GROWTH, STRUCTURE AND EVOLUTION OF THE LYTTELTON VOLCANIC COMPLEX, BANKS PENINSULA, NEW ZEALAND

A thesis submitted in fulfilment

of the requirements for the degree of

Doctor of Philosophy in Geology

at the

University of Canterbury

By

Samuel J. Hampton

University of Canterbury

2010

FRONTISPIECE

Lyttelton Harbour as a southerly blows in.

ABSTRACT

The Lyttelton Volcanic Complex, north-western Banks Peninsula, New Zealand, is comprised of five overlapping volcanic cones. Two magma systems are postulated to have fed Banks Peninsula's basaltic intraplate volcanism, with simultaneous volcanism occurring in both the north-western and south-eastern regions of Banks Peninsula, to form Lyttelton and Akaroa Volcanic Complexes respectively. The elongate form of Banks Peninsula is postulated to relate to the upward constraining of magmatism in a north-west / south-east fault bounded zone. The Lyttelton Volcanic Complex resulted from the development of a pull-apart basin, with a number of releasing bend faults, controlling the location of eruptive sites. Cone structure further influenced the pathway magma propagated, with new eruptive sites developing on the un-buttressed flanks, resulting in the eruption and formation of a new cone, or as further cone growth recorded as an eruptive package.

Each cone formed through constructional or eruptive phases, termed an eruptive package. Eruptive packages commonly terminate with a rubbly a'a to blocky lava flow, identified through stratigraphic relationships, lava flow trends and flow types, a related dyking regime, and radial erosional features (i.e. ridges and valleys). Within the overall evolving geochemical trend of the Lyttelton Volcanic Complex, are cyclic eruptive phases, intrinsically linked to eruptive packages. Within an eruptive package, crystal content fluctuates, but there is a common trend of increasing feldspar content, with peak levels corresponding to a blocky lava flow horizon, indicating the role of increased crystalinity and lava flow rheology. Cyclic eruptive phases relate to discreet magma batches within the higher levels of the edifice, with crystal content increasing as each magma batch evolves, limiting the ability of the volcanic system, over time, to erupt. Evolving magmas resulted in explosive eruptions following effusive eruptives, and / or result in the intrusion of hypabyssal features such as dykes and domes, of more evolved compositions (i.e. trachyte). Each eruptive package hosts a radial dyke

swarm, reflecting the stress state of a shallow level magma chamber or a newly developed stress field due to gravitational relaxation in the newly constructed edifice, at the time of emplacement.

Two distinct erosional structures are modelled; radial valleys and cone-controlled valleys. Radial valleys reflect radial erosion about a cone's summit, while cone-controlled valleys are regions where eruptive packages and cones from different centres meet, allowing stream development. Interbedded epiclastic deposits within the Lyttelton lava flow sequences indicate volcanic degradation during volcanic activity. As degradation of the volcanic complex progressed, summit regions coalesced, later becoming unidirectional breached, increasing the area of the drainage basin and thus the potential to erode and transport extensive amounts of material away, ultimately forming Lyttelton Harbour, Gebbies Pass, and the infilled Mt Herbert region. Epiclastic deposits on the south-eastern side of Lyttelton Harbour indicate a paleo-valley system (paleo-Lyttelton Harbour) existed prior to 8.1 Ma, while the morphology of the Lyttelton Volcanic Complex directed the eruptive sites, style and resultant morphology of the proceeding volcanic groups.

ACKNOWLEDGEMENTS

There have been many people involved in inception, undertaking and completion of this thesis. The key to this study has been the ever present and patient Professor Jim Cole. His constant support, guidance, knowledge and endless revisions of chapters, has been an integral part. Thanks to Professor Steve Weaver for listening to some crazy ideas and having the patience to join me in the field. A special thanks to David Bell for the engineering opportunities, the splendid exposures created at Black Point, to which this thesis delves into, and for your constant banter, abuse and trickery. Thanks to Associate Professor Uwe Ring, without his contribution to understanding the faults and structures of Banks Peninsula a crucial piece of the puzzle would be missing. Thanks to Professor John Bradshaw for discussions on dyking regimes, volcanic growth and tectonic environments, an endless source of knowledge. Thanks to David Shelley, for the use of field notebooks, time in the field, and comments on working hypotheses. Thanks to Dr Karoly Nemeth and Professor Shane Cronin for time in the field and constructive comments in the early to mid stages of research.

Thank you to the University of Canterbury for the Doctoral Scholarship, making this research possible. To the Mason Trust Fund, a source of funding key to the never ending fieldwork, conference attendances, and research travel.

Thank you to those in the Department of Geological Sciences who have provided support and enthusiasm over the past years; Anekant Wandres, Chris Grimshaw, John Southward, Kerry Swanson, Rob Spiers, Pat Roberts, Janet Warburton, Cathy Higgins and Vanessa Tappenden. Thanks to the postgraduates and fellow PhDs (06), of which I'm one of the last (Chad, Tom, Rose, Clinton), thank you for all of your support, banter, whisky or wine over the past years.

Thank you to my family for all the support and encouragement over the past eight years. Thank you to my Mum and Dad your enthusiasm, understanding, emergency funding, and endless support. A massive thank you to Aimee, your patience, support, encouragement, and never ending distractions has kept me in check and balanced.

TABLE OF CONTENTS

CHAPTER 2: POLAR COORDINATE TRANSFORMED (PCT) IMAGE ANALYSIS AND DEGRADATION OF LYTTELTON VOLCANO

CHAPTER 3: EPICLASTIC DEPOSITS ON THE SOUTH-EASTERN SIDE OF LYTTELTON HARBOUR

CHAPTER 4: LAVA FLOW PACKAGES OF LYTTELTON VOLCANO: DISTINGUISHING BLOCKY LAVA FLOWS FROM A'A LAVA FLOW SEQUENCES

CHAPTER 5: PRIMARY VOLCANIC LANDFORMS AND ERUPTIVE CENTRE IDENTIFICATION

CHAPTER 6: RECONSTRUCTING ERODED VOLCANIC CONES: LYTTELTON VOLCANIC COMPLEX, BANKS PENINSULA, NEW ZEALAND

CHAPTER 7: STRUCTURAL CONTROL AND FURTHER STUDY

CHAPTER 8: CONCLUSIONS

REFERENCES

LIST OF FIGURES

CHAPTER 1: INTRODUCTION

CHAPTER 2: POLAR COORDINATE TRANSFORMED (PCT) IMAGE ANALYSIS AND DEGRADATION OF LYTTELTON VOLCANO

CHAPTER 3: EPICLASTIC DEPOSITS ON THE SOUTH-EASTERN SIDE OF LYTTELTON HARBOUR

CHAPTER 4: LAVA FLOW PACKAGES OF LYTTELTON VOLCANO: DISTINGUISHING BLOCKY LAVA FLOWS FROM A'A LAVA FLOW SEQUENCES

CHAPTER 5: PRIMARY VOLCANIC LANDFORMS AND ERUPTIVE CENTRE IDENTIFICATION

CHAPTER 6: RECONSTRUCTING ERODED VOLCANIC CONES: LYTTELTON VOLCANIC COMPLEX, BANKS PENINSULA, NEW ZEALAND

CHAPTER 8: CONCLUSIONS

LIST OF TABLES

CHAPTER 2: POLAR COORDINATE TRANSFORMED (PCT) IMAGE ANALYSIS AND DEGRADATION OF LYTTELTON VOLCANO

CHAPTER 3: EPICLASTIC DEPOSITS ON THE SOUTH-EASTERN SIDE OF LYTTELTON HARBOUR

CHAPTER 4: LAVA FLOW PACKAGES OF LYTTELTON VOLCANO: DISTINGUISHING BLOCKY LAVA FLOWS FROM A'A LAVA FLOW SEQUENCES

CHAPTER 1

INTRODUCTION

1.1. Introduction

Banks Peninsula is the largest accumulation of Miocene volcanic rocks on the East Coast of the South Island, New Zealand, consisting of the eroded remnants of two large volcanoes (Figure 1.1 and 1.2; Lyttelton (11 – 9.7 Ma) and Akaroa (9.3 – 8 Ma), with intervening Mt Herbert Volcanic Group (9.7 – 8.0 Ma) and later Diamond Harbour Volcanic Group (8.1 – 5.8 Ma; Sewell et al., 1992). Although highly eroded, the morphology of both volcanoes can be seen from aerial, digital elevation models (DEM's) and satellite images (Figure 1.1). Lyttelton and Akaroa Volcanoes are viewed as large single vented volcanoes, due to symmetric forms, large basal diameters, evidence of dyking throughout their histories, and parasitic eruptive vents (Sewell, 1988; Shelley, 1987; 1988; 1992; Sewell et al., 1992).

1.2 Location and History

Banks Peninsula forms a large promontory, at latitude 43° 40'S, longitude 172° 45'E on the East Coast of the South Island, New Zealand. Banks Peninsula was initially named 'Banks Island' by Captain James Cook, from the Endeavour 15km offshore, after the expedition's botanist Sir Joseph Banks (Speight, 1917). The first inhabitants, the Maori, named the Peninsula *Te Rakaihautu* or 'the storehouse of Rakaihautu'. The Port Hills are known as *Te Whakatakanga o Te Ngarehu o Tamatea Whenua* or 'the place where Tamatea Pokai Whenua left the ashes of the fire he brought (Brown and Weeber, 1992).

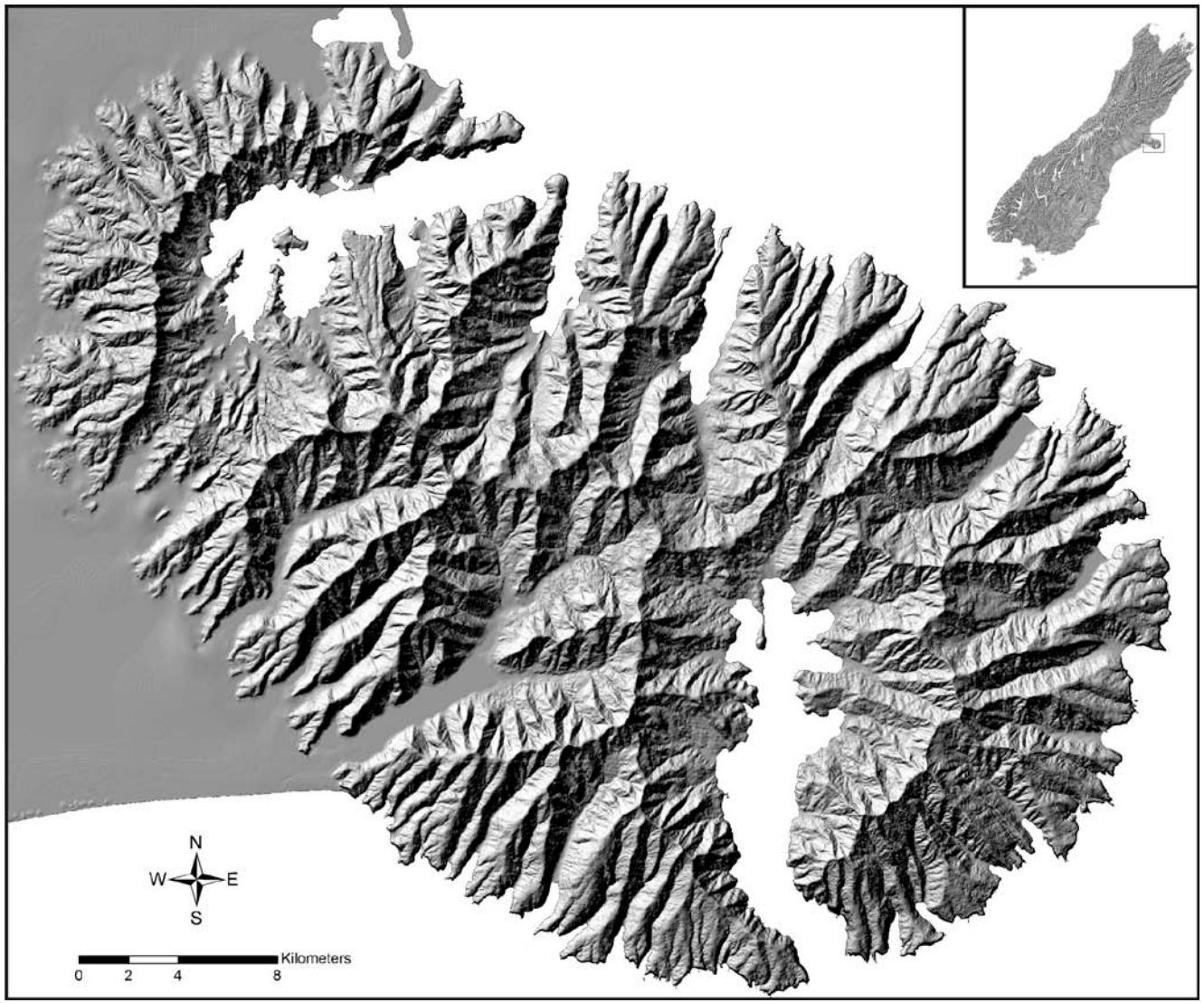

Figure 1.1. DEM of Banks Peninsula, highlighting Lyttelton Volcano to the north-west, and Akaroa to the south-east. Note the morphology of Lyttelton and Akaroa Harbours and the radial drainage about the central upper regions.

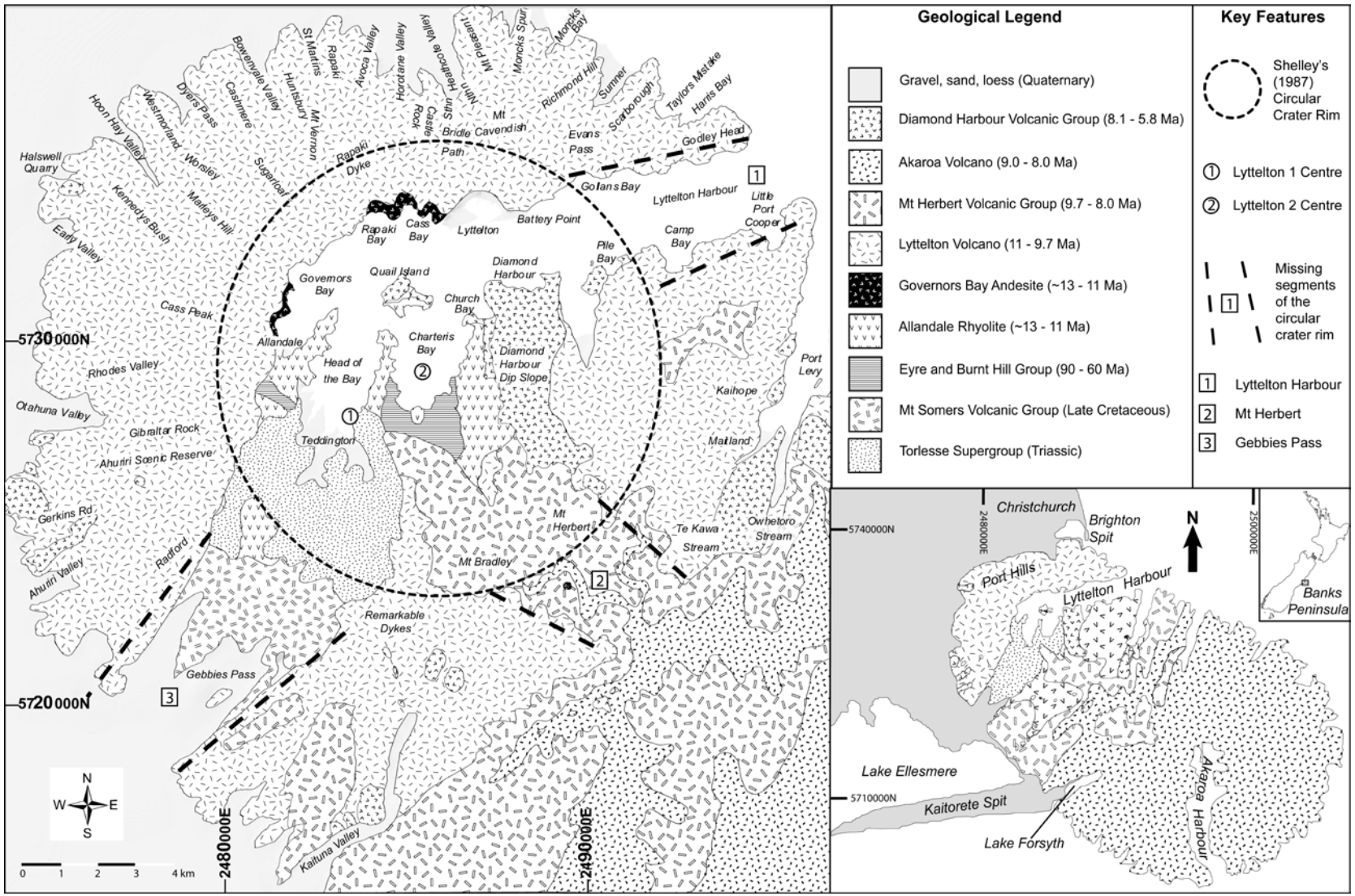

Figure 1.2. Simplified geology of Banks Peninsula and features of previous evolutionary models of Lyttelton Volcano (based on Sewell (1985) and Shelley (1987). Place names are referred to throughout the thesis are highlighted in this figure.

Maori occupation provided modifying aspects on the Peninsula, from Pa sites (fortified Maori villages; Brailsford, 1981), cultivation areas, to extensive burn offs. Maori forest clearance, chiefly by fire, had removed about one-third of Banks Peninsula's forest by the time European settlers arrived towards the middle of the nineteenth century (Johnston, 1969). The most radical changes to the Peninsula arrived with the Europeans. Extensive logging decimated forests of the Peninsula, intensified with the burning off for pastoral land. Leaving patches of original forest cover, with approximately 4% of original old forest cover remaining (Wilson, 1994). Quarrying of the volcanic rocks of Banks Peninsula provided the building blocks for many Christchurch buildings, ranging from tuff, dykes, domes, and e lava flows. Remnants of these quarries are scattered throughout the area, with one of the largest at Halswell Quarry.

1.3. Physiography

Banks Peninsula is the highly eroded remnants of a volcanic complex, primarily comprising Lyttelton and Akaroa Volcanoes (Figure 1.2; Sewell et al., 1992), that connected with the South Island by progressive deposition of alluvial gravels, now forming the Canterbury Plains (Figure 1.3), mainly during extensive glaciations (Sewell et al., 1992), and the eastward flowing rivers of the Waimakariri, Rangitata and Rakaia (Figure 1.3). Alluvial gravels overlie undulating Upper Cretaceous and Tertiary basement rocks, and are interbedded with marine deposits (Forsyth et al, 2008).

Coastal deposits to the south of Banks Peninsula are from longshore drift, redistributing gravels and sands from rivers further south. This has resulted in the formation of Kaitorete Spit and the formation of Lake Forsyth and Ellesmere (Figure 1.2; Browne and Naish, 2003). To the north, circling currents around Banks Peninsula produce an eddying effect, accompanied by the prevailing NE swell, promoting deposition of Brighton Spit (Figure 1.2).

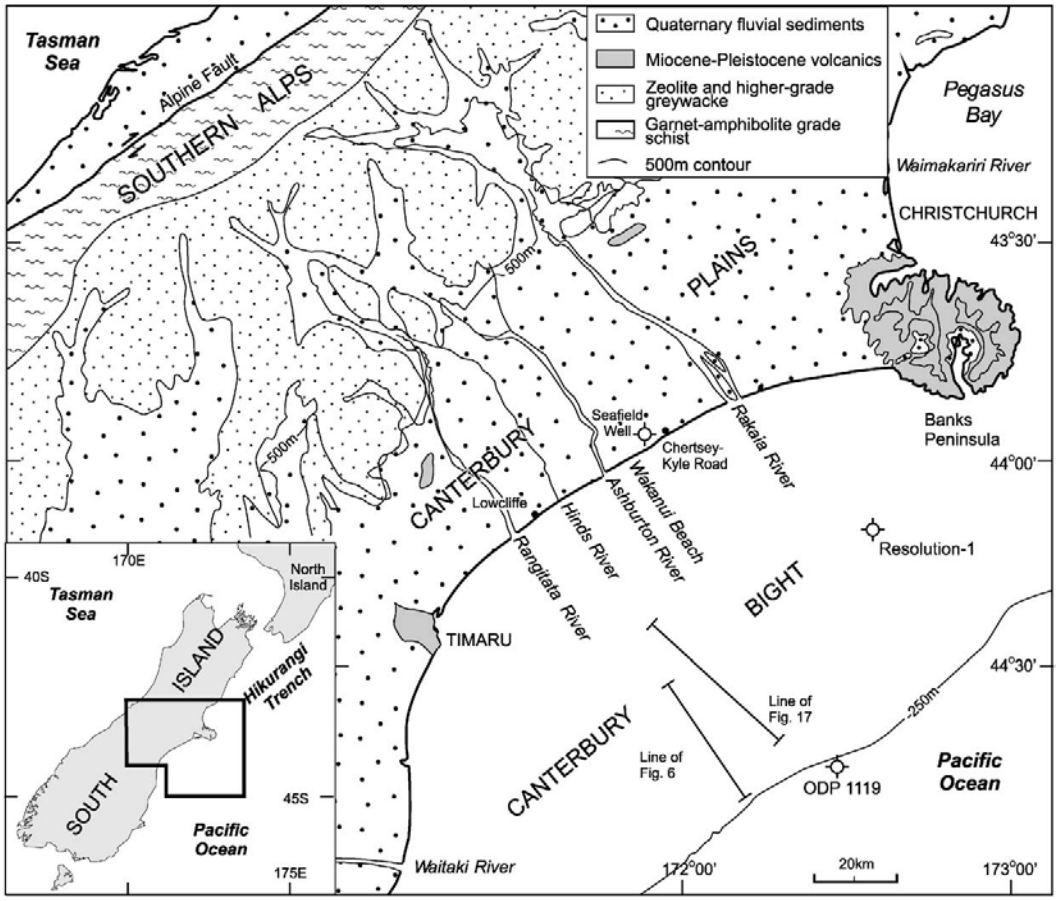

Figure 1.3. Major rivers of the Canterbury Plains, South Island. The Canterbury Plains formed due to the uplift, erosion and deposition of gravels, sourced from the greywacke rocks of the Southern Alps (Figure from Browne and Naish, 2003).

1.4. Tectonic Setting and South Island Intra-Plate Volcanism

A compressional regime, peaking as the Rangitata 'Orogeny' in the Cretaceous period, kept New Zealand on the eastern side of Gondwana (Bradshaw et al., 1981). Compression changed to extension and rifting in the Late Cretaceous (80 – 53 Ma) separating New Zealand from Gondwana, opening the Tasman Sea (Sewell & Gibson, 1988). Extensional tectonics caused warping, local basin subsidence and widespread alkalic to tholeiitic volcanism in the Canterbury region until the Late Eocene-Oligocene (Sewell et al, 1989).

During the early Miocene, tectonic activity changed to a compressional regime, causing uplift (Kaikoura 'Orogeny'), increasing sedimentation and alkalic and tholeiitic volcanism in

the South Island, including Banks Peninsula (Figure 1.4; Adams, 1981). The shutting off of volcanism in the South Island coincides with the change from predominantly strike-slip to compressional tectonics (Hoke et al., 2001). Bal (1997) concluded from studying shore platforms, that Banks Peninsula has been tectonically stable since the mid-late Quaternary.

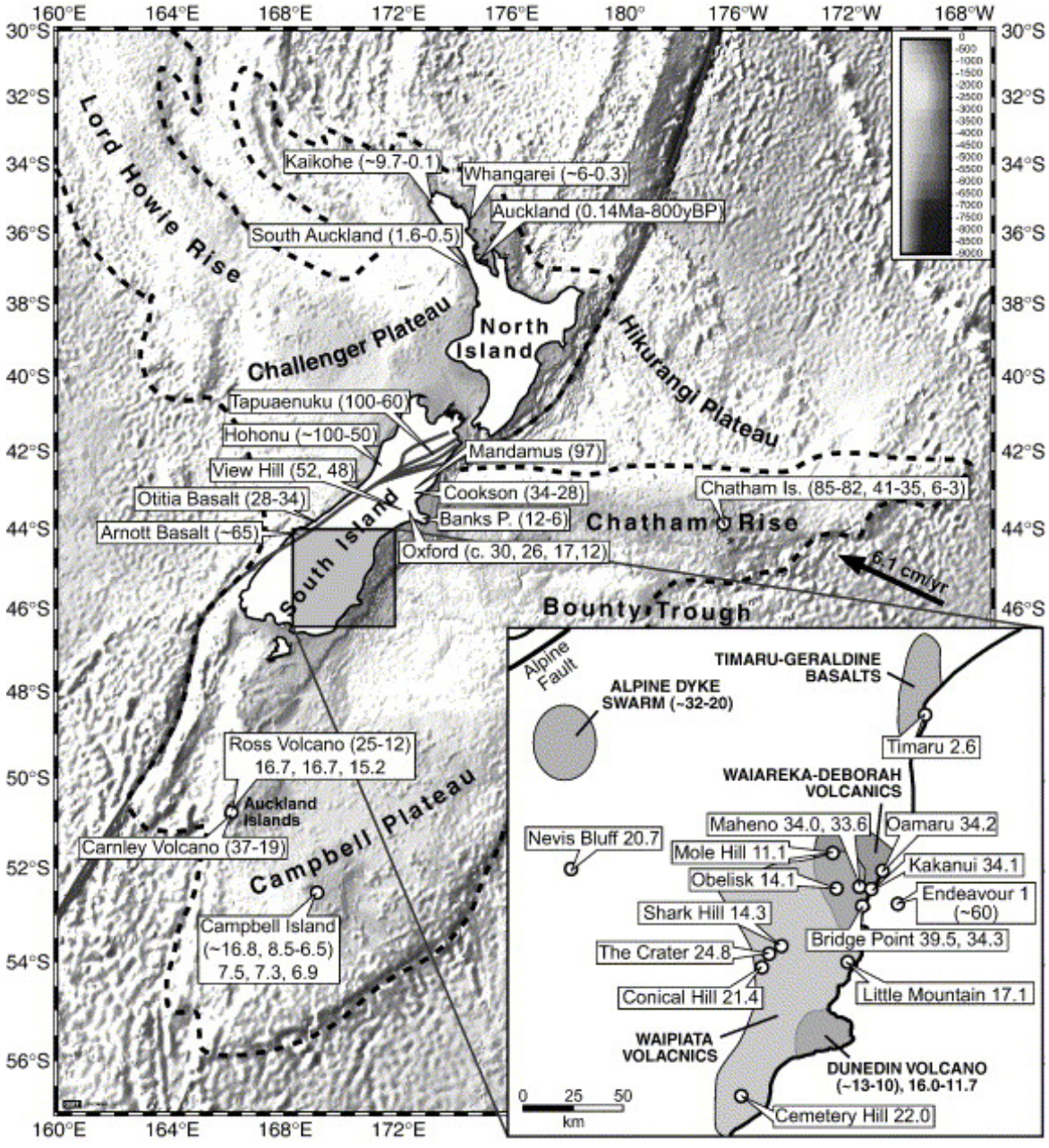

Figure 1.4. Cenozoic intra-plate volcanism in New Zealand. Each area of volcanism are labelled with approximate age ranges of volcanic activity (From Horenle et al., 2006).

Intra-plate volcanism occurred throughout the New Zealand in the Cenozoic in the North, South, Chatham, Auckland, Campbell and Antipodes Islands (Figure 1.4). Two extensive regions of intra-plate volcanism developed in the South Island in the Miocene, Banks Peninsula and Dunedin volcanic complexes (Figure 1.4). Hoke et al's (2000) study of the sub-continental mantle beneath southern New Zealand, suggested that the intra-plate basaltic volcanism was the result of thermal instabilities deep in the earth's mantle, or sourced from shallow depths in the upper mantle, caused by thermal mantle instabilities of unknown origin. Recent investigations (Finn et al., 2005; Hoernle et al., 2006; and Timm et al., 2009) have focussed on the difficulties in explaining intra-plate volcanism in New Zealand, by either a mantle plume model or continental rifting. Hoernle et al (2006) investigated intraplate volcanism in the Otago region and suggested lithospheric detachment. Timm et al (2009) has suggested this model is also appropriate for Banks Peninsula volcanism.

1.5. Banks Peninsula's Stratigraphy and Geological History

The following is a summary of the stratigraphy and geological history of Banks Peninsula, as defined through previous investigations of Banks Peninsula (Carlson et al., 1980; Weaver, 1980; Thiele, 1983; Sewell, 1985; Andrews et al., 1987; Shelley, 1987; Barley et al., 1988; Sewell et al., 1988; Weaver and Smith, 1989; Shelley, 1992; Sewell et al, 1992). Ages for Banks Peninsula volcanism stated throughout this thesis are from Stipp and McDougall (1968)

Diamond Harbour Volcanic Group (8.1 - 5.8 Ma)
Stoddart Basalt (ds)
Kaioruru Hawaiite (dk)

Church Basalt (cb)
Chateau Intrusives (ci)
Darra Basanitoid (cd)

Akaroa Volcanic Group (9.0 - 8.0 Ma)
Te Oka Formation (ae) Mt Sinclair Formation (am) Onawe Syenite (ao)
Duvachelle Gabbro (ad) Lushington Breccia (al) French Hill Formation (af)
Tikao Trachyte (at)

Mt Herbert Volcanic Group (9.7 - 8.0 Ma)
Herbert Peak Hawaiite (hh) Port Levy Formation (hp)
Orton Bradley Formation (ho)
Mt Bradley Volcaniclastic Member (hob)

Lyttelton Volcanic Group (11 - 9.7 Ma)
Mt Pleasant Formation (lp)
Lyttelton Volcanic Group (l)

Governors Bay Andesite (gb) (~13 - 11 Ma)

Allandale Rhyolite (ra) (~13 - 11 Ma)

PROBABLE UNCONFORMITY

Burnt Hill Group (Early Miocene)
Bradley sandstone (bb)

UNCONFORMITY

Eyre Group(Paleocene - Eocene)
Marine Drive Formation (em)

View Hill Volcanics (ev)

Charteris Bay Sandstone (ec)

Broken River Formation (eb)

PROBABLE UNCONFORMITY

Mount Somers Volcanic Group (80.9 Ma)
Gebbies Rhyolite (me) McQueens Andesite (mm)
Gebbies Pass Plant Beds (mer)

REGIONAL UNCONFORMITY

Torlesse Supergroup (t) (Triassic)

Figure 1.5. Stratigraphic sequence of Banks Peninsula, as published by Sewell et al., (1992).

1.5.1. Pre Lyttelton Volcanics

The basement rocks of Banks Peninsula are comprised of deformed Torlesse Supergroup (Figure 1.5) exposed in Gebbies Pass (Figure 1.2). Torlesse Supergroup are late Triassic sandstone, mudstone and chert, formed in a large submarine fan complex (Campbell and Coombs, 1966). A localised topographic high arose due to the Rangitata Orogeny (early Jurassic, mountain building phase) and localised faulting (Weaver, 1980; Thiele, 1983), providing the first building block for Banks Peninsula.

The first volcanic rocks on Banks Peninsula are the Late Cretaceous Mt Somers Volcanic Group (Figure 1.5), exposed in Gebbies Pass and McQueens Valley (Barley et al., 1988). Igneous activity produced two-pyroxene andesites and peraluminous, high-silica rhyolite lava flows, domes and ignimbrites. Within the Mt Somers Volcanic Group are the Radford Conglomerates and the Gebbies Pass "plant beds", which represent scree slope and lake deposits that formed between lava domes (Andrews et al., 1987).

In the early Tertiary, extensive erosion occurred as the area progressively became inundated by the sea (Sewell et al, 1992). During this period (50 Ma) a thin sequence of siliceous and volcanic-derived sedimentary rocks were deposited, known as the Eyre and Burnt Hill Groups (Figure 1.5; Carlson et al., 1980). Deposits include unconformities (visible breaks in sedimentation), which may relate to uplift and drowning of the area (Sewell et al, 1992).

This area then rose above sea level, the result of pre-volcanic doming or faulting, in the early Miocene (Sewell et al, 1992). Allandale Rhyolite (Figure 1.5) were erupted, producing rhyolite domes and lava flows, and later dacite (Mid-Miocene) and lava flows of the Governors Bay Andesite (Figure 1.5), were erupted from a series of vents in the proximity of the present head of Lyttelton Harbour (Sewell et al, 1992).

1.5.2. Lyttelton Volcano (11 – 9.7 Ma)

Lyttelton Volcanics formed in the Late Miocene between 11.0 and 9.7 Ma of hawaiite, subordinate basalt, mugearite lava flows and interbedded sediments (Sewell et al, 1992; Figure 1.2, 1.5 and 1.6). It is currently hypothesised that Lyttelton Volcano had two distinct centres (Figure 1.2), Lyttelton 1 at the Head of the Bay (11.0 – 10.4 Ma) and Lyttelton 2 in Charteris Bay (10.4 – 9.7 Ma) (Shelley, 1987). Shelley (1987) identified these from dyke orientations, and this was supported by Neumayr (1999) from orientations of valleys, ridge lines and lava flow trends.

Lyttelton 1 and Lyttelton 2 Volcano

Lyttelton 1 is dominantly built up of lavas with episodes of explosive volcanism that progressively built a symmetrically shaped, composite volcanic cone (Figure 1.6; Sewell, 1985; Sewell et al, 1992). Prior to the eruption of Lyttelton 2, erosion or collapse is considered to have occurred to the edifice of Lyttelton 1 (Figure 1.6; Sewell, 1988; Neumayr, 1998) with epiclastic deposits occurring at a major disconformity between flows of Lyttelton 1 and Lyttelton 2. Activity then shifted to Lyttelton 2, progressively constructing a symmetrically shaped cone similar in size and shape to Lyttelton 1. Initial lavas in-filled the eroded Lyttelton 1 cone, and then overtopped the eroded crater rim, producing a thin veneer of lava flows over the flanks. Throughout the history of both Lyttelton 1 and 2 volcanic edifices have been cut by basalt to trachyte dykes. Some dykes fed lava flows or produced parasitic cones on the flanks of the volcanoes.

Mt Pleasant Formation (10.4-9.7 Ma)

Late stage Lyttelton Volcano activity is termed the Mt Pleasant Formation (Figure 1.5 and 1.6). Activity was mainly from flank eruptions on the north-eastern and southern Lyttelton Volcano, mantling the flanks of Lyttelton 2 Volcano lava flows to the northeast. A hiatus in volcanic activity is signified by an epiclastic horizon between the lava flows of Lyttelton 2 Volcano and the Mt Pleasant Formation, although lava flows have been observed interbedded within lahar deposits (Neumayr, 1998).

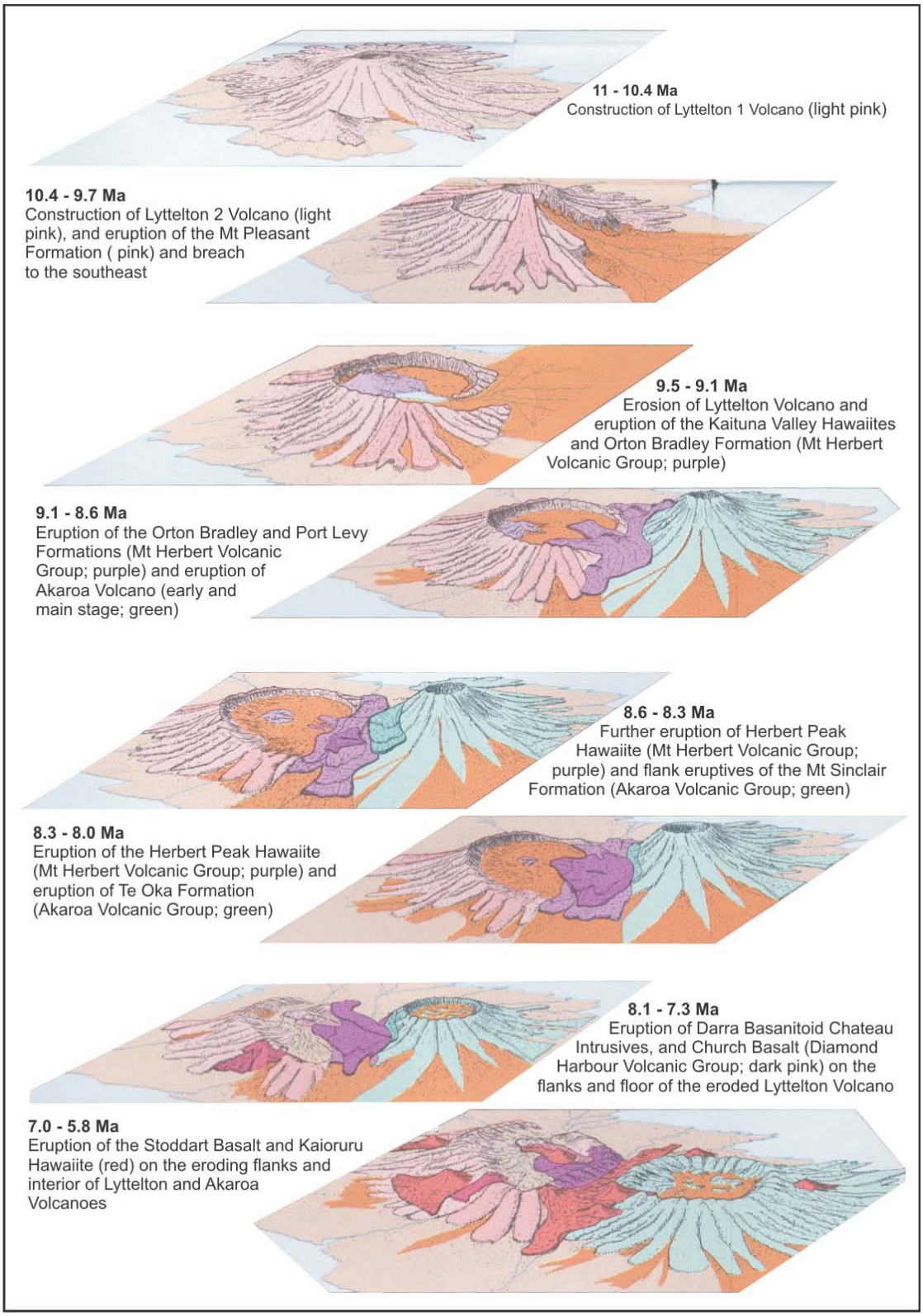

Figure 1.6. Sewell et al (1992) summary figure illustrating the history of Miocene volcanism on Banks Peninsula.

1.5.3. Mt Herbert Volcanic Group (9.7 – 8.0 Ma)

After a period of quiescence, volcanic activity shifted from Lyttelton Volcano to the Mt Herbert region (Figure 1.2 and 1.6). During this period, there was deep erosion in the crater, with breaches in the southeast, and possibly, southwest crater rim and slopes of the Lyttelton Volcano edifice. The Mt Herbert Volcanic Group (9.7 – 8.0 Ma; Figure 1.5) initially began from vents in the Lyttelton crater and then migrated south-eastwards to the crater rim breach, erupting ~100km^3 of material (Sewell, 1985).

Kaituna Valley Hawaiites (9.7 – 9.5 Ma)

The Kaituna Valley Hawaiites unconformably overlie the Lyttelton Volcanics and are the initial flows of the Mt Herbert Volcanic Group. Sewell (1985) identified boulder conglomerate deposits between the Kaituna Valley Hawaiites and Lyttelton Volcanics, and interpreted them as 'mass flow deposits', formed from the erosive debris of Lyttelton Volcano. Lava flows are grey-black, phyric, 2 – 10 m thick, and are separated by thin layers of scoracious lapilli and fine tuff. Sewell (1985) initially named these the Kaituna Olivine Hawaiites, but later (Sewell, 1988) renamed them the Kaituna Valley Hawaiites. These are lava flows constrained further volcanic activity to localised areas, and mark the renewal of volcanic activity after the Lyttelton Volcanics. Activity was probably of Hawaiian style, from monogenetic cones.

Orton Bradley Formation (9.5 – 8.6 Ma)

The Orton Bradley Formation (Figure 1.5 and 1.6) consists of the Homestead Lava Member, Mt Bradley Volcaniclastic Member, Packhorse Lava Member, and the Tablelands Volcaniclastic Member (Hampton, 2005). The formation covers an area from Mt Herbert south to Kaituna Valley and Prices Valley, and rests unconformably on Torlesse rocks, Charteris Bay Sandstone, and Lyttelton Volcanics (Sewell, 1988). Homestead Lava Member flows are the initial volcanic products within the south-southeast collapse of Lyttelton Volcano, with its vent in close vicinity to that of Lyttelton 2 (Hampton, 2005). The overlying Mt Bradley Volcaniclastic Member represents periods of fluvial activity

intensified by the surrounding collapse amphitheatre, a phase of phreatomagmatic activity, and formation of a lake late in the sequence (Hampton, 2005). This lake then provided the fuel for a second phase of phreatomagmatic activity (Tablelands Volcaniclastic Member), which is interbedded with the extensive Packhorse Lava Member Flows.

Port Levy Formation (8.9 – 8.4 Ma)

Between 8.9 – 8.4 Ma igneous activity moved further south to the northern flanks of Lyttelton Volcano (Figure 1.5 and 1.6). The Port Levy Formation consists of lava flows, welded airfall tuff, and rare dykes (Sewell, 1985; Sewell et al., 1992). The principle source of eruption was at Port Levy, erupting as small scoria cones followed by extrusion of lavas (Sewell, 1985).

Herbert Peak Hawaiite (8.5 – 8.0 Ma)

Lava erupted from a vent 50 m southeast of Mt Herbert, producing flat lying, columnar to tabular jointed, grey aphyric to phyric hawaiites that cap Mt Bradley and Mt Herbert dipping to the north at 2° (Sewell et al., 1988). Sewell (1985) noted low ash abundance, indicating activity was dominantly of Hawaiian-type, from a fissure vent eruption. The characteristic thick columnar jointed flows is linked to extrusion of lavas onto an almost flat lying surface (Sewell, 1985).

1.5.4. Akaroa Volcanic Group (9.1 – 8 Ma)

Activity occurred simultaneously at the Mt Herbert and Akaroa volcanoes (Figure 1.2, 1.5 and 1.6). Activity at Akaroa produced a 1200 km³ composite strato-shield cone, predominantly composed of alkali lavas, pyroclastics and shallow intrusives, which reached an estimated 1800m above sea level (Weaver and Smith, 1989). Activity was predominantly from a central vent (suggested as Onawe Peninsula), although minor vents on the flanks, and radial dyking did occur.

The Akaroa Volcanic Group has been classified into extrusive and intrusive rocks by Sewell et al., (1988). Extrusive rocks include the early stage Tikao Trachyte and Lushington Breccia, the main cone forming French Hill Formation (9.0 – 8.3 Ma), the flank eruptives of the Mt Sinclair Formation 8.6 – 8.3 Ma) and the Te Oka Formation (8.3 – 8.1 Ma). Intrusive rocks include the Duvachelles Gabbro (8.92 Ma) and the Onawe Syenite exposed on Onawe Peninsula, representing late stage emplacement.

1.5.5. Diamond Harbour Volcanic Group (8.1 – 5.8 Ma)

The Diamond Harbour Volcanic Group (Figure 1.2 and 1.5) incorporates the previously termed "church-type" lavas (Sewell et al., 1992), defining a volcanic group representing a phase of eruptive activity and erosional phases on the eroding volcanoes of Banks Peninsula.

Darra Basanitoid (8.1 – 7.7 Ma)

Columnar to irregularly jointed basanitoid lava flows (Figure 1.5 and 1.6), exposed on the western and eastern sides of Quail Island, and overlie Lyttelton Volcanics between Taitapu and Ahuriri (Sewell et al., 1988). Lava flows on the north-western side of Quail Island are flat lying with thin zones of auto-brecciation (Sewell, 1985). North-eastern Darra Basanitoid lavas overlie a basal yellow-brown, angular to sub-rounded, boulder to cobble conglomerate, which overlies weathered Allandale Rhyolite.

Church Basalt (8.0 – 7.3 Ma)

Columnar jointed basalt flows, interbedded with epiclastic deposits, erupted and deposited within the eroded Lyttelton Volcano (Figure 1.5 and 1.6; Sewell et al., 1988). Church Basalts are best exposed at Purau Bay, Church Bay, and Quail Island.

At Purau Bay, Church Basalts unconformably overlie Lyttelton Volcanics (Sewell et al., 1992). Basal Church Basalt lavas are overlain by a epiclastic sequence of conglomerate, interbedded with tuffaceous sandstone, and an upper, dune to planar bedded, gently

north dipping, tuffaceous sandstone. This sequence is followed by a series of lava flows, the lowest of which is being a columnar jointed, almost dome-like, crystal-rich basaltic lava, with the basal horizon incorporating the underlying sand.

On Quail Island, Church Basalts are exposed as two (20m) thick, almost flat lying, columnar jointed lava flows, overlying and separated by volcaniclastic deposits. Basal volcaniclastics are white-yellow, fine grained tuffaceous sandstone to mudstone, interbedded with poorly sorted pebble-boulder conglomerate (Sewell, 1985). Interbedded volcaniclastics are approximately 20m thick, red-yellow brown, sub-rounded to rounded pebble-boulder conglomerate, interbedded with tuffaceous sandstone and mudstones.

Chateau Intrusives (7.99 Ma)

Columnar jointed hawaiite, dome, sills, and dykes, intruding Allandale Rhyolite, Mt Bradley Volcaniclastic Member, and Church Basalt.

Kaioruru Hawaiite (6.85 Ma)

Red-brown vesicular hawaiite lavas (Sewell, 1985) exposed in the eroded interior of Lyttelton Volcano along the shore platform near Ripapa Island, Diamond Harbour, Church Bay and northern Quail Island (Figure 1.5 and 1.6; Sewell et al., 1992). The Purau Bay exposure occurs on the eastern side of the bay, underlying the Stoddart Basalts of Ripapa Island and the adjacent Peninsula. Diamond Harbour exposures are discontinuous along the shore platform of Black Point and Diamond Harbour. Kaioruru Hawaiites rest unconformably on eroded Church Basalts, with a maximum thickness (10m) at Church Bay (Sewell, 1985). Quail Island exposures are along the shore platform and reefs along the northern shoreline, are northwest dipping, and unconformably overlying conglomerates associated with the Darra Basanitoids (Sewell, 1985).

Stoddart Basalt (7.0 – 5.8 Ma)

The final phase of activity resulted in 20km³ of sheet flows and lava plugs on the eroding Banks Peninsula volcanoes and the eroded interior of Lyttelton Volcano (Figure 1.5 and 1.6). Exposures are at; Quail Island, Diamond Harbour to Purau Valley, Ripapa Island and associated peninsula, Kaituna Valley, between Taitapu and Ahuriri, and at Halswell Quarry (Sewell et al., 1988). At Quail Island, Stoddart Basalt overlies a thick sequence of brown, yellow-brown, matrix to clast supported, pebble to boulder conglomerate, with channelized sandstone layers, which rest unconformably on underlying Kaioruru Hawaiite. Purau Valley to Diamond Harbour exposure is the largest accumulation of Stoddart Basalt, forming the 5km long Diamond Harbour dip slope.

1.5.6. Post Volcanism

After volcanism ceased, Akaroa and Lyttelton Volcanoes underwent extensive erosion modifying the topography, and forming Lyttelton and Akaroa Harbours. During glacial periods, "rock flour" transported by aeolian processes was deposited, causing loess to mantle the topography (Taylor et al., 1983). Over the last 2 Ma sedimentation of the Canterbury plains occurred, connecting Banks "Island" to the South Island, forming Banks Peninsula.

1.6. Features of the Previous Theories of Lyttelton Volcano

1.6.1. Historic volcanic centre location: Dyke Regimes

Debate has surrounded Banks Peninsula's volcanic evolution since the time of the German geologist Julius von Haast (1860). Von Haast was commissioned by the Canterbury Provincial Council in 1859 to produce a geologic survey of Mt Pleasant, for the purposes of building a railway tunnel, connecting the Port of Lyttelton to Christchurch. Within his report Haast (1860) identified Lyttelton Harbour as being the remains of an extinct volcano, with lava flows around the crater rim having a quaquaversal dips about a common centre. Quail Island (Figure 1.2) was seen as the centre of the volcano, supported

by orientation of dykes. He proposed that Quail Island recorded the late phase of volcanic activity within Lyttelton Volcano, as it is not intruded by dykes, with the rest of Banks Peninsula considered to be formed by a number of volcanic systems. Later Haast (1878, 1879) modified his ideas proposing a centre of volcanism for Lyttelton Volcano south-west of Quail Island, with a trachytic radial dyke swarm occurring near the end of eruptive activity.

Speight (1917) judged from the quaquaversal dips of the flows observed on the cliffs and on the other side of the deep-cut valleys, as well as from the records of the tunnel, that the centre of the harbour corresponded to the centre of activity, but owing to the occupation of the bottom of the crater by the sea the actual site of the vent could not be definitely located. Speight (1917) deduced from the orientation of the dykes of the walls of the crater ring, that the radiated from a small area just south of Quail Island, which he regarded as the actual centre of disturbance and the precise locality of the vent. Speight (1938) further analysed Lyttelton dykes concluding that they radiate from a point a little south west of Quail Island. He followed by stating "it is unlikely, however, that the conduit up which the lava come to construct the cone itself was located at this spot. It probably lay in a somewhat eccentric position near the reef which rises to the just above sea level from the floor of the harbour between the town of Lyttelton and Quail Island."

Frost (1965) interpreted dyking regimes on Lyttelton Volcano, indicating an eruptive centre west of Quail Island. Shelley (1987) analysed dyke regimes of Lyttelton Volcano identifying two eruptive centres, Lyttelton 1 and Lyttelton 2 (Figure 1.2). Neumayr (1999) re-interpreted the location of Lyttelton 1 using orientations of valleys, ridge lines and lava flow trends, indicating a centre of volcanism slightly north-west of Shelley's (1987) Head of the Bay centre.

1.6.2. Circular Erosional Crater Rim

Crater rim features were initially considered by von Haast (1878, 1879) as secondary features when designating eruptive centre locations, a process based mainly on dyke orientations. However he recognised a crater rim on the western Port Hills, primarily above Governors Bay (Figure 1.2) associated with Lyttelton Volcano. Speight (1938) defined the caldera rim of Lyttelton as between Evans Pass at the eastern end to Gebbies Pass at the western end. He estimated this between 1000 to 1500 feet in height and at a distance approximately three miles from the centre of the cone measured radially.

It wasn't until the 1980's that the large circular crater rim of Lyttelton Volcano was hypothesised by Sewell (1985). Shelley (1987) supported this large circular crater rim theory (Figure 1.2), connecting the highest points around the erosional crater rim of Lyttelton Volcano, with a centre of rotation in Charteris Bay, reflecting the morphology of Lyttelton 2 Volcano.

1.6.3. Height Estimates of Lyttelton Volcano

Speight (1917) in the examination of the Lyttelton Tunnel recorded the average inclination of flows in the tunnel as almost exactly 15°, and this value corresponds with that obtained from observations of prominent flows exposed on the sides of valleys eroded deeply into the flanks of the volcano. Taking this value, and also the distance of the outer fringe of the hills from the centre of the volcano as approximately six miles, the height of the cone must have approached 8000 ft (2438.4 m); and if making allowance for a probable greater inclination of the flows and an increased thickness near the vent, and also for the depression of the land which has occurred since volcanic activity waned, and Speight (1917) considered it possible that the cone approached, if it did not actually exceed, 10, 000 ft (3048 m) in height.

Reconstructions of Ligget and Gregg (1965) evaluated Lyttelton as reaching a height of 1670m, while Stipp and McDougall (1968) estimated it as a shield-like 1525m, supported

by Weaver and Smith (1987) with a postulated height of 1500m. Shelley's (1992) analysis of the centres of Lyttelton Volcano suggested a summit of 2500m, similar in morphology to Mt Etna (Figure 1.7). These estimates were produced through a simple process of identifying a centre of volcanism and projecting the dip of the outer slopes towards this. Variation exists between, with Shelley's (1992) dramatically steepening outer flank dips (~>20°) based on a Mt Etna morphology, whereas Sewell et al (1992) based on lower flank dips (~12°) of a Hawaiian shield morphology. The present topography of Lyttelton is around a quarter of these estimates, with the Port Hills reaching ~500m a.s.l., with the highest point on the Peninsula, Mt Herbert at 920m a.s.l.

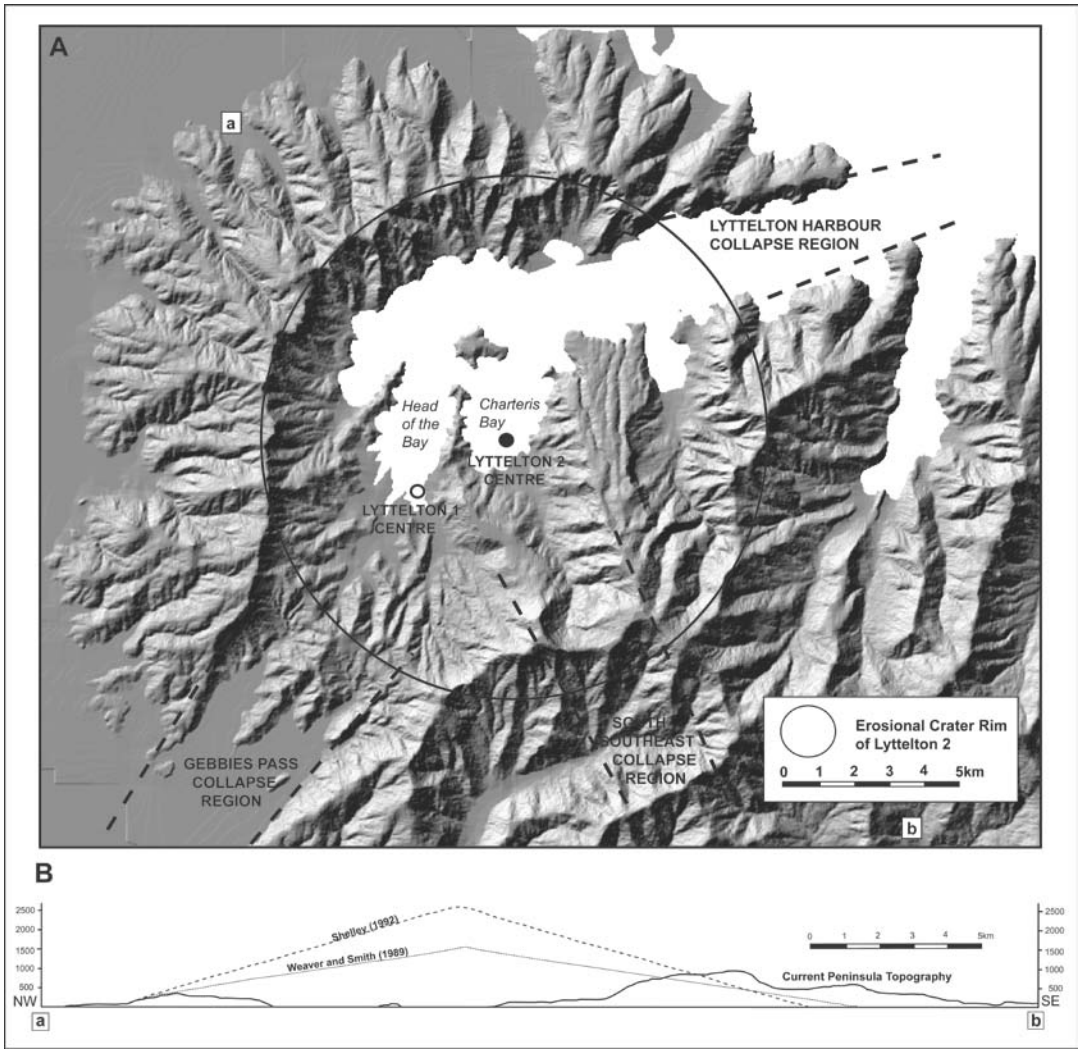

Figure 1.7. Key features of previous interpretations of Lyttelton Volcano. A) The two centres of Lyttelton Volcano, as identified by Shelley (1992), and the erosional crater rim related to Lyttelton 2, and the three collapse regions (Sewell, 1988). B) Projected heights of Lyttelton Volcano of Shelley (1992) and Weaver and Smith (1989).

1.6.4. Formation of Lyttelton Harbour

The most prominent erosive features of Banks Peninsula are the long harbours of Lyttelton and Akaroa (Figure 1.1 and 1.2). The origins of Lyttelton and Akaroa Harbours have been debated since first recognition of Banks Peninsula's volcanic origins. Ideas have varied from purely erosional incision, through to sector collapse with further enlargement.

Speight (1917) noted that "the present form of the cone is no doubt entirely different from that which it presented at the close of this volcanic phase.... Instead of the usual moderate-sized crater at the top there is now a great hollow, and evidence suggests that this form had developed to some extent before the next phase of volcanic activity began". He proposed three working hypotheses:

1. The crater been formed by explosion or collapse of the cone, the former indicating a revival of volcanic activity.
2. The crater is due to peripheral faulting causing subsidence of the original crater.
3. The crater eroded by action of streams, or by the sea, or more probably the, in some cases at all events, by a combination of both processes.

In Speight's (1943) revision of the geology of Banks Peninsula, he revisited the formation of the harbours, disregarding the possibility of caldera collapse, stating that there is no positive evidence of collapse. Within this paper he also noted the orientation of both Lyttelton and Akaroa Harbours in relation to the surrounding fault systems of the South Island. Lyttelton Harbour sits on an ENE – WSW line, which is the approximate orientation of the dominant fault lines of the north-eastern portion of the South Island. Akaroa Harbour orientation is on a NNW – SSE line, which characterise the faults of the mountain regions of Canterbury, and lies at right angles to Lyttelton Harbour.

Speight (1943) followed this with a suggestion that the harbour was the result of 1) a line of minor craters (such as Tarawera, 1886), or 2) by collapse following on the rapid outflow

of magmas along tectonic lines, the caldera in both cases being modified by erosion with the master stream draining through the sector graben if formed according to the second hypothesis. In a following statement he concluded that "the entrances (Lyttelton and Akaroa Harbours) have been chiefly formed by consequent streams which have eroded radial trench-like valleys across the outward dipping beds of a volcanic cone, and the sides of the valleys have been modified especially near the entrances by marine erosion." He considered initiation of these master valleys an accident in topography, possibly at a low point in the crater rim where a moderate summit explosion or accidental feature arose during the final stages of construction.

An important aspect of Banks Peninsula volcanic landscape interpretation is William's (1941) type classification of erosion caldera. In reviewing Speight's (1917; 1938) analysis of Lyttelton Volcano and Banks Peninsula, William's (1941) supported the erosive formation of Lyttelton Harbour, with the enlargement of the craters (Lyttelton and Akaroa Harbours) through fluviatile action, similar to that of La Palma, Canary Islands.

Sewell (1985) hypothesised three breaches in the crater rim of Lyttelton Volcano (Figure 1.2); Gebbies Pass, Mt Herbert, and Lyttelton Harbour. Sewell (1985), Weaver and Smith (1989) and Sewell et al., (1992) reflect highly on the influence of erosion forces, although collapse was perceived near the upper end of erosive forces. Collapse was accompanied by deep erosion, eating away at the soft core of the volcano, producing the distinctive harbour of Lyttelton, Mt Herbert depression and Gebbies Pass.

1.7. Purpose of Study

The volcanics of Banks Peninsula has been widely studied in terms of geochemistry. Few studies have focussed on the physical volcanology and the structural complexities surrounding volcanic groups. The main goal of this thesis is to investigate the growth,

structure, and development of Lyttelton Volcano, through examination of the physical volcanology and geomorphology of Lyttelton Volcano, Banks Peninsula.

Specific objectives to be addressed within this thesis are:

- Establishment of the volcanic stratigraphy exposed in the inner cliff faces of Lyttelton Harbour, and deposits relationships to geochemical analysis
- Establish the relationship between the outer flank geomorphology and deposits to the better exposed and investigated inner harbour exposures
- Establish the relationship between the eastern and western exposures of Lyttelton Volcano
- Determine the influence and degree of volcanic collapse in the development of Lyttelton Volcano
- Investigate the formation, timing and development of Lyttelton Harbour, through investigation of volcanics and deposits exposed in the eroded interior of Lyttelton Volcano
- Establish the origin of the epiclastic deposits in the north-eastern sector of Lyttelton Volcano.
- Determine the eruptive style, volcano type and morphology of Lyttelton Volcano
- Determine the role of radial dyking in the development of Lyttelton Volcano
- Establish the relationship between geochemical trends and eruptive cycles and the observed physical volcanology of Lyttelton Volcano
- Define structural / tectonic controls on volcanism in Banks Peninsula
- Establishment of a detailed volcanic evolution model for Lyttelton Volcano
- Discussion and comparison of the evolutionary model with basaltic to andesitic volcanoes and volcanic complexes

1.8. Field Area

The field area involved in this study covers western Banks Peninsula (Figure 1.2), and its immediate surroundings. Geological exposure is best around the sea cliffs, and inner harbour / bay regions, although these only provide a selective slice through volcanic sequences. Further exposures are located around the crater rims of Lyttelton Volcano, with only limited exposures within valleys, due to loess, sediment and vegetation cover. Fieldwork covered most of Lyttelton Volcano with isolated areas of more concern, investigated in detail. Fieldwork was covered by car and on foot, with a motor boat used for coastal regions.

1.9. Terminologies

This thesis uses the IUGS classification of igneous rock, and White and Houghton's (2006) classification for primary volcaniclastic rocks and sedimentary deposits (Figure 1.8). The term primary volcaniclastic deposits is used following White and Houghton's (2006) classification in which deposits are the direct results from a volcanic eruption, defined as pyroclastic, autoclastic, hyaloclastic and perperitic (Figure 1.9). Epiclastic deposits resulting from the weathering and reworking of primary volcaniclastic deposits are classified using the normal sedimentary rock names (Figure 1.8) of Fisher and Schmincke (1984). Component descriptions within primary volcaniclastic deposits and epiclastic deposits follow White and Houghton's (2006) component classes (Figure 1.10).

Grain size		Primary volcaniclastic deposit		Sedimentary deposit (rock name)	
(phi)	(mm)	Unconsolidated	Lithified	Unconsolidated	Lithified
>4	<1/16	Extremely fine ash	Extremely fine tuff	Clay	Mudrock, shale
3–4	1/16–1/8	Very fine ash	Very fine tuff	Very fine sand	Very fine sandstone
2–3	1/8–1/4	Fine ash	Fine tuff	Fine sand	Fine sandstone
1–2	1/4–1/2	Medium ash	Medium tuff	Medium sand	Medium sandstone
0–1	1/2–1	Coarse ash	Coarse tuff	Coarse sand	Coarse sandstone
−1 to 0	1–2	Very coarse ash	Very coarse tuff	Coarse sand	Coarse sandstone
−2 to −1	2–4	Fine lapilli	Fine lapilli-tuff	Granule	Grit, granule congl.
−4 to −2	4–16	Medium lapilli	Medium lapilli-tuff	Pebble	Pebble conglomerate
−6 to −4	16–64	Coarse lapilli	Coarse lapilli-tuff	Cobble	Cobble conglomerate
<−6	>64	Block/bomb	Breccia	Boulder	Boulder congl.

Note: The ash and lapilli grain-size ranges have been modified from that given by Fisher (1961) and derivative classifications to match and include the subdivisions within the sand and gravel ranges given by Wentworth (1922). "Extremely fine" ash replaced "fine ash" for particles finer than 4 phi (1/16 mm). Lithified sedimentary deposits with angular grains coarser than 2 mm are commonly termed "breccia."

Figure 1.8. Grain size and classification scheme for primary volcanic deposits and sedimentary deposits of White and Houghton (2006).

Process	Deposit adjective (noun)
Sedimentation from pyroclastic plumes and currents	Pyroclastic (various)
Deposition of fragments from lava, formed via air cooling	Autoclastic (autobreccia)
Deposition of fragments from lava, formed via water chilling	Hyaloclastic (hyaloclastite)
Mingling of magma with wet sediment, ~in situ deposition	Peperitic (peperite)

Note: All should be given grain-size names based on grain size and degree of lithification (Table 1).

Figure 1.9. Primary volcaniclastic deposits and sedimentary deposits of White and Houghton (2006).

Component	Key criteria	Components within deposits (*example*)
Juvenile	Primary juvenile: derived directly from erupting magma; particle contributes heat to thermal budget of transport and/or fragmentation processes. Recycled juvenile: juvenile clast recycled during the eruption that formed it; not a significant thermal contributor to depositing plume or current.	Dense to inflated fragments of chilled magma (*pumice*, *scoria*, *dense juvenile*); may be recycled. Aggregate of relatively finer-grained clasts (*accretionary lapilli*, *armored lapilli*). Crystals derived directly from the erupting magma (e.g., *juvenile feldspar*); may be recycled.
Lithic	Clast formed by fragmentation of pre-existing rock or incorporated from unconsolidated sediment. These contribute negligible heat energy to transport, depositional, or fragmentation processes.	Fragments derived from wall rock (e.g., *sandstone lithic*). Fragments of solidified magma from conduit walls, blocks of lava or dike rock (e.g., *basalt lithic*). Block of pyroclastic rock (e.g., *tuff block*).
Composite	Clast formed by mingling of magma with a clastic host, or incorporation of lithic debris into magma.	Fragments of peperite (*composite clasts*). Bomb with lithic core (*cored bomb*).

Note: Though "juvenile" is subdivided to distinguish primary from recycled clasts, it is recognized that this significant behavioral distinction can only rarely be made from ancient deposits. Composite clasts are unique in combining lithic and juvenile material.

Figure 1.10. Component classes of primary volcaniclastic deposits of White and Houghton (2006).

CHAPTER 2

POLAR COORDINATE TRANSFORMED (PCT) IMAGE ANALYSIS AND DEGRADATION OF LYTTELTON VOLCANO

2.1. Introduction

This chapter analyses features considered key in evolution of Lyttelton Volcano; the circular crater rim, eruptive centre location, and catastrophic collapse and associated epiclastic deposits exposed in north-eastern Lyttelton Volcano. Previous studies have suggested that Lyttelton Volcano developed through the growth of two large volcanic cones (Figure 1.2), with collapse occurring between Lyttelton 1 and 2, and after the construction of Lyttelton 2 (Shelley, 1987; 1992; Neumayr, 1998). Lava flows are assumed to radiate from two sources, a Head of the Bay source (Lyttelton 1), and a more complex interaction from the Charteris Bay (Lyttelton 2) overlying the eroded Lyttelton 1 surface. Collapse produced an unconformity between these two lava stacks, highlighted by Shelley (1987) as a laharic sequence exposed in the Tors and Mt Cavendish (Figure 1.2), modified by Neumayr (1998), further extending from beneath the Tors to the back of Lyttelton Township.

The chapter is divided into two sections; the first section discusses techniques of volcanic geomorphological and morphometric analysis and further develops the use of these in investigating the degraded Lyttelton Volcano, under the framework of Shelley's (1987) model. The second section reviews volcanic degradation, discussing the features of catastrophic collapse to low energy stream-flow, and relate them to features offshore and the epiclastic sequences in the north-eastern sector of Lyttelton Volcano.

2.2. DEM-Based Morphometry: Investigating Volcanic Relief

Digital elevation models (DEM's) of volcanic terrains are useful in depicting geomorphic and structural features, especially those of large scale edifices and deposits (Szèkely and Karàtson, 2004). DEM's have become increasingly used in the field of volcanic geomorphology (i.e. Aydar et al 2003; Favalli and Pareschi 2004; Norini et al 2004; Favalli et al., 2005; Jordan et al 2005; Karàtson et al 2006; Kouli and Seymour 2006) with both the images and the analysis of models enabling recognition of morphological and eruptive features. The use of DEM's in geomorphological and morphometric analysis has led to the recognition of sector collapse (i.e. Aeolian Islands, Italy; Favalli et al., 2005), highly eroded caldera complexes (i.e. Lesvos Islands, Aegean Sea, Kouli and Seymour, 2006), and the evolution of complex strato-volcanoes (i.e. Nevado de Toluca volcano, Mexico, Norini et al., 2004; Keserus Hill volcano, Hungary, et al., 2006).

2.2.1. Morphological and geomorphological analysis

Morphological and geomorphological analysis follow similar processes, condensed in this study as; visualisation, analysis, interpretation, classification, and reconstruction.

Visualisation

DEM, aerial photographs and satellite imagery, provide a basis to begin analysis and interpretation, commonly through draping aerial photographs over DEM models in Geographic Information Systems (GIS) software (i.e. ArcGIS Version 9.2, 3D visualisation application ArcScene). These models can be viewed from multiple perspectives, lighting, shading and layering.

Analysis

Analysis is typically performed within GIS software (i.e. ArcGIS Version 9.2, ArcMap) to commonly produce:

- Slope maps and slope frequency histograms, enable recognition of slope (degree) in an area (Figure 2.1A) with the histogram representing the

occurrence of slope degrees vs. area. The steepness of the terrain is depicted through the colour intensity (i.e. the steeper the slope the brighter the colour).

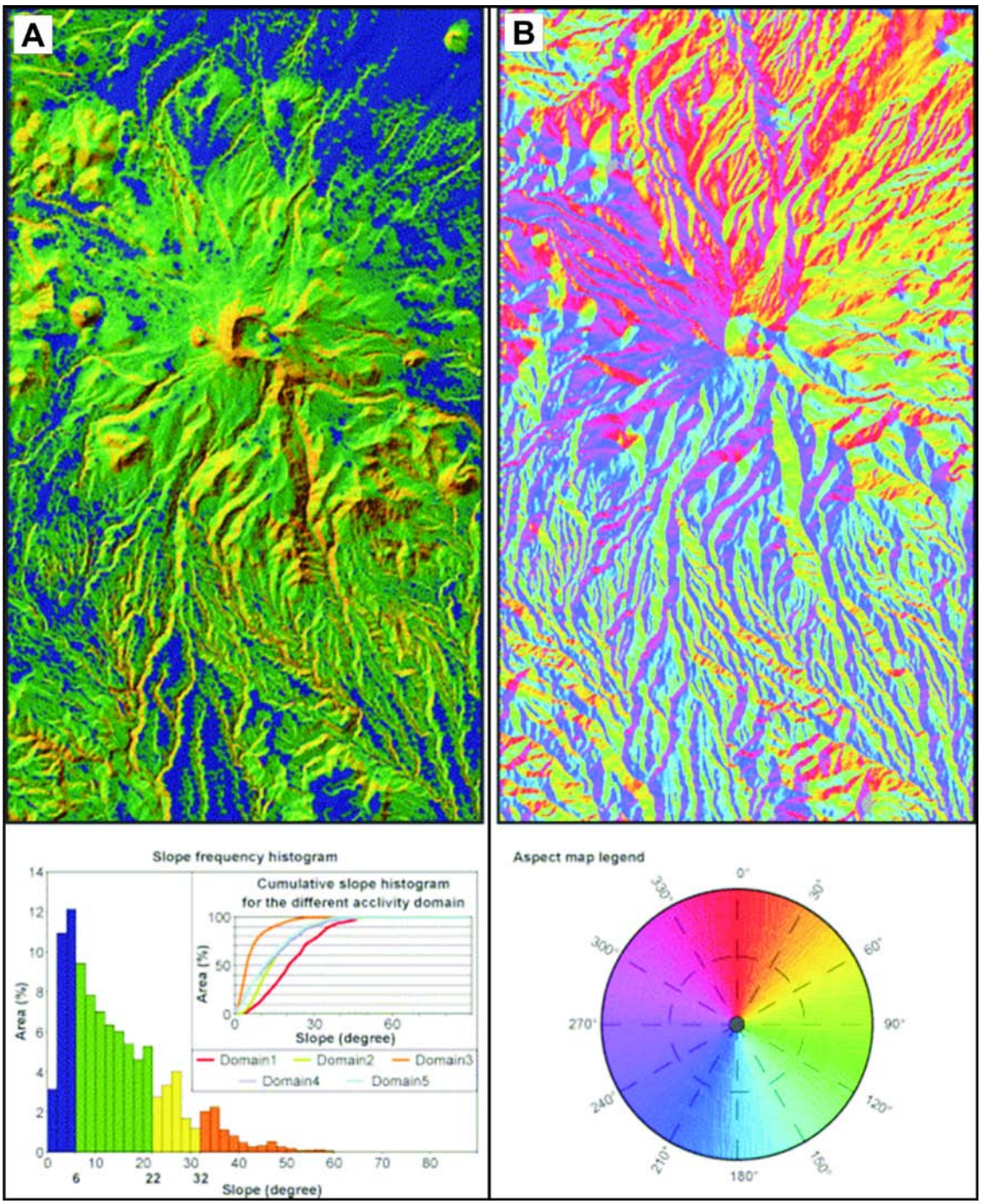

Figure 2.1. Geomorphic analysis of Nevado de Toluca volcano, Mexico (Norini et al., 2004). A) Slope map and slope frequency histogram, orange colouration depicts the steepest slopes. B) Aspect map and aspect map legend, indicating the orientation a slope faces.

- Slope aspect maps (Figure 2.1B) display the direction a slope faces. Aspect maps enable easy recognition of ridgelines, valleys, and lineaments due to colour changes.

- Drainage network analyses enable the simple recognition of current streams and valleys (i.e. Favalli and Pareschi, 2004), while the use of a Watershed tool defines catchment areas, with the intersection point of catchments orienting along ridgelines.

Interpretation

Interpretation is typically performed within GIS software (i.e. ArcMap 9.2) or computer drawing programmes (i.e. CorelDRAW X3). Through further analysis of GIS derived data key features or factors interpreted:

- Lineaments (Figure. 2.2) are commonly associated with faults (i.e. Jordan et al., 2005; Karàtson et al., 2006) or volcanic rifts (i.e. Norini and Seymour, 2006).
- Valley and ridge patterns, are closely associated to lineaments, these features will often radiate about a volcanic landform due to incision (Norini et al., 2004; Szèkely and Karàtson, 2004), or in the case of a caldera trend towards the central depression (Kouli and Seymour, 2006).
- Geomorphic features, for example major collapse scars, volcanic edifices and craters, escarpments, and canyons (i.e. Favalli et al., 2005)
- Cross sections of major structures to identify key features (i.e. crater rims, caldera collapse, lava domes or eruptive fractures (Norini et al., 2004; Kouli and Seymour, 2006)).

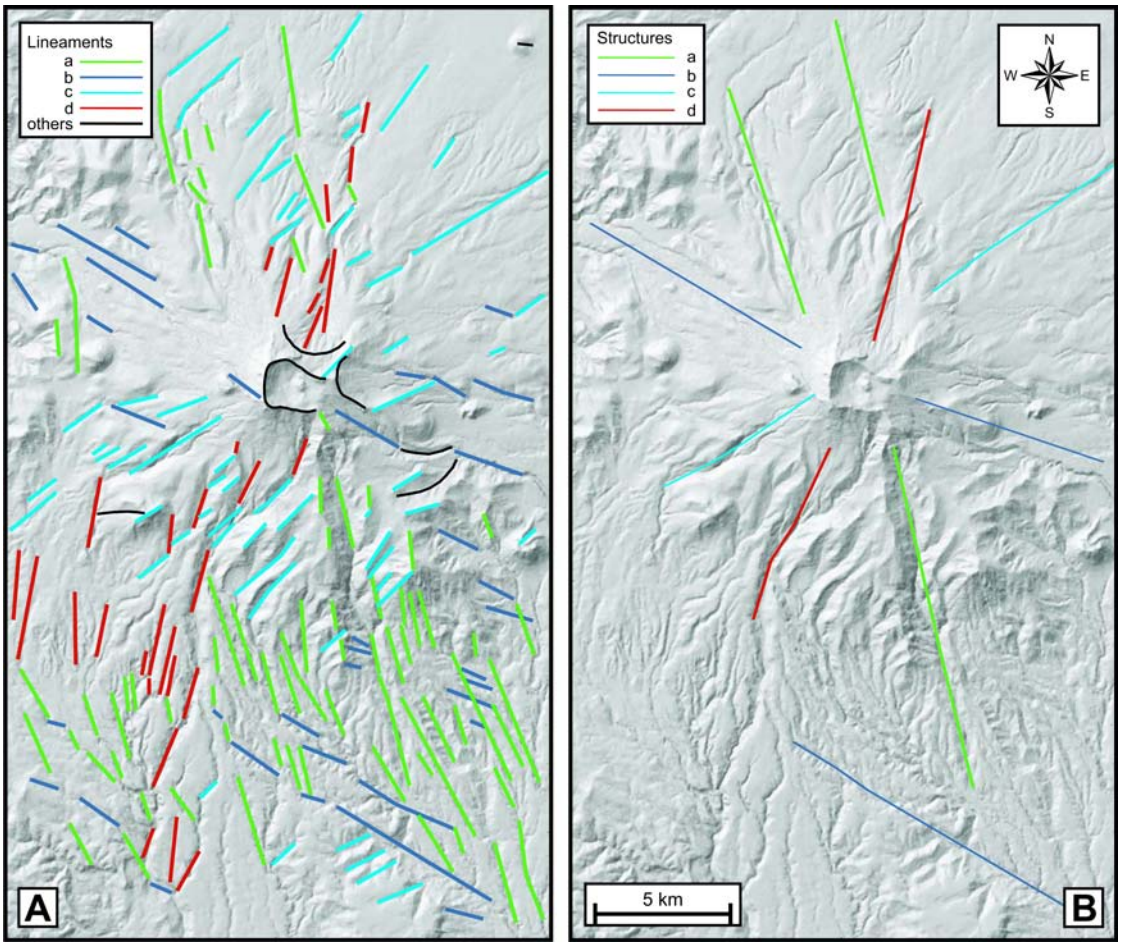

Figure 2.2. Lineament and structural analysis on Nevado de Toluca Volcano, Mexico (Norini et al, 2004). A) Identified lineament groups: a) NNW-SSE; b) NW-SE; c) NE-SW; d) NNE-SSW. B) Recognised fault structures: a) Taxco-Queratarо fault system; b) Tenago fault; c) Zacango fault; d) NNE-SSW faulting structure.

Classification

Classification is dependent on the individual study, varying from geomorphic styles (i.e. Favalli et al., 2005) to broad classification of landscape modifications (Szèkely and Karàtson, 2004).

- Geomorphic signatures are commonly used within active to relatively unmodified (minimal erosion) volcanic landforms, where the resulting geomorphology is clearly identifiable to a source and a process (i.e. a sector collapse scar on a sub-aerial volcano, to the hummocky surface and more distal volcanic fans offshore (Aeolian Islands, Italy, Favalli et al., 2005).
- Lineaments previously recognised can then be classified to their origin (Figure 2.2), with two common styles, faulting or eruptive fissure (dyking). Commonly valley and ridge trends are incorporated into this analysis with the orientation

of these commonly being affected by the surrounding tectonics or the surface geology (Norini et al., 2004; Jordan et al 2005; Karàtson et al., 2006; and Kouli and Seymour, 2006).

- Domains / sectors were defined by Norini et al (2004) on slope and aspect distribution maps, DEM's and perspective views and surface texture (Figure 2.3). Szèkely and Karàtson (2004) defined sectors based on ridge orientations (ultimately catchment regions).

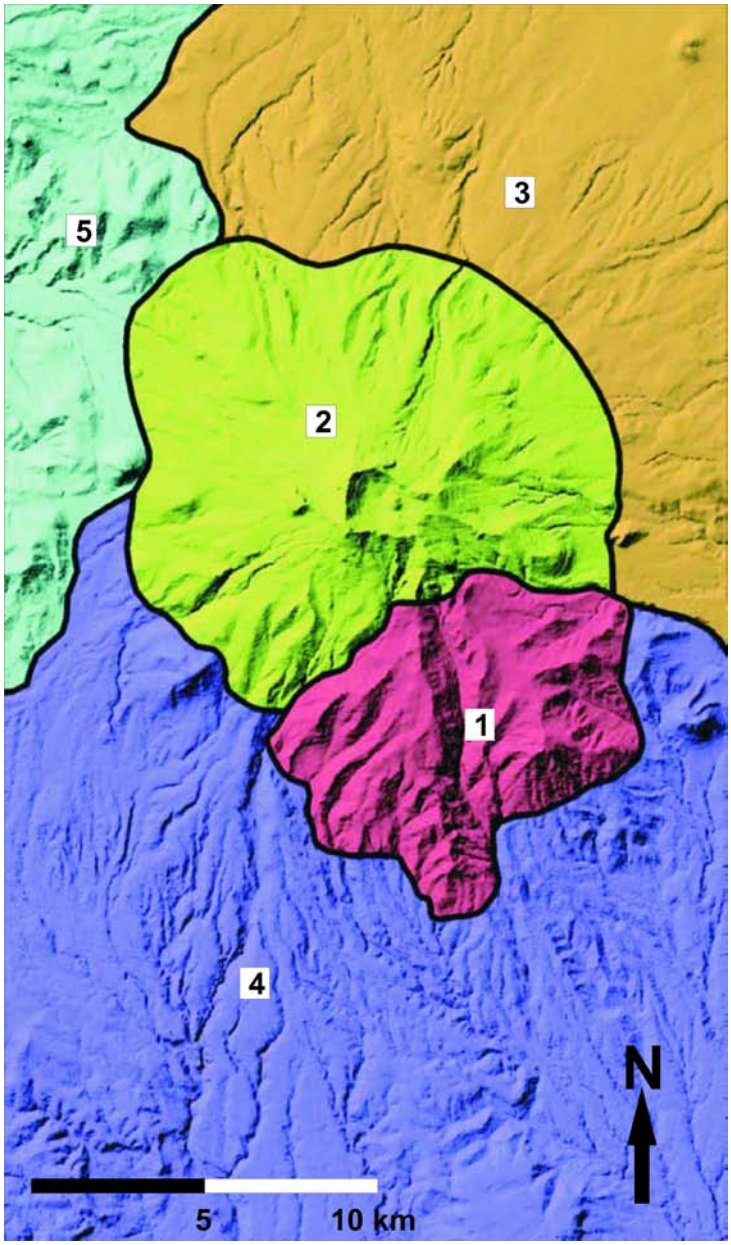

Figure 2.3. Domains of Nevado de Toluca volcano, Mexico (Norini et al., 2004). 1) irregular morphology with numerous flank ruptures. 2) Nevado de Toluca cone. 3) North-eastern lower flank of the volcanic edifice. 4) Southern DEM portion, limited by a more or less sharp slope break. 5) north-westernmost DEM portion.

Geological Models

The result or synthesis of the aforementioned analyses are broad, somewhat schematic geological models (i.e. Karàtson et al., 2005), or classifications of volcanic landforms to a specific region (Favalli et al., 2005). Szèkely and Karàtson (2004) however further analysed their data, producing a polar coordinate transformed map (PCT map), a DEM image of a once conical volcanic structure rotated and transformed about a proposed centre of volcanism (Figure 2.4).

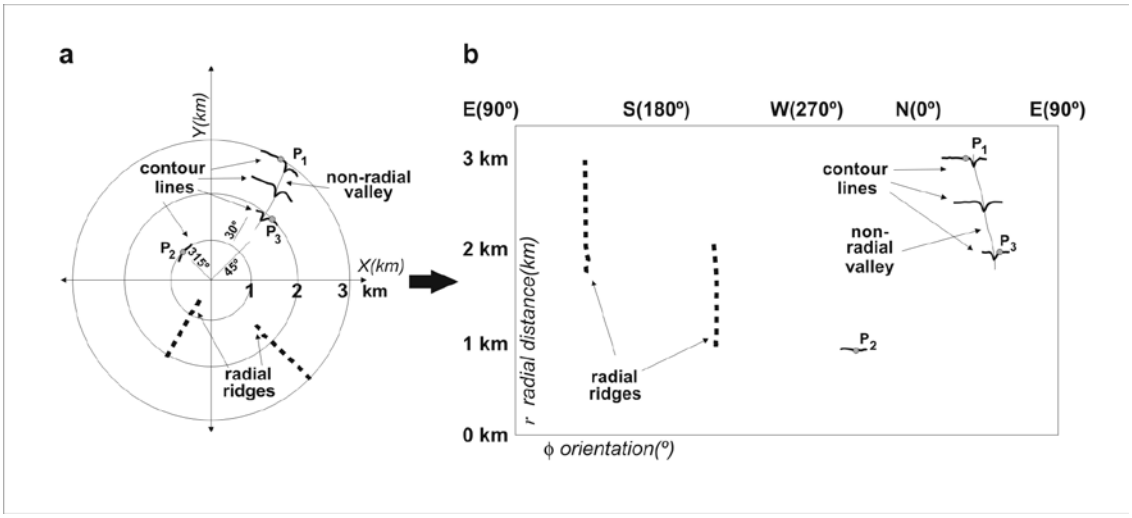

Figure 2.4. Transformation of conical volcanic features of a DEM to a PCT map. A) Schematic cone volcano with both radial and non radial valley and ridges. B) PCT map, crater rim displayed along the bottom axis, parallel to each other and perpendicular to crater rim are radial ridges, whereas the non-radial valley is at an oblique angle to the crater rim.

A polar Coordinate Transformed map (PCT's) is the result of transforming DEM data around a single point; in this instance proposed centres of volcanism (Szèkely and Karàtson, 2004). A polar coordinate transformed map images any concentric and radial features to a radius-axis parallel or angle-axis parallel feature, while any non-concentric and non-radial features will become scattered (Figure 2.4). The data for a PCT image is obtained by running an Avenue script in ArcView GIS 3.2 (details in Szèkely and Karàtson, 2004). The script requires inputs of the centre of volcanism (Cartesian coordinates), the volcano radius (radial distance), and the number of divisions required (relating to overall resolution). The script produces a text file with three categories (angular coordinates, radial coordinates, and angular resolution). This

data is then converted to a grid file and displayed in Surfer 8 (a contouring and 3D surface mapping program produced by Golden Software) as shaded relief images.

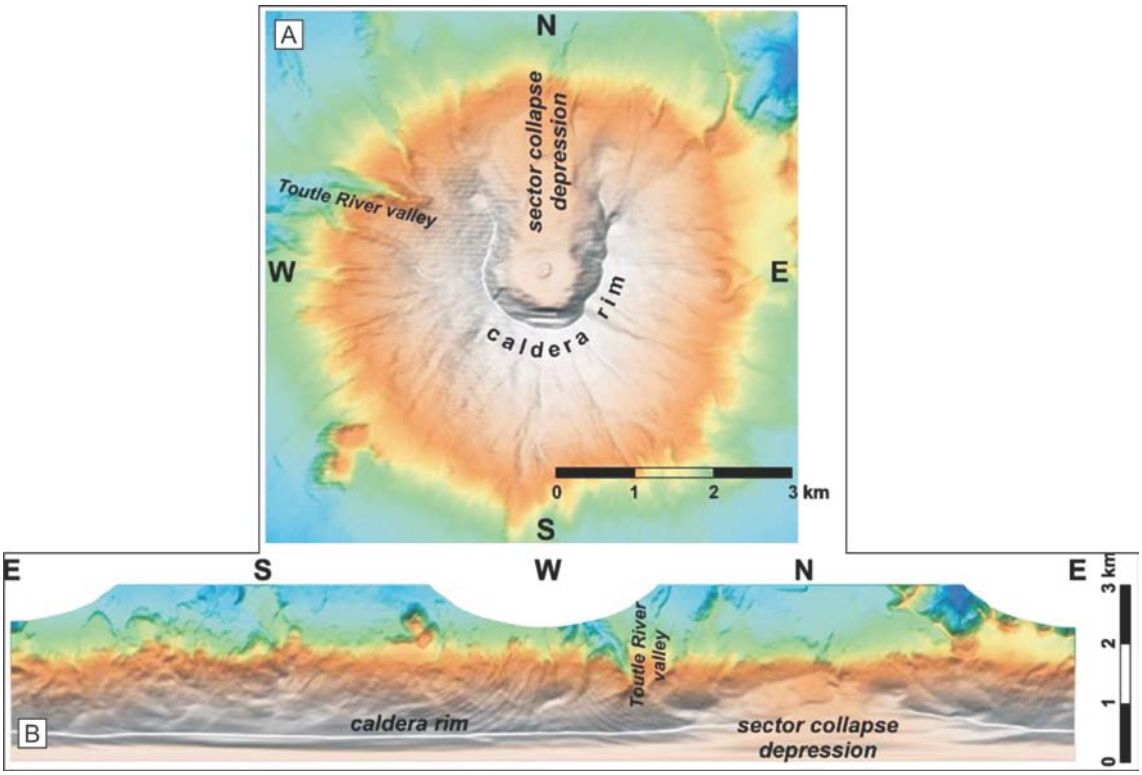

Figure 2.5. Digital elevation model (DEM) of Mt St Helens and transformed PCT map. A) Mt St Helens with the defined 1980's sector collapse amphitheatre and circular crater rim. B) PCT map of Mt St Helens, sector collapse depression is defined by a break in the circular crater rim, almost parallel to the base line, which represents the volcanic centre.

The resulting image presents a transformed DEM as a rectangle, with the bottom axis representing the single point of rotation, or centre of volcanism. This image presents features of the volcano, which either support the proposed centre of volcanism or disprove the hypothetical centre. The production of these images also enables the further recognition of sectors of the volcano, for example:

1) Related to the centre of volcanism (i.e. radial and concentric features);
2) Related to the centre of volcanism but are modified through later volcanism or erosion; or
3) Unrelated to the proposed volcanic centre. Szèkely and Karàtson (2004) produced an example PCT of Mt St Helens (Figure 2.5) where a defined sector

collapse depression (1980 collapse event) is evident, as well as the near-circular caldera rim and radiating valley systems.

Szèkely and Karàtson's (2004) study highlighted PCT maps as a useful tool in identifying catastrophic collapse regions on both highly eroded (Borzsony Mountains, Hungary) and recent volcano's (Mt St Helens, USA; Figure 2.5; Szèkely and Karàtson, 2004). As catastrophic collapse is proposed to have occurred throughout the evolution of Lyttelton Volcano (Shelley, 1987; 1992; Sewell et al., 1992), the methodology of producing a PCT map in the identification of both catastrophic collapse and associated geomorphic signatures on a large conical volcano is undertaken.

2.2.2. Morphometry Analysis: Lyttelton Volcano

DEM-based morphometry is a method of reconstructing volcanic relief and paleo-surfaces from primary landforms. Investigation of Lyttelton Volcano follows the key aspects outlined above.

Visualisation

Lyttelton Volcano is viewed through DEM's (a 10 m cell size / resolution DTM, supplied by GNS, New Zealand, projected coordinate system GD 1949 New Zealand Map Grid, on the 1949 Geographic coordinate system), aerial photographs (geo-referenced Tiff files from www.linz.govt.nz. on the projected coordinate system GD 1949 New Zealand Map Grid), GoogleEarth satellite imagery, and 3d perspectives in both ArcGIS 9.2 programme ArcSCENE (Figure 2.6), in which aerial photographs are draped over a DEM.

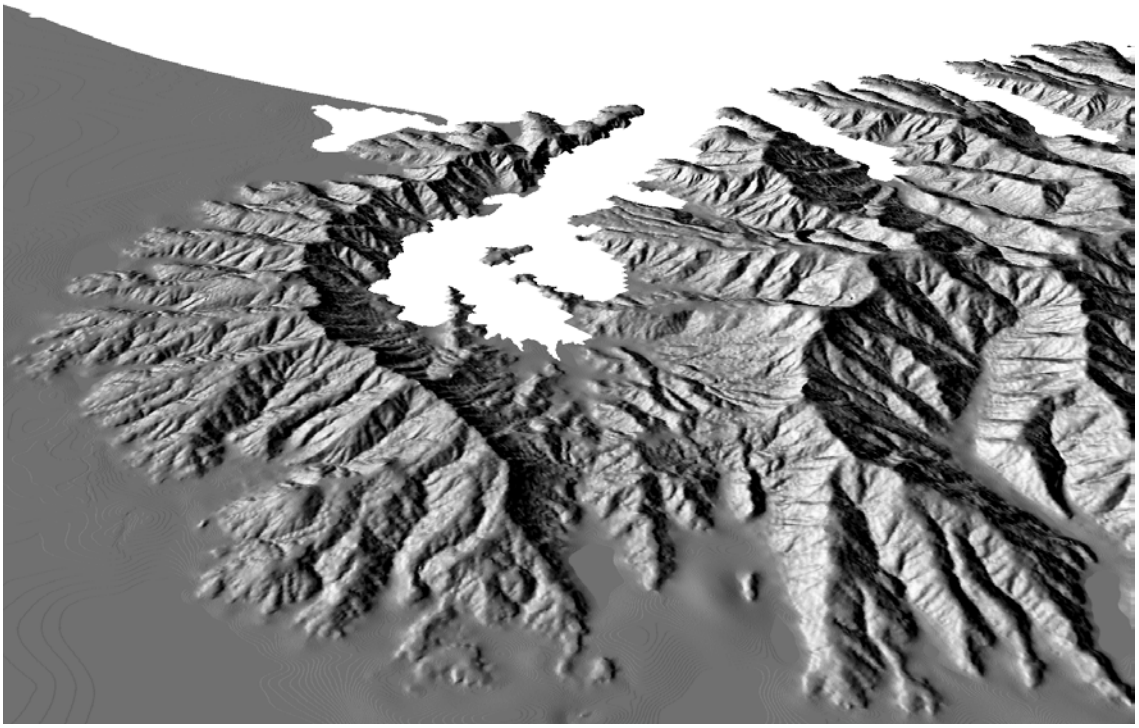

Figure 2.6. ArcSCENE view to the northeast of Lyttelton Volcano, of a 10m resolution DEM supplied by GNS. Gebbies Pass is the depression in the foreground, Lyttelton Harbour extends towards the northeast.

Analysis

Analysis was performed in ArcMAP 9.2. Slope maps (Figure 2.7A) and aspect maps (Figure 2.7B) were developed through 3D Analyst Tools in Arc Toolbox. Stream networks are calculated from DEM's using the Flow Accumulation function in Arc Toolbox (Figure 2.8A). Watersheds (Figure 2.8B) are produced in ArcMAP 9.2., using Arc Toolbox, hydrology and Watershed tool, derived stream networks, and identified pour points.

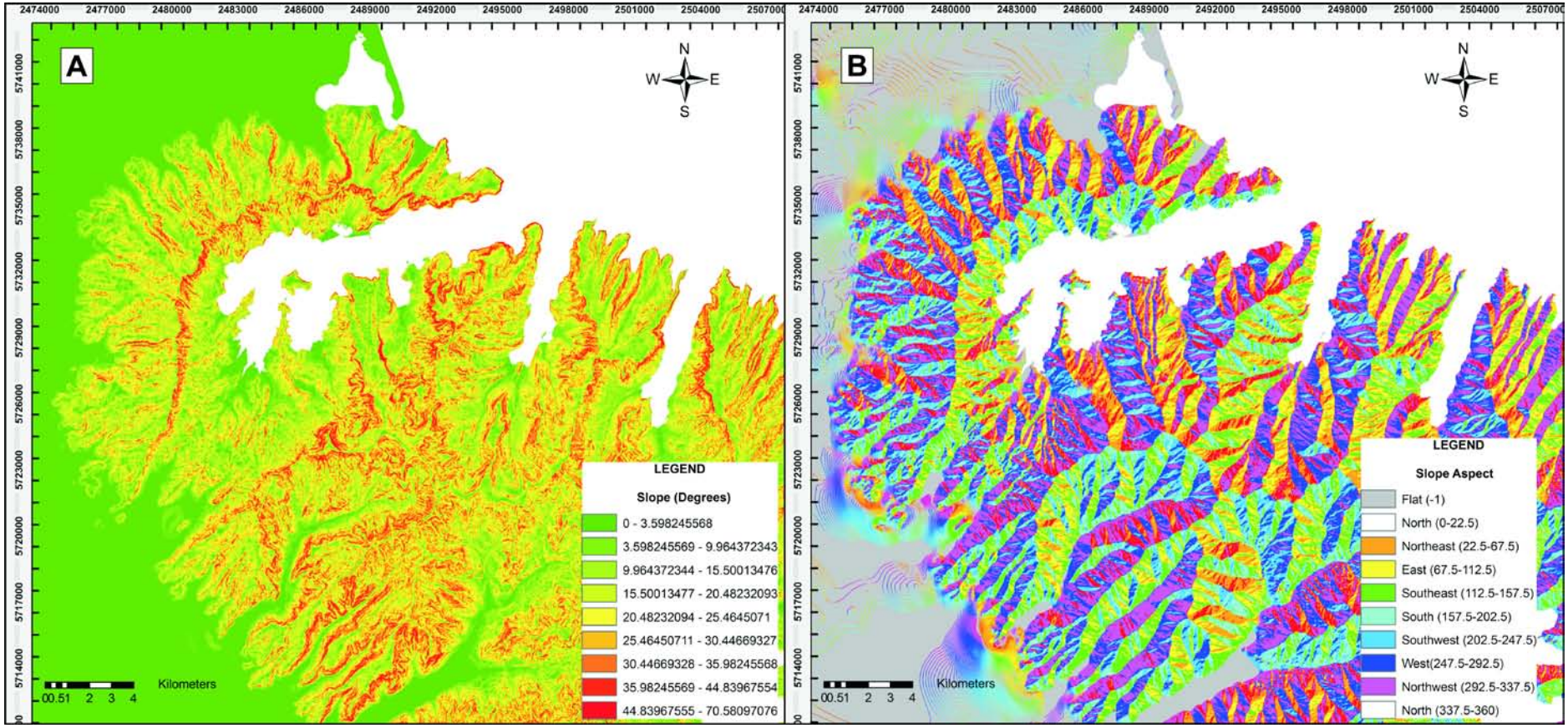

Figure 2.7. A) Slope map of western Banks Peninsula. Red colourations indicates steep slopes, primarily located around the termed "erosion caldera" (Williams, 1941) or crater rim (Shelley, 1992) of Lyttelton Volcano. **B)** Aspect map of western Banks Peninsula. Clearly visible is the somewhat radial valleys of the western Port Hills, and the highly variable central regions of Banks Peninsula, primarily related to Mt Herbert Volcanic Group Volcanism, post Lyttelton Volcano.

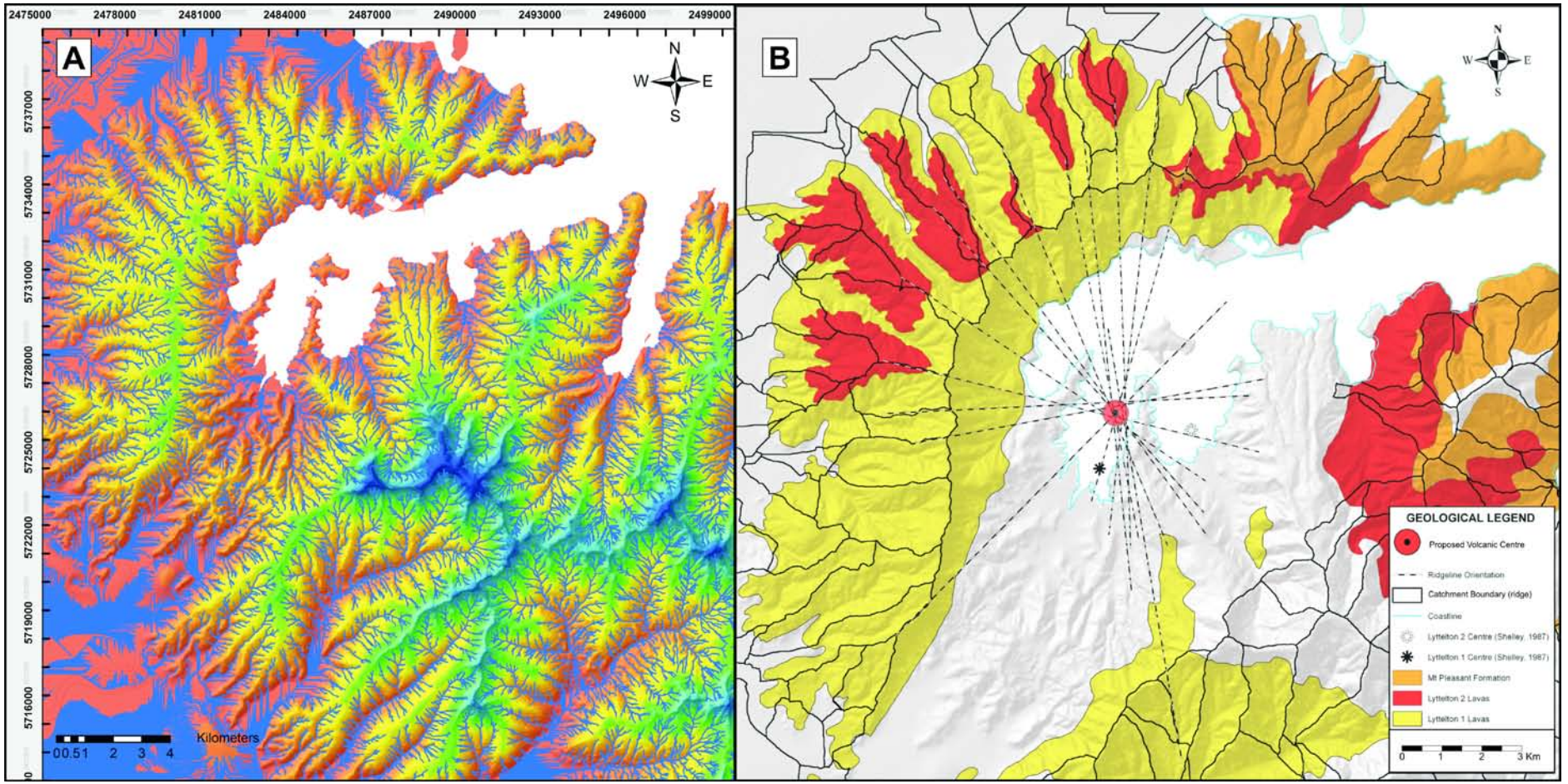

Figure 2.8. A) Drainage network analysis of western Banks Peninsula. A radial drainage pattern is evident on the western Port Hills, while more random dendritic drainage is expressed in central Banks Peninsula. The relatively younger drainage of the Diamond Harbour dip-slope is clearly observable extending into the harbour. **B)** Catchment analysis boundaries of western Banks Peninsula, marked in black. Colourations depict geological contacts, the three stages of Lyttelton's volcanism, as reviewed by Neumayr (1998). A simplistic ridgeline orientation analysis is displayed, identifying the centre of volcanism. The identified centre is north of Shelley's (1987) eruptive centre of Lyttelton 1 and is close proximity to Neumayr's (1998) eruptive centre location for Lyttelton 1 Volcano.

Interpretation and Classification

Interpretation and classification is intrinsically related and is combined in this next phase of analysis of Lyttelton Volcano. Based on interpretation there are two regions of pronounced erosion on western Banks Peninsula, Lyttelton Harbour and Gebbies Pass, indicated by significant depressions and steep bounding slopes (Figure 2.7A and B). Aspect models (Figure 2.7B) and drainage networks (Figure 2.8A) indicate a somewhat radial drainage network in the western side of Lyttelton Volcano (Port Hills). The interior regions of Banks Peninsula have a complex slope and drainage network, related to Mt Herbert Volcanism, an aspect beyond the scope of this initial investigation. This phases of volcanism infilled a depression on the south-east side of Lyttelton Harbour (Sewell, 1985; Sewell et al., 1992), producing the now highest point in Banks Peninsula, Mt Herbert, highlighted by a plateau surrounded by steep dips (Figure 2.7A). The youngest volcanism (Diamond Harbour Volcanic Group) is clearly evident in all images (Figure 2.7 and 2.8), with the younger drainage pattern (Figure 2.8A) indicating erosion incised this surface directed towards Lyttelton Harbour.

Classification of western Banks Peninsula follows the identification of sectors (Figure 2.9). In this study sectors have been defined through slope and aspect distribution maps, DEM's and perspective views and surface texture (i.e. slope, aspect, drainage and watershed), and more importantly the geological context (i.e. type of rock unit as defined from existing published geological maps (Sewell., 1985; Sewell et al., 1992., Neumayr;, 1998).

On Lyttelton Volcano five distinct sectors are recognised (Figure 2.9): Sector 1, areas of unmodified Lyttelton 1 and Lyttelton 2 Volcanics, unmodified, relates to these areas having not undergone significant morphological changes due to proceeding phases of volcanism, or significant erosion (excluding interior harbour regions); Sector 2, areas of modified Lyttelton 1 and Lyttelton 2 volcanism, primarily overlain by subsequent volcanism or highly disturbed by erosion; Sector 3, Mt Pleasant Formation, late stage volcanism of Lyttelton Volcano, relatively unmodified surfaces; Sector 4 Post Lyttelton Volcano eruptives, encompassing Mt Herbert Volcanic Group, Akaroa Volcanic Group, and Diamond Harbour Volcanic Group activity; Sector 5, exposed basement lithologies,

deposited prior to Lyttelton Volcano, sector indicates pronounced erosion in these areas, stripping off volcanic cover.

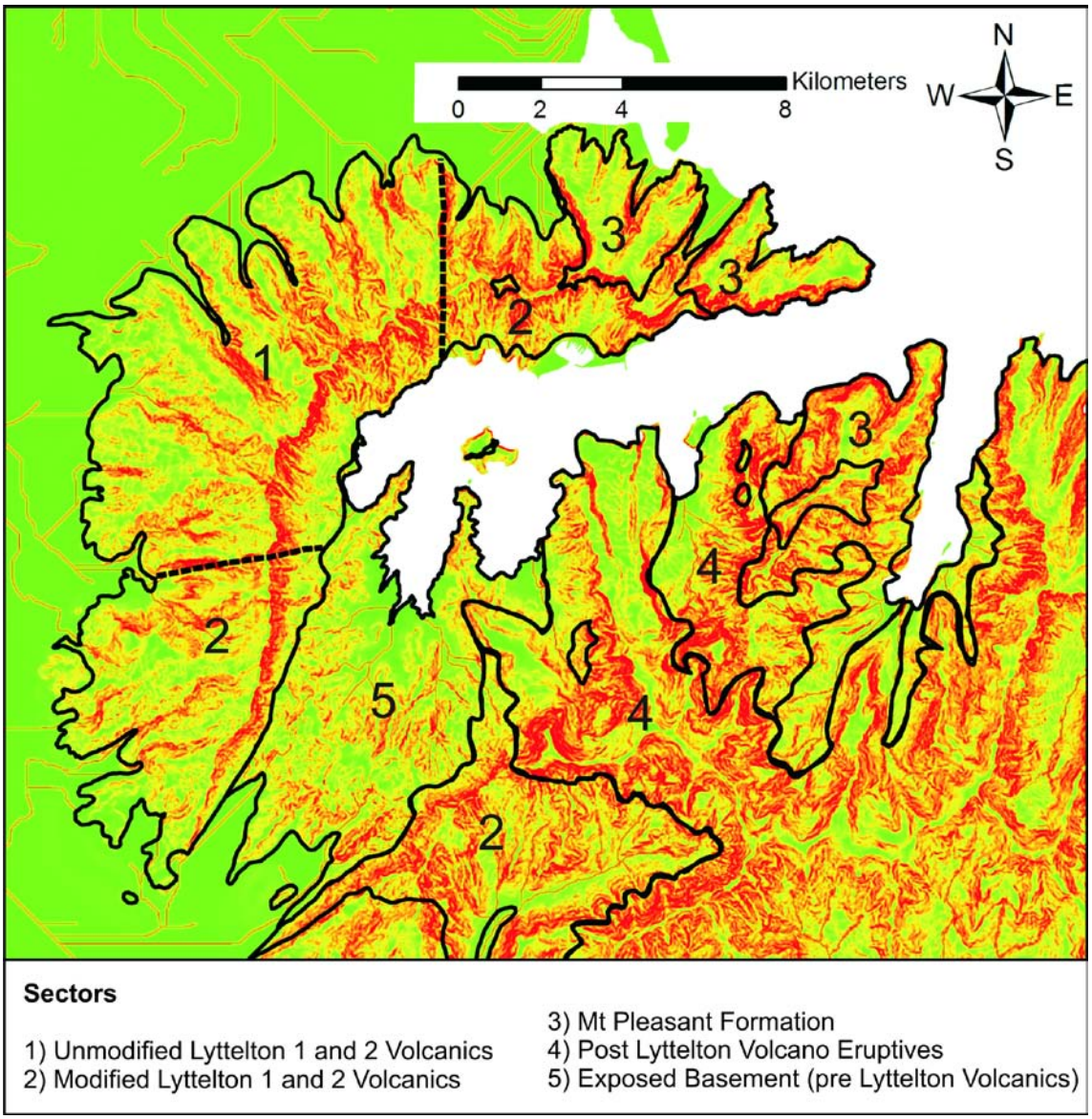

Figure 2.9. Morphometric sectors of Lyttelton Volcano identified through slope and aspect distribution maps, DEM's and perspective views and surface texture, and geological context. The term unmodified is used to indicate surfaces where limited covering of subsequent volcanism occurred as well as limited erosion, excluding the inner harbour regions. Details of each sector are discussed in text.

PCT Map

As outlined earlier creation of a PCT map is obtained through the transformation of DEM data through the use of an Avenue script in ArcGIS 3.2. Prior to running this script three input criteria's need to be establish, centre of volcanism, volcano's radius (radial distance) and the number of divisions required (relating to the overall resolution).

The centre of volcanism for the point of rotation selected in the creation of the PCT map is based on a simplistic analysis of Lyttelton Volcano's ridge system (Figure 2.8B). A simplistic ridge analysis was performed through catchment / drainage analysis, with lines between catchments indicating ridges. Ridge analysis then identifies the straightest ridgelines in western Banks Peninsula, in areas relatively unmodified from subsequent erosion or volcanism. These trends are projected towards the harbour, source of volcanism, resulting in the identification of the proposed centre for PCT map transformation (Figure 2.8B). The resulting centre location is north of Shelley's (1987) Lyttelton 1, yet similar in position to Neumayr's (1998) revised centre for Lyttelton 1 Volcano.

The radial distance is calculated as 12000m, based on the point of rotation and the extent of sub-aerial volcanic deposits. A 100m resolution PCT map was hypothesised as the final output, the resulting division required was 120 divisions, over the 12000m radius, giving the 100m resolution required.

The PCT map of Lyttelton Volcano was produced in conjunction with Balazs Szèkely (Institut fur Geowissenschaften, Univesitat Tubingen, Germany) and David Karàtson (Space Research Group, Department of Geophysics, Eotvos University, Budapest, Hungary). The proposed eruptive centre was used as the point of rotation for PCT map construction using a 10m resolution. The Avenue polarization script was run at Canterbury University, with the data, in spreadsheet form being transformed into a PCT map by Balazs Szèkely, analysed in Surfer.

Radial ridge and valley features from the selected point of rotation should result in perpendicular lineation's parallel to each other on the PCT map (Szèkely and Karàtson, 2004). In examination of the PCT map no clear parallel features are recognisable. On the Port Hills section an almost radial arrangement of valley systems is evident, however these do not parallel each other or intersect the crater rim at right angles. The resulting conclusion is that the western sector / Port Hills of Lyttelton Volcano are not radial about an eruptive centre at the Head of the Bay, Lyttelton Harbour. It is also acknowledged here that Shelley's (1987) model also reflected on the development of

the circular crater rim of Lyttelton Volcano as the resulting feature produced from Lyttelton 2. With that being said it was hypothesised by Shelley (1987; 1989) that due to the underlying structure of Lyttelton 1 the resulting erosional features of Lyttelton 2 (ridge and valleys) in the north-western and western Port Hills (Figure 1.2) orient to a Lyttelton 1 centre.

In examination of the crater rim in the PCT map (Figure 2.10), an idealised straight line as that of the Mt St Helens (Figure 2.5) example is not produced. What is evident is an arcuate crater rim line, constant at oblique angles to the proposed centre. This could relate to extensive erosion since volcanism ceased, the point of rotation not being at the correct concentric point, or that the circular crater rim feature is more complex than that of a simplistic volcanic cone.

Initial usage and construction of the PCT map was to highlight and examine the proposed collapse regions of Lyttelton Volcano. Within this, the PCT map does display the three sectors of Lyttelton Volcano, hypothesised to have formed through collapse (Sewell, 1985). In comparison to the sharp near-parallel sides of the Mt St Helens collapse scarp (Figure 2.5), no such features are apparent, with the proposed collapse regions broadening not narrowing, as they ascend towards the hypothesised eruptive centre.

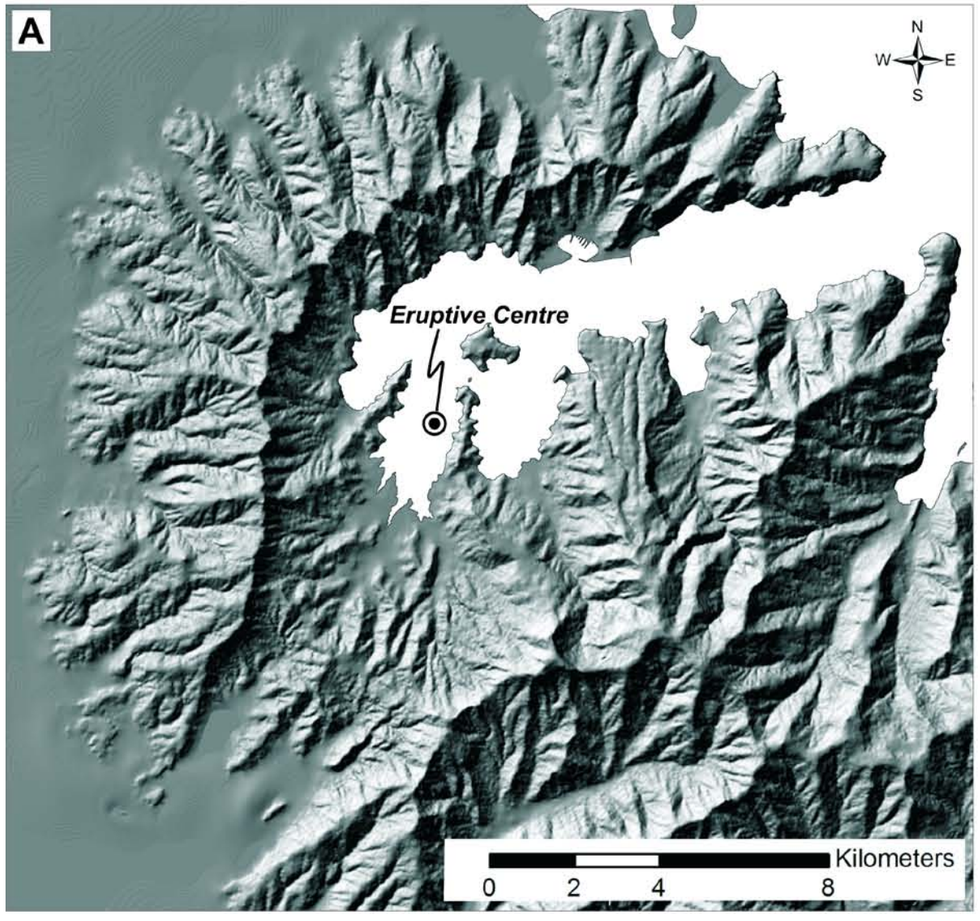

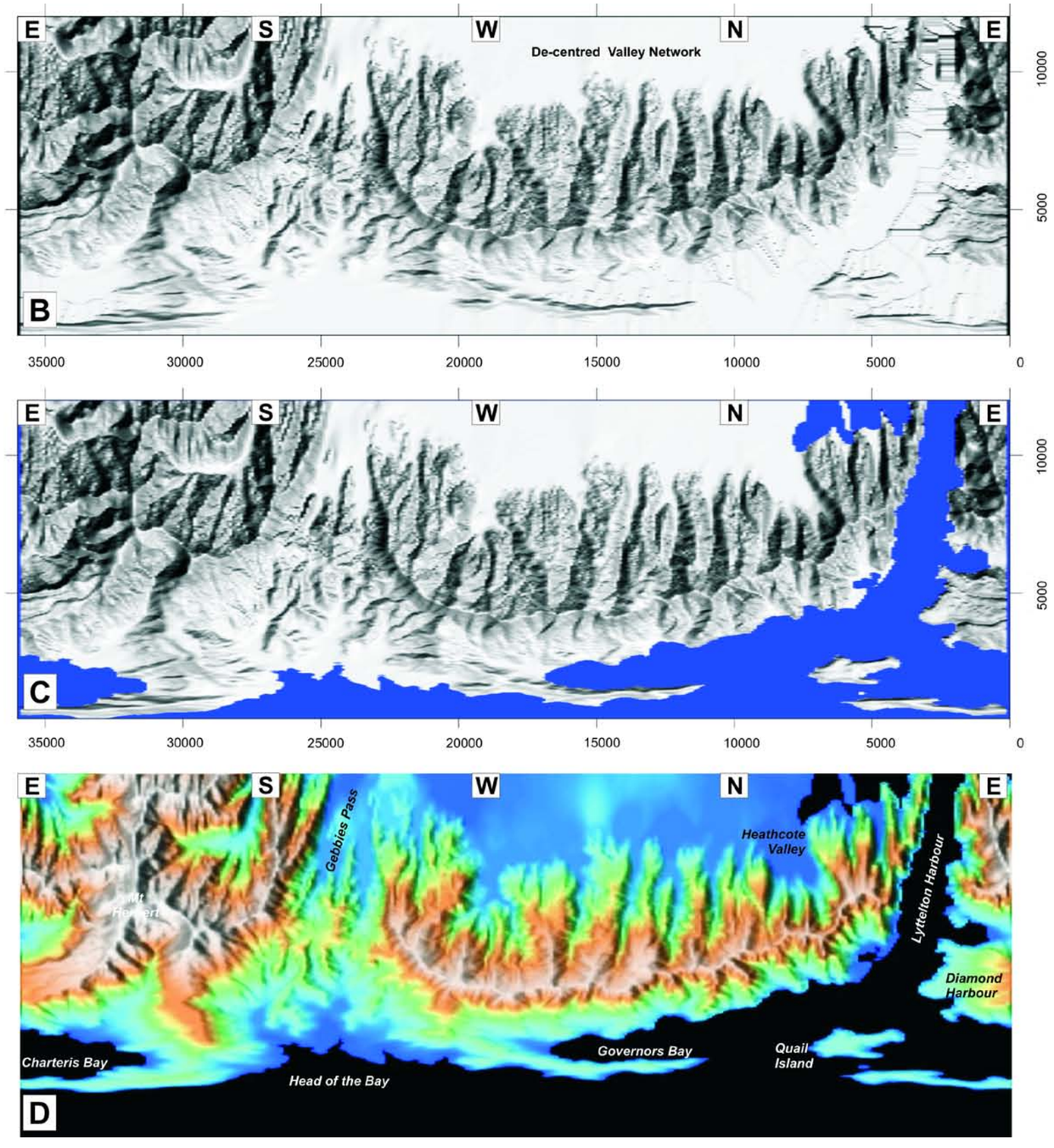

Figure 2.10. PCT map of Lyttelton Volcano. A) DEM displaying the previously identified eruptive centre, used as the point of rotation in production of the PCT map. B) Initial PCT map, with the de-centred radial valley of north-western Port Hills highlighted, note that the point of rotation (eruptive centre) is the base the PCT maps. C) Infilled harbour, estuary and bay areas, with key topographical points labelled. D) Topographic height raster image produced in surfer, of note is the white crater rim of the Port Hills being oblique to the point of projection

2.3. Volcanic Degradation

Volcanic degradation occurs, pre, syn or post-eruptively, an aspect acknowledge within facies analysis of volcano successions (Nemeth and Martin, 2007). Strato-volcanoes are comprised of primary volcanic deposits (i.e. lava flows, domes, pyroclastic deposits) and secondary epiclastic deposits (i.e. debris avalanche deposits, debris flow deposits). A ring plain or volcaniclastic apron forms around a strato-volcano through the accumulation of both primary volcanic and secondary epiclastic deposits (Neall, 1975; Mathisen and McPherson, 1991; Palmer and Neall, 1991; Schmincke, 2004; Karatson and Martin, 2007), with the redistribution of primary volcanic materials taking place immediately after or during the course of an eruption, when volcanic processes rapidly initiate secondary volcanic deposits (i.e. lahars, debris avalanche; Smith and Lowe, 1991; Nemeth and Martin, 2007). An example of this is the syn-eruption and remobilisation of pyroclastic material, and the reworking of this material during inter-eruptive periods forming secondary epiclastic deposits (Figure 2.11; Smith and Lowe, 1991).

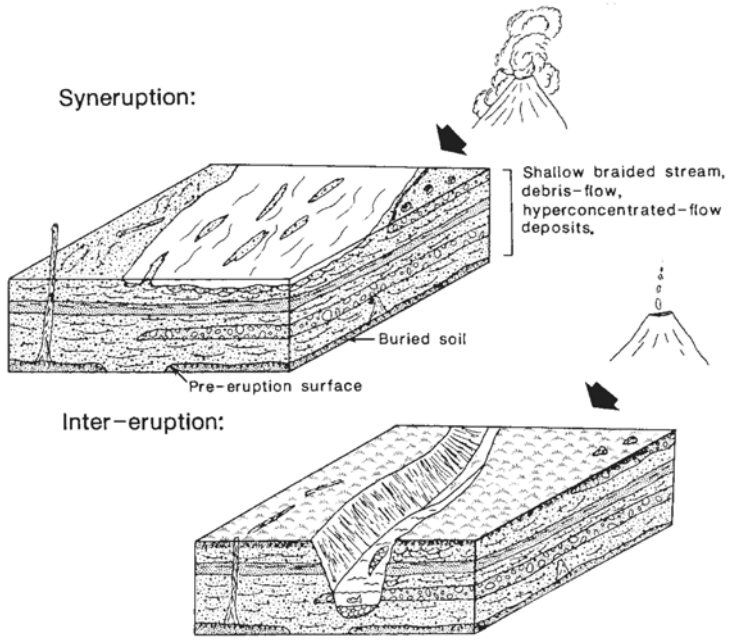

Figure 2.11. Syn-eruptive and inter-eruptive sedimentary facies on the flanks of a strato-volcano, as depicted by Smith and Lowe (1991)

2.3.1. Volcanic Facies

Volcanic degradation is best discussed in terms of volcanic facies analysis. Facies, either sedimentary or volcanic is defined as "a mapable rock unit that has common textural, compositional, and internal structural features indicative for a well defined source, transportation and depositional mechanism" (Nemeth and Martin, 2007). As strato-volcanoes commonly have complex evolutions (i.e. Ruapehu; Palmer and Neall, 1991) a facies approach is readily applied (Hackett and Houghton, 1989; Mathisen and McPherson, 1991; Palmer and Neall, 1991; Cronin et al., 1996). A common approach in both non-volcanic and volcanic settings is the division of facies into distal, medial and proximal (Vessel and Davies, 1981; Wright et al., 1981). Hackett and Houghton (1989; Table 2.1.), Riggs and Busby-Spera (1990), and Mathisen and McPherson (1991; Figure 2.12) further developed this concept of volcanic facies incorporating vent facies (central, flank and satellite).

Association	Principal Lithofacies	Minor Lithofacies	Other Notable Features
Central and flank vent	Irregular lava domes and plug like intrusions -- welded fall deposits – vent breccias	Thin lavas -- lahar deposits	Tectonically over-steepened dips -- alteration
Proximal cone-building	Massive and auto-brecciated lava flows -- lahar deposits	Fall tephra-reworked sediments -- dikes -- block and ash flow deposits	Complex gully-filling morphology -- numerous apparent stratigraphic inversions
Distal ring plain	Hyper-concentrated and normal stream deposits -- lahar deposits -- fall deposits	Debris avalanche deposits -- lava flows -- loess	Fall deposits strongly wind influenced
Satellite vent	Strombolian bomb beds -- phreatomagmatic surge and fall deposits -- aa lava flows	Reworked sediments -- distal fall deposits from composite volcano	Relatively primitive chemical composition

Table 2.1. Facies association for Ruapehu Volcano (Hackett and Houghton, 1989).

2.3.2. Degradational Deposits / Features

Volcanic degradation processes include catastrophic collapse resulting in debris avalanche formation to low energy stream flow. This continuum of processes is best reviewed in Coussot and Meunier (1996) classification of mass movements on steep slopes (Figure 2.13), which can easily be applied to the volcanic facies environments.

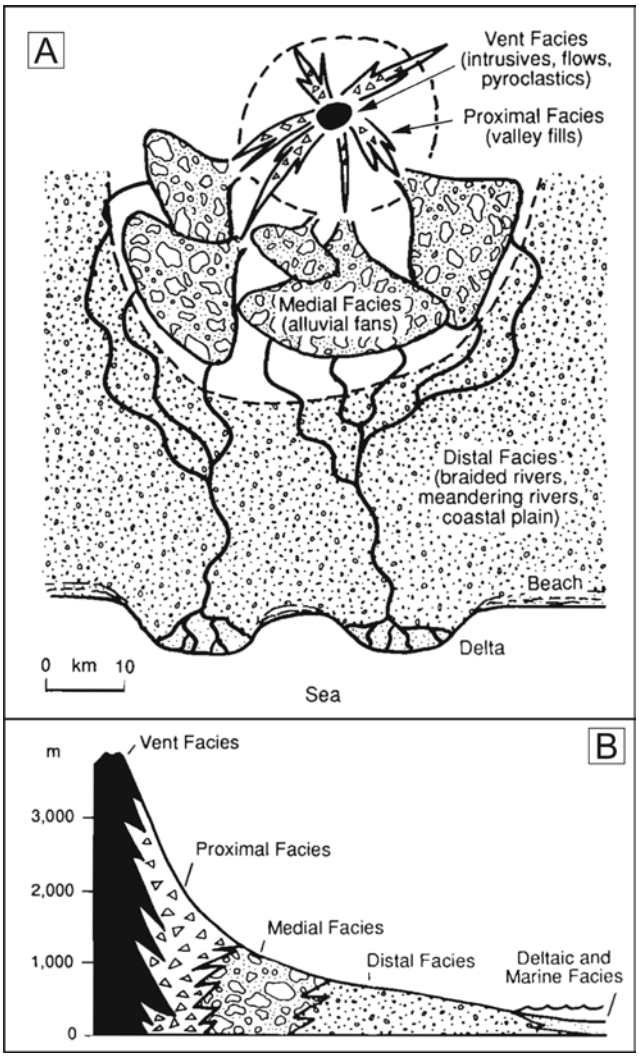

Figure 2.12. Volcanic facies environments of Mathisen and McPherson (1991) (after Vessel and Davies, 1981).

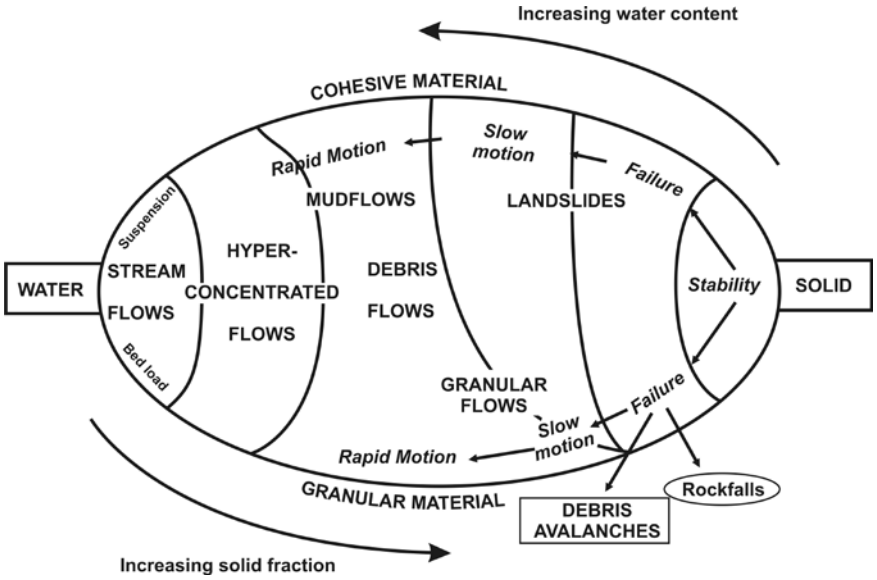

Figure 2.13. Classification of mass movements on steep slopes as a function of solid fraction and material type (Coussot and Meuinier, 1996).

Volcanic Collapse / Debris Avalanches

Catastrophic volcanic collapse results from destabilisation of an edifice resulting in large scale destruction of the upper summit region (Figure 2.14). Collapse can be triggered by explosive eruptions (Ponomareva et al., 1998), intrusion of new magma (Elsworth and Voight, 1996; Voight and Elsworth, 1997), earthquakes (Voight and Elsworth, 1997), volcanic spreading (Borgia et al., 1992; Van Wjk de Vries and Francis, 1997) or magma chamber inflation (Lo Giudice and Rasa, 1992).

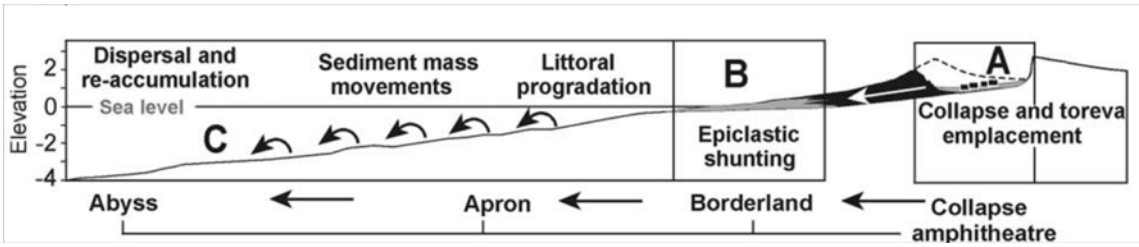

Figure 2.14. Roa (2003) sediment transfer model of the the Bejenado debris avalanche, sourced from the Cumbre Nueva embayment on La Palma, Canary Islands. Section A is typified by collapse features (hummocks and lateral levees) and toreva blocks, confined in a proto-canyon. Section B is area of debris avalanche and volcaniclastic fan above sea level. Section C represents the remobilisation of debris avalanche derived and volcaniclastic fan material.

Volcanic collapse commonly form near-parallel-sided, amphitheatre-like depressions, opening downslope. Depressions are typically surrounded, or partly bounded, by steep cliffs which may be in excess of a kilometre in height (McGuire, 1996; Tibaldi, 1996; 2001). Volcanic collapse generate debris avalanches, of which there are three main types (Ui et al., 2000):

1) Bezymianny-type volcanic debris avalanche – blast induced collapse (Mt Bezymianny, Russia; Belousov, 1996);
2) Bandai-type volcanic debris avalanche – major phreatic eruption induced collapse (Bandai volcano, Japan; Yamamoto et al., 1999);
3) Unzen-type volcanic debris avalanche – earthquake induced parasitic dome destabilisation (Mt Unzen, Japan; Ui et al., 2000).

Material in a sector collapse (2.13) is transported as debris avalanches, debris flows or epiclastic deposits (Figure 2.14, forming features, such as toreva blocks, hummocky surfaces and marginal levees (Figure 2.15; Ui et al., 2000).

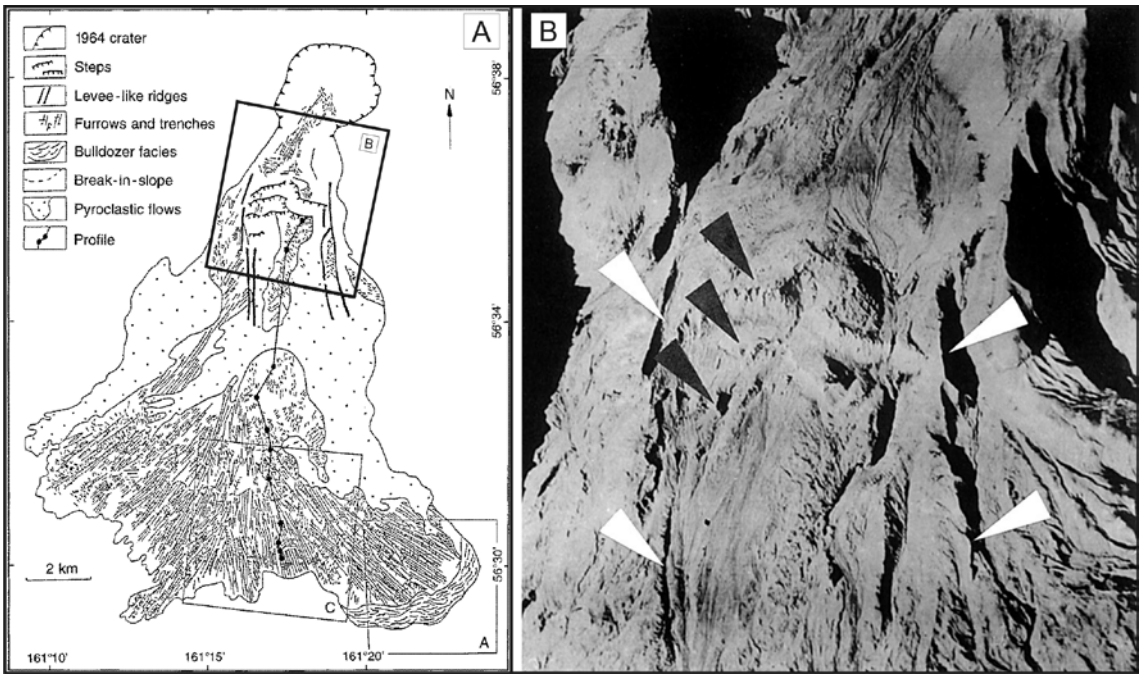

Figure 2.15. Belousov et al., (1999) geomorphic mapping of debris avalanche deposits on the southern flank of Shiveluch volcano, Kamchatka, Russia. A) Key features highlighted of the 1964 collapse of the crater, the levee-like ridges, furrows and trenches in the upper collapse amphitheatre, extending down-slope into terrain dominated by levee like ridges and hummocks. The distal reaches of the avalanche is marked by what is termed bulldoze facies. B) Aerial photograph of the region marked B in A, the crater regions is further beyond the top of the photograph. Black arrows highlight three steps (depicted in A), whereas the white arrows mark longitudinal levee-like ridges

The morphology of volcanic debris avalanches commonly exhibit hummocky morphology (Figure 2.15; i.e. Shiveluch volcano, Kamchatka, Russia; Belousov et al., 1999). Hummocky topography, in the medial to distal reaches, are the result of transport of megaclasts (Ponomareva et al., 1998; Clavero et al., 2002), with hummocks being larger and more closely spaced in proximal areas of deposition (Nemeth and Martin, 2007). Hummocks reach tens of metres across, with interior of blocks exhibiting jigsaw-fit cracks (Figure 2.16), progressively opening with debris avalanche distances, incorporating matrix into these cracks (Nemeth and Martin, 2007).

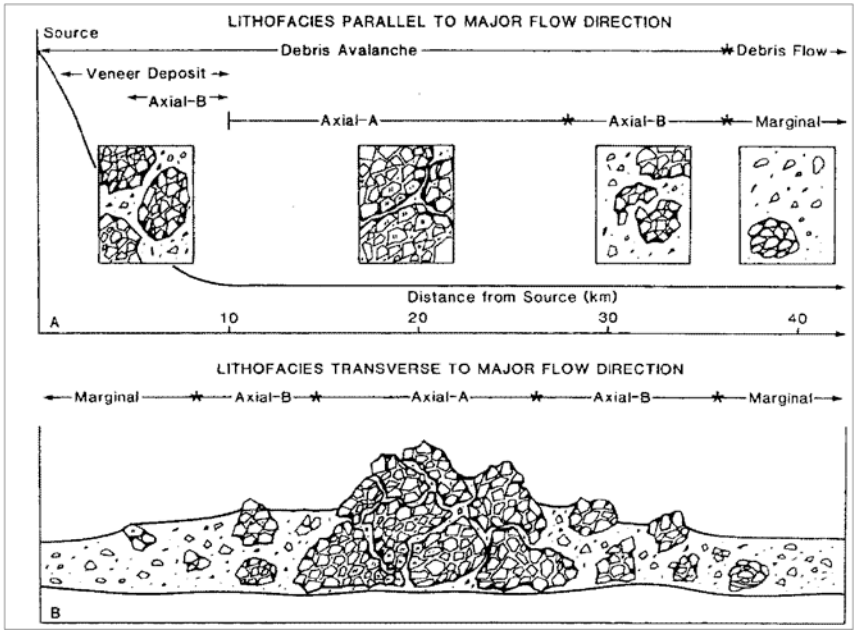

Figure 2.16. Lithofacies associated with debris avalanche deposits grading away from source to debris flow, note the massive internal structures (from Palmer et al., 1991).

Toreva blocks (Figure 2.14) are gigantic blocks of the volcano that slid towards the mouth of the amphitheatre during the collapse event, commonly having intact, rotated original stratigraphy of the collapse volcano (Wadge et al., 1995). In the Sacompa collapse in Northern Chile (Wadge et al., 1995) toreva's formed a barrier between the amphitheatre and the rest of the debris avalanche. Associated with collapse are levees (Figure 2.15), extending from the upper collapse amphitheatre to distal reaches of the debris avalanche

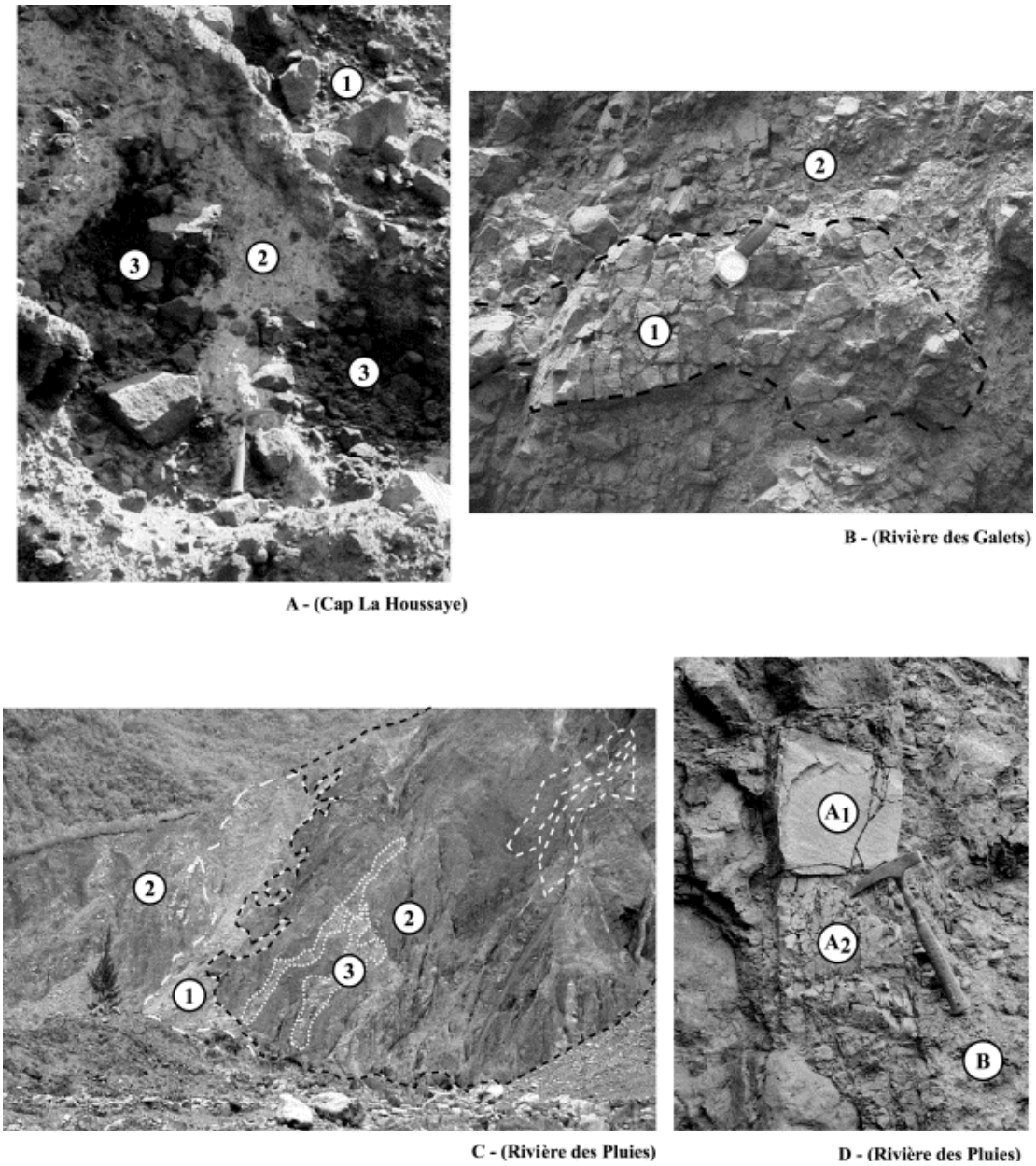

Figure 2.17. Debris avalanche deposits and block facies of Piton des Neiges Volcano (Reunion Island; Bret et al., 2003). (A) Saint-Gilles debris avalanche deposit. Legend: (1) block facies; (2) matrix facies; (3) shattered blocks. (B) A shattered block in the block facies of Rivière des Galets debris avalanche deposit. Legend: (1) shaterred block; (2) block facies. (C) 'Grand Eboulis' outcrop in Rivière des Pluies. Legend: (1) matrix; (2) megablock; (3) shattered and tilted lava flows in the megablock. (D) Typical jigsaw fractures in the block facies of Rivière des Pluies debris avalanche deposits. Legend: (A1) fractured block; (A2) typical jigsaw cracks; (B) matrix.

Debris avalanches are characterised by a block (megaclast-rich) facies and a matrix facies (Figure 2.16; 2.17; Palmer and Neall, 1991; Ui et al., 2000). Block facies are comprised blocks up to hundreds of metres in diameter and deformed pieces of the source volcano (Cacho et al., 1994; Reubi and Hernandez, 2000), displaying distinct signs of both mechanical stress and internal fracturing, forming distinctive jigsaw fit textures (Palmer et al., 1991), with some if these blocks preserving original 'in-situ'

volcanic successions (Nemeth and Martin, 2007). Matrix facies are chaotic poorly sorted mixture of fractured clasts from various sources of the volcano (Reubi and Hernandez, 2000). Continuations of topographic structures are also evident offshore within modern examples, as submarine volcanic flank channels / valleys (Gee et al., 2001; Tibaldi, 2001; Masson et al., 2002).

Lahars: Debris Flow – Stream-Flow

With runout and entrainment of surface water, volcanic debris avalanches transform into debris flows, then into hyper-concentrated flows and normal floods downstream (Figure 2.13; 2.18; Smith and Lowe, 1991; Vallance, 2000). The spectrum of volcanic mass flows (Figure 2.18), incorporating debris flows to hyper-concentrated stream flows of volcanic origin are termed lahars (Smith and Lowe, 1991; Fisher and Schmincke, 1994; Lavigne and Thouret, 2000; Vallance, 2000). Smith and Lowe (1991) proposed that the term lahar, be used to describe the process of formation and not the deposit. The type of lahar flows is dependent on the ratio of sediment to water (Figure 2.18), with a lahar current having various flow phases (i.e. debris flow, followed / accompanied by hyper-concentrated flow; Nemeth and Martin, 2007). The resulting textural characteristics of a lahar flow defines the type of flow (Table 2.2; Palmer and Neall, 1991; Nemeth and Marti, 2007) and lahar facies type (Figure 2.19; Vallance, 2000).

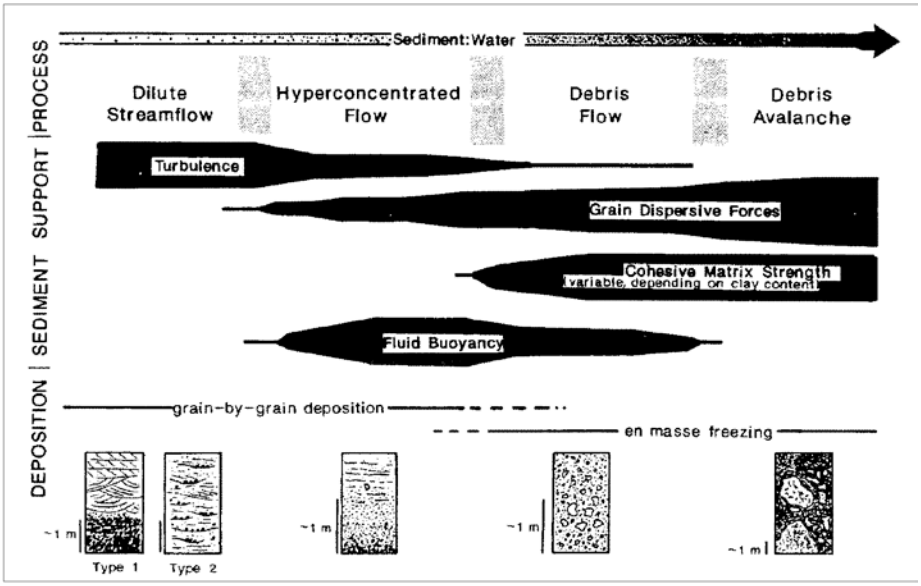

Figure 2.18. Spectrum from dilute streamflow to debris avalanche (from Smith and Lowe, 1991).

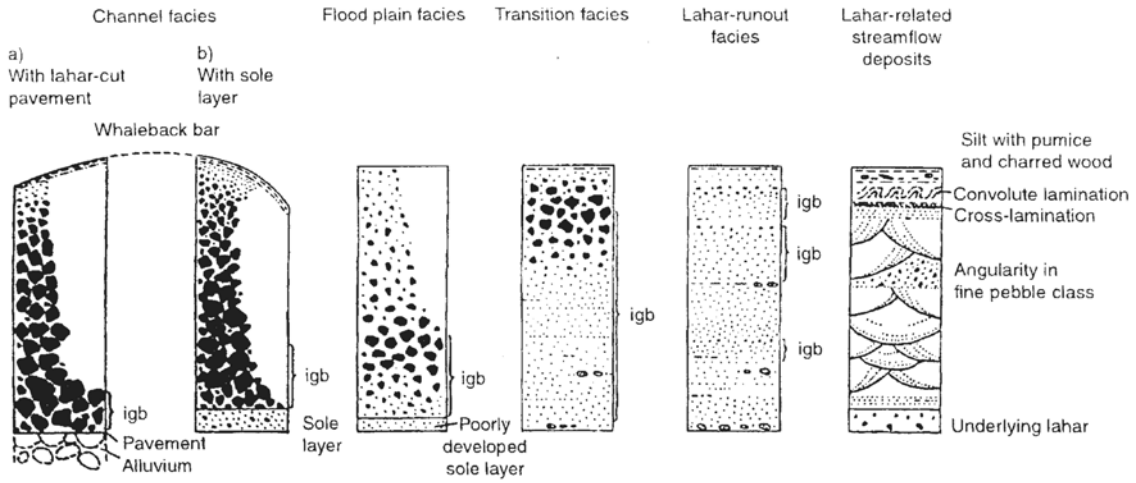

Figure 2.19. Facies types of laharic deposits (Vallance, 2000).

Lithofacies	Description	Bed Thickness	Geometry and Basal Contact	Interpretation
Dcm	Clast supported, non-graded. Thin matrix-supported, inversely graded base. Matrix, poorly sorted, fine-coarse sand + granules. Maximum clasts 0.7-3.0m.	0.2-4.3	Lenticular with scoured base or tabular with planar, non-scoured base	Debris flow
Dmm_1	Matrix supported, non-graded. Thin inversely graded base. Matrix, poorly sorted fine-coarse sand + granules. Maximum clasts 1.7-1.2m.	0.7-1.6	Tabular with non-scoured base	Debris flow
Dmm_2	Matrix supported, non-graded. Thin inversely graded base. Matrix, poorly supported fine-very coarse sandy mud. Mud is rich in allophone. Rip-up clasts of lignite, tephra, diamicton, and sand. Maximum clasts 0.1-7.0m.	0.2-17.0	Tabular with non-scoured base	Debris flow
Dmg	Matrix-supported, graded. Inverse, normal, and inverse to normal grading. Matrix, poorly sorted fine-very coarse sand + granules. Maximum clasts 0.01-0.15m.	0.1-1.5	Tabular with planar, non-scoured base or lenticular with scoured base	Debris flow
Gm	Clast-supported gravel. Non-graded or normally graded. Tightly packed cobbles and boulders. Matrix, poorly sorted, medium-coarse sand. Imbricated. Scoured base.	0.2-1.0	Tabular or lenticular	Longitudinal bars or channel lag
Sgb	Poorly bedded, moderately to poorly sorted sand. Alternating fine and coarse beds to 5cm thick of coarse sand + granules and fine-medium sand. Commonly with layers of sub- to well-rounded pumice. Occurs in sequences that fine or coarsen upward with no internal scour surfaces. Base of the intervals are planar and non-scoured.	0.4-1.2	Tabular	Hyper-concentrated flow
Spb	Well bedded, moderately to poorly sorted sand. Alternating coarse and fine layers of coarse sand + cobbles and coarse to very coarse sand. Beds are non-graded, have internal scours, and are discontinuous. Bases are scoured or on scoured.	0.2-1.5	Tabular	Deposition in broad channels
Ss	Low angle, trough cross-bedded sand draping and filling shallow scours. Sets to 0.2m thick. Moderately well to poorly sorted medium-very coarse sand and granule layers. Gravel lags, mud drapes, and well rounded pumice.	0.2-2.0	Lenticular	Scour and fill by shallow, high-discharge flow
St, Sp, Sh	Moderately to moderately well sorted, medium-coarse sand. High angle trough and planar cross beds. Sets to 3m. Horizontal laminations to 2mm. Scoured bases and convolute bedding.	0.3-0.7	Tabular or lenticular	Dunes
Sr	Moderately sorted, very fine-medium sand. Scoured bases and convolute bedding. Fines upward into silt.	0.1-0.2	Tabular	Waning flow, overbank flow
Fl, Fsc	Finely laminated very fine sand, silt and mud. Structure-less sand and mud.	0.1-0.2	Tabular or lenticular	Waning flow, overbank flow
C	Lignite, macerated organic debris and wood. Underclay and pumice stringers.	0.2-0.5	Tabular	Swamp
T	Sandy loam. Root cast and rootlets. Organic rich tops in some beds.	0.1-0.8	Tabular	Reworked tephra, paleosol

Table 2.2. Lithofacies, descriptions, deposition and flow types of Palmer and Neall (1991).

2.4. Lyttelton Volcano Analysis

The following reviews degradation products in distal to marine facies, and proximal cone-building facies, in particular reviewing aspects of catastrophic collapse / debris avalanche deposits in these environments and compares these to deposits of Lyttelton Volcano previously linked or termed to originate from catastrophic collapse.

2.4.1. Seismic Profile Analysis

Large scale volcanic debris avalanches due to volcanic collapse have been recognised on oceanic volcanoes (Figure 2.20), such as Hawaii (Carracedo et al., 1999), Canary Islands (Gee et al., 2001; Masson et al., 2002; Hurlimann et al., 2000; 2004; Perez-Torrado et al., 2006), Monserrat (Le Friant et al., 2004), Reunion (Oehler, 2008), with the offshore morphologies of these reflected in both seismic profiles (Figure 2.21) and swath bathymetry. In the analysis of submarine flanks of volcanoes, landslide blocks are recognisable as large coherent angular blocks, commonly surrounded by debris avalanche hummocky terrains (Moore et al., 1989; Moore and Chadwick, 1995; Le Friant et al., 2004; Favalli et al., 2005).

In the previous models of Lyttelton Volcano, sector collapse or catastrophic collapse is hypothesised to have occurred at least two times to the northeast flank of Lyttelton Volcano (Shelley, 1987; 1992; Neumayr, 1998), with the latter collapse resulting in the formation of Lyttelton Harbour. On Lyttelton Volcano exposure of these distal deposits is limited due to the covering of the Canterbury Plains gravels, and the Pacific Ocean surrounding much of the Peninsula. The resulting investigation revolves around analysing seismic records offshore of Lyttelton Volcano to identify features common to a distal volcanic ring plain.

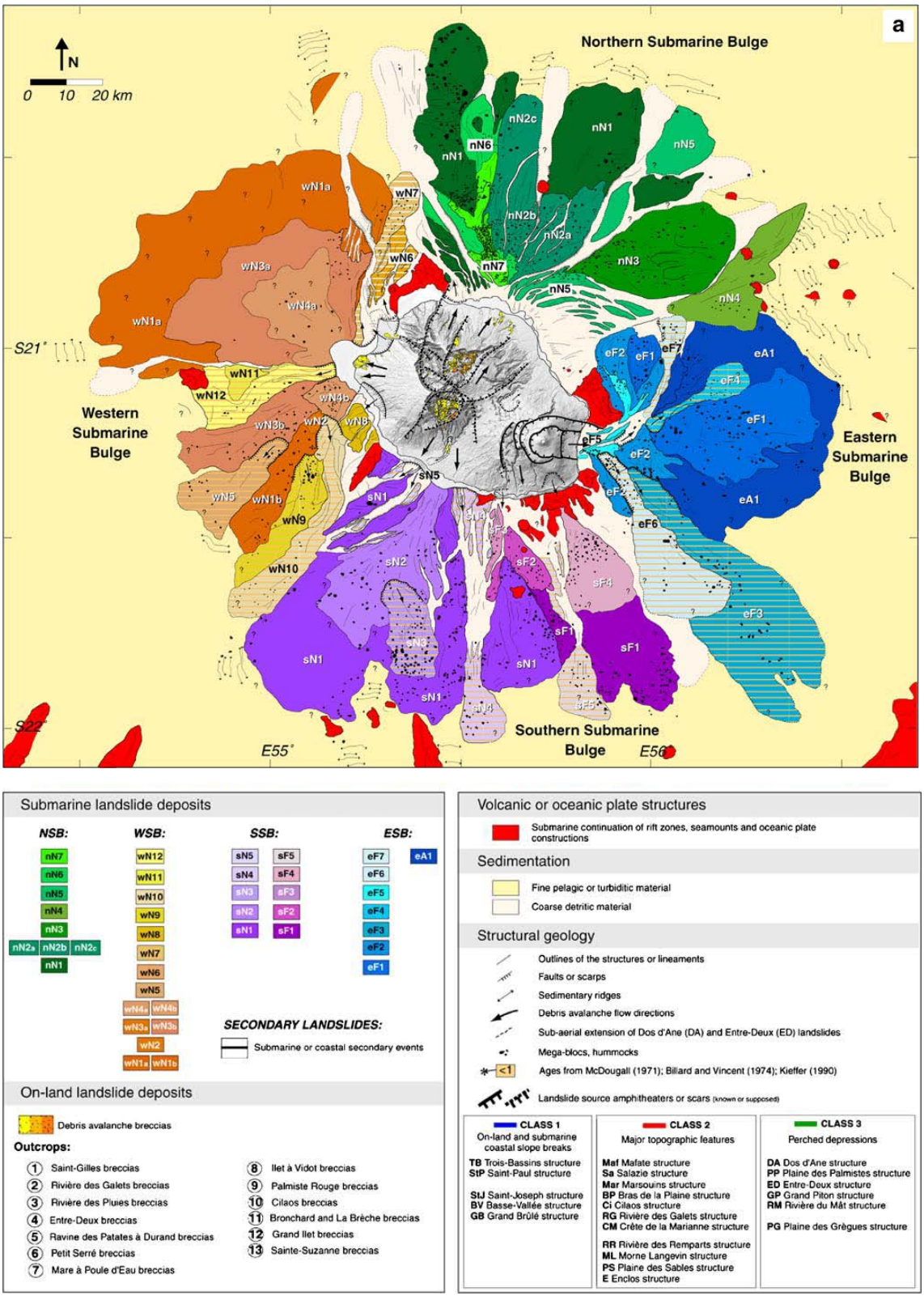

Figure 2.20. Detailed map on the subaerial and proximal submarine parts of the Reunion Volcanoes. On land, outcrops of debris avalanches and the main topographic features interpreted as the potential source zones of the landslides are overlaid on a DEM (from Oehler et al., 2008).

Limited geophysical research has been obtained for Banks Peninsula and the surrounding seafloor. Most seismic lines and interpretations were produced during the late 1960's to 1970's in pursuit of oil and gas deposits. Two seismic lines in close proximity to Lyttelton Volcano are Mobil Exploration Lines 72-6 (Figure 2.22) and 72-7 (Figure 2.23). Mobil Exploration Line 72-6 (Figure 2.22) extends from offshore Pigeon Bay towards the Waimakariri River. No large-scale debris avalanche features are depicted within this record, what is evident is the westward dipping volcanic platform and the incision of the Waimakariri River at the north-western end of the section (Figure 2.22). Mobil Exploration Line 72-7 (Figure 2.23) extends from offshore Lyttelton Harbour to the east. This seismic profile also displays the outer slope of Banks Peninsula, and the complex incised channel system to the east (Figure 2.23).

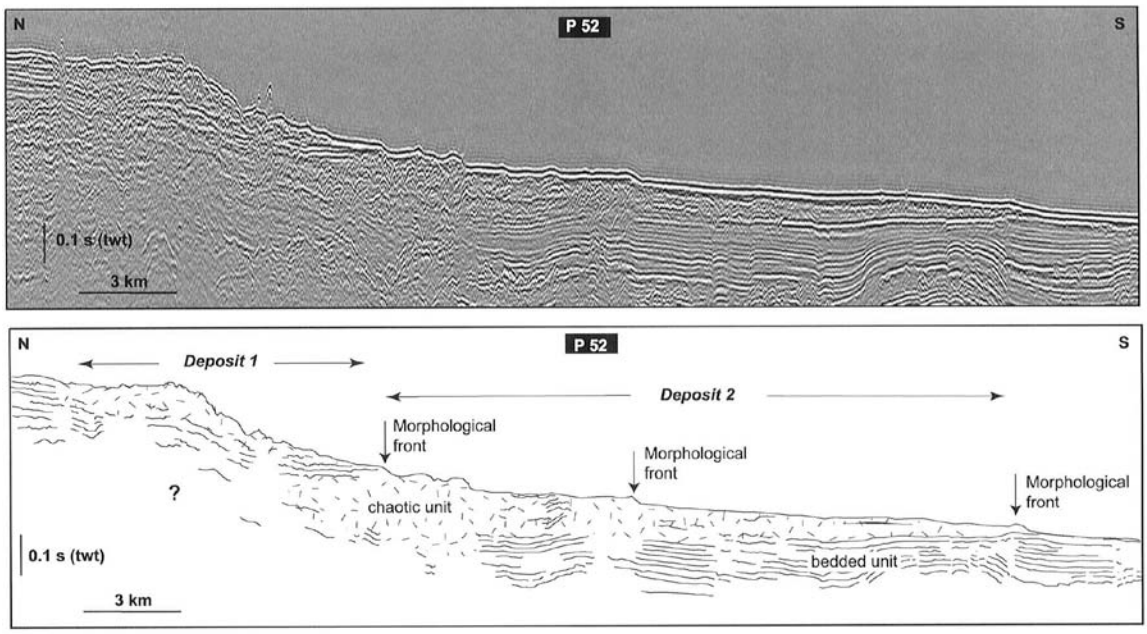

Figure 2.21. Seismic profile, Line 52 of Le Friant et al., (2004) study of Monserrat, West Indies, with interpreted section below. Deposits 1 and 2 relate to debris avalanche deposits, identified by incoherent-chaotic units, when compared to sub-horizontal, well-bedded sedimentary layers.

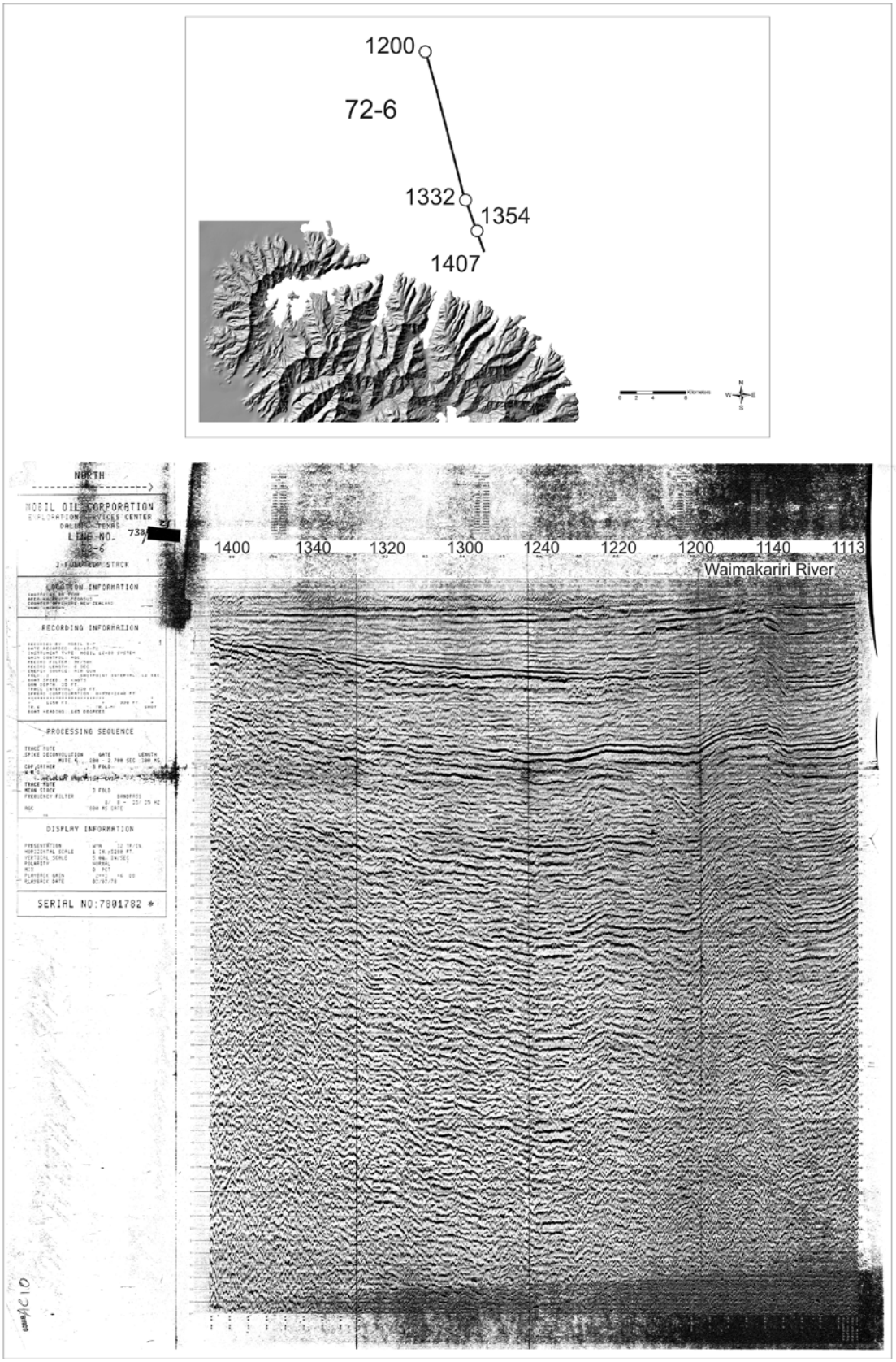

Figure 2.22. Mobil Oil Corporation seismic line MOBIL72: Line name 72-6 (http://www.crownminerals.govt.nz/cms/petroleum/technical-data). Seismic lines begins where Lyttelton sector collapse deposits should be apparent, while reflectors display a basin deepening away from the volcano's flanks. Hummocky features between shot points 1113 - 1200 are produced from the Waimakariri River outflow.

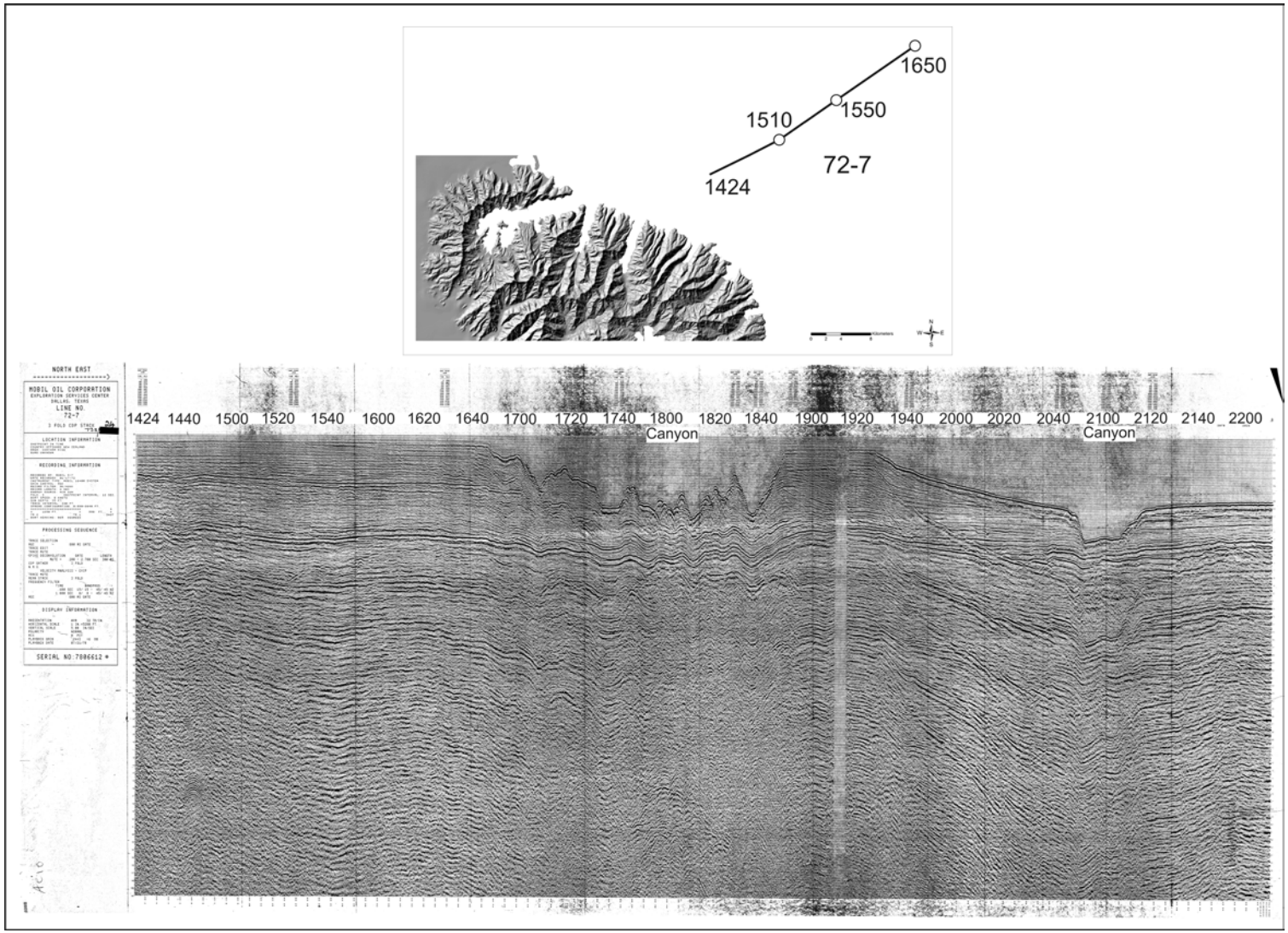

Figure 2.23. Mobil Oil Corporation seismic line MOBIL72: Line name 72-7 (http://www.crownminerals.govt.nz/cms/petroleum/technical-data). Initial shot points are off shore and in alignment with Lyttelton Harbour, the direction collapse would have propagated towards. Near parallel seismic reflectors are apparent from shot point 1424 t0 1600, where after distinct canyon features of the Pegasus Canyon predominate.

2.4.2. North-Eastern Lyttelton Volcano Epiclastic Deposits

The north-eastern sector of Lyttelton Volcano contains the most extensive epiclastic sequences deposited during Lyttelton Volcano activity. These were initially viewed as long duration erosive / degradational phases, representing hiatuses in volcanic activity (Weaver, 1980; 1985; Altaye, 1989). Shelley (1992) suggested these epiclastic deposits represented the break in activity from Lyttelton 1 to Lyttelton 2, since which time, deposits have been used to identify the horizon between Lyttelton 1 and Lyttelton 2. Various studies on Lyttelton Volcano have focused on epiclastic deposits, importantly Neumayr (1998) and Irvine (2003), each redefining the boundaries of Lyttelton 1 / Lyttelton 2, and Lyttelton 2 / Mount Pleasant Formation Flows.

Neumayr (1999) study focussed on the geochemistry of the Lyttelton 1 lava stack, with the approximate termination of this sequence at the laharic horizons between the Tors and Mt Cavendish. Irvine (2003) filled in further descriptive aspects of these epiclastic deposits, but this study was limited to a somewhat sedimentological study within stream-flow to debris-flow. Descriptions of units were reviewed and further investigated in the field, where exposures had been overlooked or unobserved this was incorporated.

This section focuses on the stratigraphic relationship, description, interpretation of flow types and paleo-flow directions and uses these to hypothesise mechanism and source of epiclastic horizons in north-eastern Lyttelton Volcano.

Location and Stratigraphy of Epiclastic Horizons

Epiclastic deposits of north-eastern Lyttelton Volcano occur in six regions (Figure 2.24), the Tors to Mt Cavendish, Sumner valley, Evans Pass, Battery Point, slopes of Cass and Rapaki Bays, and the Rapaki Track.

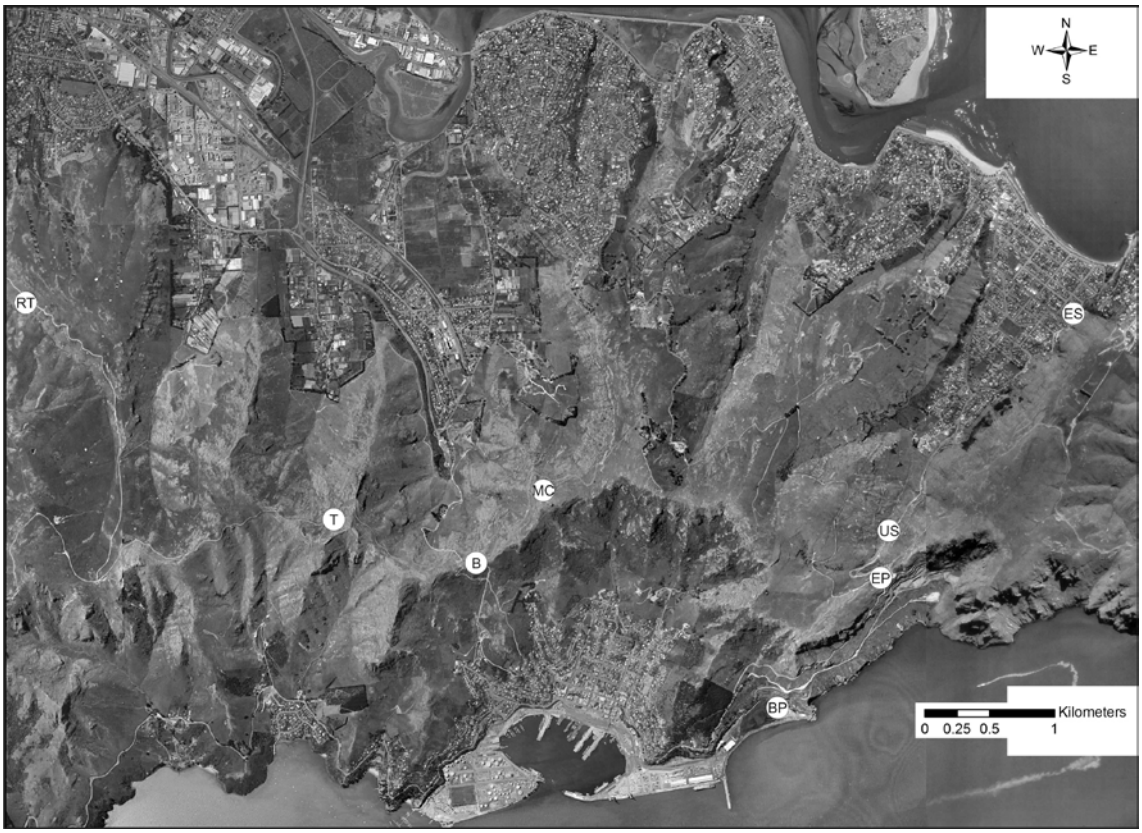

Figure 2.24. Epiclastic horizon locations of north-eastern Lyttelton Volcano. RT, Rapaki Track epiclastic deposits; T, Tors epiclastic deposits; B, Bridle Path epiclastic deposits; MC, Mt Cavendish epiclastics; BP, Battery Point epiclastic; EP, Evans Pass epiclastic; US, Upper Sumner Valley epiclastic deposits; ES, eastern Sumner epiclastic deposits. Aerial photographs are from www.linz.govt.nz.

Castle Rock to Mt Cavendish

The Tors to Mt Cavendish sections are exposed in road cuts on both Lyttelton and Heathcote sides of Mt Cavendish, and mantle the upper slopes of the spur SW of the Bridle Path. Epiclastic deposits between the Castle Rock and Mt Cavendish overlie aa to blocky lava flows, eroded scoria cones, and pyroclastic layers. Deposits are overlain by lava flows and intruded by dykes of basaltic to trachytic compositions. Lahar deposits occur in three main regions (Fig. 2.24 and 2.25); Castle Rock – Tors, Castle Rock – Bridle Path, Bridle Path – Mt Cavendish.

Castle Rock

Between Castle Rock and the back section of the Tors on the Summit Road (Figure 2.25) is a series of epiclastic deposits with thin hawaiite – mugearite lava flows interbedded with deposits (Weaver, 1980). Deposits are red-brown, massive, non-graded, medium sand to pebble matrix supported, sub-angular, polymict volcanic

conglomerate (Weaver, 1980; Irvine, 2003). The summit road cuts deposits at right angles, providing ideal cross sections of flows. Within the lahar deposits are channels, with channel bases being boulder-rich. Sections also display the variation within flows, from boulder-rich debris, to matrix-rich deposits. Clasts within these horizons are highly variable in composition, size and angularity, with larger clasts being basaltic.

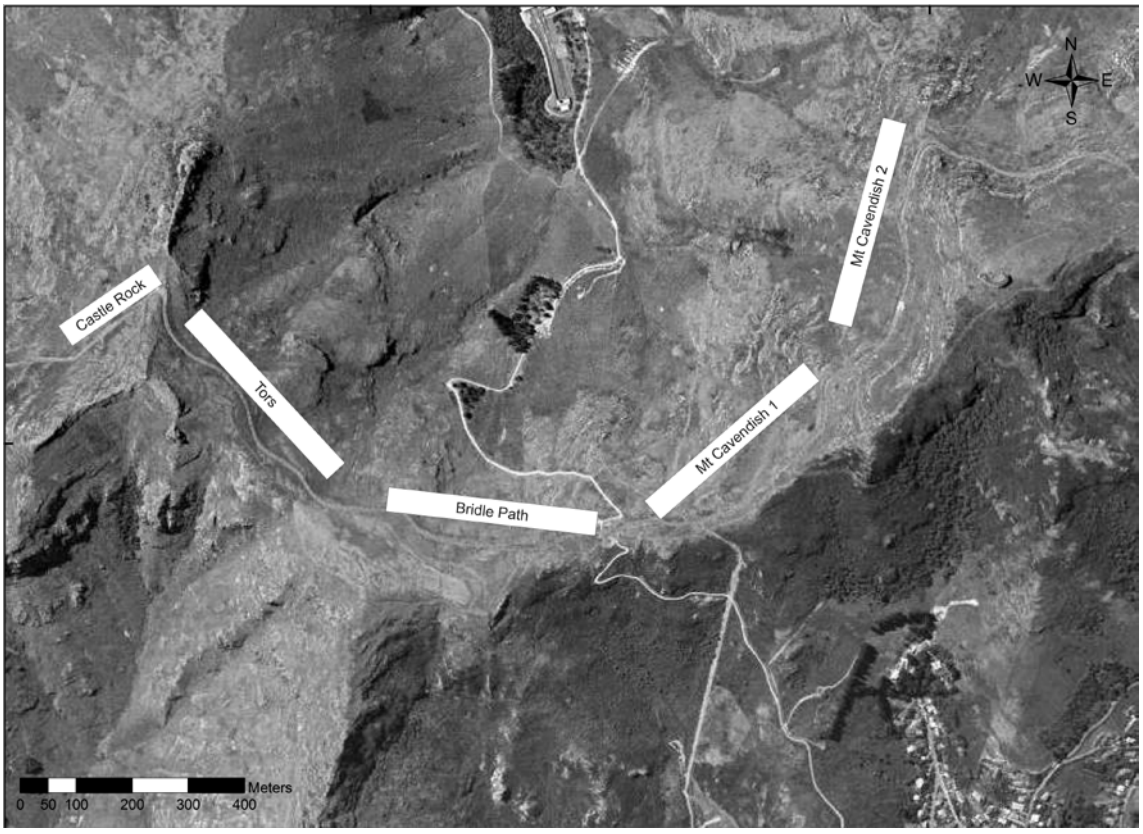

Figure 2.25. Location of epiclastic sequences between Castle Rock to Mt Cavendish. Highlighted sections are discussed in text.

Tors to Bridle Path

The Tors sequence of epiclastic deposits, exposed along, above and below the road section between the Bridle Path and Castle Rock (Tors section; Figure 2.25) is the largest on Lyttelton Volcano. This sequence is comprised of four epiclastic deposits interbedded with three or four hawaiite – mugearite flows, cut by various dykes (Figure 2.26) and sills, and capped by lava flows (Weaver, 1980, Irvine, 2003).

Deposits are predominantly matrix supported, up to 2m boulder-rich conglomerate (Figure 2.26). Clast-rich layers are often found at the base with fines-rich layers at the

top or base of layers. Clasts within the epiclastic deposits are highly variable in angularity and size with larger clasts being basaltic in composition. Epiclastic deposits to the southeast have similar characteristics, yellow – dark brown, coarsely bedded, inversely graded, fine sand to granule matrix supported, sub-rounded to rounded, polymict conglomerates, with clast concentrated zones, and very fine to coarse sand lenses (Irvine, 2003). Towards the top of the sequence epiclastic deposits become more oxidised, and is then capped by a thin horizon (<80cm) of red brown medium to coarse ash pyroclastic material.

In sections parallel to assumed flow direction, clasts align along flow lineation's (Figure 2.27), indicating a dip / flow direction away from Lyttelton Town centre. Channels in road sections are near to perpendicular to flow orientations, with basal clasts in channels being larger with crude stratification occurring above (Figure 2.27).

The basal contact of this epiclastic sequence is best exposed at the Bridle Path end. At higher levels, on the ridge facing Lyttelton township, basal boulder-rich epiclastic deposits directly overlie a highly brecciated lava flow, of either rubbly a'a or blocky rheology (Figure 2.27). On the Heathcote Valley or north facing slopes this contact is marked by Highly weathered, cream-white, fresh yellow-green, phenocryst-rich, medium-coarse ash with angular juvenile lapilli-sized fragments. Deposits are crudely layered with iron-pan surfaces. These deposits correlate with further juvenile fragmented deposits in the roadside, south of Bridle Path. These deposits consist of agglutinated spatter interbedded with medium-coarse red ash. On the Bridle Path extending into Heathcote Valley deposits consist of angular basaltic fragments in a medium-coarse, cream-white ash matrix.

Figure 2.26. Stratified epiclastic deposits of the Bridle Path sequence. A) Larger clasts are aligned with flow direction, to the southwest. Note the dyke intruding the epiclastic deposits to the left of the photo. B) Rounded basaltic clasts, in a matrix supported epiclastic horizon.

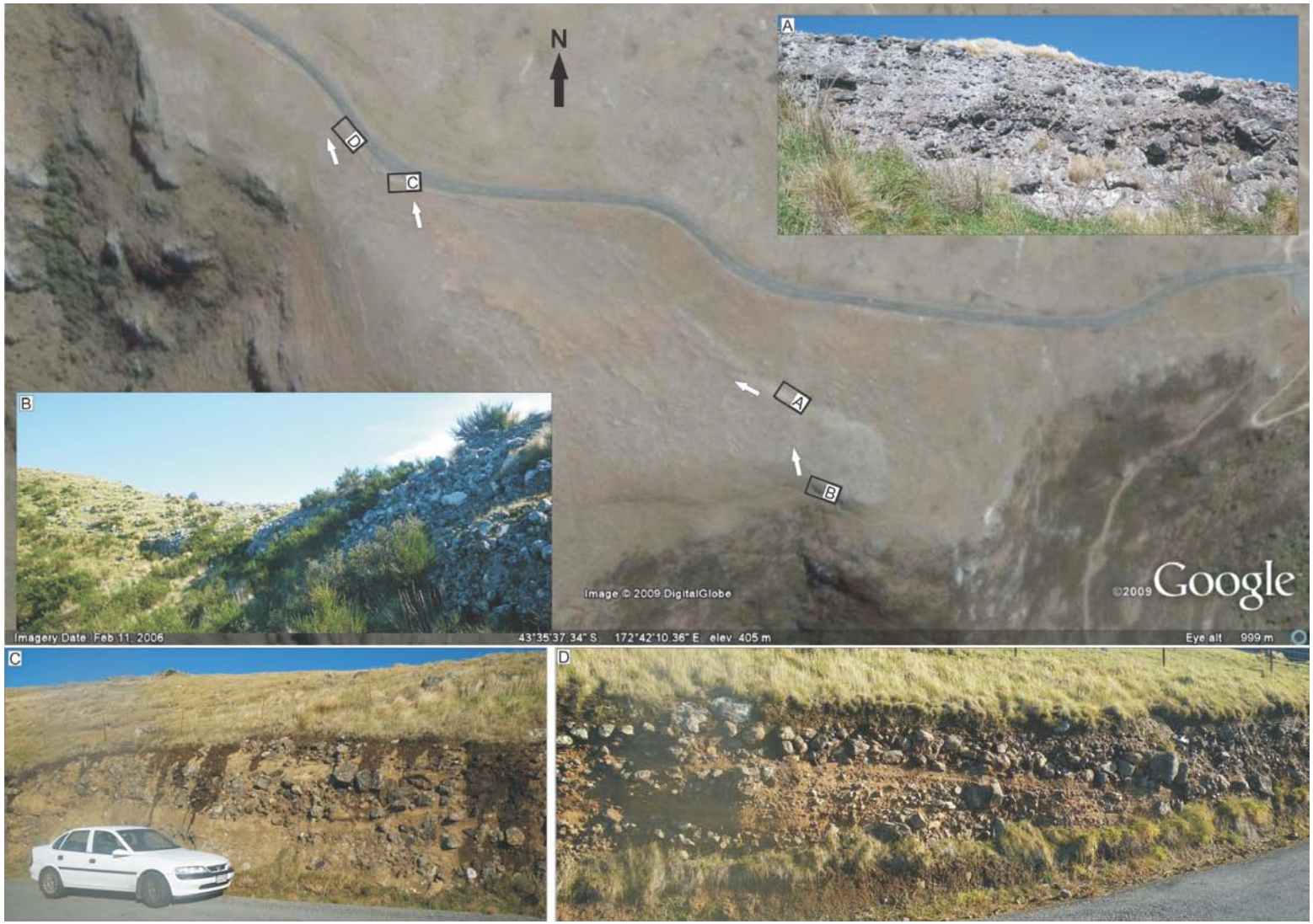

Figure 2.27. Flow direction indicators of the Tors – Bridle Path Sequence. Background figure indicate locations of figure A-D with associated white arrows in the approximate flow direction as interpreted from outcrop. A) Stratified laharic deposits dipping towards the view and to the right. B) Laharic deposits overlying a brecciated lava flow, deposits are dipping away from the viewer. C) Channelized laharic deposits, trending towards the viewer. D) Stratified laharic layers dipping to the right

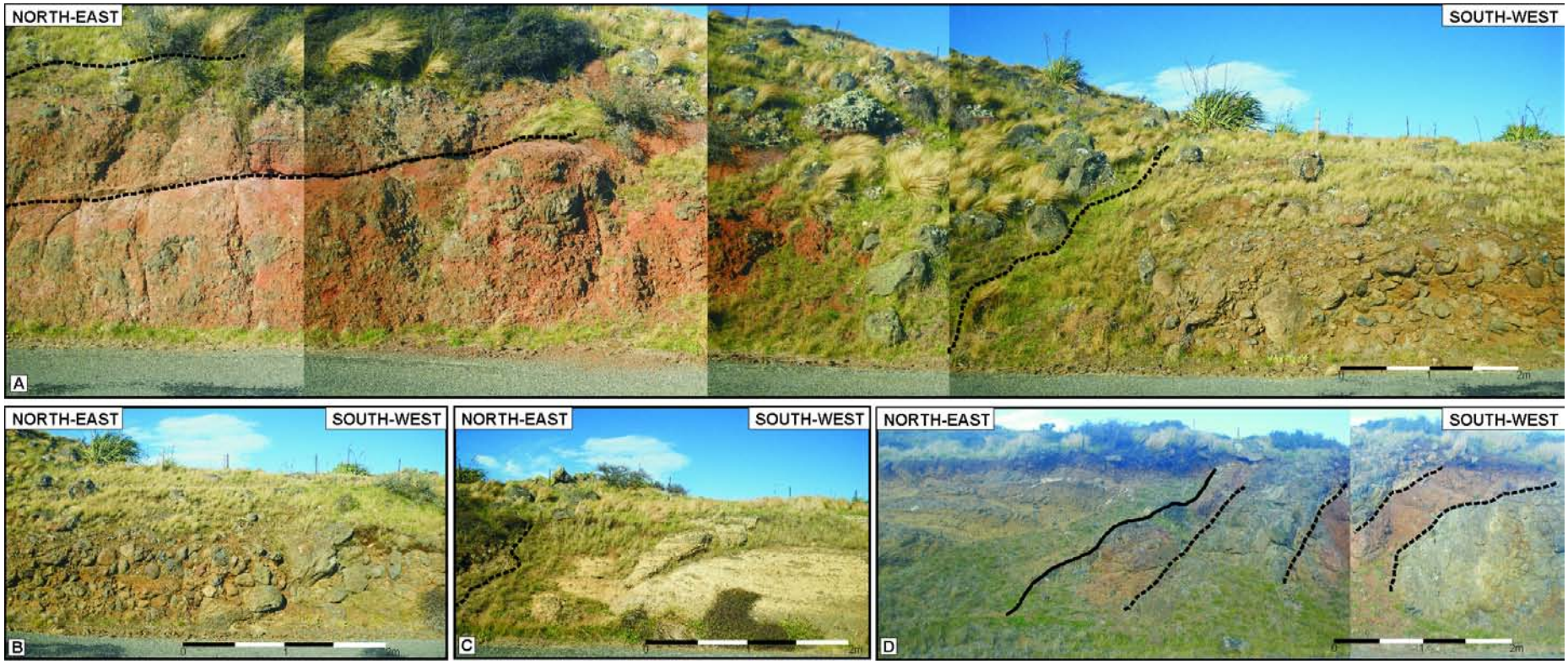

Figure 2.28. Scoria cone of the Mt Cavendish 1 sequence. A) The northern stratified welded agglutinates, red ash, scoria and basaltic fragments dip to the north-east, and have been incised by epiclastic deposits. B) Incised epiclastic deposits comprised of matrix supported conglomerate. C) Coarse ash deposits with flattened basaltic lava fragments. The north-eastern end marks the contact between ash deposits and epiclastic deposits with a matrix sourced from the incised ash. D) South-western end of the Mt Cavendish section, stratified crystal-rich ash deposits are intruded by dykes, along the margin with red pyroclastic layers.

Mt Cavendish 1

The Mt Cavendish section consist of a north-eastern side (Figure 2.25 and 2.28) consisting of pyroclastic deposits intersected by epiclastic deposits, and overlain by lava flows, while the south-western side is somewhat devoid of pyroclastic material, with a significant section being covered by slope-wash, beyond thus section are lava flows intersected by dykes. Pyroclastic deposits have four distinct units (Figure 2.28):

Cream – yellow, crystal tuff with an ash matrix. Cream – yellow, crystal tuff with coarse angular lapilli basaltic clasts, in an ash matrix (Figure 2.28D). Near flat lying, cream – yellow fine to coarse ash deposits, with flattened vesicular lava fragments (Figure 2.28C). This unit is intersected by channelized epiclastic deposits (Figure 2.28C). These poorly sorted, matrix supported, sub-rounded, polymict conglomerates (Figure 2.28B), are similar in composition to previously described epiclastic deposits of Mt Cavendish. Of importance is the incorporation of the surrounding pyroclastic material, which decreases away from the contact (Figure 2.28C). Limited coarse ash deposits are exposed to the northeast of this epiclastic unit, prior to the overlying stratified welded agglutinates, red pyroclastic, scoria and basaltic fragments (Figure 2.28A). Lava fragments increase up section, becoming increasingly more magmatic, grading into agglutinated lava flows, with a stratigraphically younger lava flow sequence continuing above.

Mt Cavendish 2

Three separate epiclastic deposits have been identified on the Summit Road below Mt Cavendish (Figure 2.25 and 2.29). The stratigraphically oldest is exposed ~30m south of the Gondola line, above the upper lava flow sequence of Mt Cavendish 1. Deposits are brown – tan, coarsely bedded, normally graded at the base, inversely graded at top, poorly indurated, poorly sorted, fine sand to granule matrix supported, sub-rounded, polymict conglomerate, with fine sand lenses (Irvine, 2003).

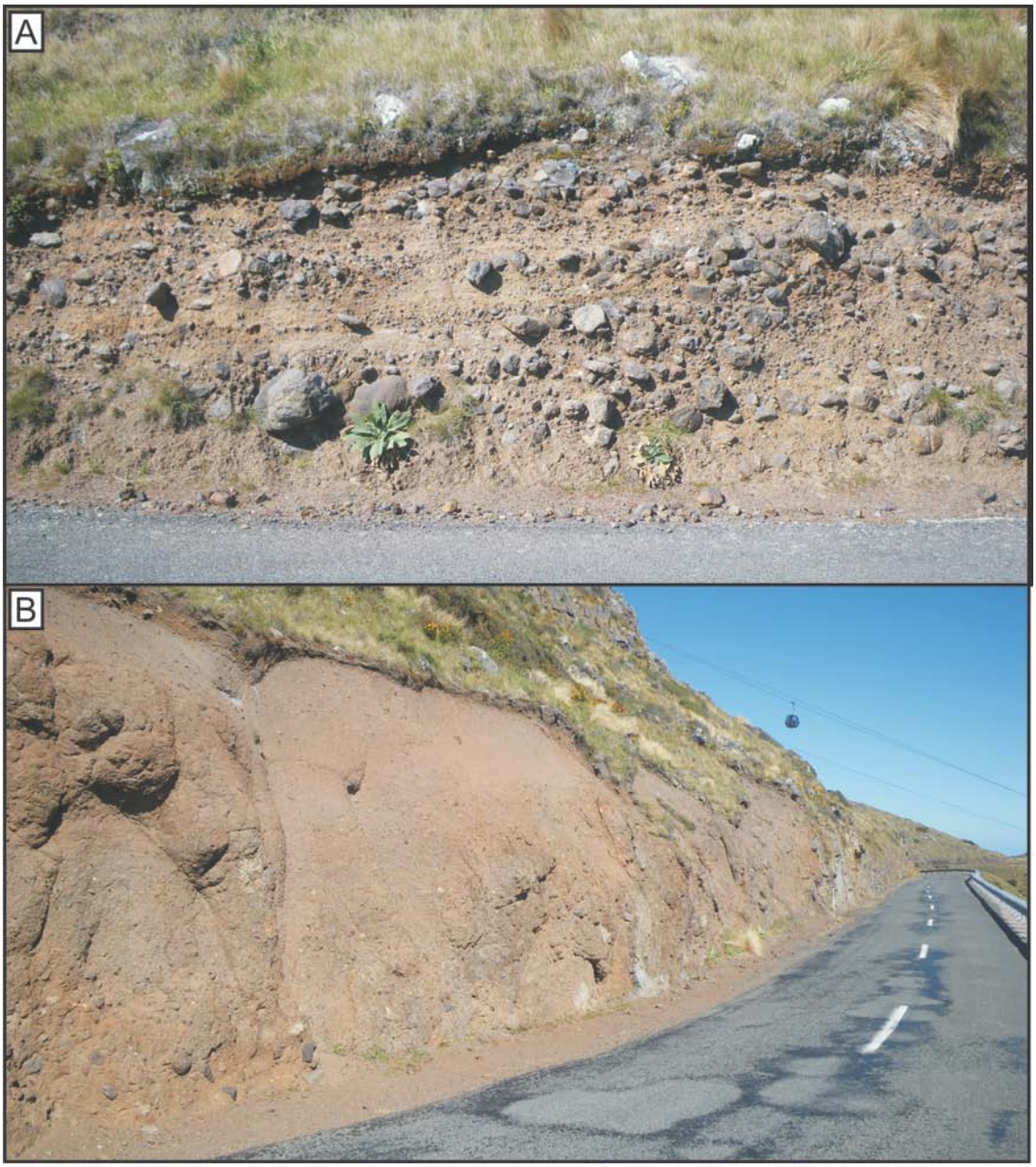

Figure 2.29. Epiclastic deposits of the Mt Cavendish section. A) Middle clast-supported to clast-poor, epiclastic horizon. B) Epiclastic deposits at the apex of the Summit Road, note the lack of clasts within the upper sequence.

The second deposit is exposed beneath the gondola line (Figure 2.29A). Deposits are grey – brown – orange, poorly indurated, poorly sorted, sub-rounded clast-supported, crudely stratified, polymict volcanic conglomerate. Upper and lower deposits are typically normally graded at base, becoming inversely graded up section. In the middle of this sequence is a red – orange, fine sand to granule matrix supported layer, clast-rich layer (Irvine, 2003).

The third epiclastic deposit, exposed on the bend on the Summit Road (Figure 2.29B), is a grey – brown / red, massive, poorly indurated, poorly sorted, medium sand to granule matrix supported, sub-angular to angular, polymict volcanic conglomerate (Irvine, 2003). Larger clasts are limited within the upper horizons of this deposit, with a distinct red banding occurring beneath the overlying lava flow. This sequence of epiclastic deposits is intruded by both basaltic and trachytic dykes. One prominent dyke intersects the epiclastic deposit (upper two units) repeatedly, due to the road cut intersecting the strike of the dyke (Figure 2.29B).

Battery Point

Battery Point epiclastic deposits are exposed in batter faces above the coal store to the south of Battery Point (Figure 2.25 and 2.30), approximately 1km from Lyttelton Township. These deposits were originally described by Coates (1976) as one lahar, approximately 1m thick, with rounded volcanic clasts in an ash-mud matrix, with the base of this deposit being comprised of grey / white, gray, red and rusty orange clasts (<10cm long) in a yellow-white tuff matrix. Irvine (2003) divided this sequence into a lower and an upper deposit.

Figure 2.30. Battery Point epiclastic exposures. Distinct red pyroclastic-rich red epiclastic layers weathered black comprise much of the lower batter face, with brecciated lava flows overlying. The sequence is intruded by multiple near-vertical dykes.

The lower lahar is described by Irvine (2003) as a tan, massive, non-graded, poorly indurated, slightly vesicular fine sand to granule matrix supported, polymict volcanic conglomerate (~1.1m thick, ~100m long exposure). The upper deposit is grey, changing

to orange up sequence, massive, non-graded, poorly indurated, fine to coarse sand matrix supported, polymict volcanic conglomerate, with occasional carbonised wood fragments (Irvine, 2003).

Sumner Valley

Sumner epiclastic deposits are exposed in the lower cliff faces on the eastern and side of the valley, and on the road leading up Sumner Valley and the road intersection at Evans Pass (Figure 2.24).

Eastern Sumner Valley

Epiclastic deposits of eastern Sumner (Figure 2.24) are exposed in the lower cliff faces on the eastern side of the valley, and are capped by a'a lava flows. At the north-eastern end of Sumner Road, is an exposure of gently eastward dipping, orange-brown, roughly stratified, poorly indurated, fine sand to granule matrix supported at base grading into clast supported, sub-angular, polymict volcanic conglomerate (Irvine, 2003), correlated with deposits in a quarry ~150m away (Coates, 1976). At the base of the deposit is a orange-yellow, massive, poorly indurated, moderately sorted, fine – medium sand, sandstone, which grades into the overlying epiclastic deposit (Irvine, 2003).

Upper Sumner Valley

The Evans Pass Road lahar is an extensive deposit outcropping for ~500 in road cuts, and correlated to scrappy outcrops in farmland on the opposite side of the valley ~200m away (Figure 2.24; Neumayr, 1998, Irvine, 2003). This deposit is divided into an upper and lower unit.

The upper unit, is comprised of tan, coarsely bedded, inversely graded, poorly sorted, coarse sand to granule matrix-supported at the base grading up into clast-supported, polymict volcanic conglomerate (Irvine, 2003). The base of this deposit has a yellow, massive, poorly indurated, moderately sorted, fine – medium, volcaniclastic sandstone (Irvine, 2003). The lower units, approximately 300m down the road, is an orange-brown, crudely bedded, normally graded at the base, to inversely graded at the top,

poorly sorted, coarse sand to granule matrix supported, sub-rounded, polymict volcanic conglomerate (Irvine, 2003). This epiclastic sequence probably has a continuation on the western side cliff faces of Sumner Valley.

Evans Pass

A small lensoid lahar exposed in the road cutting at the junction of Sumner, Evans Pass, and the Summit Roads (Figure 2.24) is described as a tan, massive, poorly indurated, poorly sorted, coarse silt to matrix supported, polymict volcanic conglomerate (Irvine, 2003).

Rapaki Track Epiclastic deposits

Rapaki Track epiclastic deposits outcrop near the start of the track (100m above S.L.) and are last encountered further up the track, around 190m (A.S.L; Figure 2.24). Deposits overlie weathered basalt lava flows and are interpreted to be interbedded with lava flows, due to sporadic exposure. Deposits are poorly sorted, matrix to clast supported conglomerate, clasts range from coarse lapilli to boulder (up to 70cm), in a red brown, poorly to moderately indurated, fine to coarse lapilli matrix. Clasts are red basaltic, grey phenocryst-rich basaltic clasts, highly weathered basalt clasts, and cream to green trachyte.

2.5. Discussion

2.5.1. Epiclastic Interpretation

The first recognition of lahar deposits on Lyttelton Volcano was by Coates (1976), describing two exposures at Battery Point, Lyttelton Harbour, which he correlated with an extensive pyroclastic horizon in a quarry to the west of Windy Point. Weaver (1980) described the thick epiclastic sequence between Castle Rock and Mt Cavendish, designating them as a late degradational phase in the construction of the Lyttelton cone, later (Weaver et al., 1985) considering these deposits as degradational phases accumulating in stream channels, on the eroding Lyttelton cone.

It was not until Shelley (1992) that the laharic horizons of the north-eastern sector of Lyttelton Volcano were considered to represent the boundary between Lyttelton 1 and Lyttelton 2 Volcanoes. In Neumayr's (1998) study of Lyttelton Volcano, he adjusted the Lyttelton 1 and Lyttelton 2 boundary because of newly identified epiclastic deposits on the south side of the Tors and correlated these to outcrops in Lyttelton and at Battery Point. He also suggested that the Tors - Mt Cavendish epiclastic deposits represented the boundary between Lyttelton 2 and the late stage Mt Pleasant Formation flows. More recently Irvine's (2003) study suggested that Neumayr (1998) mistakenly identified rubbly aa lava flow tops and remnants of eroded scoria cone deposits as lahar deposit.

What was lacking from these previous studies was interpreting these units in the scale of Lyttelton Volcano and what they actually represent within the growth and degradation of the volcano.

In investigating the epiclastic deposits of north-eastern Lyttelton Volcano, deposits were observed at various stratigraphic horizons within the overall structure of Lyttelton Volcano, and not as one defined horizon as suggested by Shelley (1987). Each epiclastic sequence is distinct, with limited correlations between major deposit locations identifiable during mapping or by later projections. Deposits are primarily interpreted as debris flows, hyper-concentrated flows and stream flows (Table 2.3) that deposited on the proximal slopes of Lyttelton Volcano.

Locality	Characteristics	Interpretation
Castle Rock	Massive, non-graded, medium sand to pebble matrix supported, sub-angular, volcanic conglomerate. Channels	Debris flows
Tors to Bridal Path	Matrix supported, < 2m boulder-rich conglomerate, coarsely bedded, inversely graded, fine sand to granule matrix supported, sub-rounded to rounded, conglomerate; very fine to coarse sand lenses; channelled	Hyper-concentrated flows
Mt Cavendish 1	Poorly sorted, matrix supported, sub-rounded, conglomerate	Debris flow
Mt Cavendish 2 (lower)	Coarsely bedded, normally graded at the base, inversely graded at top, poorly indurated, poorly sorted, fine sand to granule matrix supported, sub-rounded, conglomerate, with fine sand lenses	Debris flow to stream flow
Mt Cavendish 2 (middle)	Poorly indurated, poorly sorted, sub-rounded clast-supported, crudely stratified, conglomerate	Debris flows
Mt Cavendish (upper)	Poorly indurated, poorly sorted, medium sand to granule matrix supported, sub-angular to angular, volcanic conglomerate	Debris flow to hyper-concentrated flow
Battery Point (lower)	Massive, non-graded, poorly indurated, slightly vesicular fine sand to granule matrix supported, volcanic conglomerate	Debris flow
Battery Point (upper)	Massive, non-graded, poorly indurated, fine to coarse sand matrix supported, volcanic conglomerate	Debris flow
Eastern Sumner Valley	Roughly stratified, poorly indurated, fine sand to granule matrix supported at base grading into clast supported, sub-angular, volcanic conglomerate	Debris flow - channelized
Eastern Sumner Valley (base)	Massive, poorly indurated, moderately sorted, fine – medium sand, sandstone	Hyper-concentrated flow
Upper Sumner Valley (upper)	Coarsely bedded, inversely graded, poorly sorted, coarse sand to granule matrix-supported at the base grading up into clast-supported, conglomerate, basal massive, poorly indurated, moderately sorted, fine – medium, sandstone	Hyper-concentrated flow overlain by debris flow
Upper Sumner Valley (lower)	Crudely bedded, normally graded at the base, to inversely graded at the top, poorly sorted, coarse sand to granule matrix supported, sub-rounded, conglomerate	Debris flow transitioning to hyper-concentrated flows
Evans Pass	Massive, poorly indurated, poorly sorted, coarse silt to matrix supported, conglomerate	Debris flow
Rapaki Track	Poorly sorted, matrix to clast supported, conglomerate	Debris flow

Table 2.3. Lyttelton Volcano epiclastic deposit description and interpretations, following the classification of Palmer and Neall (1991).

2.5.2. Pyroclastic Interpretation

Distinct pyroclastic horizons are exposed beneath the Bridle Path epiclastic deposits and the incised by the Mt Cavendish 1 epiclastic deposits. In the examination of these units distinct similarities are recognised with Vespermann and Schmincke (2000) scoria cone facies (Figure 2.31). Description and scoria cone facies association of pyroclastic

deposits encountered at both Mt Cavendish 1 section and beneath the Bridle Path sequence are proposed (Table 2.4).

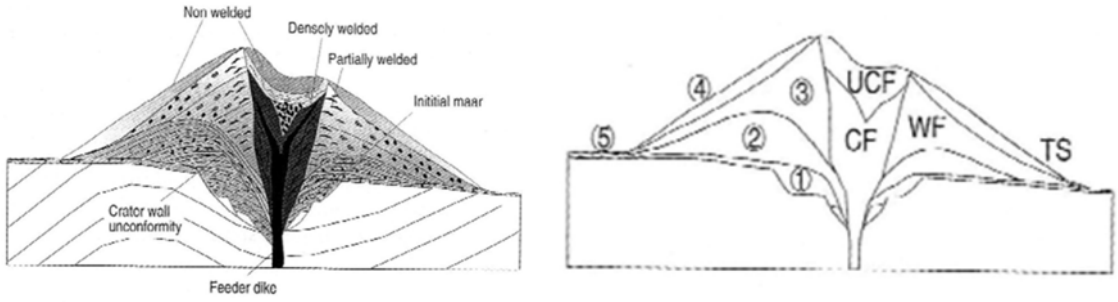

Figure 2.31. Vespermann and Schmicke (2000) classification of scoria cone facies. 1 — initial phreatomagmatic units, 2 — strombolian units with intercalated phreatomagmatic beds, 3 — strombolian eruption formed cone facies, 4 — post-strombolian talus, 5 — distal fallout tephra, CF = crater facies, UCF = upper crater facies, WF = wall facies, TS = talus slope

	Description	Unit	Facies
Mt Cavendish 1	Cream – yellow, crystal tuff with an ash matrix	Initial phreatomagmatic units	Crater facies
	Cream – yellow, crystal tuff with coarse angular lapilli basaltic clasts, in an ash matrix	Initial phreatomagmatic units	Crater facies
	Near flat lying, cream – yellow fine to coarse ash deposits, with flattened vesicular lava fragments	Strombolian units with the intercalated phreatomagmatic beds	Crater / wall facies
	Stratified welded agglutinates, red pyroclastic, scoria and basaltic fragments	Strombolian eruption formed cone facies	Wall facies
	Agglutinated lava flows	Strombolian eruption formed cone facies	Wall facies
Bridle Path	Phenocryst-rich, medium-coarse ash with angular juvenile lapilli-sized fragments	Distal fallout tephra	Talus slope
	Agglutinated spatter interbedded with medium-coarse red ash	Strombolian eruption formed cone facies	Wall facies

Table 2.4. Mt Cavendish and Bridle Path pyroclastic deposit descriptions, unit classification and associated scoria cone facies, as defined by Vespermann and Schmincke (2000).

From Vespermann and Scmincke (2000) scoria cone facies classification (Fig 2.31) the pyroclastic deposits exposed at both Mt Cavendish 1 section and beneath the Bridle Path section are remnants of scoria cones on the flanks of Lyttelton Volcano (Table 2.4). The Mt Cavendish 1 scoria cone, although now highly eroded the original

structure is transacted by the road. From north to south (Figure 2.28), the main vent lava flows overlie welded agglutinated lavas of the scoria cone, underlying this horizon are the Strombolian crater wall facies, the interior of the cone records the initial phreatomagmatic stages of the scoria cones development, the southern crater wall facies are intersected by various dykes and overlain by lavas. Bridle Path pyroclastic deposits indicate a scoria cone existed in this area prior to the deposition of the overlying epiclastic deposits. The vent area is hypothesised to be near the Bridle Path saddle, with near vent deposits (limited exposures) in this area, and crater wall facies exposed in road cuts (dipping away from this region) to the south.

2.5.3. Origin of Epiclastic Deposits

Determination of the origin of the epiclastic horizons of Lyttelton Volcano is an important aspect in understanding the evolution of the volcano. All of the observed epiclastic horizons are in medial to proximal volcanic facies, and therefore if this represents a volcanic debris avalanche or collapse horizon then close to source debris avalanche structures should be apparent, e.g. jigsaw fit block fracture (Figure 2.17), toreva's, and levees. Within analysis these features are not immediately obvious with the epiclastic deposits having typical features debris flow to stream flow (Figure 2.18), commonly associated with long-term processes of volcanic degradation and aggradations (i.e. Palmer and Neall, 1991). With this being stated these deposits may represent the remobilised deposits of a debris avalanche, the following discusses key features of the epiclastic deposits.

Clasts and Relationships with Underlying Lithologies

Clasts within the epiclastic deposits are variable, with larger clasts being basaltic (Figure 2.32). Weathering of clasts is also variable with some clasts being relatively fresh, whereas others have distinct weathering rinds or are completely altered. Highly altered clasts are common within the epiclastic deposits of the Tors region, with trachytes altering to a cream-white, and in the past (Irvine, 2003) have been interpreted as rhyolitic clasts. Also within this zone are what appear to be altered tuffaceous sandstone and mudstones, suggestive of hydrothermal alteration.

Figure 2.32. Clast and matrix compositions and variation. A) Clast-rich matrix supports larger sub-angular basaltic clasts. Band C) Weathered white matrix surrounds highly variable basaltic clasts. D) Vesicular basaltic clast. E) Angular basalt clast surrounded by rounded granule to cobble-sized clasts. F) Fresh flow banded basalt, surrounded by weathered clasts. G) Elongate vesicle, magmatic clast, indicative of deposition near to source.

With most clasts being sub-angular to sub-rounded, a remobilisation or incorporation of volcanic material into volcanic mass flows is the most probable source mechanism. Clasts on the volcanic slopes and in pre-existing drainage networks would have been undergoing degradational processes, producing the observed rounding, indicating long-lived degradation and aggradation.

Channel Features

Clast alignment reflects flow lineation, suggesting pulsating deposition. Clasts within channels are larger in the base of channels, with alignment of clasts occurring stratigraphically higher within channels. Channels and stratified epiclastic horizons are useful paleo-flow indicators. The best sections to refine the flow directions and therefore postulate source regions are the Castle Rock to Mt Cavendish section, and the Battery Point section.

Epiclastic deposits between Mt Cavendish and Castle Rock dip away from a point south of the Lyttelton Township (Figure 2.27). The Summit Road provides two transects through laharic deposits, one at right angles and the other parallels flow direction (Figure 2.27). At the edge of the cliff facing towards Lyttelton Harbour epiclastic layers are sub-parallel to one another, indicating a flow direction from the northeast. A further aspect of the Mt Cavendish sequence is the erosional channelized epiclastic deposit on the northern side of the scoria cone (Figure 2.28). This lahar incise through the inner crater region of the scoria cone, incorporating the ash-rich inner crater facies, decreasing in abundance into the flow interior, indicating a flow direction from the east.

Channels are common within the Battery Point section, with their orientations reflecting flow direction and underlying topography, an important aspect in the understanding of a paleo-topography. Channels exposed on the batter faces at Battery Point have a similar orientation to the present day Sumner Valley, indicating a paleo-valley existed during the time of deposition.

2.5.4. Evidence of Collapse

Various dykes intrude through lava flow sequences, scoria cones and epiclastic horizons, in the Tors-Bridle Paths and Mt Cavendish sections. If as hypothesised in previous studies this epiclastic-rich horizon is the result of debris avalanche. In volcano's that have pronounced sector collapse, the proceeding dyking will parallel the ridges of the u-shaped collapse amphitheatre (Figure 2.33; i.e. Mt Etna; McGuire and Pullen, 1989; Acocella and Neri, 2009). If collapse occurred in this region then the resulting dyking would be oriented NE-SW, under a collapse at a similar orientation to the present day harbour. In analysis dykes in this region reflect orientations oblique to almost perpendicular to this hypothesised collapse trends.

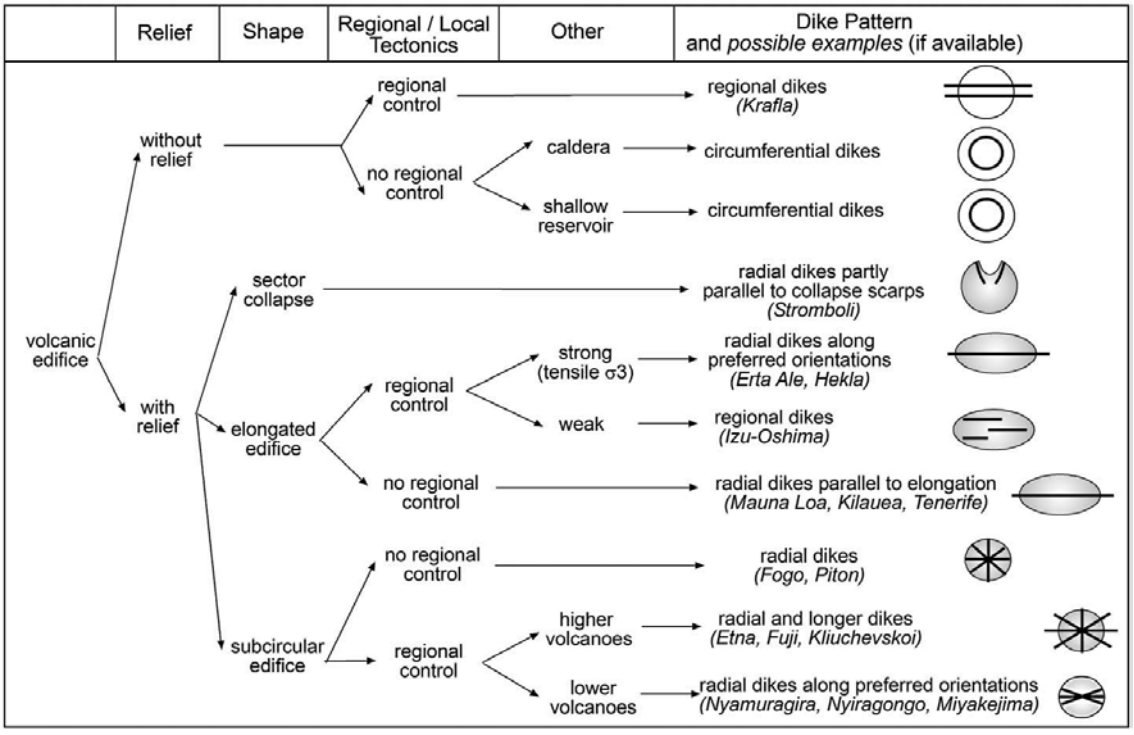

Figure 2.33. Acocella and Neri (2009) summary diagram of dyke patterns due to edifice shape, relief and tectonics. Note the radial dyke pattern parallel to sector collapse scarps.

Previous Catastrophic Collapse Associated Deposits

Explosive collapse associated deposits have been previously interpreted at Battery Point, by Coates (1976) and Neumayr (1998). At the base of the lower lahar deposits are grey or white fragments, with other rocks of gray, red and rusty orange, 10cm long in a yellow-white tuff matrix (Coates, 1976). Coates (1976) interpreted this as an ignimbrite, an interpretation that Neumayr (1998) supported, suggesting that this

horizon represents a violent eruption associated with rhyolitic magmas, triggering sector collapse to the eastern flank of Lyttelton Volcano. The white clasts interpreted as rhyolite can be traced up to the hill crest above, where a trachyte dyke is exposed in the ridge line above. This trachyte is highly weathered, white, and clearly the source of this so called 'rhyolite'. Also occurring on the north-western bench faces are reworked epiclastic deposits and recent slopewash deposits, full of weathered white clasts, with a loess-rich matrix, suggesting these identified rhyolitic horizons are more recent and not associated with a catastrophic collapse of Lyttelton Volcano.

2.5.5. Syn-Eruptive Deposits

Edifice destruction is rapid and episodic (Palmer and Neall, 1991), with volcanic debris avalanches delivering large amounts of sediment to a ring plain in a single sedimentation event burying the surrounding ring plain landscape, followed by long periods of slow sedimentation and local fluvial dissection. This is recorded in the rock record as periods of long term quiescence (low sedimentation post event) or relatively low frequency eruptions (tephra layers; Palmer and Neall, 1997). In comparison edifice construction on the Taranaki ring plain is recorded as "unconformity bounded vertical sequences in deposits of lahar dominated systems" with sequences as packages of sediment related to different eruptive periods (Palmer and Neall, 1991). This syn-eruptive process is best expressed in Giordano et al (2002) emplacement model of rain-generated lahars at Roccamonfina, Italy, following an ignimbrite eruption (Figure 2.34).

In the analysis of Lyttelton Volcano the epiclastic horizons of the north-eastern sector are not a continuous horizon, but are periodic degradational phases separated by eruptive products (pyroclastic and lavas). A primary argument against a prolonged period of degradation on Lyttelton Volcano is the occurrence of lava flows interbedded within the epiclastic deposits, indicating ongoing effusive eruptive activity during volcanic degradation. Due to the lava flow location and flow orientations of interbedded flows, the ongoing activity was probably from a central vent. The occurrence of relatively intact scoria cones at the time of epiclastic incision and

deposition suggests typical slope degradation, rather than a pronounced catastrophic collapse of the volcano, disrupting the surrounding volcanic slopes.

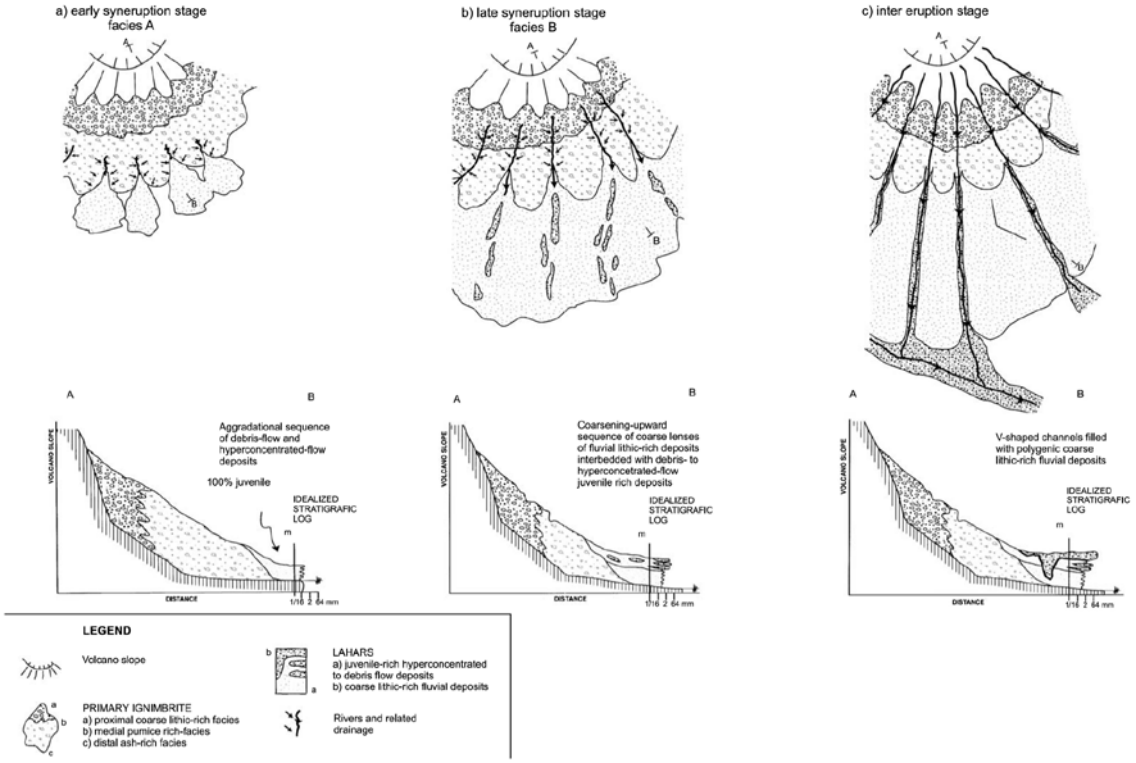

Figure 2.34. Generation and emplacement of rain generated lahars at Roccamonfina (Giordano et al., 2002). a) early syn-eruption stage: distal erosion forming hyper-concentrated and debris flows. b) late stage eruption: drainage network incises up-slope, lahars are interbedded with fluvial conglomerate. c) inter-eruption stage: restoration of drainage network and the removal and redistribution of pyroclastic debris.

Primary and remobilised pyroclastic materials are observed in some of the epiclastic deposits, indicating contemporaneous volcanic activity. Within the Mt Cavendish sequence vesicular juvenile clasts are present indicating incorporation of recent eruptives. Whereas the Upper Sumner epiclastic sequence matrix-rich horizons are comprised of reworked ash, with incorporation of fragments and clasts into the debris flow. Also within this sequence are thin tephra beds, with no entrained clasts, suggesting explosive events produced tephra which was either reworked or deposited in close proximity to the eruptive source.

Based on these observations it is suggested that epiclastic sequences deposited on the mid to lower flanks of Lyttelton Volcano, with those of upper Sumner Valley forming

through rain triggered mass flows remobilising near to source tephras (Prof. Shane Cronin pers. comm. 2007). Rain-induced epiclastic deposits have been recognised as key redistributors of loose volcanic material during periods of quiescence, intensified in zones of bare landscape (Davidson and DeSilva, 2000). The presence of such remobilised tephra deposits on Lyttelton Volcano indicates a landscape with low levels of vegetation in the mid to lower flanks.

2.6. Summary

- Neither the major radial valley system nor the circular erosional crater rim of Lyttelton Volcano, are concentric to a Head of the Bay eruptive centre.
- No distinct volcanic collapse features (e.g. avalanche deposits) are evident in seismic profiles offshore of Lyttelton Volcano.
- Epiclastic deposits are comprised of remobilised sub-angular to rounded volcanic material, commonly with paleo-channels, and are devoid of typical near-source collapse associated features.
- Epiclastic horizons occur as distinct horizons interbedded with Lyttelton lava flows, and not as a single horizon marking an unconformity between Lyttelton 1 and 2.
- Epiclastic deposits are interbedded with lava flows, and have a reworked pyroclastic matrix, indicating ongoing eruptive activity accompanying volcanic degradation and deposition on the flanks of Lyttelton Volcano.
- Channel features indicate paleo-valley systems, with those of the Tors-Bridle Path region indicating flow directions from a source near to Lyttelton Township.
- Epiclastic horizons on Lyttelton Volcano represent periods of volcanic degradation on the vent and proximal slopes of Lyttelton Volcano, with aggradation occurring in proximal to distal volcanic facies environments.
- Volcanic activity was ongoing during times of deposition, with the epiclastic deposits often having a matrix largely of reworked primary-pyroclastic material, and being interbedded with lava flows.

CHAPTER 3

EPICLASTIC DEPOSITS ON THE SOUTH-EASTERN SIDE OF LYTTELTON HARBOUR

3.1. Introduction

This chapter describes the epiclastic deposits exposed at Black Point, on the south-eastern side of Lyttelton Harbour (Figure 3.1), which has previously been mapped (Sewell et al, 1988; 1992) as Allandale Rhyolite and Diamond Harbour Volcanics. In a recent subdivision on Black Point (Black Rock Estate; Figure 3.1), a new epiclastic sequence has been exposed, with the basal and upper contacts exposed, providing stratigraphic constraint on the timing of deposition of the deposits. This sequence overlies both Allandale Rhyolite and Lyttelton Volcanic Group lavas, and is interbedded with and overlain by Diamond Harbour Volcanic Group (Figure 3.1). Lyttelton Harbour is contentious within the development and erosive history of Lyttelton Volcano, and this chapter provides a new stratigraphic context to the origin, morphology and timing of formation of Lyttelton Harbour, a key aspect in the erosive history of Lyttelton Volcano.

Other epiclastic deposits have been recognised on and around the eroded Lyttelton Volcano (Figure 3.1), with key exposures identified at Quail Island (Sewell, 1985), Purau (Dorsey, 1981), Mt Herbert, Mt Bradley, and Kaituna Valley (Sutton, 1993; Hampton, 2005). Through detailed examination of the Black Point sequence and relationship to the surrounding stratigraphic sequence, depositional environments can be established. These can then be compared to other epiclastic deposits to define the erosive / post volcanic history of Lyttelton Volcano.

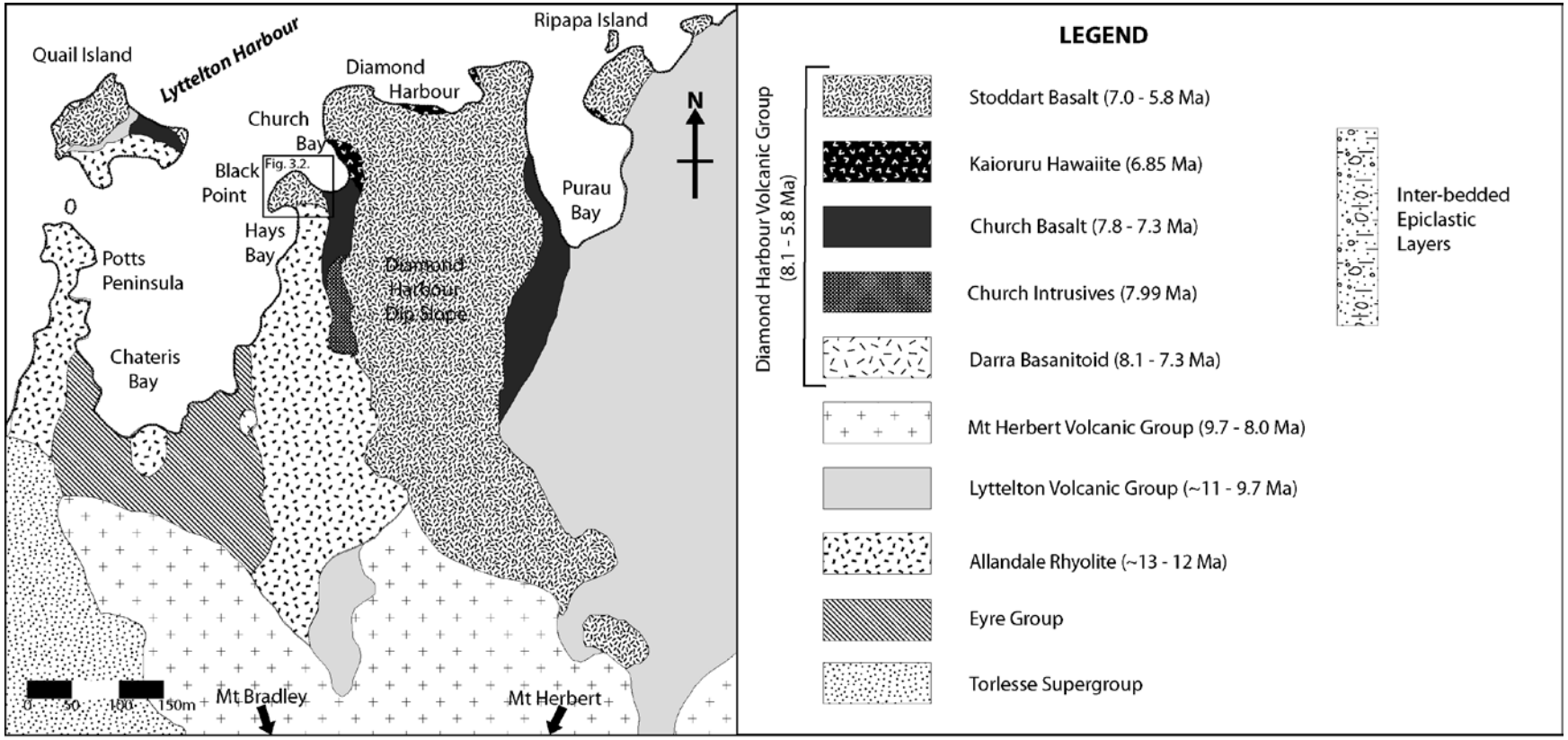

Figure 3.1. Simplified geological map and schematic stratigraphic section for south-eastern Lyttelton Harbour.

3.2. Lyttelton Harbour Epiclastic Deposits

Large sequences of epiclastic deposits are exposed in the upper reaches of both Kaituna and Purau Valleys, on the shoreline of Purau Bay, above Tableland Spur in Charteris Bay, Quail Island, and on Black Point between Hays and Church Bay (Black Rock Estate; Figure 3.1). Epiclastic sequences occur at various stratigraphic horizons (Figure 3.2), unconformably overlying Allandale Rhyolite (~13 – 12 Ma) and Lyttelton Volcanics (~11 – 9.7 Ma), and interbedded with Mt Herbert Volcanic Group (9.7 – 8.0 Ma) and Diamond Harbour Volcanic Group lava flows (8.1 – 5.8 Ma). Interbedded epiclastic deposits have been incorporated within formation descriptions, but stratigraphically represent depositional periods between eruptions.

3.3. Stratigraphy of Black Point

Epiclastic deposits at Black Point show a complete sequence from basal contacts to the overlying volcanic groups (Figure 3.2). The epiclastic sequence is exposed in recent road-cuts (produced during subdivision), and the shore platforms between Church and Hays Bays. Deposits overlie Allandale Rhyolite and are interbedded with initial Diamond Harbour Volcanic Group lavas, giving a time of deposition between 8.1 and 7 Ma. Overall, conglomerates young to the west, and dip into Lyttelton Harbour.

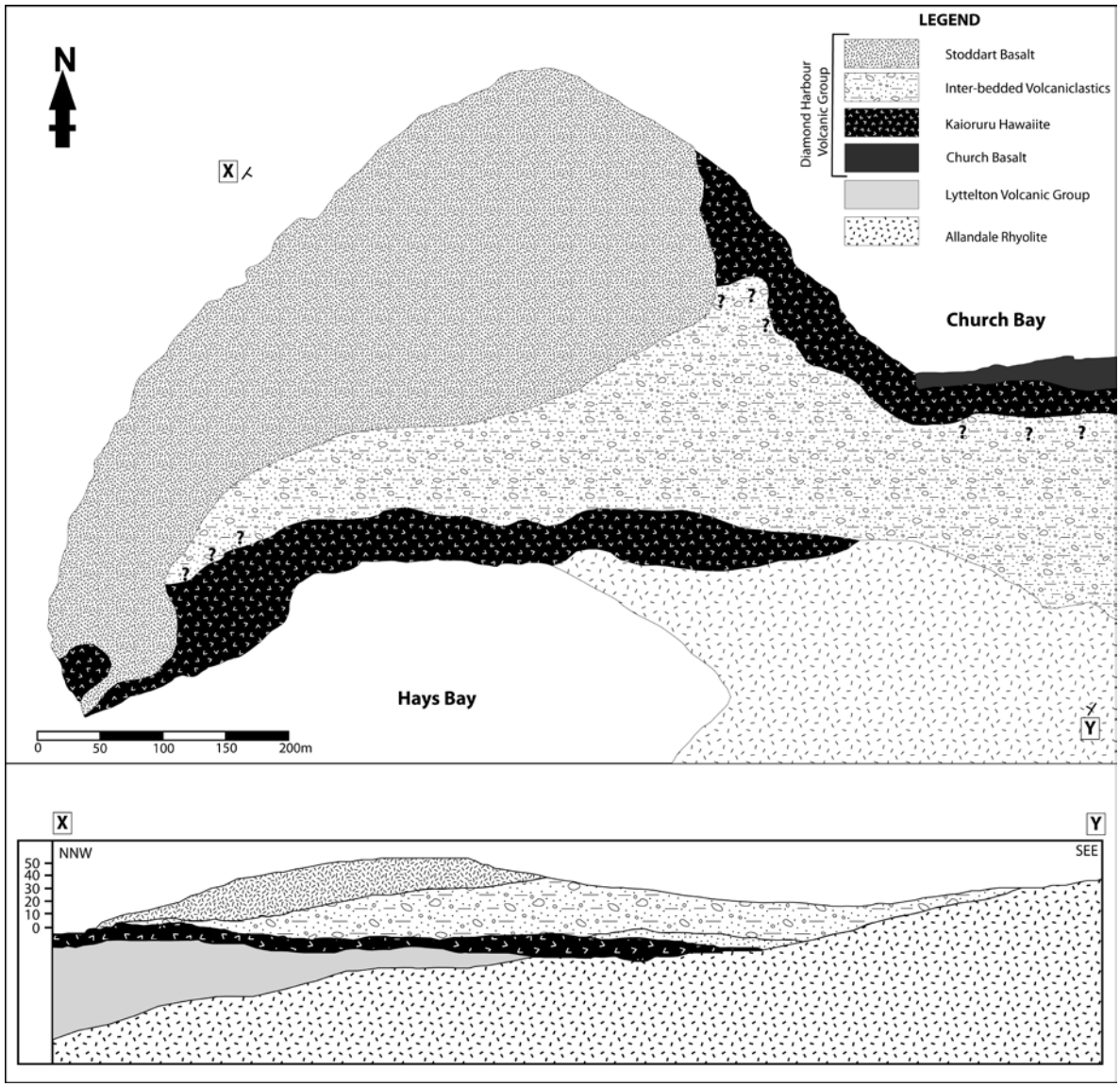

Figure 3.2. Geology of Black Point, of note is the lack of Lyttelton Volcanics in plan view and the hypothesised incorporation within the cross section as a thinning SEE dipping eroded surface.

3.3.1. Main Sequence

Underlying Units

Allandale Rhyolite is the predominant basement on the south-eastern side of Hays Bay (Figure 3.2). This unit drops steeply towards the west and north. The contact between the Allandale Rhyolite and the epiclastic deposit is exposed 10m beneath the road (Figure 3.3), dipping to the northwest. Within this exposure there is a gradation from un-weathered cream-white rhyolite, to highly weathered cream-orange rhyolite (80cm),

above which is a horizon (1m) of highly weathered rhyolite, comprising poorly indurated rhyolite clasts surrounded by a highly weathered rhyolite matrix, before grading into a rhyolite clast-rich, medium sand, matrix-supported conglomerate (Figure 3.3). Only the basal ~1m region of this conglomerate is rhyolite-clast-rich with limited basaltic clasts. Rhyolite clasts are angular and highly weathered, decreasing in size away from the contact, whereas basalt clasts proportionally increase up section, with the largest clast being 1m by 80cm, 3m from the basal contact. Basaltic clasts vary from highly weathered to fresh, with larger clasts being angular boulders and the smaller <cobble clasts being well rounded. The matrix within layers also varies from tuff rich to lapilli rich.

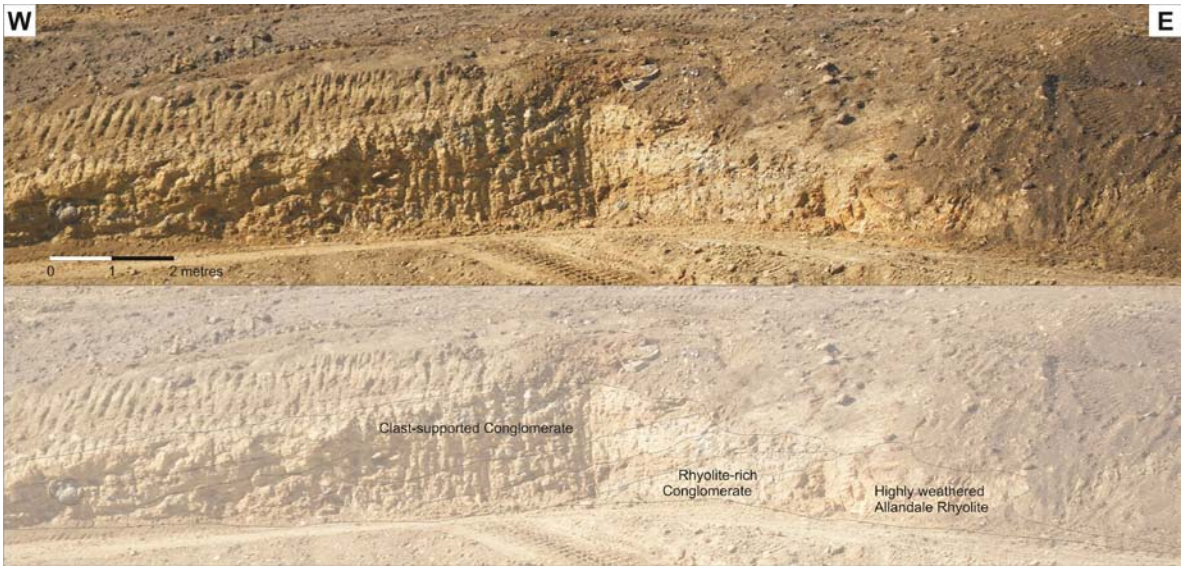

Figure 3.3. Rhyolite overlain by basal rhyolite clast rich conglomerate, grading into a basaltic clast-rich conglomerate.

Underlying Kaioruru flows are exposed within a road cutting 70m uphill from the shore platform, with two distinct lava flows dipping to the east. No contacts are seen between epiclastic rock units and these lavas, but stratigraphic relationships indicate the lavas lie beneath the epiclastic sequence. These lavas can be correlated to a further exposure overlying Allandale Rhyolite further downhill, and then to the shore platform on the south-western side of Black Point.

Basal Tuffaceous Sandstone and Mudstone

Lying stratigraphically below the main epiclastic sequence is a series of inter-bedded mudstones and sandstones (Figure 3.4). Four distinct units are recognised within this sequence, exposed in various road cuttings. 1) A pale cream, normally thinly bedded (<5cm), normally graded, moderately to well sorted, medium to fine sandstone. The basal sequence of normally graded layers are typically thin (<4mm) medium sandstone layers grading into fine sand above. Thin (<2mm) red-brown, irregular wavy layers are interspersed throughout this unit, near or at the top of graded beds. 2) A cream-brown to orange, moderately indurated, thinly bedded (<5cm), medium to fine sand (Figure 3.C). Brown-purple, fine sandstone layers are inter-bedded throughout (Figure 3.4 B), with the medium grained sand layers having white fragments (highly weathered feldspar) and being slightly normally graded. 3) A purple-brown very well sorted, very thinly bedded (<1cm), normally graded, fine sandstone. Basal areas of normally graded layers are slightly coarser and yellow-cream in colour. 4) A light yellow / cream, white speckled, poorly indurated, massive well sorted, medium sandstone.

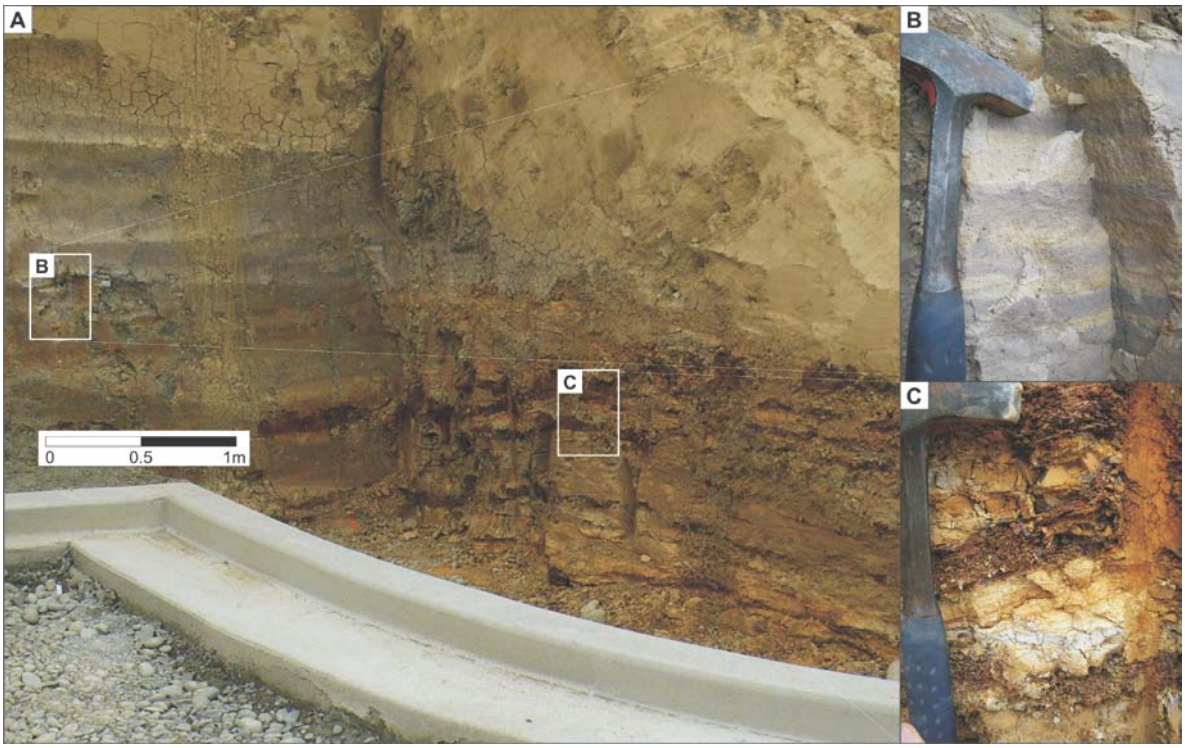

Figure 3.4. A) Basal tuffaceous sandstones and mudstones at the end of a newly cut right of way. B) Cream to purple bedded mudstone. C) Iron-rich horizons with the lower cream tuffaceous sandstone.

Main Sequence

Overall, the main epiclastic sequence, along the crest of the Black Point (Figure 3.2, 3.5, 3.6, 3.7), comprises matrix-supported conglomerate with lenses / layers of tuffaceous mud to sandstone. Pyroclastic content increases towards the top of the sequence, indicated by red colouration, accompanied by vesiculated volcanic clasts, grading to the initial lava flows of the Stoddart Basalt, Diamond Harbour Volcanic Group. This sequence is then capped by loess, loess colluvium, and a soil horizon.

Conglomerates are matrix-supported, sub-rounded to sub-angular, pebble to boulder sized, with layers varying from clast-rich to clast-poor. The matrix is cream to oxidised brown (weathered white), fine sand to granule (volcanic clasts). Distinctive sinuous iron pan layering / veining exists throughout deposits, highlighting banding / layering of clasts. Conglomerates are classified into lithofacies, using the classifications of Calvari and Groppelli (1996); Sohn et al., (1999); Sohn, (2000); Vallance (2000); and Roa (2003).

Facies A: Matrix-Clast Supported Conglomerate

Facies A (Figure 3.8, 3.9) is a massive, matrix-clast supported, pebble to boulder (<50cm by 50cm), clast-rich to clast-poor conglomerate. Clasts are sub-angular with smaller clasts being sub-rounded (average size of 12cm diameter). Clasts are predominantly fine grained basalts with weathered rinds, producing a thin white exterior on some clasts. Variation not only occurs in clast size and weathering extent (Figure 3.8, 3.9), but within angularity and elongation or platy-ness, with the longest axis in flow direction. Tuffaceous mudstone and sandstone clasts are also present but are minor components (~5-10%). The matrix varies from cream / orange to moderately weathered (increasing towards top of cuttings) cream oxidised brown, fine sand to granule. Deposits are intersected by oxidised iron stained fractures and layers, in some cases concentrated along remnant bedding and shear planes (Figure 3.6).

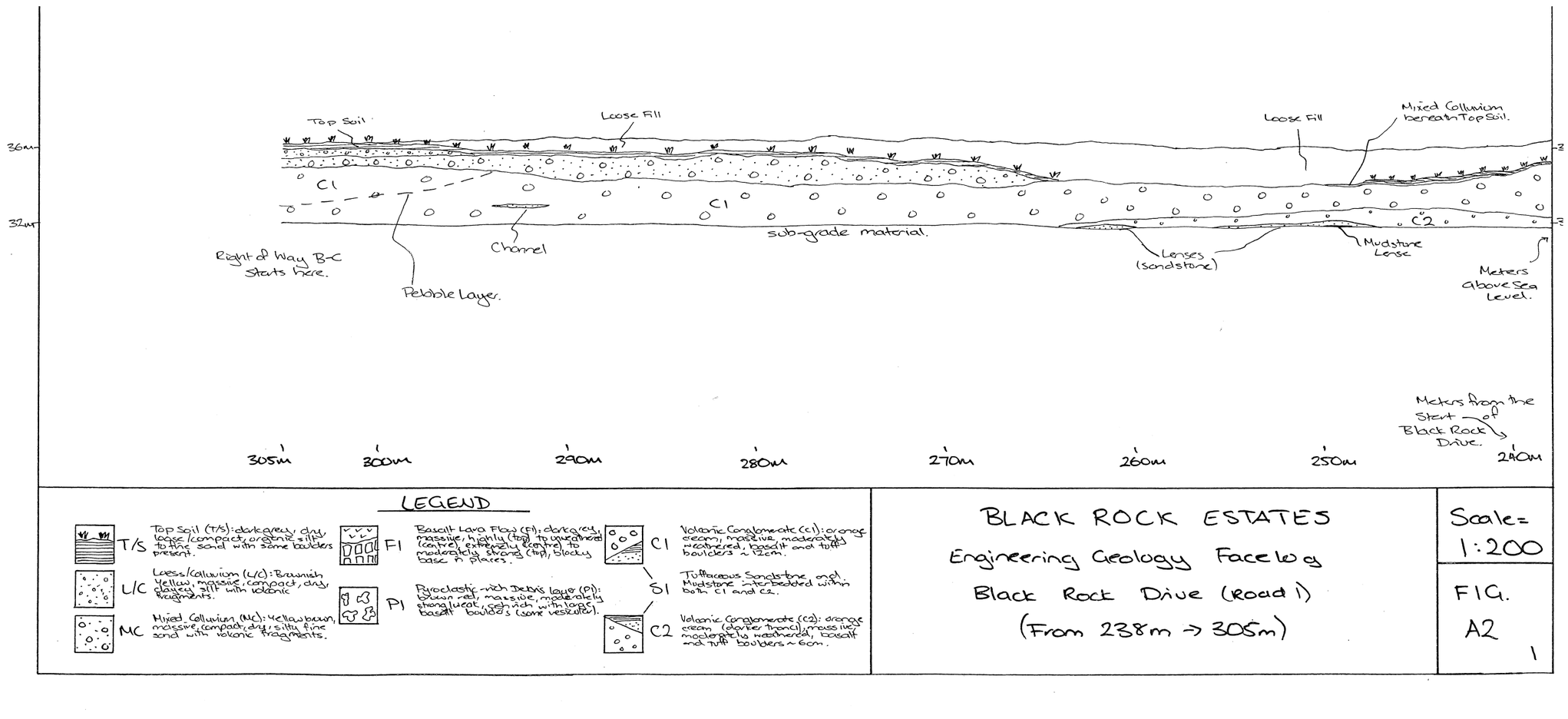

Figure 3.5. Face log of the main sequence of conglomerate along the main right of way in the Black Point subdivision. Note the main conglomerate horizons; C1 refers to matrix-clast supported conglomerate facies, C2 refers to matrix supported conglomerate facies. S1 to interspersed tuffaceous units, exposed as lenses or channels with the exposure.

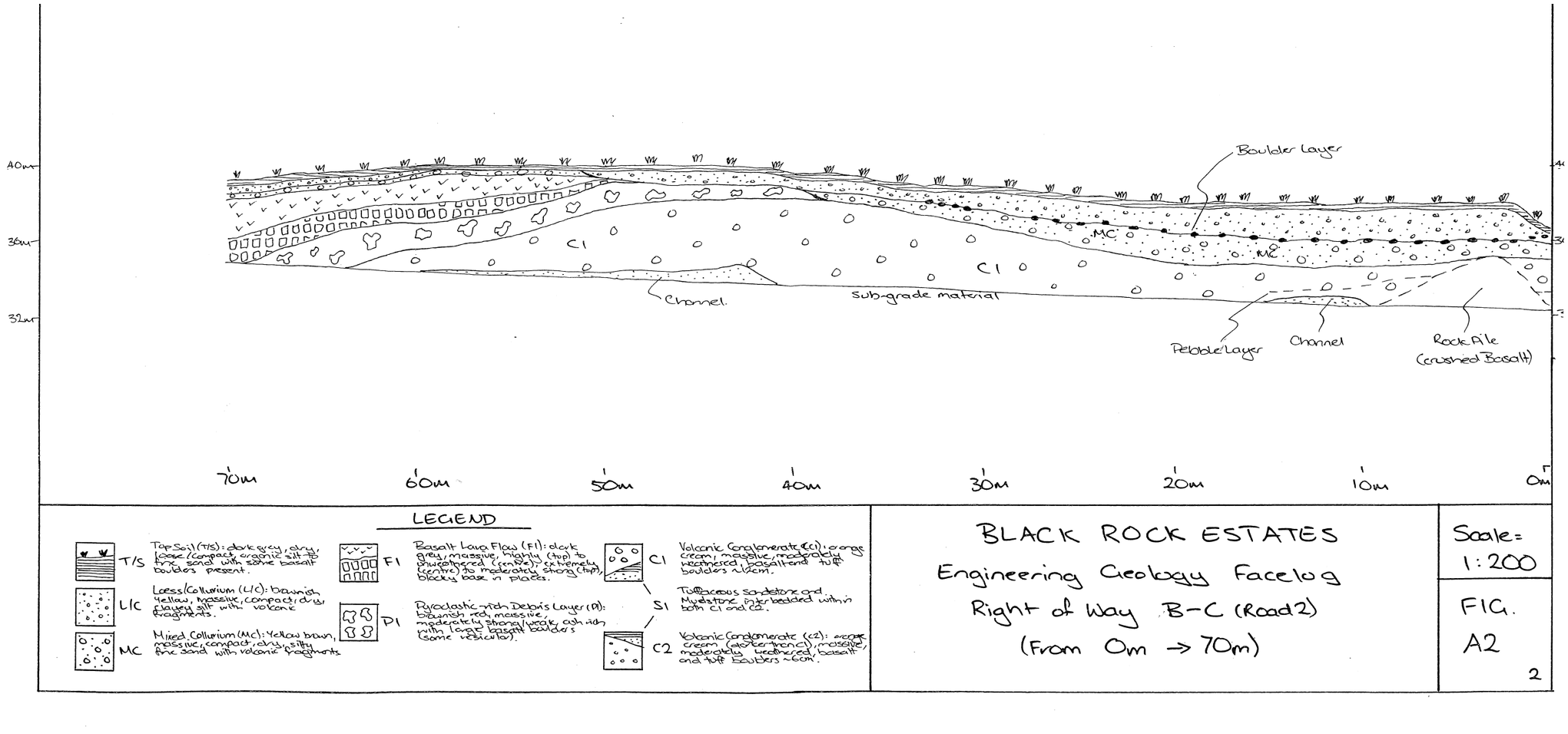

Figure 3.6. Face log at the end of the main right of way at the Black Point subdivision. S1, interspersed tuffaceous sandstone units are encountered as lenses at the base of faces. Of significance in this section is the contact between conglomerate facies and the pyroclastic horizon (F1) and lava flow of the Diamond Harbour Volcanic Group (D1).

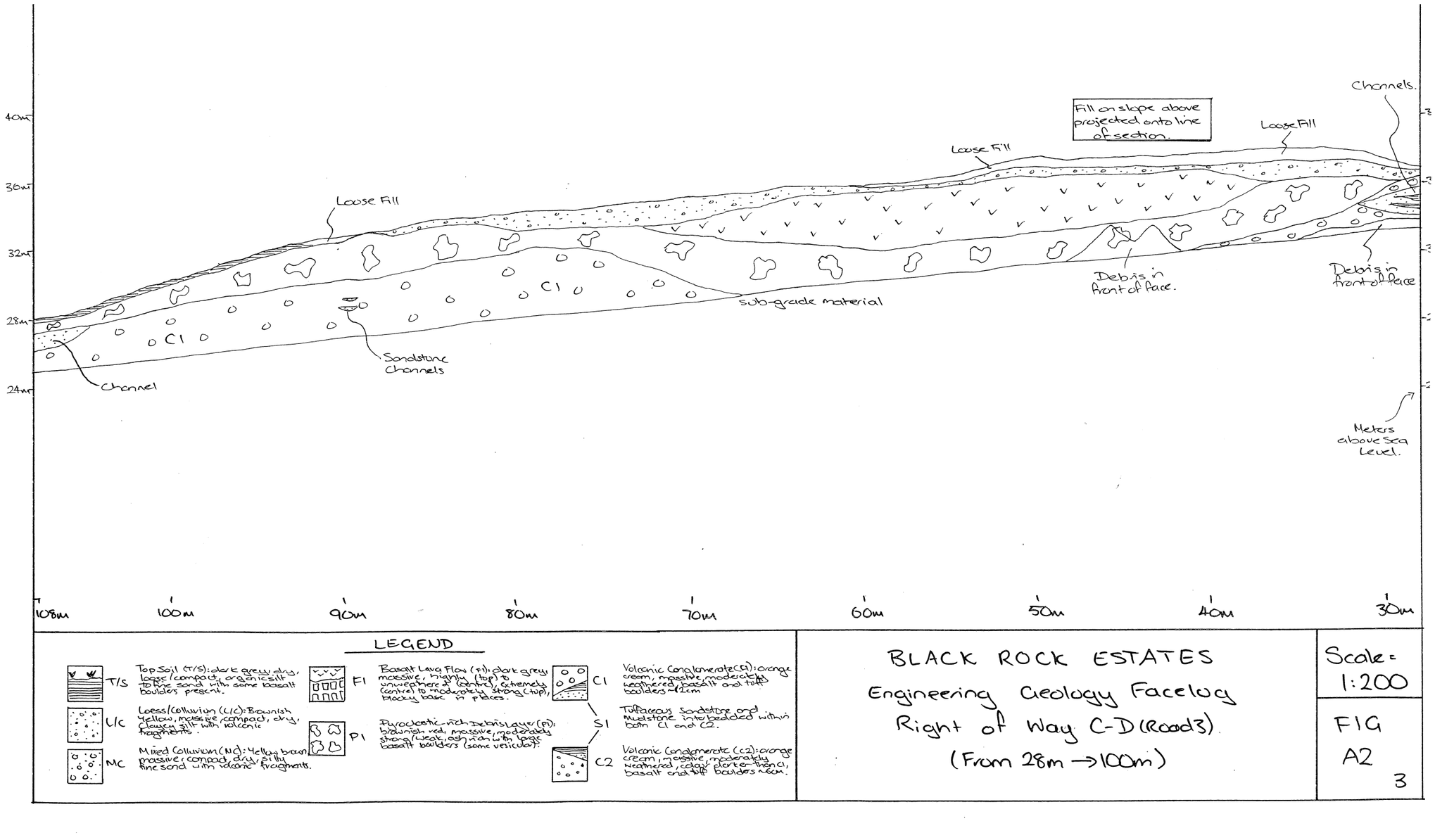

Figure 3.7. Face log highlighting the contact between conglomerate and interspersed tuffaceous units and the overlying pyroclastic-rich horizon and lava flow of the Diamond Harbour Volcanic Group. Of significance is the channelized lava flow and the underlying clast alignment (within conglomerate) indicating channel existence prior to lava flow emplacement, an aspect further highlighted in text and within Figure 3.11.

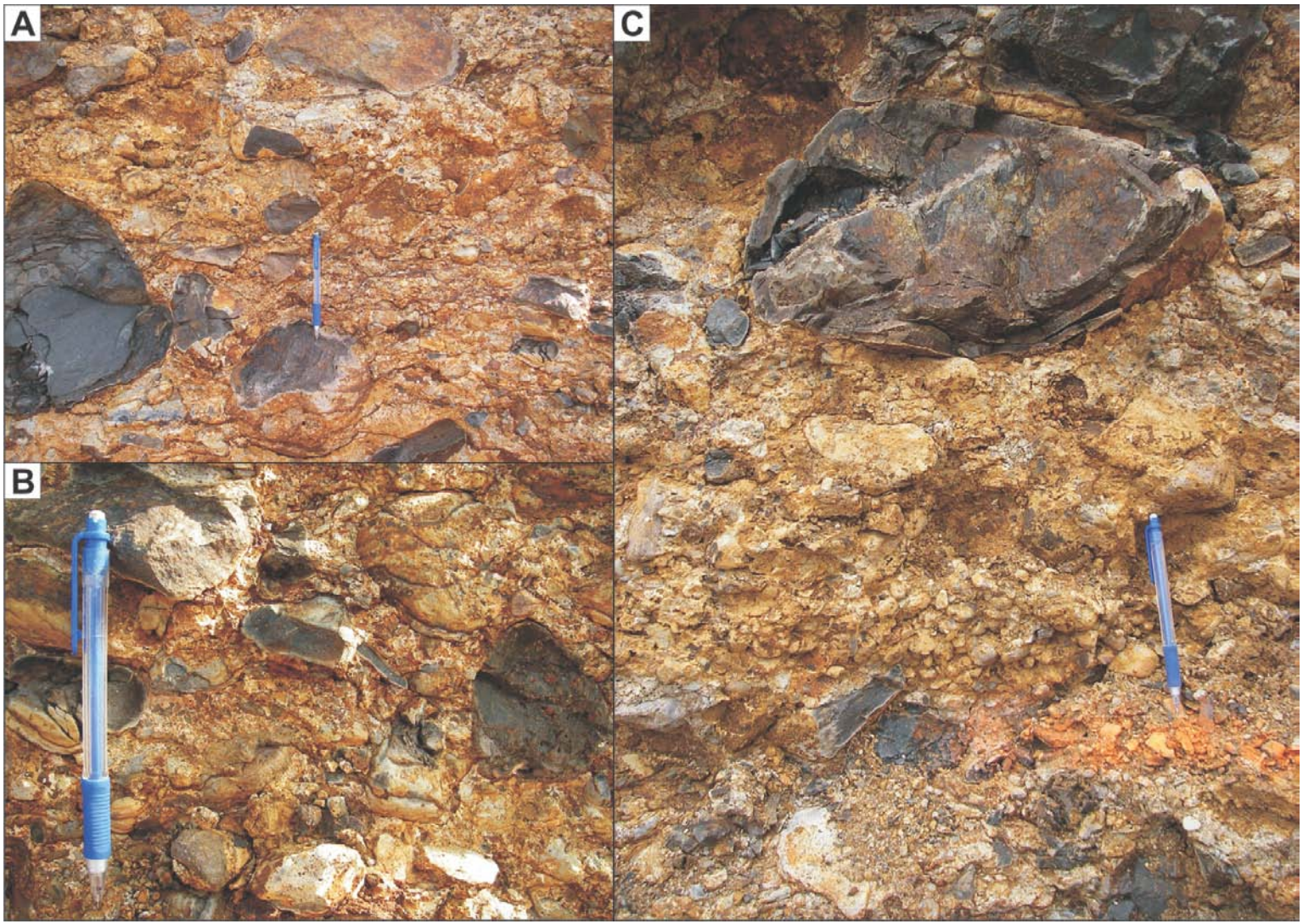

Figure 3.8. Clasts within the main sequence conglomerate. A) Sub-rounded to sub-angular clasts within a tuffaceous matrix. Note secondary iron staining. B) Weathered white outer layers on basaltic clasts, next to un-weathered fresh, aphyric basaltic clast (right hand side). C) Spheroidally weathered / onion skin weathered rind basaltic clast in a clast supported, pebble matrix. Pencil is 15cm long.

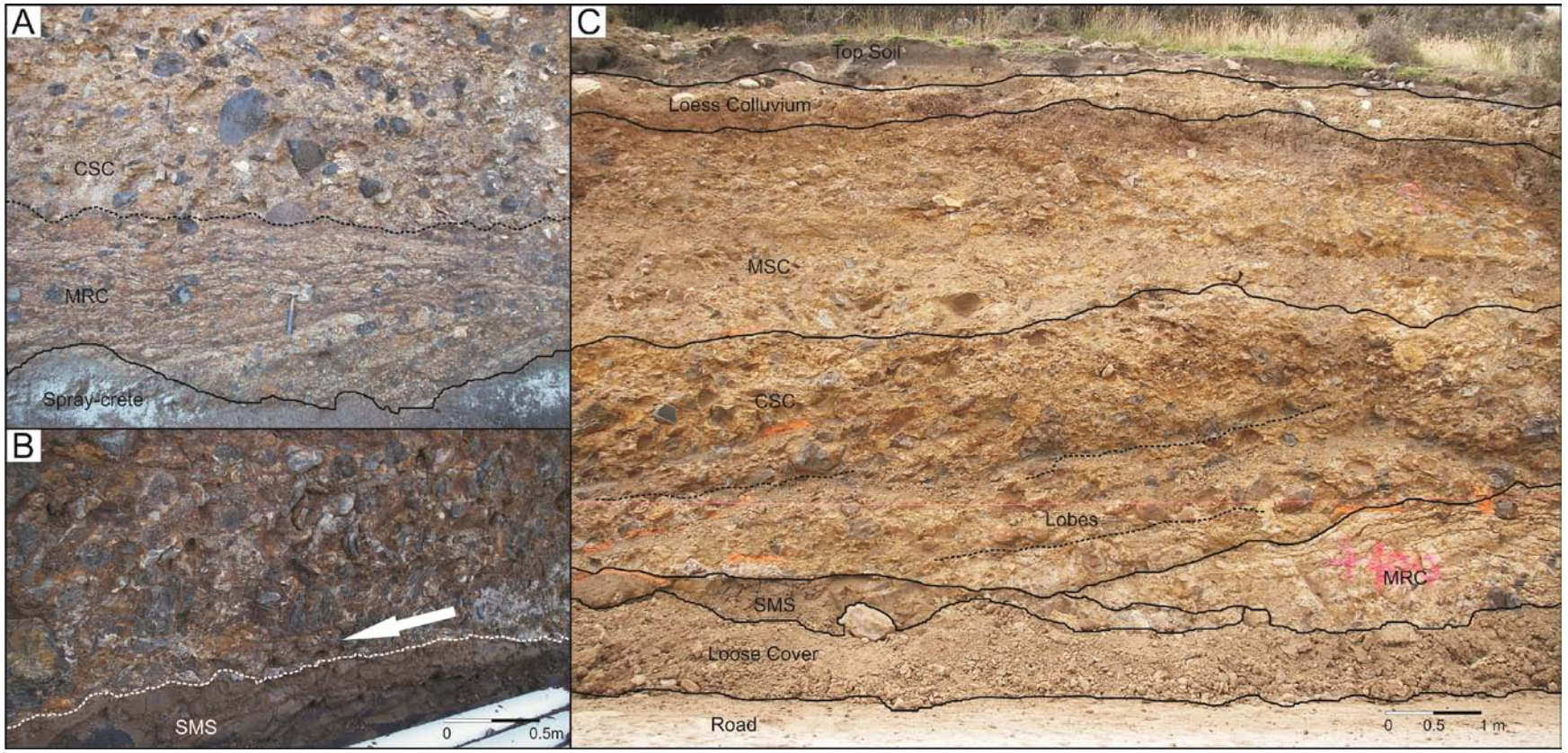

Figure 3.9. Bedding structures within the main sequence. A) Iron stained veining with a matrix-rich horizon (MRC), above which is a clast supported, poorly sorted conglomerate (CSC). B) Sheared basal tuffaceous mudstone (SMS), shears formed during debris flow emplacement, flow direction from right to left (arrow). C) Basal mudstone(SMS) overlain by a matrix-rich conglomerate (MRC) grading into clast supported conglomerate (CSC), which is capped by matrix supported conglomerate (MSC). Deposition of conglomerate is from right to left, forming lobes (black dashed lines) that thin away from source.

Facies B: Matrix Supported Conglomerate

This facies is similar to facies A, but is a slightly darker cream to orange, massive matrix-supported conglomerate (Figure 3.9). The unit is moderately weathered, with a similar clast variation to facies A (< boulder), but with granule-sized basaltic clasts being the predominant clast type. Tuffaceous sandstone clasts are still present but at a lower percentage than facies A. The matrix is fine sand to pebble, with clasts up to boulder (average size 12cm diameter). Clasts are predominantly basaltic with some moderately-indurated tuffaceous sandstone clasts.

Facies C: Interspersed Tuffaceous Units

Sandstone lenses occur throughout the sequence (Figure 3.6 and 3.7), with one of the largest being ~3m wide by 30cm deep. Lenses have channelized bases with flat tops; basal regions are sub-rounded clasts rich, matrix supported with the medium sandstone matrix supporting clasts and increasing up section (Figure 3.7 and 3.9). The top 2cm of the lens is pebble-granule-rich, with sub-rounded clasts of various compositions (red tuffaceous sandstone, basalts, red-scoriaceous clasts). At the base of the main section (Figure 3.9), is a cream brown, slightly bedded (indicated by volcanic fragment alignment), poorly indurated, sub-angular, lithic to lithic poor layered, medium to coarse grained tuffaceous sandstone.

Clast Compositions and Weathering Profiles

There is variation in composition, size, roundness, and weathering of clasts (Figure 3.8). Within the main sequence of conglomerates, clasts are predominantly basaltic, with weathered rhyolite clasts decreasing from the base of the section upwards, although there is a slight increase at the top of the sequence. Weathering of basaltic clasts within this unit is variable, with clasts having highly weathered outer rims, almost onion-skin weathering profiles (in an outcrop which has only recently been cut), to very fresh basaltic clasts (Figure 3.8). Weathered basaltic rinds reduce with increasing angular, vesicular clast and pyroclastic content near the top of the conglomerate sequence. Some tuffaceous

sandstone clasts are incorporated within the conglomerate units, and are more indurated than the interbedded tuffaceous mud to sandstones, indicating lithification prior to erosion and deposition.

Overlying Contacts

The top of the conglomerate unit is marked by an increase in pyroclastic components, both ash and fragmented basaltic clasts (Figure 3.6, 3.7, 3.11). The pyroclastic-rich layer is red-brown, varying between moderately to well indurated, fine sandstone (Figure 3.11). Clasts within the top red horizon of the conglomerate become less highly weathered basaltic clasts, with increasing vesicular basaltic clasts proportions (Figure 3.11). Large tuffaceous sandstone clasts are also present within these upper horizons. Vesicular clasts grade into the overlying Stoddart Basalt lava flow. Above this lavas flows become more massive, producing the flat lying lavas exposed on the northern point of Black Point, which then dip suddenly towards the harbour (NW).

3.3.2. Hays Bay Shore Platform Exposure

On the western side of Hays Bay (Figure 3.2) is an irregular contact between basement lithologies (Allandale Rhyolite and Lyttelton Volcanics), epiclastic deposits, and the Kaioruru Hawaiite and Stoddart Basalt of the Diamond Harbour Volcanic Group (Figure 3.12 and 3.13). On the shore platform a complex interaction between highly spheroidally weathered Kaioruru Hawaiite and Stoddart Basalt is exposed (Figure 3.12). This contact is marked by thin tuffaceous sandstone lenses / layers underlying the flow-aligned, vesicular, Kaioruru Hawaiite. On the western end of the Peninsula the relatively thin Kaioruru Hawaiite lavas drape over a pre-existing topographic high (Figure 3.12 and 3.13), steepening from ~10° to 45–50°. Conglomerate is exposed beneath this contact further to the east, where it dips steeply towards the harbour (Figure 3.13), and may only represent a thin epiclastic unit. The irregularity of the contact between Lyttelton Volcanic Group, conglomerate, and Diamond Harbour Volcanic Group lavas (Kaioruru Hawaiite) is evident

through the orientation of the vesicular horizons (Figure 3.13) and the draped lavas exposed on the shore platform and the cliff faces above.

3.3.3. Church Bay Shore Platform Exposure

The western shore platform of Church Bay (Figure 3..2) provides an exposure of epiclastic deposits interbedded with Church Basalts and overlain by Kaioruru Hawaiite and Stoddart Basalt (3.11). The base of the epiclastic sequence is poorly exposed, with limited exposures highlighting conglomerate matrix and smaller clasts infilling the irregular surface of brecciated basaltic lavas, palagonite ash and volcanic ejecta. The epiclastic sequence is a well indurated, sandstone to iron matrix-supported conglomerate. Clasts are variable, ranging from sandstone and mudstone, red oxidised lavas, rhyolite, and sub-angular to well rounded basaltic clasts. Basaltic clasts are up to 1m by 0.5m (boulders), with the longest axis aligned to the flow direction (NE; Figure 3.14). Throughout the exposure are fine to medium tuffaceous sandstone lenses with coarse sand to pebble clasts.

The epiclastic sequence is overlain by a thin (30-50cm) vesicular dark grey basaltic lava flow, followed by a red, highly vesicular, vesicle banded, flow oriented, large hornblende rich pahoehoe lava flow (Figure 3.14C and D). The contact between lavas is conformable / gradational, with lower sections of the overlying lavas showing similar vesicle alignment in a lower 10-20cm zone, becoming vesicle-poor for ~1m (stratigraphically), before grading back into an elongate vesicle rich, grey black lava (Figure 3.14D). The lower grey to red lava flow unit represents the Kaioruru Hawaiite, whereas the conformable overlying lavas are those of the Stoddart Basalt (Diamond Harbour Volcanic Group). Towards Lyttelton Harbour, the true irregularity of the conglomerate surface is expressed as localised dip direction changes of the overlying Kaioruru Hawaiite (Figure 3.14B). With overlying Diamond Harbour Volcanic Group lavas dropping in elevation from the hillside to the shore platform, changing progressively from solid to more brecciated scoriaceous lava.

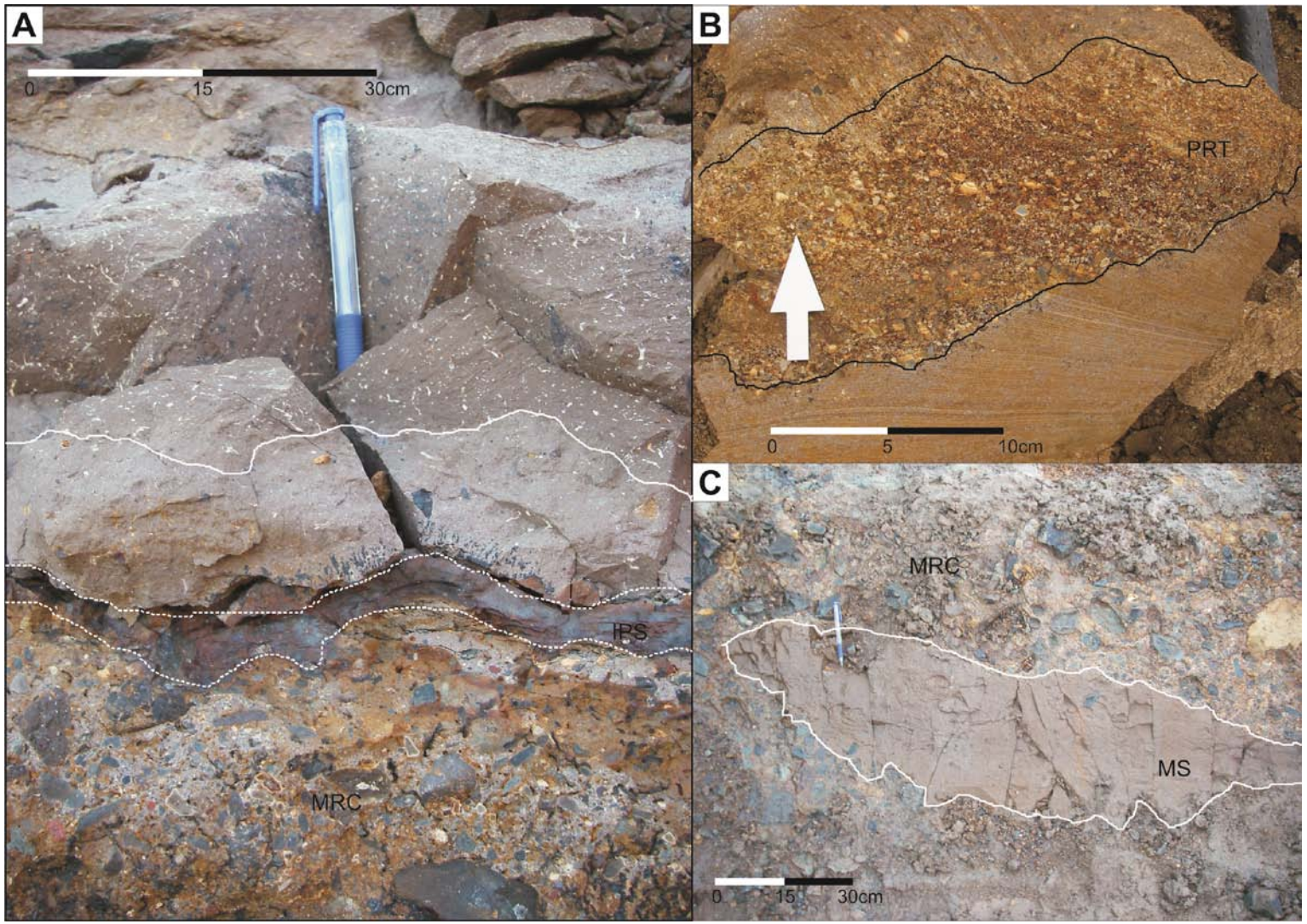

Figure 3.10. Tuffaceous mudstone deposits. A) Tuffaceous mudstone overlying a matrix-rich upper horizon of the conglomerate facies. Contact is marked by an iron pan surface. B) Secondary iron staining in tuffaceous mudstone. Mudstone is separated by a pyroclastic-rich tuffaceous horizon. C) Debris flow incorporated mudstone, fracturing within the clast indicates incorporation within flow, suggesting previous deposition and semi-lithification.

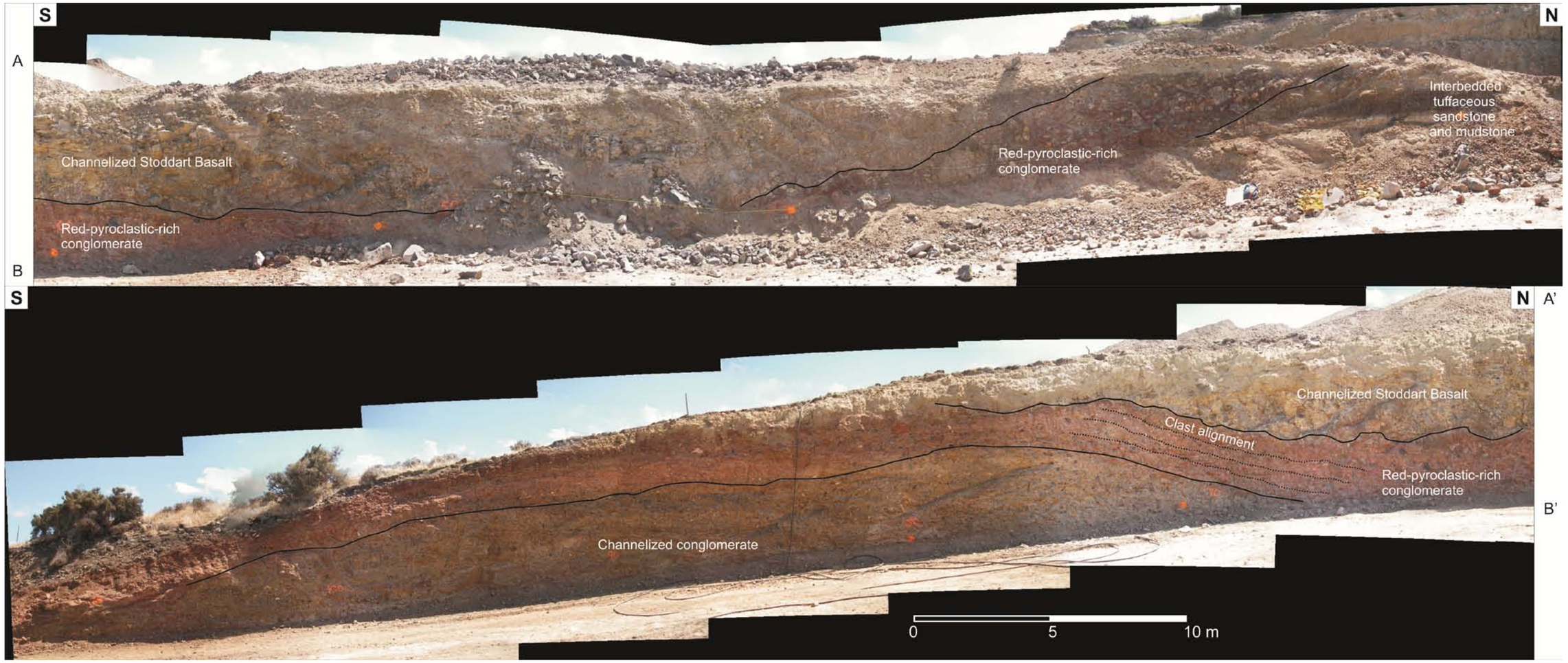

Figure 3.11. Channelized Stoddart Basalt overlying a red pyroclastic-rich conglomerate horizon, and underlying channelized conglomerate. Clast alignment in the both the channelized conglomerate and pyroclastic conglomerate mimic the contact of the overlying lava flow.

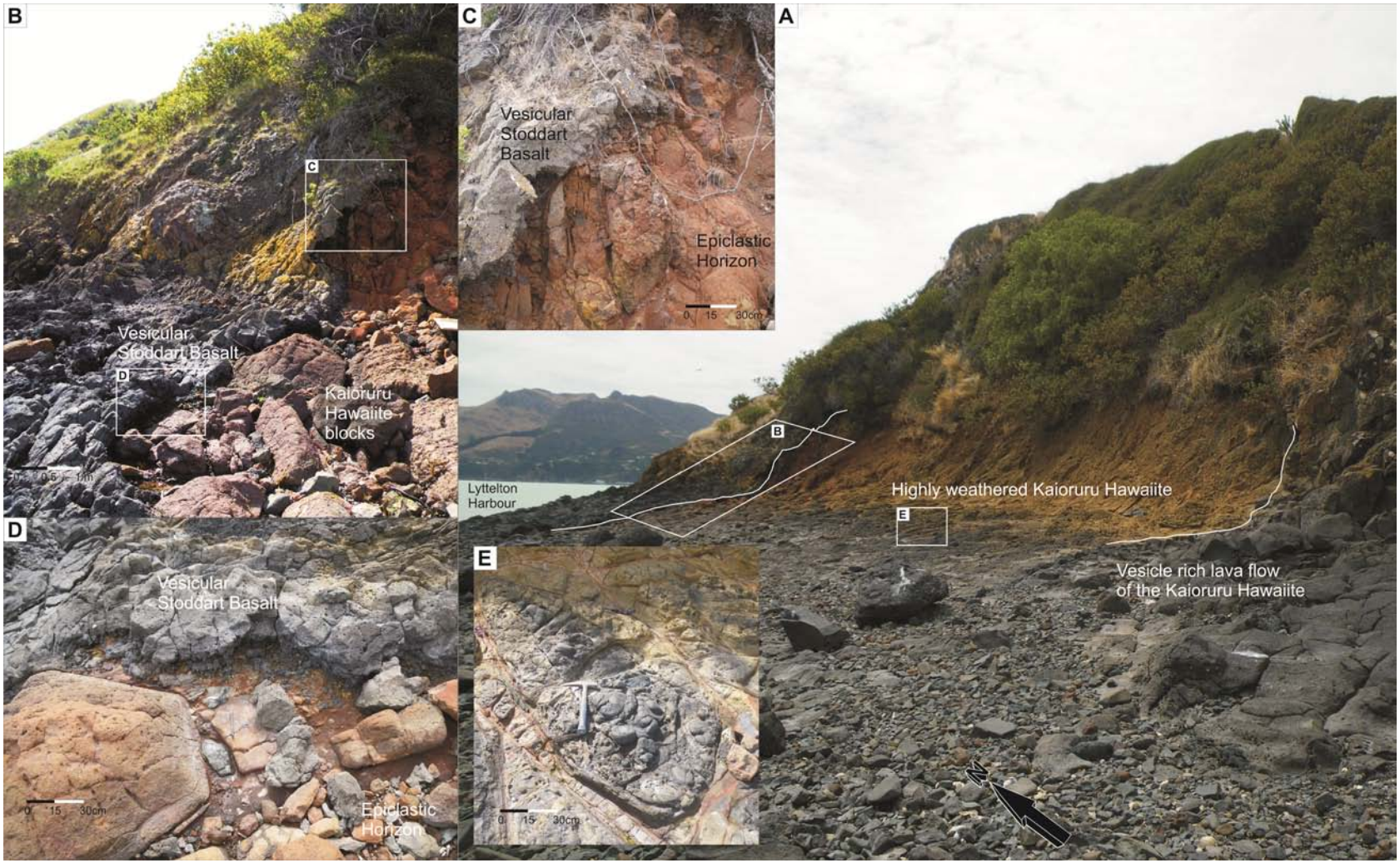

Figure 3.12. Stoddart Basalt overlying Kaioruru Hawaiite at the Hayes Bay shore platform. A) Vesicle-rich Kaioruru Hawaiite overlies a highly spheroidally weathered, Kaioruru Hawaiite. B, C, D) The contact between the Kaioruru Hawaiite and Stoddart Basalt is marked by a epiclastic horizon, related to the main epiclastic sequence. D) The highly spheroidally weathered Kaioruru Hawaiite.

Figure 3.13. Kaioruru Hawaiite lava flows at the western end of the Hayes Bay shore platform. Flows dip from east to west, with flow contacts and foliations (white lines) indicating that flows steepen in dip (arrow) towards Lyttelton Harbour (left side of photo).

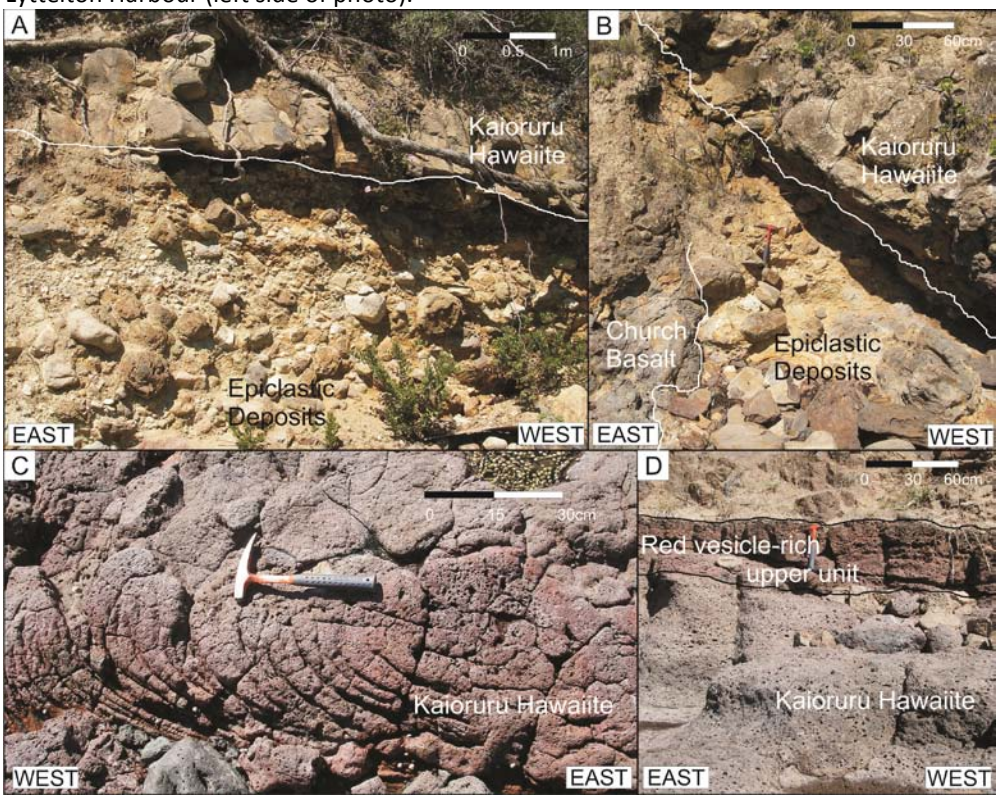

Figure 3.14. Church Bay exposures of epiclastic sequence and overlying Kaioruru Hawaiite. A) Clast-rich epiclastic overlain by thin Kaioruru Hawaiite. B) Erosional contact between underlying Church Basalt, a thinned epiclastic layer and steeply dipping Kaioruru Hawaiite. C) Ropey pahoehoe texture in the Kaioruru Hawaiite. D) Cross section view of the red, vesicle-rich Kaioruru Hawaiite, note this is the same horizon as seen in C.

3.4. Interpretation and Origin

3.4.1.Basal Units

Highly weathered rhyolite beneath the main epiclastic sequence indicates a surface that was mostly devoid of Lyttelton Volcanics prior to deposition of the conglomerate. The decreasing rhyolitic clasts component upwards in the conglomerate sequence (Figure 3.3) suggests progressive covering or exclusion of rhyolite as a source material. This basement rhyolite surface descends in height from the east to west, with the farthest western outcrop of the rhyolite at 10m above sea level (Figure 3.2). Kaioruru Hawaiites on-lap to the Allandale Rhyolite, the contact between the two dips to the east, but the exposure of Kaioruru Hawaiite drops in height to the south, indicating flow directions from the north-east.

3.4.2. Conglomerate

Conglomerate units have distinct characteristics of debris flow, hyper-concentrated flows to stream flow deposits (Sohn et al., 1999; Sohn, 2000; Lirer et al., 2001). Sohn et al., (1999) defined six facies and interpreted their origins (Table 3.1). From these classifications and interpretations the origin of Black Point epiclastic deposits is reviewed.

Basal Tuffaceous Units

Significant tuffaceous sandstone and mudstone occur at the base of the conglomerate sequence in the central regions of the peninsula (Figure 3.4). This sequence has no conglomerate inter-beds. Tuffaceous sandstone and mudstones (Figure 3.4) are finely normally graded beds (<10cm), indicating waning flow regime or depositional pulses in a relatively low energy environment (Sohn et al., 1999). No distinct channel morphologies are encountered with these deposits, suggesting a broad depositional area. Cream layers are similar in composition and appearance to the conglomerate matrix, while the red-brown layers are finer grained, with colouration reflecting oxidised horizons.

Facies	Description	Interpretation	References
Clast-Supported Conglomerate with Muddy Matrix	Medium to thick bedded, massive and ungraded, pebble to cobble sized, subangular to subrounded, and generally elongate clasts, in a poorly sorted muddy matrix, conglomerate	Debris flows (laminar shear)	Johnson 1970; 1984; Fisher 1971; Enos 1977
Clast-Supported Conglomerate with Sandy Matrix	Medium to thick bedded, massive and ungraded, pebble to cobble sized, subangular to subrounded, and generally elongate clasts, in a poorly sorted granular coarse sand, conglomerate	Debris flows dominated by frictional grain interactions	Kim et al. 1995; Sohn et al. 1997
Sand-Matrix-Supported Conglomerate	Medium- to thick-bedded, pebble-to-cobble, are poorly clasts aligned conglomerate, overlain by stratified sandy deposits	Turbulent heavily sediment-laden debris flow to hyper-concentrated flood flow	Lowe 1982; Todd 1989; Druitt 1995
Stratified Pebbly Sandstone	Thin, discontinuous interbeds parallel to bedding, generally ungraded, well- to crudely stratified pebbly coarse- to fine grained sand sandstone	Flood-flow deposits, sediment laden turbulent hyper-concentrated flood flow	Harrison and Fritz 1982; Pierson and Scott 1985; Smith 1986, 1987; Blair 1987; Smith and Lowe 1991; Best 1992
Thinly Stratified Sandstone	Thinly stratified or horizontally laminated, coarse- to fine-grained sandstones, centimeters to decimeters thick	Waning stage sheet floods or water flows, dewatering of debris flows, or reworking of surficial deposits by sheetwash during storms	Gloppen and Steel 1981; Ballance 1984; Wells 1984
Fine-Grained Homogeneous Deposits	Fine-grained deposits intercalated between gravelly and sandy beds Beds are homogeneous massive or stratified, purple, clay to muddy sand to gravelly sandstones, containing scattered granule to fine pebble clasts Thin sheetlike layers of discontinuous interbeds or meter-thick, laterally persistent beds	Inactive segments of alluvial-fan surfaces that were inundated only by occasional floods or/ Long period of fan abandonment and slow suspension sedimentation	

Table 3.1. Sohn et al., (1999) facies of epiclastic deposits and interpreted origin.

Facies A and B: Matrix-Clast Supported Conglomerate

This facies has similarities to the clast-supported, conglomerate with muddy matrix and clast-supported, conglomerate with sandy matrix of Sohn et al., (1999). Conglomerates have a distinctive layering identifiable in clast alignment, with the majority of clasts long axes aligned NNW to NNE (Figure 3.9). Stony imbrications (indicating flow directions to the NNW) are present throughout the deposit, indicating laminar shear within flow (Fisher, 1971). Tuffaceous-rich basal regions have localised fluid injections (Figure 3.9), which when combined with the evidence of flow alignment (stony imbrications) of clasts, suggests sediment laden debris flows (Figure 3.15; Lowe, 1982; Kim et al., 1995; Sohn et al., 1997).

Within the main sequence are shears (Figure 3.9), occurring in the interbedded tuffaceous sandstone layers, and in the matrix-rich conglomerate (Figure 3.9). Shears are observed in the basal sandstones propagating into the upper conglomerate sequence, accentuated by iron staining (Figure 3.9). The basal shear zones are the result of the friction generated at the base of these flows, as the water component reduces with flow distance (Assoc. Prof. Tim Davies, per comm. 2008). Shearing debris flows occur where particles are denser than the fluid with concentrations greater than 40% (Vallance, 2000).

Clast imbrications or flow alignment is related to flow regime either at the head of debris flows or in the interior (Figure 3.15; Sohn et al., 1999). The head of the flows are often, coarse grained angular clast-rich, which results in a dry, frictional flow perimeter, with the overall flow over run-out distance being normally graded (Figure 3.15; Sohn et al., 1999; Vallance, 2000). The lobate shape of deposits also supports an origin by debris flow formation, with clast-rich layers having clast alignment mimicking the lobed front of a debris flow (Figure 3.9C and 3.15). Stratification (Figure 3.9) within deposits may be due to transitional or hyper-concentrated flows, with variable grading being the result of the lateral and longitudinal variation of flows (Figure 3.15; Vallance, 2000).

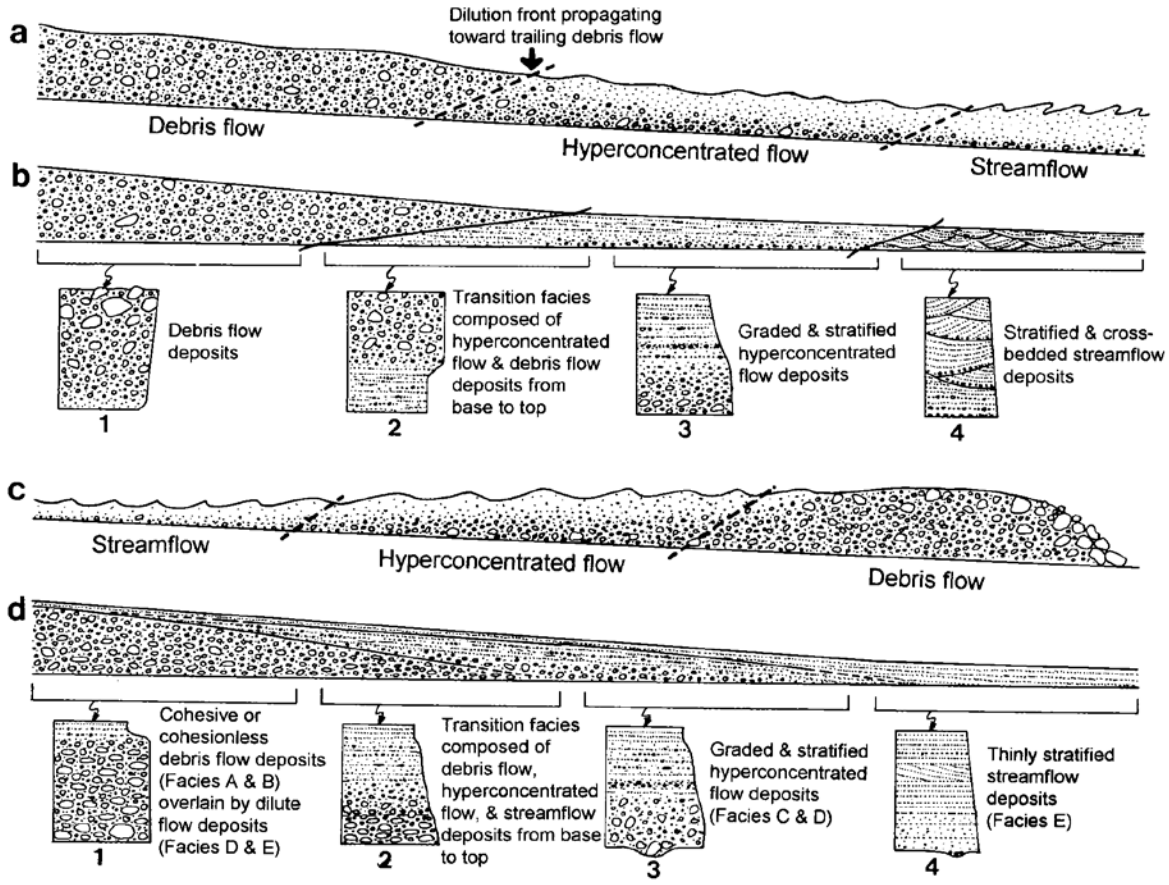

Figure 3.15. Sohn et al., (1999) transition models of stream-flow to debris flow (a), and debris flow to stream-flow (c), with interpreted stratigraphic sequences as flows proceed (b and d).

Facies C: Interspersed Tuffaceous Units

Where interbedded tuffaceous sandstone and mudstone lenses are intersected at ~90° to flow direction distinct channel structures can be observed (Figure 3.5, 3.6 and 3.7), leading to the interpretation of localised deposition in channels incised in the conglomerate (Sohn et al., 1999), hypothesised as meander bends in this debris flow dominated environment.

Channels

Channel structures, up to 10m across occur, with the larger clasts being near or in the axis of large channel structures, and smaller clasts aligned parallel to the channel structure, reflecting channel infill. The overlying Stoddart Basalt lava flow is also somewhat channelized (Figure 3.7 and 3.11), when observed at right angles to flow direction (in the

end road cutting). Channels could be the result of erosive debris flow, scouring the basal contacts (Lirer et al., 2001) or drainage incision, during periods of lower sedimentation (Palmer, 1991).

A distinct relationship between clast alignment and lava flow morphology can be established (Figure 3.7 and 3.11), in which clast orientation appears to reflect a channel orientation at the same orientation to the contact with the lava flow, with the northern end of this contact overlying a deposit of tuffaceous sandstone and mudstone, representing a low energy channel infill. Alignment of clasts within the conglomerate indicates paleo-flow directions at similar orientations to infilled channels, with incorporated clasts also reflecting this flow direction.

Overlying Contact

This pyroclastic sequence (Figure 3.6, 3.7 and 3.11) overlying and interbedded with the main epiclastic sequence is related to the overlying lava flow, with the red colouration resulting from the primary pyroclastic component or a baking / alteration from the overlying Stoddart Basalt lava flow. The basal contact of the overlying flow is unusual, with vesicular fragments being ripped or pulled away from the overlying flow during emplacement. This is similar to a peperite (Dr. K. Nemèth, pers comm. 2008), in which a lava flow interacts with soupy to wet sediments, resulting in fragmentation and incorporation of this material in the basal regions (Martin and Nemèth, 2007), implying the pyroclastic-rich conglomerate sequence was wet. The basal Stoddart Basalt flow mimics the underlying alluvial fan morphology (Figure 3.11), infilling a channel oriented to the NW.

The western side of Black Point is devoid of Church Basalt, with contacts within the Kaioruru Hawaiite marked by thin epiclastic layers (Figure 3.12). Thin sandstone layers infill small paleo-depressions on the Kaioruru Hawaiite, indicating a low energy

depositional setting, when compared to the major epiclastic sequence. These deposits, like the rest of the Black Point were capped by Stoddart Basalt.

This eastern sequence (Figure 3.14) reflects interbedded Church Basalts lavas with conglomerate, inferred to lie unconformably on Allandale Rhyolite and Lyttelton Volcanic Group. Interbedded epiclastic units are stratigraphically near the top of the Church Basalts. Clasts composition indicates variable sources, with incorporation of primary volcanic material, on or at the interbedded boundaries. Clast orientations indicate flow directions towards Lyttelton Harbour, with the channelized Kaioruru Hawaiites indicating similar down-flow directions and source regions to the southeast (Figure 3.14). These thin lavas are then covered by the thick Stoddart Basalt sequence. Stoddart Basalts on the shore platform are marked by brecciated, explosive hyaloclastic breccia, indicating magma water interaction during time of emplacement. The thick lava flow sequence above is crudely columnar jointing indicating flow and cooling took place away from water interaction.

3.4.3. Origin of Clasts and Tuffaceous Sediments

Clast Source

After initial rhyolite-rich conglomerate, basaltic clasts predominate. Matrix composition remains relatively similar throughout the entire conglomerate sequence until the appearance of pyroclastic-rich matrix ash and clasts at the top of the sequence, excluding the interbedded tuffaceous sandstone and mudstone layers. Clast composition is a direct indicator of source region. Highly weathered, white rinds on basaltic clasts (Figure 3.8C) are probably from the older Lyttelton Volcanics, with weathering variation dependent on exposure pre-deposition. Fresher basaltic samples are either freshly exposed Lyttelton Volcanics, Mt Herbert Volcanic Group, or Diamond Harbour Volcanic Group lavas (see Chapter 1) towards the top of the sequence. Tuffaceous sandstone clasts are probably from the basal volcaniclastic sequence of the Mt Herbert Volcanic Group, further

discussed in matrix source origin. Weathering rinds may also be indicative of clast alteration in-situ after emplacement. A similar relationship has been encountered on the Tongariro ring plain (Lecointre et al., 2002), with highly weathered rinds / onion-like peeling outer margins.

Tuffaceous Sediments

A key question is the source of the feldspar-rich, tuffaceous matrix, mudstones and sandstones deposits. The source region for these tuffaceous deposits is to the southeast of Black Point (Figure 3.1 and 3.2). In this region prior to the eruption of the "church-type" lavas, Allandale Rhyolite, Lyttelton Volcanic Group and Mt Herbert Volcanic Group were exposed. No tuffaceous deposits have been acknowledged or exposed in this region associated with the Allandale Rhyolite and the Lyttelton Volcanics. However, the Mt Herbert Volcanic Group has significant exposure of tuffaceous deposits (Hampton, 2005).

The Mt Herbert Volcanic Group erupted between 9.7 to 8.0Ma, in the region of Charteris Bay and central Banks Peninsula. Initial eruptions of the Mt Herbert Volcanic Group were phreatomagmatic (Mt Bradley Volcaniclastic Member (Hampton, 2005) and the Tablelands Volcaniclastic Member (Sewell, 1985; Sutton, 1987)). These eruptions occurred in the upper reaches of Charteris Bay to upper Purau Valley, south-east to east of Black Point. In the examination of the tuffaceous sandstone and mudstone units some evidence of hydrothermal alteration (sulphurous fragments) and vesicular basaltic fragments support this interpretation, as does the existence of lithified to semi-lithified tuffaceous sandstone clasts.

Matrix and Tuffaceous Sandstone Compositions

As foraminifera, marine insects, egg cases (Dorsey, 1981), and freshwater algae (Sewell, 1985) have been identified from similar deposits at Diamond Harbour and Quail Island, paleontology of the tuffaceous sandstone and mudstone units was undertaken to identify fossils. Of the four samples sieved (75µm), dried and analysed under binocular microscope

no fossils were identified. All deposits had similar compositions under the microscope, being predominantly weathered white – cream feldspar, glassy to white quartz fragments, basaltic fragments, remnant iron pan layers, and yellow sulphurous fragments. The clay rich matrix material was not analysed.

3.5. Discussion

3.5.1. Black Point

This sequence provides a unique area in which the erosion of Lyttelton Volcano and the formation of Lyttelton Harbour can be analysed. Deposits display features common to facies associated with a composite volcano's ring plain (Mathisen and McPherson, 1991), with frequent lateral facies variation in localised areas. The following provides a synthesis of the Black Point sequence.

Two epiclastic units occur in the sequence at Black Point. The first is interbedded with the Church Basalts, covered by the Kaioruru Hawaiite and Stoddart Basalt, and the second is the main sequence overlying Allandale rhyolite and interbedded with Kaioruru Hawaiite and capped by Stoddart Basalt.

The eastern shore platform indicates epiclastic deposits were being deposited throughout eruption of the Church Basalts (7.8 – 7.3 Ma). Lava flows dip to the north (into the present Church Bay), indicating a source direction to the south. Flow indicators in the epiclastic unit also align to the south, with clast types reflecting erosion to the underlying Allandale Rhyolite, Lyttelton Volcanics and Mt Herbert Volcanic Group. The contact between this lower sequence and the Kaioruru Hawaiite is highly eroded, with Kaioruru Hawaiites unconformably overlying the epiclastic deposits exposed in the cliffs above the shore platform before dropping into an eroded channel within the Church Basalts infilled with epiclastic deposits and then Kaioruru Hawaiite. Kaioruru Hawaiites descend in height to the west, and are then conformably overlain by the Stoddart Basalt. Stoddart Basalt that

reached low levels within the proto-Lyttelton Harbour interacted with water, fragmenting producing the hyaloclastic deposits on the northern end of Black Point.

The main epiclastic sequence of Black Point overlies a paleo-high of Allandale Rhyolite, on the southeast of the present day harbour. This paleo-high was progressively covered as Lyttelton Volcano developed, then became exposed as Lyttelton Volcano underwent extensive erosion, degrading to a state similar in topography to the present day. A hypothesised cross section through Black Point (Figure 3.2) indicates the relationship between the descending rhyolite high and the onlapping Kaioruru Hawaiite, infilling and overlying epiclastic sequence and the overlying Stoddart Basalts. The contact between Kaioruru Hawaiite and the Allandale Rhyolite is based on limited exposure, but is assumed to be highly irregular. Also highlighted in the cross section is the necessary removal of Lyttelton Volcanic Group material prior to the deposition of the epiclastic sequence.

Kaioruru Hawaiites stratigraphically overlie the rhyolite high to the west, although the epiclastic sequence directly overlies rhyolite to the east (uphill) and may underlie Kaioruru Hawaiite as a wedge, thinning from the northeast to southwest. Kaioruru Hawaiites erupted at 6.85 Ma, from a source vent hypothesised to the east, now covered by Stoddart Basalt flows. These lavas infilled the irregular topography of the eroded rhyolite and underlying Church Basalt and epiclastic sequence.

Lower tuffaceous sandstone and mudstone beds reflect a low energy depositional environment, isolated from the main epiclastic sequence, although stratigraphic relationships indicate it later became covered. This depositional low point existed due to the Allandale Rhyolite descending to the west, with Kaioruru Hawaiite lavas covering this highly irregular surface producing further localised depressions. This resulted in a low lying depression, in which tuffaceous sediments accumulated. The lack of fossil remnants within this sequence indicates an environment not conducive to biologic activity, through rapid sedimentation or anaerobic conditions.

The main epiclastic sequence represents a series of debris flows following a valley system depositing as an alluvial fan system, controlled by eroding basement lithologies (Allandale Rhyolite and Lyttelton Volcanic Group lavas) and the Mt Herbert Volcanic Group. Sandstones and mudstone layers are indicative of paleo-depressions on the alluvial plain, while smaller tuffaceous sandstone lenses are low energy deposits in small meander bends, deposited during fluvial dominated periods. Channel orientations throughout the conglomerate sequence indicate the axis of predominant drainage had limited migration overtime, primarily draining between the NWW and NNE, into a proto-Lyttelton Harbour, between ~7.8 to 6.8Ma, based on stratigraphic relationships. This fan was fed with debris from the exposed Allandale Rhyolite, Lyttelton Volcanic Group, Mt Herbert Volcanic Group lavas and tuffaceous units, and towards the top of the sequence with primary volcanic fragments of the Stoddart Basalt.

Epiclastics were preferentially deposited in this area due to the control of the Allandale Rhyolite basement high, Lyttelton Volcanics and Mt Herbert Volcanic Group, with the overall paleo-valley system later being infilled by the Diamond Harbour Group lava flows. An important aspect of the main epiclastic sequence is the exclusion of the Church Basalts and Kaioruru Hawaiites prior to the Stoddart Basalt lava flows. The Church Basalt were small localised eruptions on the eroding Lyttelton Volcano (Sewell, 1988). In examining the location of the Church Basalts, they are confined to the north of the Allandale Rhyolite high, limited to the low lying regions as the top of the conglomerate was at significant elevation, and the morphology of the fan surface restricted flows to the topographic lows to the side of the fan surface. It is hypothesised that the Church Basalt in this region were being erupted contemporaneously with the early stages of deposition of the conglomerate, exposed in the eastern shore platform.

The main sequence of Black Point however overlies middle to upper lava flows of the Kaioruru Hawaiite on the western shore platform. This indicates the main sequence of epiclastics were deposited contemporaneously throughout the eruption of the Kaioruru

Hawaiite, as the contact between Kaioruru Hawaiite and the overlying Stoddart Basalt is marked by a thin red epiclastic horizon on the shore platform. Kaioruru Hawaiites overlying the main epiclastics sequence are highly irregular, defining the upper surfaces of epiclastic. Where this contact is observable the Church Basalt lavas descend rapidly over the conglomerate, supportive of the lobate morphology of the alluvial fan and individual debris flows. The Kaioruru Hawaiite follow a similar deposition regime as the Church Basalt, but had a larger alluvial fan surface to erupt over, due to eruptive centre location, suggested to be covered by the Stoddart Basalt lava flows of the Diamond Harbour dip slope.

The Stoddart Basalt erupted during the last stages of the main epiclastic sequence, highlighted by the red, pyroclastic rich horizon at the top of the sequence. Stoddart Basalt flows are found stratigraphically lower on the eastern side of Black Point (Figure 3.2), suggesting that as these lavas flowed from the east, they progressively infilled the lower regions of the proto-Lyttelton Harbour, and resulted in the thickest Stoddart Basalts being focussed to the north-eastern side of the Peninsula.. These lavas had limited coverage over the rhyolite high, supporting the concept that Stoddart Basalts were channelized by the underlying lithologies. Initial flows at low levels interacted with water, reacting explosively forming hyaloclastic breccia. On the north-western end of Black Point flows drop steeply over the lobate edge of underlying lithologies, producing the lavas that cap Black Point and the steeply dipping lavas of the shore platform and cliffs.

The following provides a summary of deposition and emplacement for the Black Point epiclastic sequence.

1. Extensive erosion to Lyttelton Volcano, uncovering basement Allandale Rhyolite, and removal of Lyttelton Volcanic Group flows.
2. Eruption and deposition of the interbedded epiclastic sequence and the Church Basalt at the low lying edges of the alluvial fan.

3. Eruption of the Kaioruru Hawaiite over the low lying areas of Allandale Rhyolite and Church Basalt. Contemporaneous deposition of the epiclastic sequence, beginning with the basal, rapidly depositing tuffaceous sandstone and mudstone. At higher levels an alluvial fan system began to develop in this region, fed from the larger paleo-valley to the east.
4. Continued eruption of Kaioruru Hawaiites at lower areas of the alluvial fan complex, mantling the channelized fan surface.
5. Eruption of the Stoddart Basalts, producing a thick series of lava flows, sourced in upper Purau Valley, which further mantled the fan surface, invading Lyttelton Harbour.

3.5.2. Relationship to Epiclastic Deposits in the Interior of Lyttelton Volcano

As discussed earlier epiclastic deposits are exposed from the upper valleys to the shore platforms on the eroded Lyttelton Volcano. These units are of significance as they indicate erosive and depositional time periods, bounded by volcanic activity, and provide key marker horizons in the erosional stages for Lyttelton Volcano.

Highlighted within this study is the development of an alluvial fan system, which invaded the eroded interior of Lyttelton Volcano. Of significance is the timing of deposition of conglomerates constrained through the interbedded and overlying Diamond Harbour Volcanic Group lava flows. When combining the hypothesised model of deposition of Black Point with the previously observed sequences around Lyttelton Volcano, a schematic model of Lyttelton Volcano's erosive state at distinct time periods can be suggested.

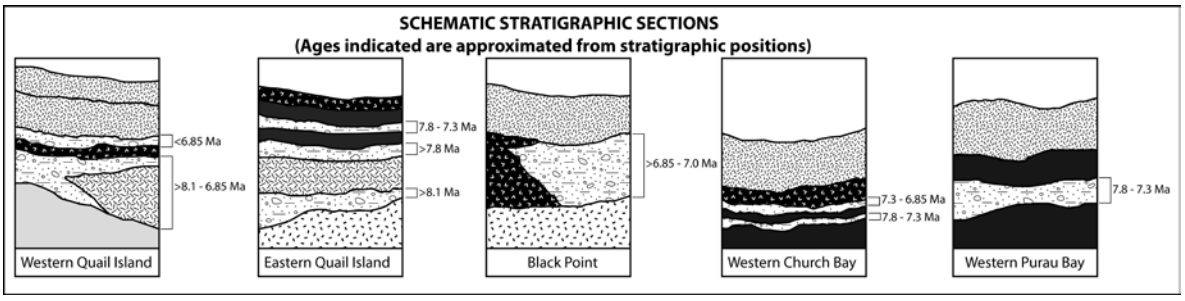

Figure 3.17. Schematic stratigraphic sections of the epiclastic deposits exposed around Lyttelton Harbour. Sections are a synthesis of Dorsey (1981), Sewell (1985) and Sewell et al., (1988), further refined through field studies within this study.

Figure 3.17 provides schematic stratigraphic sections of key conglomerate exposures about Lyttelton Harbour. Key aspects of these sequences are the epiclastic horizons separating lava flows of the Diamond Harbour Volcanic Group. The following (Figure 3.18) highlights stages of volcanic activity and deposition in the interior of the eroding Lyttelton Volcano.

A proto-Lyttelton Harbour (Figure 3.18A) had to be in existence by at least 8.0 Ma based on the age determinants for the earliest Diamond Harbour Volcanic Group lavas (Stipp and McDougall, 1968), a minimal age as based on field observations and those of Sewell (1985) conglomerate underlies these unit. It is suggested that Lyttelton Harbour would have been in a similar erosional state as today, with a predominant drainage network down the harbour, but with relative sea level being well below present levels

Localised eruptions (Figure 3.18B) of the Darra Basanitoid (8.1 – 7.3 Ma) also occurred in the eroded Lyttelton Volcano, exposed on the western and eastern sides of Quail Island. Church Basalt (7.8 – 7.3 Ma) was confined to lower areas around the edges of alluvial fans, becoming interbedded with units. The source of Church Basalt is unknown, although possible vents are exposed on Tableland Spur and to the south of Mt Herbert summit (Sewell, 1985). There is no evidence that the alluvial fan system of Black Point extended to the conglomerate sequences exposed at Quail Island (Figure 3.17), as the two are at different stratigraphic heights, and have different channel orientations and clast imbrications, and the non-existence of significant epiclastic deposits on the western shore

platform of Black Point. This leads to the suggestion that several fluvial systems were feeding into a larger proto-Lyttelton Harbour (Figure 3.18B), which at the time was draining down its current orientation (NNE).

There was a large alluvial fan system on the south-eastern side of proto-Lyttelton Harbour and smaller alluvial systems in the base of the harbour, draining the upper harbour (Charteris Bay, Head of the Bay, Governors Bay and Gebbies Pass; Figure 3.1), with clast lithology supporting this. The extent of the south-eastern alluvial fan system was probably confined to a region where Black Point epiclastic deposits mark the southerly extent, and the thin Purau Bay epiclastic deposits marks the northern extent, with the overall morphology of the valley system feeding this alluvial system highlighted through the infilling lava flows of the Kaioruru Hawaiite (Figure 3.18C), Diamond Harbour Volcanic Group. Extensive Stoddart Basalt lava flows erupted in the upper reaches of Purau Valley (Sewell, 1985), and were directed down this paleo-valley system invading proto-Lyttelton Harbour. An aspect further investigated in Chapter 6.

It is hypothesised that the north-western side of proto-Lyttelton Harbour was not as deeply eroded as the eastern side, as the late stage epiclastic sequence underlying the Stoddart Basalt dips to the southeast, indicating high topography to the north-west (Figure 3.18D). This is further supported as flows of the central area of Lyttelton did not flow further to the northwest. Since eruptive activity ceased Lyttelton Harbour has undergone significant erosion, the flat lying lavas of the Diamond Harbour Volcanic Group have remained relatively intact, with a young paleo-drainage system evident on the upper surface of the Diamond Harbour dip slope. Low lying Diamond Group flows now form Quail Island and various shallow reef and island systems throughout Lyttelton Harbour, indicating the extent to which these lavas flowed.

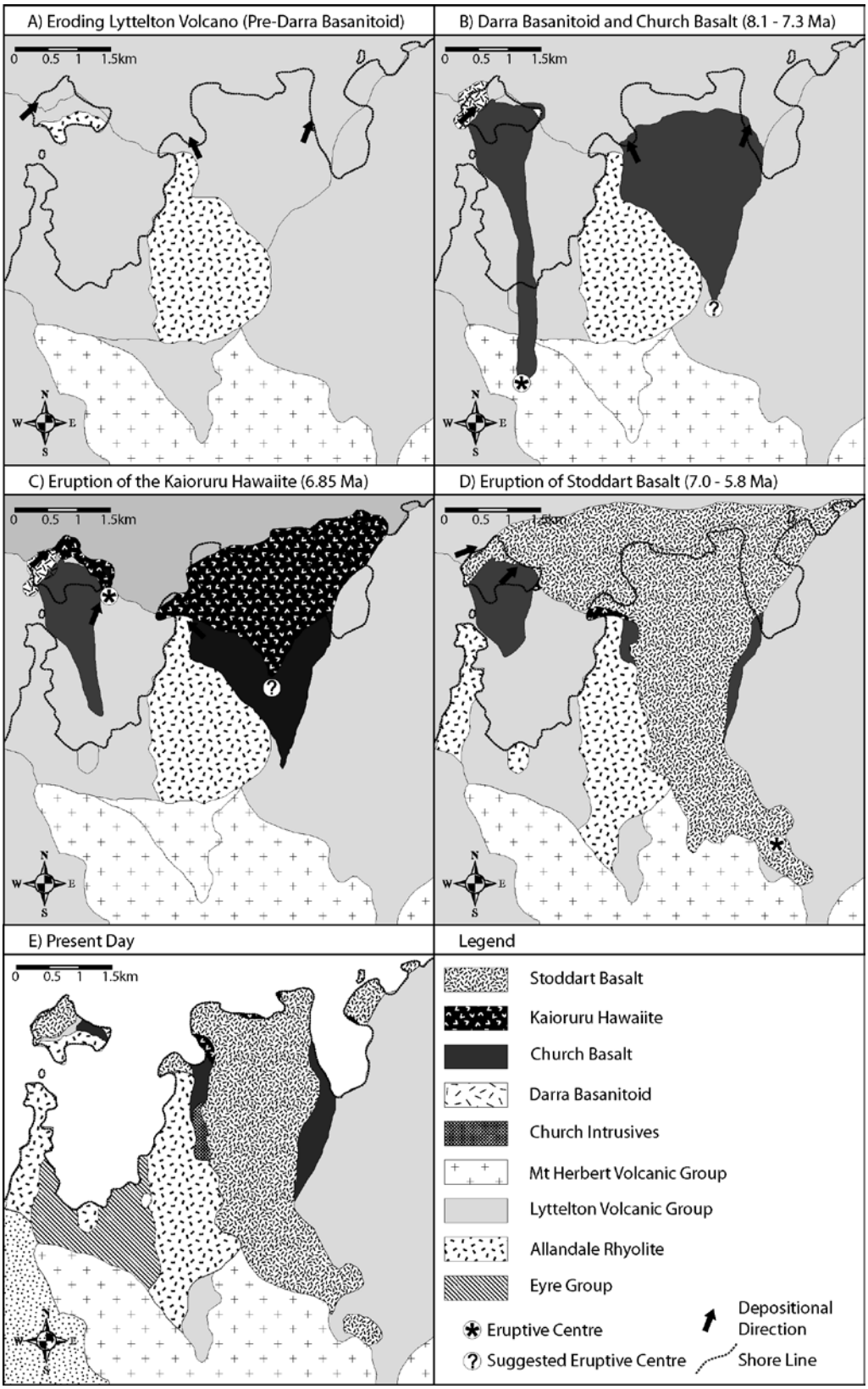

Figure 3.18. Schematic evolutionary model of central Lyttelton. Eruptive centres of the Darra Basanitoid and Church Basalt are speculative.

3.6. Summary

- Epiclastic deposits on the south-eastern side of Lyttelton Harbour indicate deposition within the highly eroded Lyttelton Volcano since 8.1 Ma.
- Basal conglomerates of the main epiclastic deposit at Black Point overlie and incorporate Allandale Rhyolite, indicating a deeply eroded Lyttelton Volcano.
- Clast lithology and morphology is dependent on bedrock exposure prior to deposition, with some weathering rinds formed post-deposition due to in-situ alteration.
- Clast alignment and channel orientations indicate a depositional system dipping to the NNW to NNE, into a paleo-Lyttelton Harbour.
- Black Point conglomerates are deposited from debris flows and transitional hyper-concentrated debris flows, in an alluvial fan system.
- Tuffaceous sandstone and mudstone indicate localised deposition in meander bends and paleo-depressions on the alluvial system.
- The alluvial system and proceeding volcanism was directed into paleo-valley systems, topographically controlled by the underlying basement and surrounding Lyttelton Volcanics and Mt Herbert Volcanic Group.
- Tuffaceous sandstone clasts and matrix components of the Black Point deposits are suggested to have originated from the volcaniclastic deposits of the Mt Herbert Volcanic Group.
- Lava flows of the Stoddart Basalt infill paleo-channels within the Black Point epiclastic deposits. Basal Stoddart Basalt lava flows are perperitic, indicating fragmentation of lavas by soupy-wet tuffaceous sediments.
- The north-western side of proto-Lyttelton Harbour was not as eroded as the eastern side, limiting the extent of the infilling Diamond Harbour lavas.

CHAPTER 4

LAVA FLOW PACKAGES OF LYTTELTON VOLCANO: DISTINGUISHING BLOCKY LAVA FLOWS FROM A'A LAVA FLOW SEQUENCES

4.1. Introduction

Lyttelton Volcano is comprised of lava flows, and interbedded clastic deposits (Sewell, 1985), that Shelley (1987) considered to radiate about two eruptive centres, Lyttelton 1 and Lyttelton 2. Lava flows are primarily a'a, however this study has recognised distinct thick lava flow horizons, comprised of extensive brecciated material, exposed on the inner slopes of Lyttelton Harbour. This chapter investigates these brecciated horizons, reviewing the classification system of a'a and blocky lavas, and provides detailed description and analysis of three brecciated exposures, and discusses a summary classification for a'a to blocky lava flow characteristics of Lyttelton Volcano.

4.2. Physical Characteristics of A'a and Blocky Lava Flows

A'a and blocky lava flows represent end members of basaltic-andesitic flow regimes (Kilburn, 2000). A'a lavas are flows with extremely irregular surfaces, usually covered by fragments of broken crust that are typically decimetres thick, with thickness controlled by cooling (Kilburn, 2000), while blocky lava flows have fractured surfaces, usually covered by blocks (up to a metre) with smooth, planar and angular surfaces (Kilburn, 2000). Blocky lava is commonly confused with rubbly a'a lava flows (Williams and McBirney, 1979). In this study we follow MacDonald's (1953) classification, with a'a being "characterised by a rough, jagged, spinose and generally clinker surface"; and the term blocky "restricted to a type in which the fragments lack the characteristic spininess of a'a", and follow the typical downstream change in crustal morphology, of pahoehoe, cauliflower a'a, rubbly a'a, to blocky lava flows (Kilburn and Guest, 1993).

A'a lava flows initially advance as sheets, with intermediate lavas advancing through fracture and flows, but finishing as near-solid masses that fragment throughout their thickness (Kilburn, 2000). Blocky flow fronts advance as crumbled snouts of debris, primarily due to fracturing of lava to form flow fronts 10's of metres thick, whereas typical a'a flow fronts are less than 20m in thickness (Kilburn, 2000). The external and internal surfaces and structures of a'a and blocky lava flows are distinct, and it is used in this chapter to further distinguish a'a and blocky lavas within the brecciated sequences of Lyttelton Volcano.

4.2.1. A'a Lava Flows

In contrast to pahoehoe lavas, a'a lava flows are jumbles of rough, clinkery, and spinose fragments, ranging from small chips to blocks measuring metres. Williams and McBirney (1979) classified three types of a'a flows:

1. Rubble flow: a flow of small loose, and semi detached fragments.
2. Clinker flow: a flow in which fragments measure more than several centimetres across.
3. Furrowed flow: a flow in which surface forms are intermediate between those of a'a and pahoehoe.

Kilburn and Guest (1993) defined two key a'a surface textures / block components on Mt Etna:

1. Cauliflower: Crust twist upwards as cauliflower-like protrusions. These break to give fragments up to decimetres across. Surfaces are grey-black, often glassy, and rough and spinose at the millimetre scale.
2. Rubbly: Crust fractures downward to yield rounded rubble up to metres across, often with an ochre-black granular surface (resembling granulated sugar), millimetres deep. The surface is fractured and highly irregular, with rubble tending to infill surface depressions, and may leave upstanding sections of massive lava exposed.

Two features common in a'a flows are ogives and tumuli. Ogives (complex downstream folds), formed though surface buckling, may form on the surfaces of both cauliflower and rubbly a'a, with wavelengths and amplitudes of the order of 10m and 1m respectively (Kilburn and Guest, 1993). Tumuli are uplifts of the solidifying vesicular crust of a flow, formed through magmatic pressure (Nèmeth and Martin, 2007). Tumuli formation is common in pahoehoe but can occur in a'a lava flows, as that observed at Mt Etna (Duncan et al., 2004).

4.2.2. Blocky Lava Flows

MacDonald (1953) stated that the "block lava is distinguished from true a'a by the fact that the individual fragments are relatively smooth polyhedral blocks bounded by dihedral angles; lacking the spinose character of typical a'a". Williams and McBirney (1979) defined blocky lava as "flows made up largely of detached, polyhedral blocks with plane or slightly curved faces and conspicuous dihedral angles. The blocky tops almost invariably pass downward into massive, unbroken lava in the interior, and this in turn grades into an auto-brecciated basal layer."

Blocky lavas are similar in appearance to a'a lava flows. Avery (2000) highlighted three distinct differences between the two flow types, based on Ruapehu's basaltic-andesite lavas:

1. The upper surface of block flows consist of fragments that are more regular and have smoother faces than a'a lava.
2. Blocky lavas are covered by a greater number of blocks than a'a flows.
3. Blocky flows are not as common as pahoehoe and a'a flows, mainly because they represent a late stage of flow development, which is not always reached.

Avery (2000) highlighted the fact that blocky lava flows exist in a variety of terrains, but tend to form in areas of low relief, where lavas have a slow advance rate. Surface features of blocky lava flows were identified by Williams and McBirney (1979), with one flow being described as having "arcuate, alternating ridges of non-vesicular to and highly vesicular blocks." Also noted was fluidal banding in siliceous block flows, with these features being contorted and cut by ramp-like shear planes. Avery (2000)

observed ramping structures where the interior massive lavas ramped over and around fragmented and folded flow-banded blocks.

4.2.3. Defining Characteristics of A'a and Blocky Lava Flows

Block Morphologies

Block morphology is the key distinguishing feature between a'a and blocky lava flows. MacDonald (1953) described the outer surfaces of a'a blocks as being exceedingly rough, irregular and spiny, medium to coarse sand in appearance. Kilburn and Guest (1993) described this sugary texture of clasts as sub-angular, equant protrusions resembling granulated sugar, and become more abundant with depth in the upper part of the flow. McDonald (1972) suggested this resulted from attrition along fracture surfaces in the flow. Kilburn and Guest (1993) hypothesised two mechanism of formation; the first due to rapid cooling of newly exposed surfaces, producing millimetre size irregularities, the second by tearing, where tiny cracks form along incipient planes of failure. Blocks have few abrasion features, with the minimal abrasion forming fine dust on many flows (MacDonald, 1953). Spinose blocks are commonly connected to the solid internal flow component, developing through squeeze-up through cracks in the flow surface (Jaggar, 1930).

Matrix

Interstitial spaces within a'a flows are filled with rubbly scoriaceous debris with clasts size ranging from 5-30cm, with the majority of clasts being fragments of the adjacent larger blocks (Avery, 2000). Fragmented material usually makes up the bulk of a blocky lava flows thickness, but some massive central lava is typical (Avery, 2000). Blocky lavas have a larger abundance of blocks, and block size and shape, when compared to a'a flows (Avery, 2000). While "both the fragmental and massive parts of block lava flows generally contain a larger proportion of glass than do the corresponding portions of a'a lava flows" (MacDonald, 1953).

Flow Interiors

A'a flows are divided into three parts with gradational boundaries: upper and lower, comprise lava flow crusts and fractured inner lavas, forming fragmented clinker that may be welded together (welded clinker or flow breccia; MacDonald 1953); middle, massive lava with irregular elongate vesicles, drawn out in response to internal flow (Cas and Wright, 1987). Whereas the massive internal layer of blocky lavas occurs near the base of the flow as a continuous bed or as a series of lenses grading upward and laterally into the breccia (MacDonald, 1953). In the internal solid lava component of both a'a and blocky flows, platy joints form (Avery, 2000). These 1-2cm platy joints closely follow the underlying surface, ramping (over larger blocks) and bending in various directions, throughout the flow (MacDonald, 1972). MacDonald (1953) considered platy joints to result from extremely high viscosity, with the friction within the flow creating sheets, which interact like a stack of cards. Cas and Wright (1987) attribute this flow foliation to shear partings in a laminar flow, and in ancient rocks can commonly be confused with densely welded tuffs.

Squeeze-ups

Squeeze-ups or the upward injection of coherent lava into brecciated lava are the forms produced from the hotter flow interior shearing upward and forward, into the overlying breccia front. Squeeze-ups are observed at all three exposures. Squeeze-ups have a distinct alignment of phenocryst and elongate vesicles on the outer margins. Squeeze-ups bifurcate as they ascend into the overlying brecciated lavas, partially losing coherency to become detached brecciated blocks.

Shear Planes

Shearing is commonly associated with a'a and blocky flows, being most pronounced at the sides and base of flows where friction levels are highest (Avery, 2000). MacDonald (1972) hypothesised that it is this ramping and irregularities with flows that form the upheaval of lava surfaces, and the formation of small hills on the tops of blocky lava flows. Accompanying platy lavas are massive jointed, flow banded, flow interiors, which are proportionally smaller in blocky lavas, compared to the interior of a'a flows

(MacDonald, 1972). Avery (2000) noted discontinuous columnar jointing in the upper half of massive flow interiors.

Levees

An a'a lava flow is typified by a large central channel bounded on each side by levees. Levees form from the cooled debris fallen from the sides of the frontal zone (Kilburn and Guest, 1993). Levees act as an insulator, enabling flows to have extensive run-out distances. Kilburn and Guest (1993) termed two types of levees, single lateral levees and multiple, medial and compound levees. Single lateral levees confine flows to a single channel, with levee sides becoming stable with spreading only at the flow front. Single lateral levees are classified into:

1. Massive Levees: have internal tripartite structure of channel material. Common in the distal zone of evolved flow. In a'a flows external margins dip outwards at 40-50°.
2. Overflow Levees: Common in middle and upper reaches of flows. These have layered interiors (massive lava alternating with auto-brecciated horizons), the massive lava levels representing channel overflow. Progressive overflows may produce outward dipping external surfaces up to 25°.
3. Debris Levees: Accumulations of poorly-sorted lava fragments and cauliflower a'a. Outward dipping external slopes are between 30-35°.
4. Accretionary Levees: Outer surfaces are comprised of welded lava debris. Appear close to vents as narrow, upward tapering walls, tens of cm wide and 1-2m tall. External and internal surfaces dip at greater than 50°.
5. Swollen Levees: Lateral intrusion of channel lava, causing swelling and may lead to internal levee auto-brecciation to local extrusions through the levee exterior.

Avery (2000) states that levee structures do not form on blocky lava flows due to the high viscosity lavas, resulting a fan array of multiple flow tongues. MacDonald (1953) provided limited discussion on levees of blocky lava flows, although indicates that the overall structure of block flows is common to a'a flows, to which one has to assume

incorporates levees. Cas and Wright (1987) in review of lava flows state that short block flows sometimes have well developed levees.

4.3. Lyttelton Lava Flows

4.3.1. Lava Flow Analysis

Analysis of Lyttelton Volcano lava flows was through field observation supported by aerial photograph analysis (Figure 4.1). This allowed major lava flows to be identified on aerial photographs, imported into ArcScene (ArcGIS Version 9.2), and draped over a 10m resolution DEM.

This technique was used to highlight Lyttelton Volcano's lava flow sequences. What became immediately apparent is the irregularity of flows, and the oblique angular relationship between lava flows and the circular crater rim (Figure 4.1). Shelley (1987) and Neumayr (1998) suggested this relates to the differences between Lyttelton 1 and Lyttelton 2, with the mantling of Lyttelton 2 flows over a highly eroded surface of Lyttelton 1.

In this study no major singular unconformity has been encountered. What is recognised are distinct lava sequences, younging to the north-east. Lava sequences primarily comprise a'a lava flows, however there are distinct horizons of primarily brecciated material, forming cliff-like exposures that are traceable from the erosional crater rim to low regions on the interior western slopes of Lyttelton Harbour. Epiclastic / laharic horizons also occur within lava sequences (previous chapter), but are interspersed with lava flow units, indicating ongoing eruptive activity and degradational phases.

Ten of these horizons have been recognised and traced on aerial photographs (Figure 4.1) on the north-western side of Lyttelton Harbour. In the field these are 10's of metres high, distinct cliff exposures, with a rubbly / blocky appearance easily discernable from the thinner, stratified, a'a lava flows.

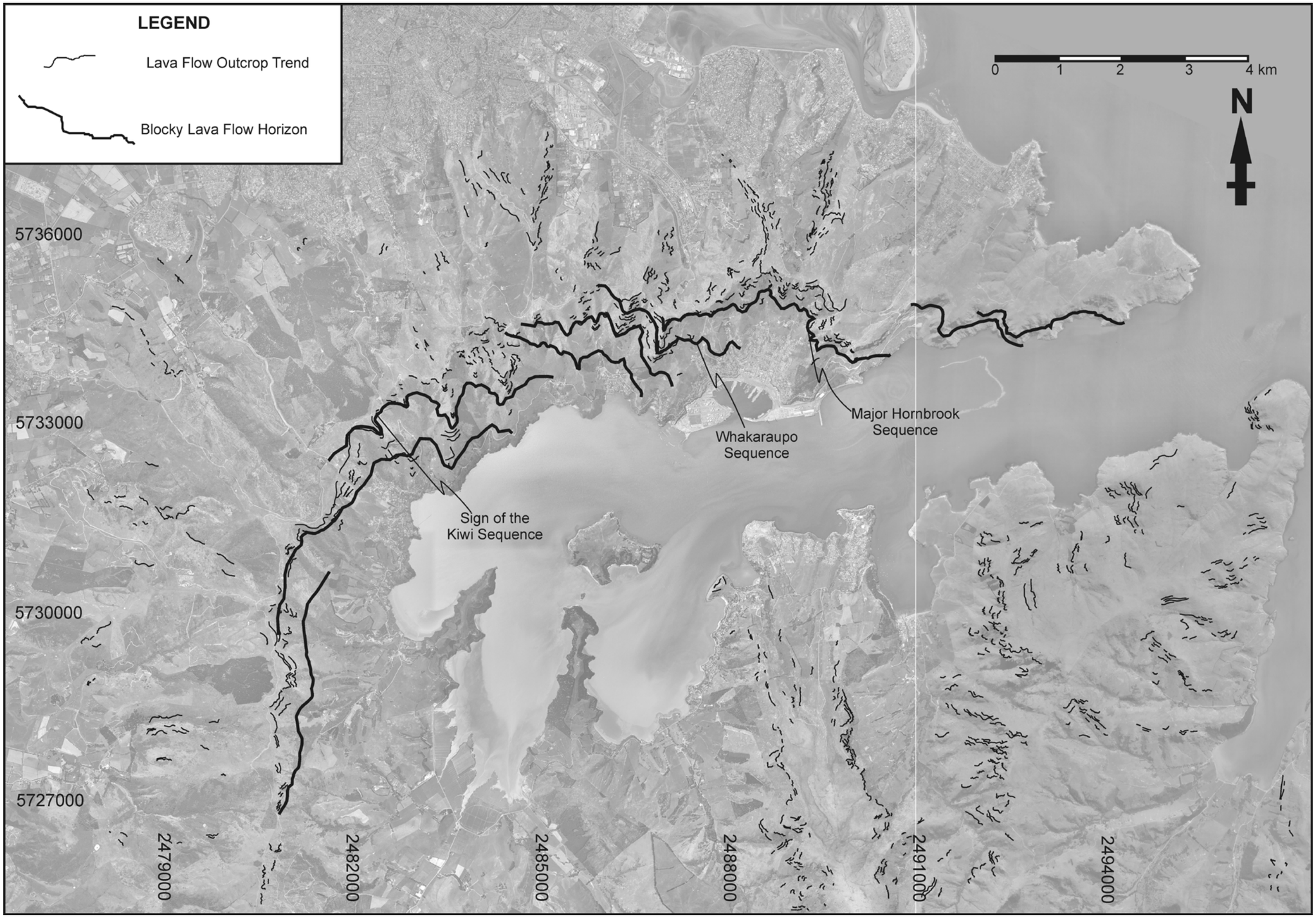

Figure 4.1. Lava flow analysis of Lyttelton Volcano. Major lava flow outcrops traced onto aerial photograph enable the identification of overall lava flow trends rather than localised, highly variable flow directions. A'a to blocky lava flow horizons in the northern sector of Lyttelton Volcano.

4.3.2. Description of Brecciated Horizons

Brecciated horizons are best exposed on the inner, north-western, slopes of Lyttelton Harbour (Gebbies Pass to Lyttelton Township; Figure 1.2), often dropping in height from the erosional crater rim to sea level. Ten brecciated lava flow horizons are exposed on the western inner harbour walls of Lyttelton Harbour. Three of these sequences are discussed in detail; the Sign of the Kiwi Sequence, Whakaraupo Sequence, and the Major Hornbrook Sequence (Figure 4.1).

Sign of the Kiwi Sequence

The Sign of the Kiwi sequence (Figure 4.1) descends in height to the northeast, into Lyttelton Harbour. Brecciated deposits overlie lavas, exposed on the south eastern side of the spur, and are intruded by the Multiple Dykes, and are in turn overlain by lavas. The highly irregular upper surface of the brecciated lava has been eroded, channelizing the overlying 30m wide lava flow. Brecciated lavas can be traced further to the south-west in the Hoon Hay Reserve.

The main exposure of brecciated lavas is on the north-eastern cliff faces above the Coronation Hill Track (Figure 4.2), with internal flow structures exposed along the Summit Road. Deposits form distinct on the northern face. The base of the sequence is exposed in the track beneath the main exposure, where channelized, thinly jointed lava flows, overlie porphyritic massive lava. Thinly jointed lavas are overlain by blocky material, with flows having rubbly tops. At the intersection between coherent lava and rubbly flow tops, vesicle orientations indicate shearing of the solid, vesiculated lava, into the rubbly top. These flows dip north-west dipping, and have a channelized appearance, highlighting the somewhat arcuate cooling pattern.

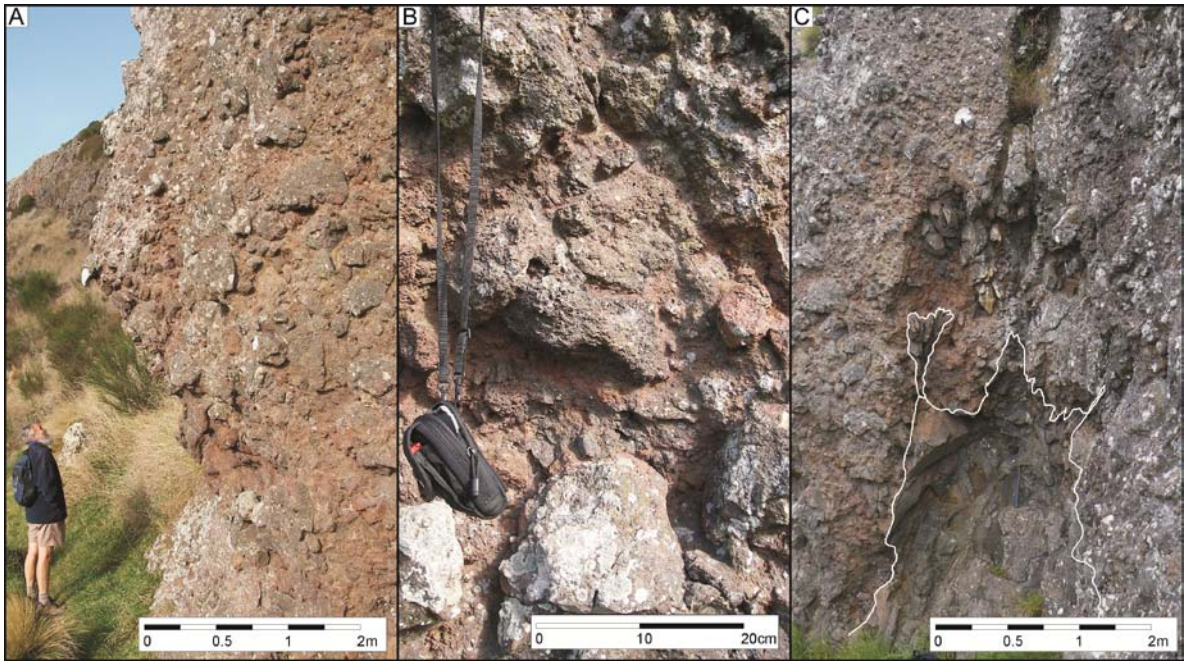

Figure 4.2. Internal lava flow features of the Sign of the Kiwi Sequence. A) Rubbly block-rich lava flow dipping to the north-west (to viewer) on Coronation Hill Track. B) Vesicle-rich to vesicle-poor blocks; note the more irregular shape of the central vesicular block. C) Near vertical squeeze-up structure, massive lava becomes more brecciated away from base of squeeze-up.

One major shear zone is observable on the north-eastern face (Figure 4.2C). At the base of this shear zone is a near vertical squeeze-up, slightly dipping to the north-east. This squeeze-up has distinct smooth sheared lava surfaces (023/57°E and 024/72°E), with an arcuate form and aligned vesicles. The squeeze-up loses coherency, becoming further brecciated, as it inter-fingers the brecciated material. The petrography of this squeeze-up is porphyritic, phenocryst-rich (30-40%: augite (<5mm); olivine; plagioclase) basalt.

The surrounding blocky material (Figure 4.3A) consists of sub-angular to angular, lapilli to block fragments, with majority being 30cm in diameter. Blocks are comprised of grey to weathered red oxidised, vesicular and non-vesicular blocks / fragmented lava in a red-brown matrix. Vesicle-rich blocks have elongate, irregular aligned vesicles, in a porphyritic, crystal-rich (50%) groundmass, similar in composition to the squeeze-up. Non-vesicular blocks are similar in composition to the squeeze-up and vesiculated blocks, yet have a lower phenocryst percentage than both and variation in feldspar content.

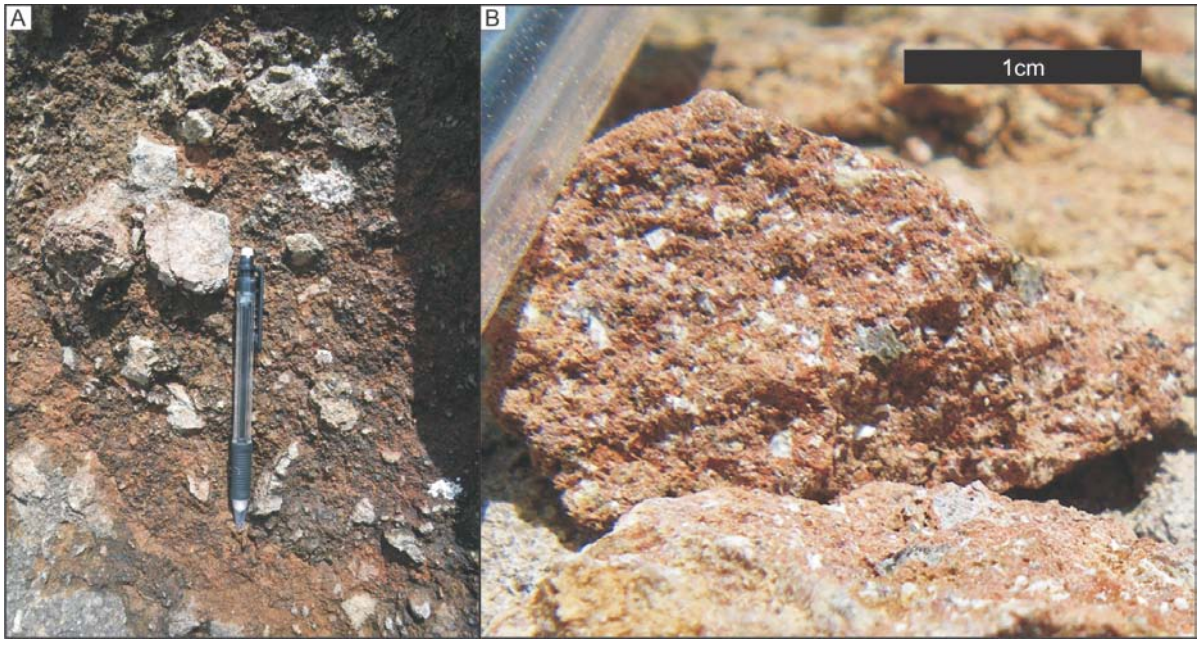

Figure 4.3. Matrix components of the Sign of the Kiwi sequence; A) Matrix supported component of flows exposed in the Summit Road. B) Fresh sample of crystal-rich matrix found at A. This matrix has a distinct primary pyroclastic origin and is poorly to moderately indurated. Pencil is 15cm long.

Further up the sequence (stratigraphically) a small lava flow is exposed, bounded by blocky material. The basal contact of this flow grades from rubbly lava blocks to solid lava, becoming more vesicular to the top, before grading into the overlying brecciated material. The composition of the lava flow is similar to the previously described blocks and squeeze-up. This flow (043/18°NW) thins rapidly uphill (SE), into a thin vesiculated lava flow.

The road cut section along the Summit Road, just north of the Multiple Dykes, exposes the flow interior. The strike of this face is 60°, and highlights channelized lava flows (~300° trend of flow), squeeze-ups and late stage dyke intrusion. Channelized flows have solid, coherent interiors, with aligned elongate vesicles on the outer margins. Brecciated blocky fragments surround these channelized flows. Brecciated material is matrix-supported, poor to moderately indurated, red, phenocryst-rich, fine ash (Figure 4.3A). In less weathered exposures phenocrysts of feldspar, augite and olivine can clearly be designated (Figure 4.3B).

Whakaraupo Sequence

The Whakaraupo sequence (Figure 4.1 and 4.4) is exposed in the ridge south-west of Lyttelton Township, which descends in height to the north-east towards Lyttelton Township. The best outcrop exposure is on the Stan Helms Track (part of the Whakaraupo Track), west of Lyttelton Township. The following descriptions are from the main cliff exposure and isolated exposures of the same brecciated horizon:

Figure 4.4. View north-east toward the Whakaraupo sequence. In the foreground is the main cliff exposure with traceable outcrops to the east, towards Lyttelton Township.

The Whakaraupo sequence is comprised of thick brecciated lava blocks with irregular inter-beds of more massive and platy jointed lavas. In localised areas basaltic to trachytic dykes intrude these brecciated deposits, with the largest being a 5m wide trachytic dyke. The base of this brecciated deposit irregularly overlies porphyritic lavas. This brecciated sequence produces a thick horizon within Lyttelton Volcano, approximately 60m thick, including associated coherent lava flows.

The best exposure of brecciated deposits is in a 30m high, north-west facing cliff, the base of which is marked by a thinly, platy jointed lava flow with a brecciated top. This platy jointed flow is a defined horizon beneath the flow, and unusually is at a higher elevation on the outer flank side (NW) than the expected summit. This lower lava has top and basal flow breccias, but further up the section the flow becomes progressively brecciated, with more angular fragments. Brecciated material occurs beneath this coherent lava, viewed across valley to the south. The platy lava flow intersected within the main cliff exposure can be traced to the south, but appears to taper out.

On the north-western cliff face two distinct structures are evident at outcrop scale. The first is a flow boundary dipping ~44° NE halfway up the exposure, and the second a series of ~6 south-west dipping (40°) shears. At the northern end of the outcrop a shear plane dips 091/32°SE. This orientation is similar to sheared faces on angular blocks with elongate vesicles. At the southern end on the top of the cliff a shear plane (272/35°S) displaces a foliated block (Figure 4.5), producing a distinct stepped base. A further shear plane on the very end of the point had a similar orientation (271/46°S).

Isolated continuations of this brecciated horizon descend towards Lyttelton Township. Within these exposures deposits are comprised of well indurated, clast-dominant, brecciated lava. Clasts vary from aphyric, vesicular (elongate), to flow aligned / lineated (figure 4.6). Blocks are < 1m in dimension, and commonly have planar surfaces on at least two sides. The matrix consists of fragmented brecciated lava, similar in composition to the surrounding blocks (Figure 4.7).

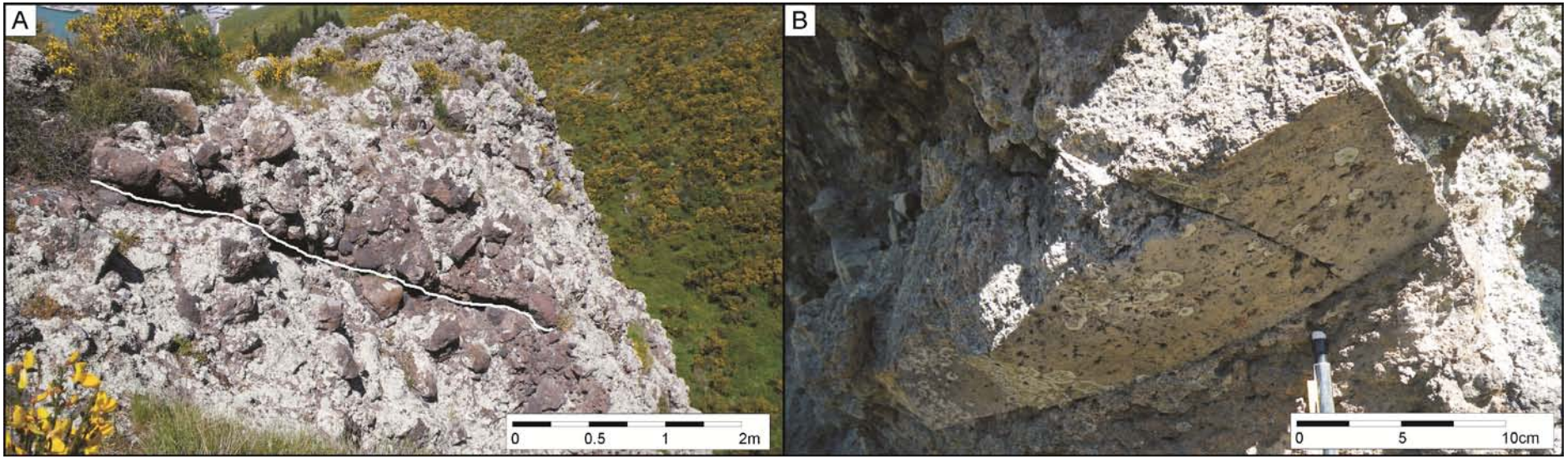

Figure 4.5. Shear plane (A) and dihedral plane block (B) of the Whakaraupo sequence.

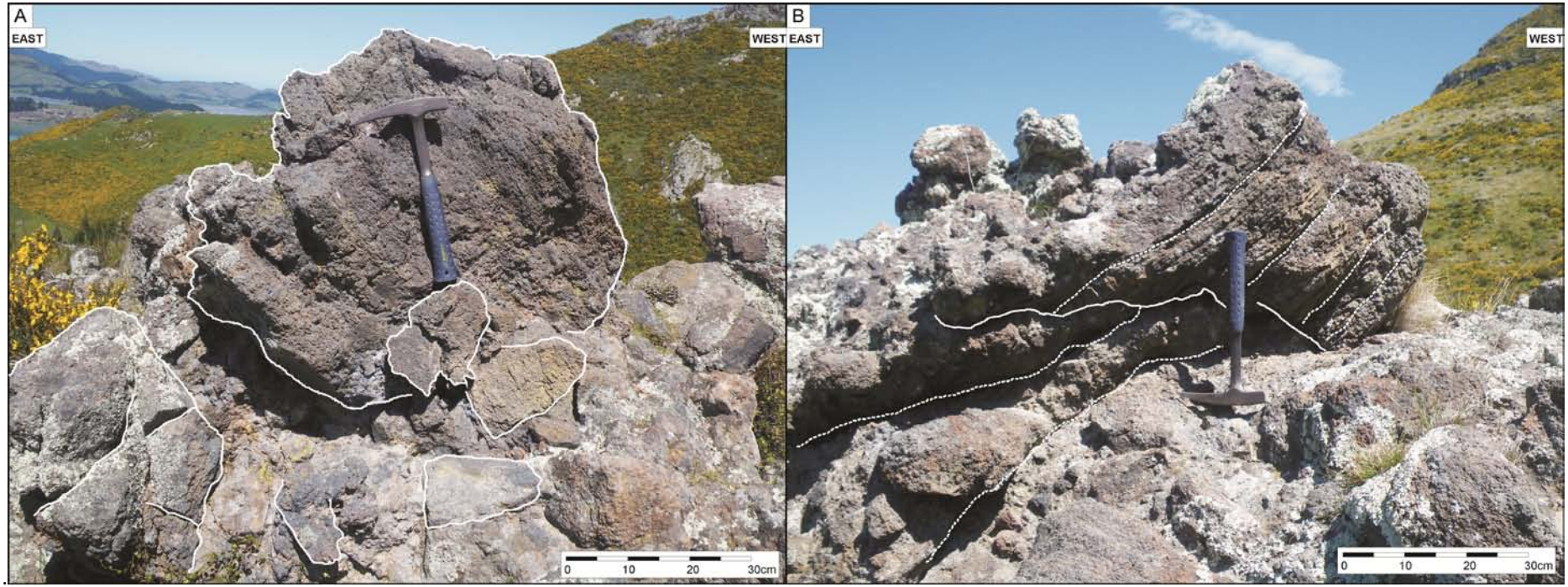

Figure 4.6. Flow banded and ramped blocks of the Whakaraupo sequence: A) Isolated flow banded block surrounded by dihedral planed blocks. B) Vesiculated block intersected by basal shears.

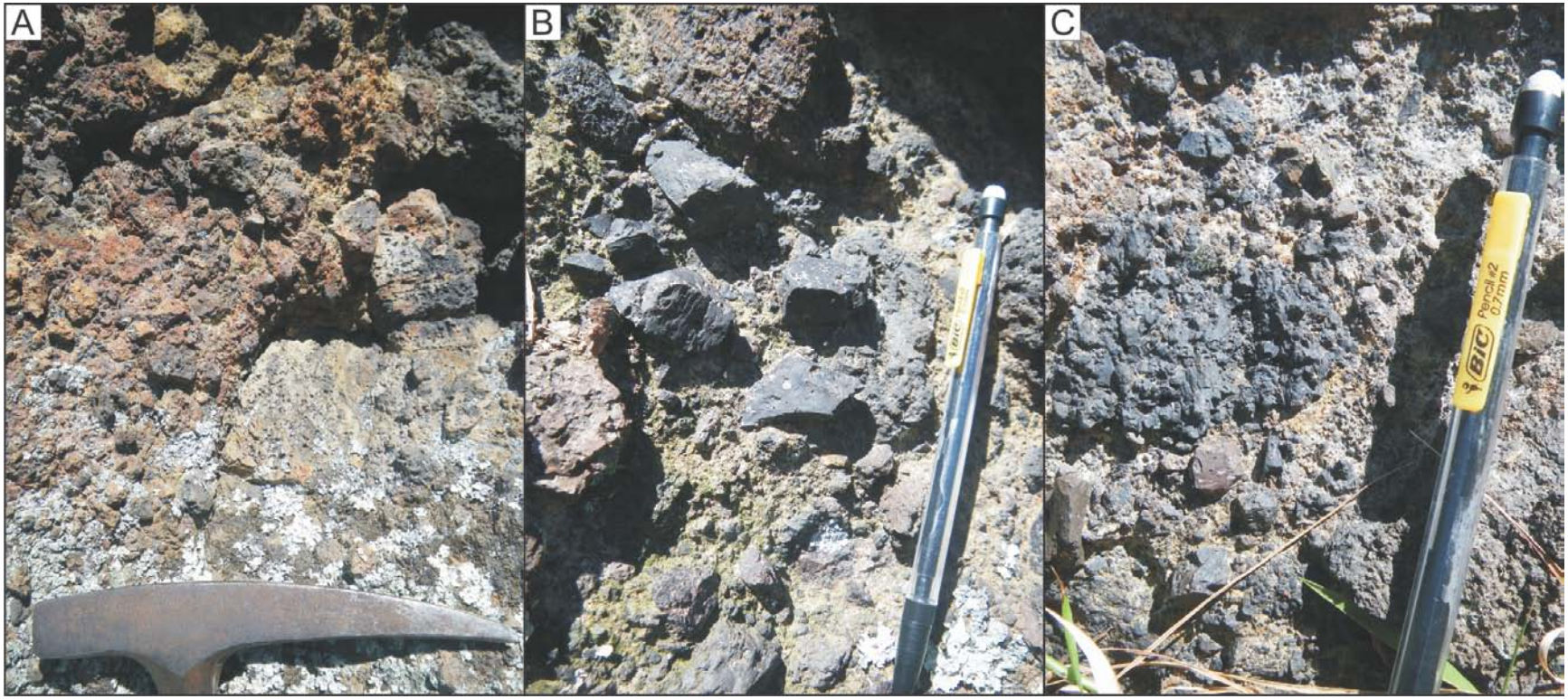

Figure 4.7. Fragmented block types and matrix in the Whakaraupo sequence; A) Rubbly surfaced and pitted angular dihedral plane blocks. B) and C) Dihedral plane blocks within a brecciated matrix.

Figure 4.8. Near vertical jointed lava injections near the top of the Whakaraupo sequence: A) Solid interior lava surrounded by agglutinated layer intersecting brecciated lavas. B) View to the west of continuation of A in outcrop, with clearly visible vertical jointing / structure.

Intersecting this brecciated horizon are irregular channelized lavas. A smaller channelized flow (plan view) displays multiple, almost chilled margins / vertical jointing (10's cm; 105/40°SSE), thickening towards the massive interior (>1m). This channel is somewhat lobate, comprised of purple-grey, fine porphyritic, flow banded basalt.

A distinct spur intersects the brecciated sequence, stratigraphically towards the top of the flow. This spur is arcuate in shape, and comprised of similar material to the brecciated sequence, but has more primary magmatic components (Figure 4.8), with near vertical fluidised lava layers, interbedded with fragmented blocky material, surrounding solid lava (104/84°S).

Major Hornbrook Sequence

The Major Hornbrook blocky lava flows form a horizon traceable from the south-west of the Bridle Path to cliff and road cuttings on Evans Pass Road (Figure 4.1). The spur to the east of Lyttelton is comprised of Lyttelton lavas, a trachyte sill (Windy Point Sill; Altaye, 1989), brecciated lavas, extensive near-vent pyroclastic deposits and covered by further Lyttelton lava flows. Exposure from Bridle Path to the main exposure on the Chalmers Loop Track, overlies Lyttelton Lavas, and is overlain by laharic horizons, the Mt Cavendish Scoria Cone, and thick near vent pyroclastic deposits.

Distinction between the blocky lava flows and the surrounding volcaniclastic and scoria cone deposits has been a key feature highlighted in the past, an aspect reviewed in Chapter 2. The key to distinguish these in the field is that most scoria deposits are highly stratified, dipping irregularly in comparison to the overall volcanic structure, whereas volcaniclastic deposits have sub-rounded fragments, of varying lithologies, and a definite fluvial origin.

The logged exposure of this sequence is from the Y-junction on the Chalmers Loop Track. Brecciated lavas have highly irregular basal contacts with underlying lavas, and are capped by near vent pyroclastics and welded spatter. The stratigraphic thickness of this unit is 35 – 40m. The Chalmers Loop Track exposure is divided into and described as five 'faces' (Figure 4.9). Stratigraphically faces 1 and 2 are the lowest, face 3 the flow

interior, and 4 and 5 exposing the upper surface of the flow. The basal contact is not exposed.

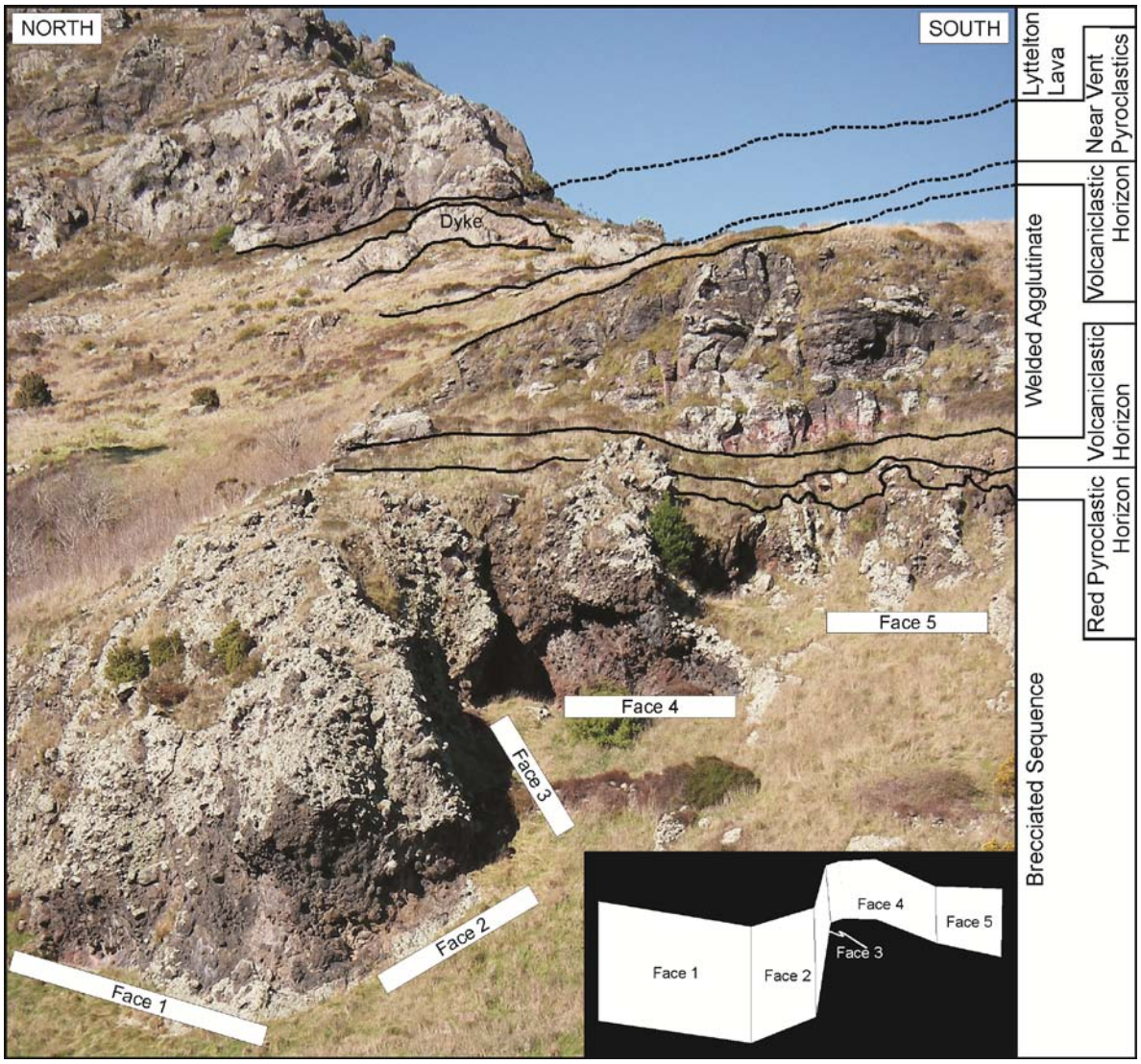

Figure 4.9. Blocky lava flow horizon of the Major Hornbrook sequence, with the exposure separated into five faces**.** A simplistic stratigraphy of the overlying units is displayed to the right hand side of the figure.

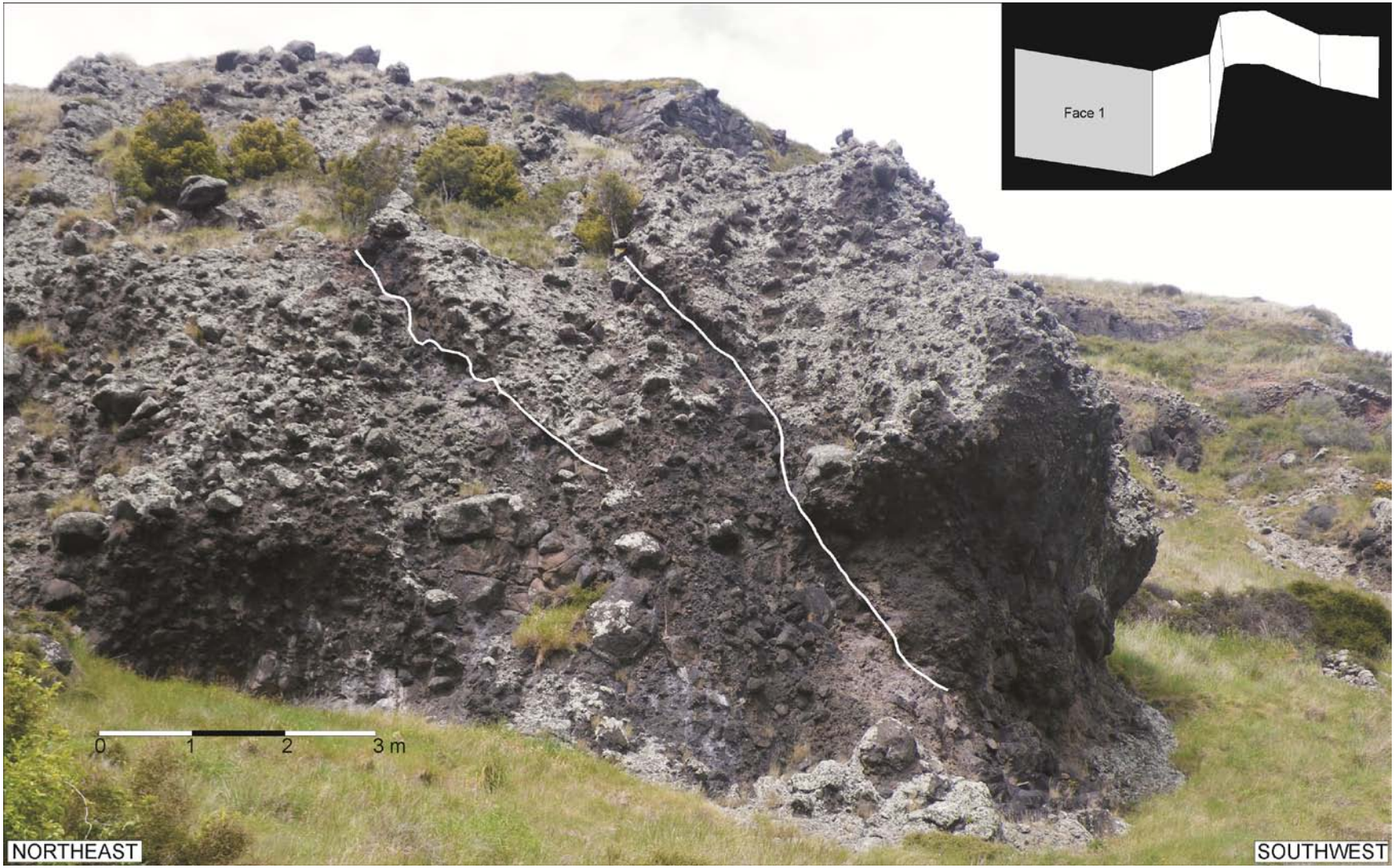

Figure 4.10. Face 1 of the Major Hornbrook sequence. Note the lack of block orientation on the left side of outcrop, and the shear planes (white lines) intersecting the interior of the face and dipping to the right.

Face 1 (250° Strike)

This face (Figure 4.9) displays no orientation of blocks, appearing to be massive, with the only evidence of shearing being at the southern end of the face (Figure 4.10; 174/63NE and 179/72NE). On one of these planes a large block is sheared, with the infilling matrix of similar type to that of the block components (Figure 4.11A). The majority of blocks have a weathered, black, granular appearance, are angular, and have distinct sheared surfaces. Blocks are phenocryst-rich, varying from vesicle-rich to non-vesicular, but of similar hand specimen mineralogy and appearance, suggesting a similar source. Some red porphyritic clasts are observed, although these seem to be accessory flow components. The matrix (Figure 4.11B and C) is comprised of black, angular fragmented pieces of larger blocks, within weathered, cream-brown, sugary textured medium to coarse grained fragments.

Face 2 (180° Strike)

A squeeze-up structure is found at the base of the southwest face (Figure 4.9). Here massive lava progressively fingers out into the blocky, brecciated components. Near vertical elongate remnant phenocryst and vesicle alignment is apparent in the lower region, indicating an upward flow of lava. The contact with the brecciated lava is sharp to gradational, with fragments of the same lithology as the squeeze-up making up the majority of the angular fragments in close proximity. Shears within this main squeeze-up are oriented 165/56NE, 137/32NE, and 156/52NE, with variation due to their arcuate shape. Associated on these shear surfaces are striations, with a recorded trend and plunge of 165/32NNW.

The squeeze-up is comprised of porphyritic, phenocryst-rich (>60%), grey black, basalt, with cream-white euhedral feldspar phenocrysts (<5mm), and fine orange phenocrysts. Outer surfaces have smooth angular faces, with aligned holes formed due to weathering out of flow-aligned feldspars. Also associated with these angular faces are striations, formed through shearing. Weathered surfaces have a granular, coarse, sugary texture. Along this face a horizon can be traced, dipping ~12° to the east, with the long axis of blocks conforming to this.

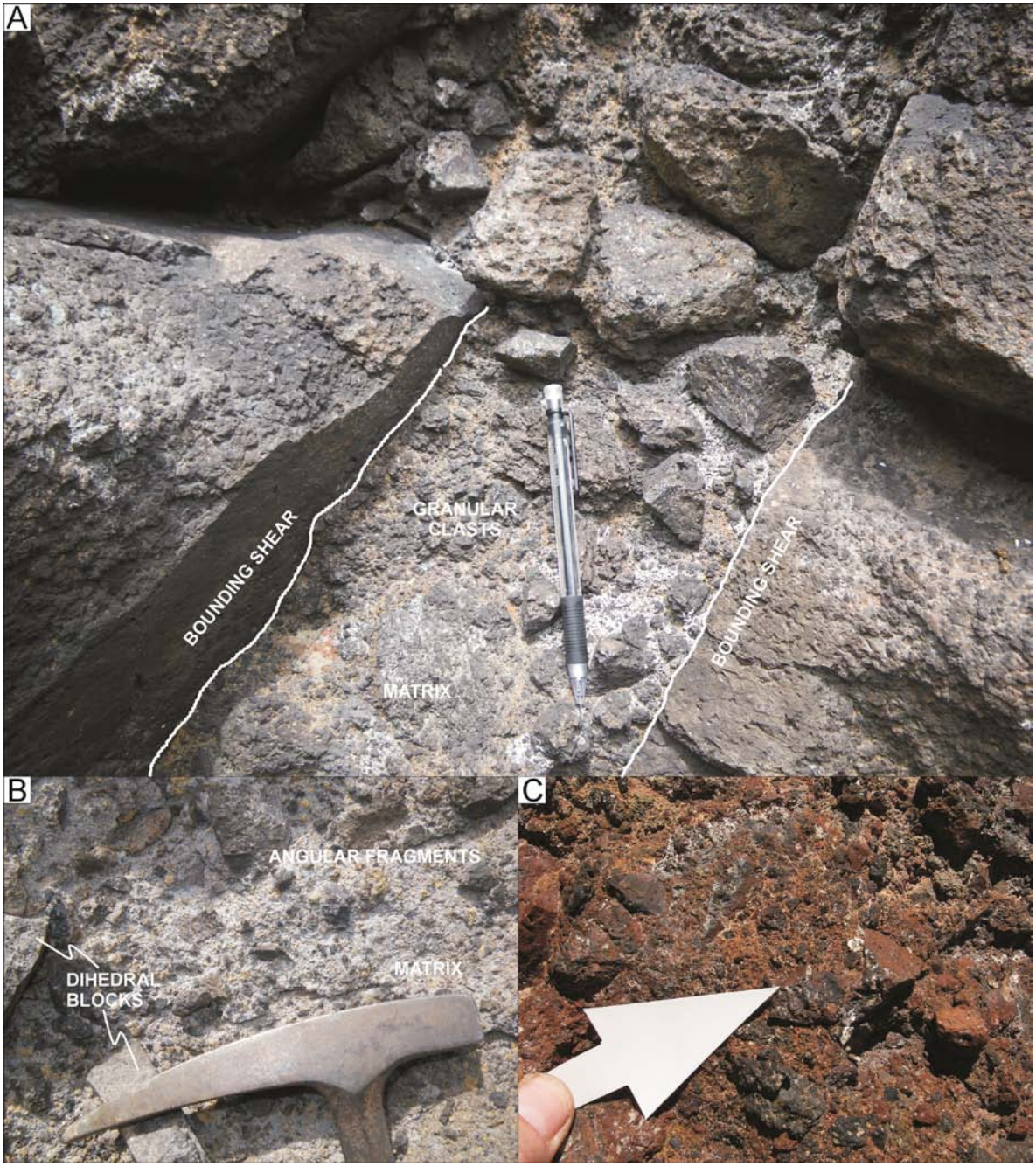

Figure 4.11. Brecciated matrix components. A) Large blocks sheared apart (parallel bounding sheared surfaces) infilled with brecciated dihedral to granular clasts, in a clast supported matrix. B) Close up of a brecciated matrix, note the dihedral block at the end of the hammer and the highly angular matrix fragments. C) Crystal-rich fragmented blocks with dihedral planes are common matrix components.

Figure 4.12. Shear planes within the Major Hornbrook sequence Face 3.

Face 3 (080° Strike)

This face exposes blocky lava intersected by at least 6 planes (Figure 4.12; 048/54°NW). Planes offset / shear blocks, progressively down-dropping the top surface to the NW (Figure 4.13). Block composition is similar to the previous exposure, although this face is more lichen covered, and weathered red-brown.

Figure 4.13. Fractured block along shear plane in Face 3, indicating thrusting of the lower sequence towards the east.

Face 4 (226° Strike)

Planes from Face 3 (Figure 4.9) extend into the face, but the main feature is a squeeze-up into the blocky breccia (Figure 4.14). Solid lava extends down to the base of this cliff. From this basal exposure a flow orientation is recorded at 226/88NW, supported by aligned vesicle trails. Towards the top of the exposure there is a further lava squeeze-up (124/62NE), splaying upwards from 40cm to over 1.5m in width.

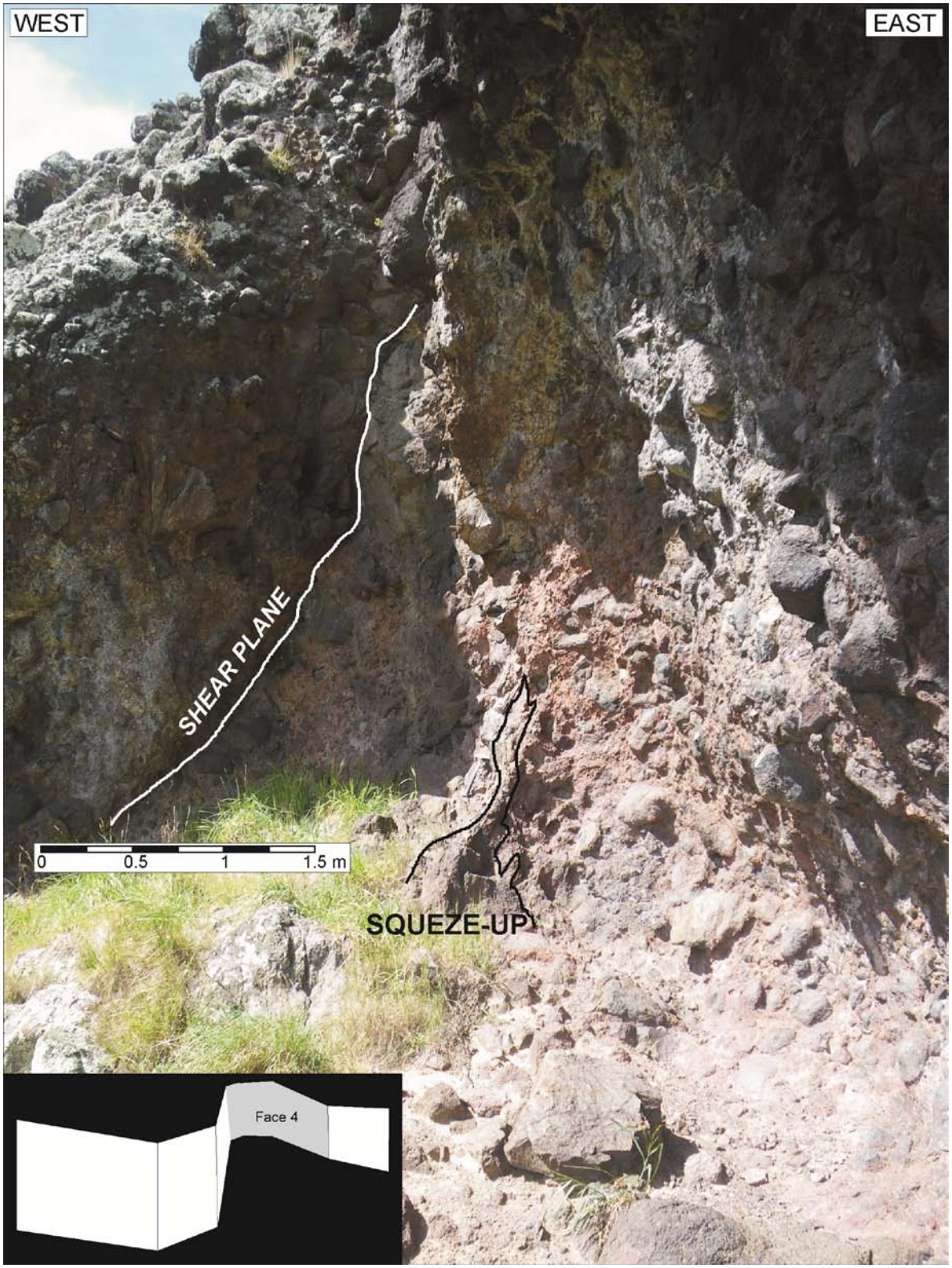

Figure 4.14. Face 4 of the Major Hornbrook sequence. A squeeze-up structure in the foreground of the figure extends into to the base of the cliff and vertically up the face.

Face 5

Face 5 (Figure 4.9) provides a section through the top section and contact of this blocky lava flow exposure. The top of the blocky lava has a low component of matrix infilling interstitial spaces between blocks, when compared to lower the lower exposures (Faces 1-4). This has resulted in the proceeding red, phenocryst-rich, fine ash to infill these spaces (Figure 4.15). This infilled lava is capped by a thin (<10cm), red, pyroclastic, phenocryst-rich, medium ash, similar to the infilling ash, which grades into a clast-supported, vesiculated, block, volcaniclastic layer (Figure 4.15). Clast size is >granule to boulder, primarily sub-angular, of various lithologies (red, fine porphyritic basalt; aphyric basalt; porphyritic basalt; vesicular basalt), with the majority being similar in composition to the underlying blocky lava fragments / blocks.

This sequence is overlain by a thin, welded spatter lava / vent agglutinate (320/11NE), a relatively thin volcaniclastic horizon, then a thin platy aphyric lava flow. This sequence is stratigraphically overlain by a highly vesicular phenocryst-rich, pink-grey welded pyroclastic unit (Figure 4.16), overlain by lavas, and intruded by highly irregular dykes. This pyroclastic unit can be linked to a thick sequence exposed on the eastern side of Lyttelton (just north of the spur above Buckley's Bay), and stratigraphically to the thick red pyroclastic horizon, overlying blocky lavas in the Harbour Quarry Road above Battery Point.

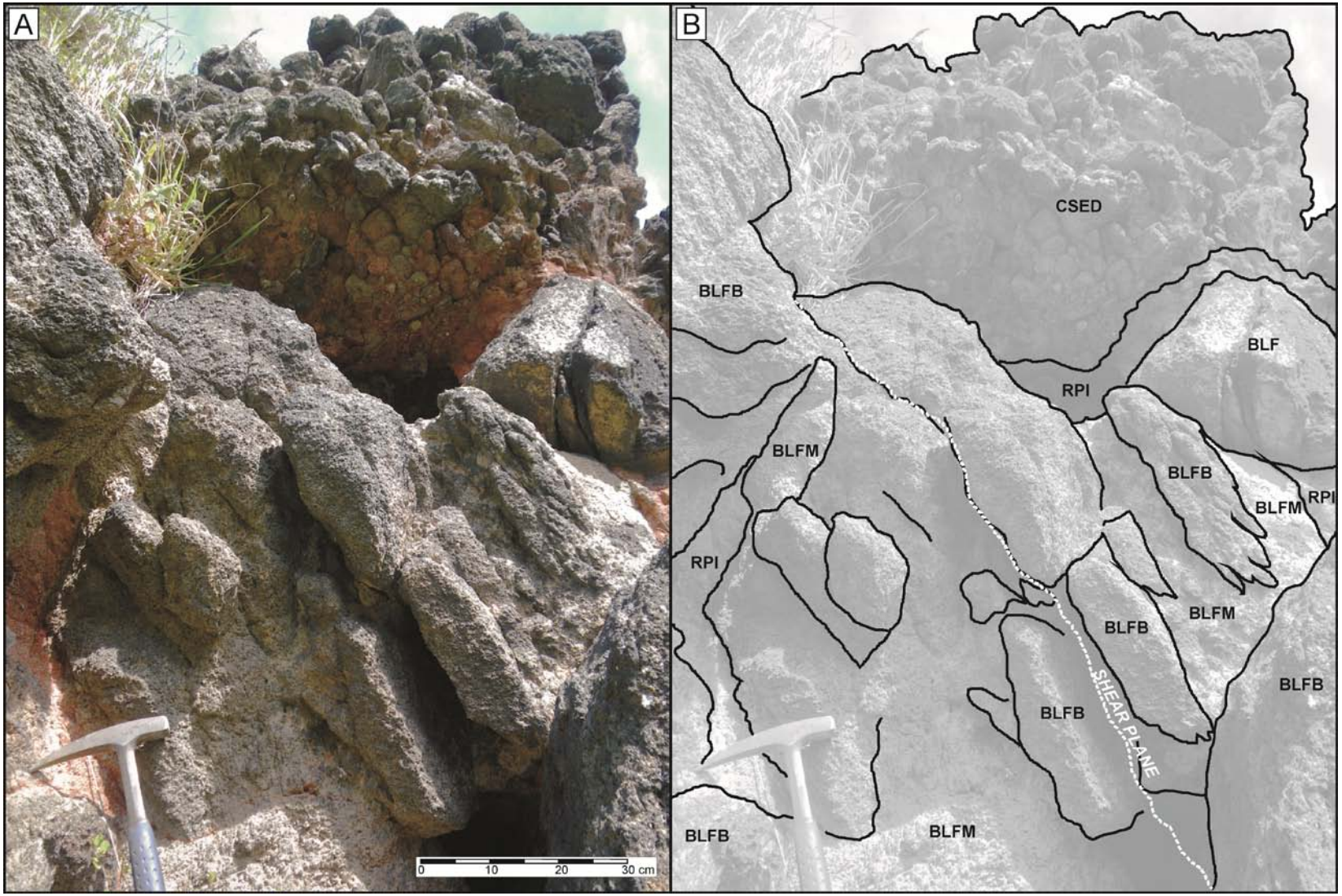

Figure 4.15. Red pyroclastics, near hammer, infilling the interstices between blocks at the top of the Major Hornbrook blocky lava. This sequence is covered by a thin red, pyroclastic horizon, grading into a clast supported volcaniclastic deposit (top of figure).

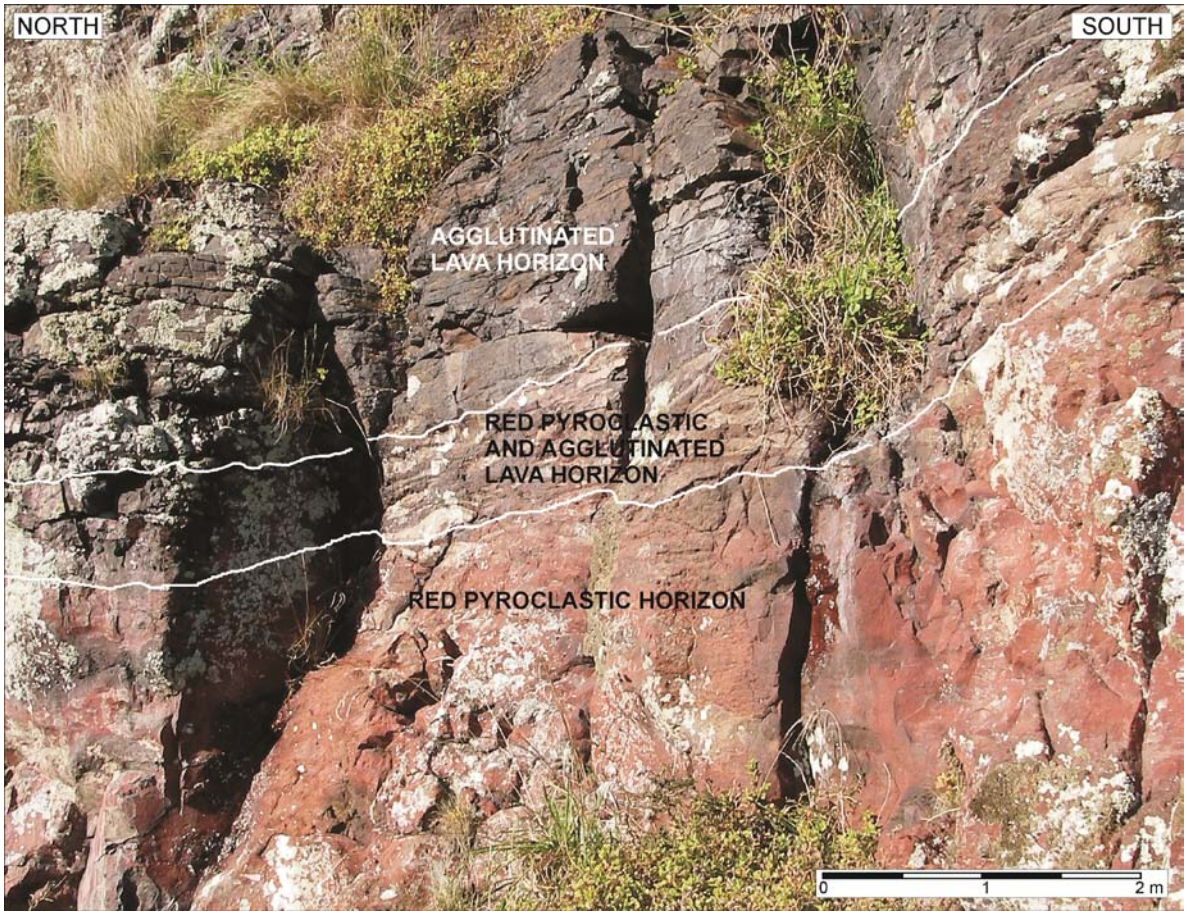

Figure 4.16. Red pyroclastic horizon grading into welded agglutinate, exposed above Face 5 of the Major Hornbrook sequence.

4.4. Characteristics of Lyttelton Volcano's Brecciated Lava Sequences

The following reviews the main structural features of Lyttelton Volcano's brecciated lava flows sequences, key to classification of flow types on the end-member spectrum of a'a to blocky lava flows.

4.4.1. Block Morphologies

Block morphology is a key defining factor in the classification of a'a to blocky lava flows, with both texture and angularity having distinct characteristics. A'a lavas are regarded as having a spinose or rubbly texture, as well as being slightly more vesicular, features common to the brecciated components of the Sign of the Kiwi sequence (Figure 4.17A). Surfaces of these blocks are sub-angular, almost globular, similar in

description to Kilburn and Guest's (1993) a'a lava flow surface. Blocks with rounded appearances also display a change in colouration to ochre-grey.

Blocky lavas can have similar spinose block to a'a but at lower proportions, and have polyhedral shaped blocks with smooth dihedral angled planes / surfaces (MacDonald, 1953). Both the Whakaraupo (Figure 4.7) and Major Hornbrook (Figure 4.12 and 4.14) sequences have blocks that conform to this description, often being displaced or sheared along larger scale structures / planes (Figure 4.17B and 4.18). MacDonald (1953) noted that the vesicularity within blocks of blocky lavas is less than a'a, indicating a higher density than a'a flows.

A key distinguishing factor of blocky lavas recognised by MacDonald (1953) was that most blocks have smooth surfaces, with a polyhedral shape bounded by dihedral angle. Blocks within flows may show variation of smoothness on faces (Figure 4.18 A), with a single block having some smooth faces, blocks with rough, spinose exteriors still exist but are less common (MacDonald, 1953). Major Hornbrook and Whakaraupo blocks are primarily angular, with at least two planar sheared faces (Figure 4.5B), while the rest have a weathered sugary texture (Figure 4.7 and4.12). Associated with these dihedral planar faces of blocks at Whakaraupo and Major Hornbrook sequences are lineation or slikenslide planes (Figure 4.18), indicating brittle shearing during flow emplacement. Cas and Wright (1987) in discussing the viscosity of blocky flows, indicate that the high viscosity producing high yield strengths produce these striated and gouged margins.

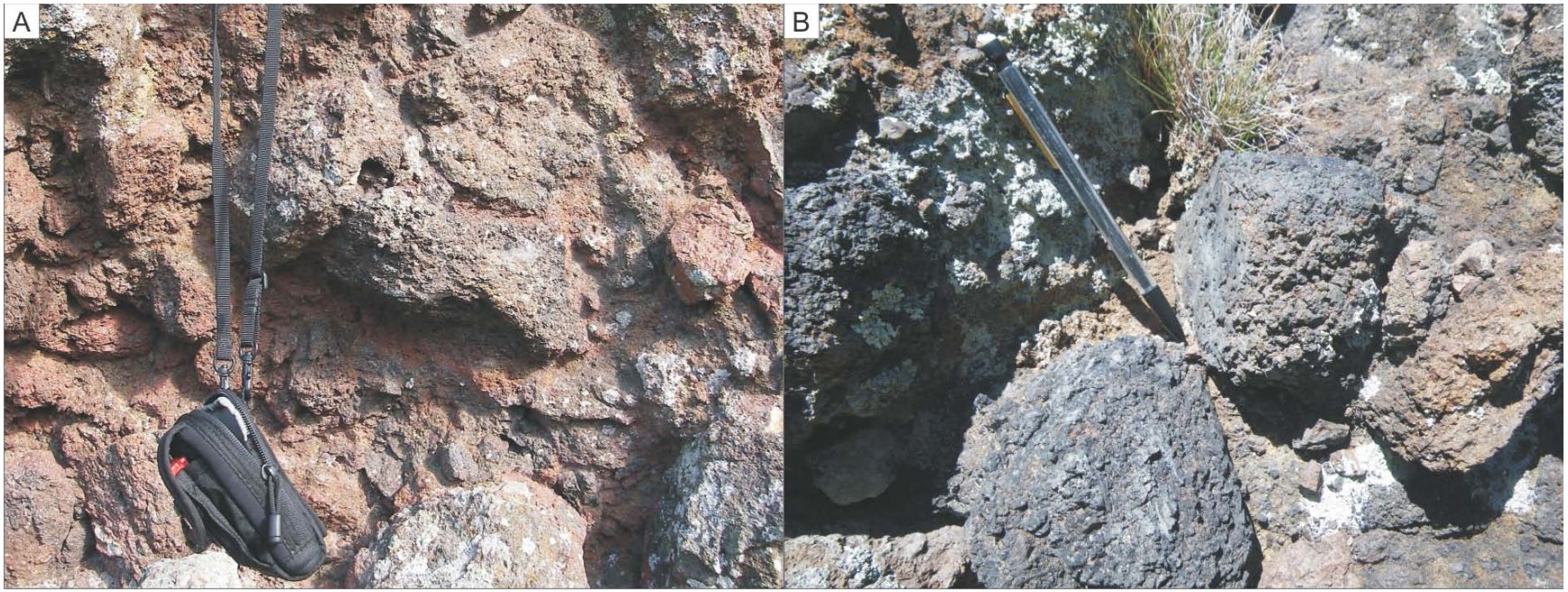

Figure 4.17. Block morphologies: A) Vesicular, globular blocks of the Sign of the Kiwi sequence. B) Spinose, sugary texture surfaces on dihedral plane blocks at the Whakaraupo sequence.

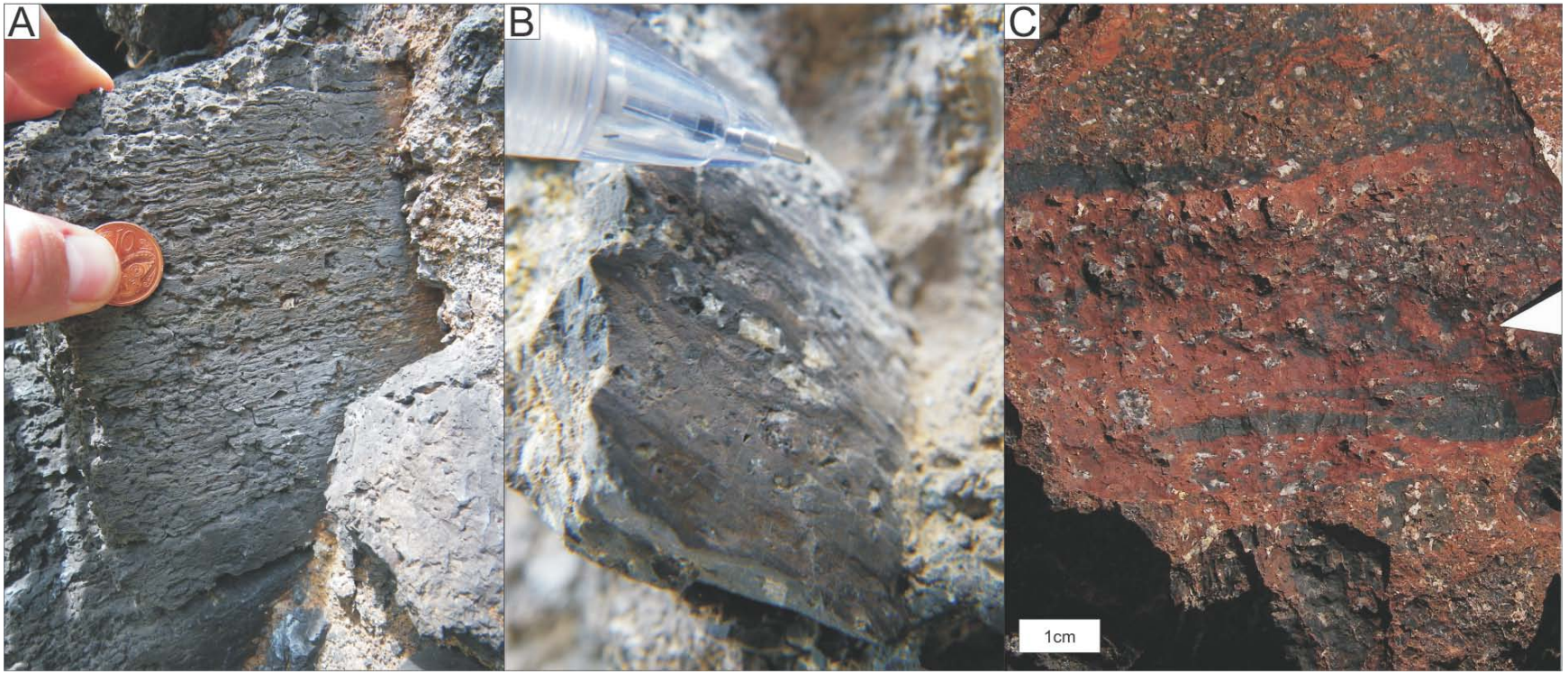

Figure 4.18. Small scale features of block components within blocky lava sequences; a key aspect is that none of these features align to the overall flow structure: A) Lava flow banding on a dihedral plane surface, note the crystal alignment also in flow direction. B) Flow banding with matching crystal alignment. C) Phenocryst-rich block with lensoid, black phenocryst-poor zones.

4.4.2. Matrix

Blocks in a blocky flow are closely spaced when compared to a'a, resulting in a higher rate of attrition, producing a higher percentage of interstitial material on the surface (McDonald, 1953). The matrix of all brecciated sequences on Lyttelton Volcano is co-depositional. The Sign of the Kiwi sequence matrix has a high primary pyroclastic component, whereas the Whakaraupo and Major Hornbrook sequences are primarily comprised of highly brecciated block material.

Both the Whakaraupo and the Major Hornbrook sequences contain angular fragments similar in composition to the main flow lithologies (Figure 4.7 and 4.12). Obviously sheared larger blocks at the Whakaraupo and Major Hornbrook sequences are often fractured, producing an almost jigsaw fit, with fracture spaces infilled by smaller brecciated blocks (Figure 4.12), which constitute the matrix of the flow. The Sign of the Kiwi sequence (Figure 4.17) is slightly more matrix supported and less indurated than those of Whakaraupo and Major Hornbrook. The upper surface of the Whakaraupo Track brecciated sequence is unlike the rest of the flow, appearing to lack matrix, hence the ability of the proceeding red pyroclastics being able to infiltrate and infill the top metre of the flow (Figure 4.15), suggesting emplacement of matrix has a component of gravity settling.

4.4.3. Flow Interiors

Two types of flow interiors are exposed at the Sign of the Kiwi and Whakaraupo sequences. No channelized lavas were observed within the Major Hornbrook sequence. Multiple small channelized coherent to platy jointed lavas of the Sign of the Kiwi sequence are best exposed on the Summit Road section. These are typical of a'a flows, with rubbly basal regions and flow tops. Away from the more coherent channelized flow interiors, flows commonly have irregular platy joints. Large scale channelized interior lavas are best expressed within the Whakaraupo sequence, where multiple coherent lava channels are observed (Figure 4.19). The platy jointed lava at the base of the main cliff exposure at Whakaraupo is an extensive horizon continuing to the east and west. This extensive horizon was initially viewed as a welded spatter horizon, a concept acknowledged by Cas and Wright (1987), but when examined as a

whole an interior channelized lava flow is hypothesised with a projected flow orientation and outcrop exposure on a 191° bearing.

Figure 4.19. Platy jointed channelized lava flow interiors within the Whakaraupo sequence. A) Thinly spaced jointing within an aphyric, fine grained, weathered pink-brown basalt. B) Side view of platy jointed lava, note the curvature in the jointing beneath hammer.

4.4.4. Squeeze-ups

Exposures of squeeze-ups at the Major Hornbrook faces (Figure 4.14) have arcuate jointing / planes with lineation's displaying the same orientations as the surrounding sheared dihedral faced blocks. The squeeze-up exposed in Face 4 (Figure 4.14) at Major Hornbrook not only indicates an upward squeeze-up direction but with the base of the cliff the coherent lava structure continue enabling a recording of flow direction based on orientation of this and flow aligned phenocryst.

The squeeze-up structures at the Whakaraupo sequence are observed along an arcuate ridge, which from a distance looks like a coherent lava flow plane. But when observed at right angles to this plane vertical up-thrusting of lava is evident (Figure 4.8). In a closer examination of this feature a distinct primary magmatic component

can be seen agglutinating to the outer brecciated lavas (Figure 4.8), forming irregular, almost wavy layers of lava and brecciated material outside of the coherent squeeze-up.

4.4.5. Shear Planes

Shear planes are only observed at the Whakaraupo and Major Hornbrook sequences. The most defined shear planes are those on Face 3 of the Major Hornbrook sequence (Figure 4.12). These planes result in the offsetting of the whole outcrop, with planes being observed to descend to the south, and then to the west along Face 2, with the cliff of face 1 being defined along the plane itself. Projection of these shear planes extends them to the southeast, intersecting face 5. On a shear plane on Face 3 a block is dissected along a plane (Figure 4.13) indicating the lower surface thrust under the overlying breccia. An important indicator, reflecting the model of shear plane formation within both blocky lava flows.

Shear planes within the Major Hornbrook sequence possibly relate to the external friction acting at the edges of the flow, forming complex levee structures (Kilburn and Guest, 1993). While shear planes in the Whakaraupo sequence are in close proximity to the platy jointed, solid lava interior of the flow, suggesting these features are typical of the ramping shear structures of a blocky lava flow.

A key aspect is to differentiate between the recorded planes on dihedral blocks and the major shear planes (Figure 4.20). In analysis of these features it appears dihedral block planes are perpendicular to shear planes at the Major Hornbrook sequence, with the shear planes having a similar strike to the recorded flow orientation of squeeze-up structures.

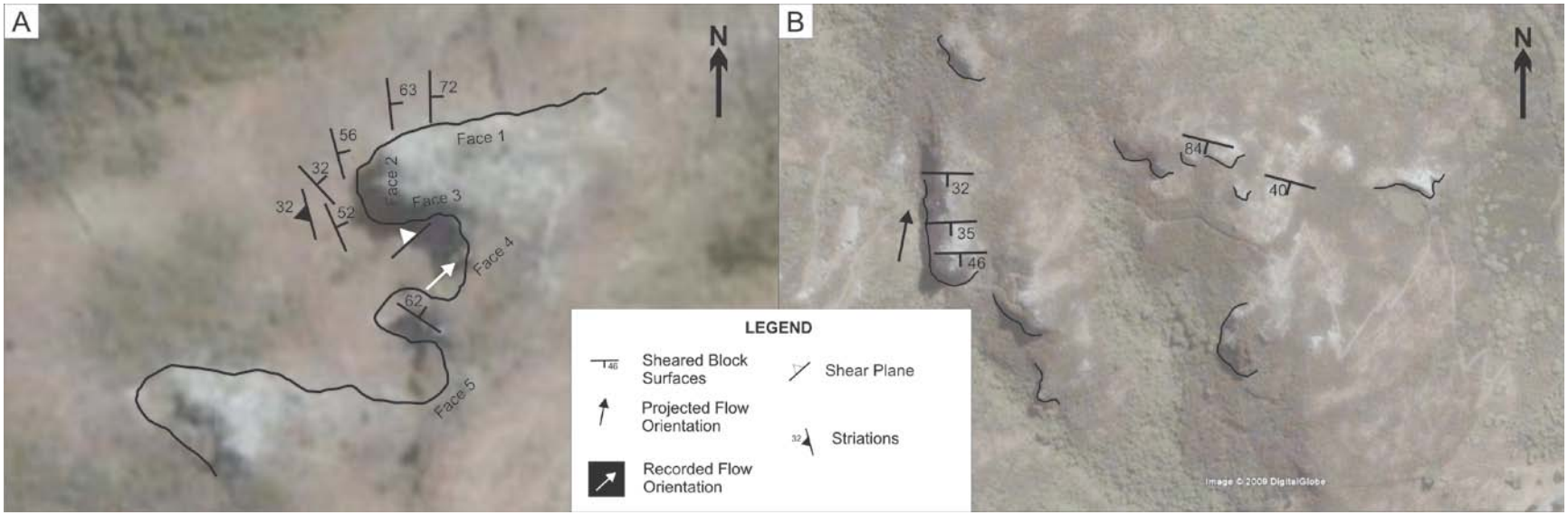

Figure 4.20. Detailed measurements of the Major Hornbrook (A) and Whakaraupo (B) blocky lava sequences. The white arrow in A, reflects the flow orientation recorded in a squeeze-up trace at the base of Face 4. Whereas in B the black arrow is a projected flow orientation based in sheared block measurements forming approximately at right angle to flow direction.

4.4.6. Levees

Distinct levee structures were observed in the Summit Road at the Sign of the Kiwi exposure. Levees are identified through the relationship of channelized lava, indicating these are of a low profile, with no distinct shear surfaces. Limited evidence exists for levee structures at the Whakaraupo or Major Hornbrook sequences. However the major planes running through Face 3 of the Major Hornbrook sequence could reflect the sheared outer regions of a channelized blocky lava flow. Features in support of this analysis are the similarity in the flow direction indicators within the squeeze-ups.

4.4.7. Summary of A'a to Blocky Lavas on Lyttelton Volcano

The three lava flow sequences represent a spectrum from rubbly a'a to blocky lavas on Lyttelton Volcano (Figure 4.21, 4.22, Table 4.1). The Sign of the Kiwi sequence represents a rubbly a'a lava flow field; the Whakaraupo sequence a transitional rubbly a'a to blocky lava flow; and the Major Hornbrook sequence a moderately high grade blocky lava flow.

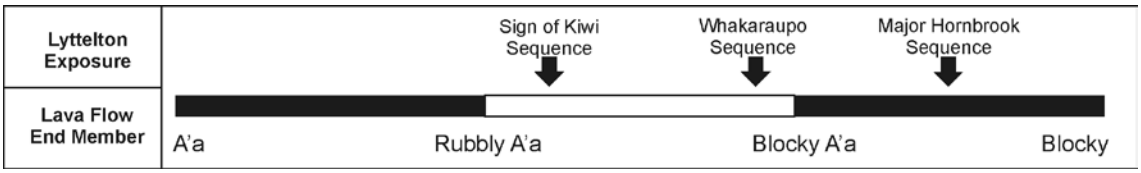

Figure 4.21. A'a to blocky lava flow end-members and the classification of brecciated horizons of Lyttelton Volcano.

Table 4.1 highlights the key distinguishing features used in this study to classify the brecciated horizons on Lyttelton Volcano, while Figure 4.22 depicts schematic cross-sections. The key distinguishing factor within flow types is block morphology. Rubbly a'a blocks are spinose, angular, and have a somewhat globular form. Blocky lava flow blocks are primarily, polyhedral with dihedral planes, marked by lineations (shears). Blocks often have a weathered sugary texture, formed due to the pitted weathering of flow oriented / banded phenocrysts. Limited finer-grained primary pyroclastic material is incorporated into the matrix of blocky lava flows when compared to rubbly a'a, where this makes up the dominant interstitial infill.

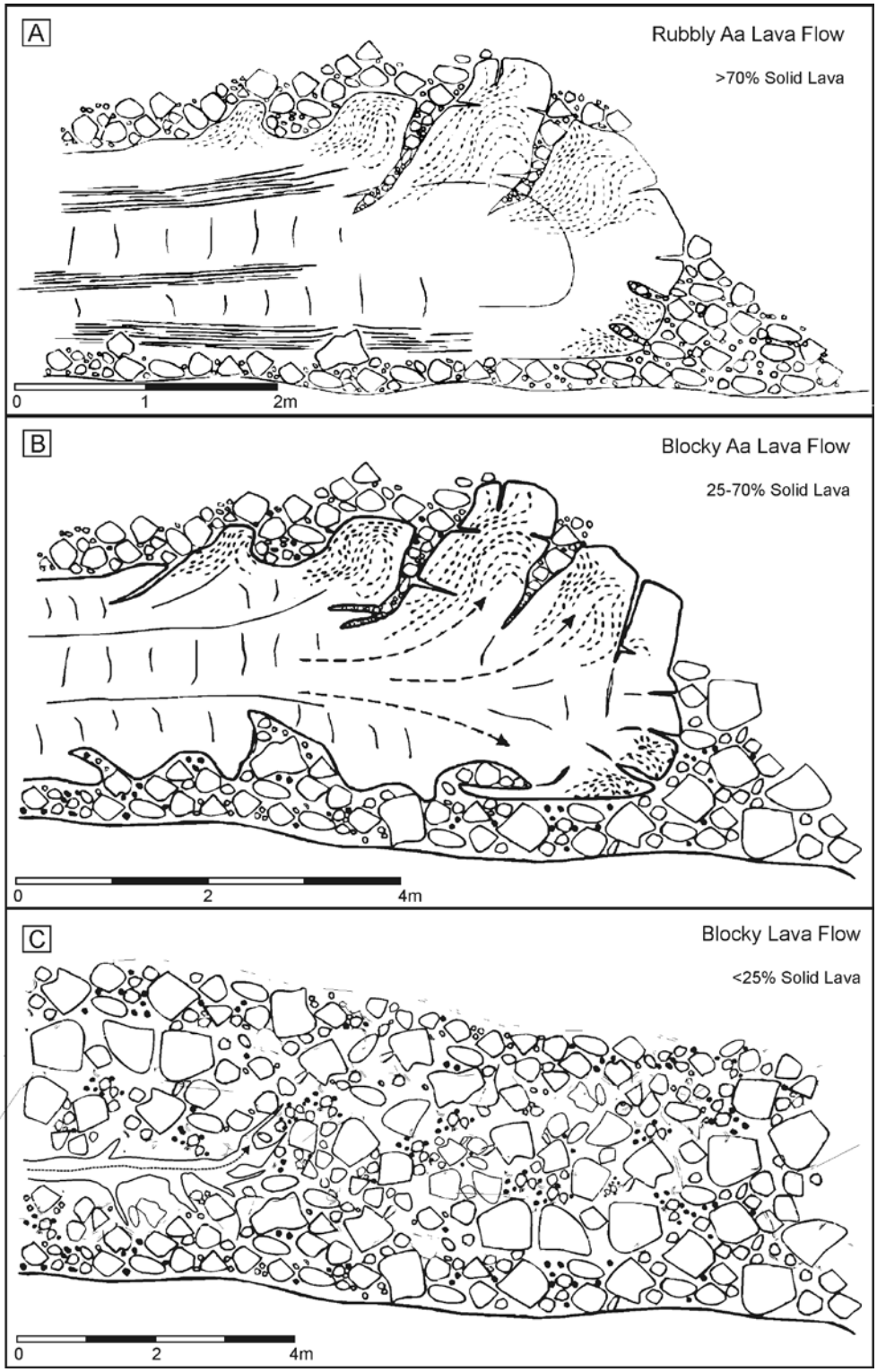

Figure 4.22. Schematic cross sections of rubbly a'a, blocky a'a and blocky lava flows: A) Schematic cross section of a rubbly a'a lava flow of Ruapehu (modified from Avery, 2000). Note the internal columnar jointed massive lava, fragmental basal and upper sections, and ramping structures. B) Schematic cross section of a blocky a'a lava flow of Ruapehu (modified from Avery, 2000). Internal lava is still pictured in this cross section, however becoming further brecciated towards the upper, lower and frontal regions of the flow. Arrows indicate the propagation direction of magma and the resulting squeeze-up / ramping structures. C) Schematic cross section of a blocky lava flow, note the lack of solid magmatic components and thin squeeze-up propagation from the interior of the flow.

A further aspect in the differentiation of flows is the solid magmatic component when compared to the brecciated / blocky components. In rubbly a'a flows this component is broadly classified as >70%, in blocky a'a 25-70%, and in blocky flows <25% (Figure 4.22; Table 4.1). In blocky flows the limited magmatic components are intersected at squeeze-up structures, with the injections being controlled by the shear dynamics of the flow (Figure 4.22).

	Rubbly A'a	**Blocky A'a**	**Blocky**
Example	Sign of the Kiwi	Whakaraupo	Major Hornbrook
Surface	Compact	Loose	Loose / porous
Block Morphology	Spinose Rubbly Sub-angular Globular	Spinose Rubbly Polyhedral Dihedral planes Lineation's (shears) Flow banded Weathered sugary texture	Spinose (low %) Polyhedral Dihedral planes Lineation's (shears) Flow banded Weathered sugary texture
Matrix	Pyroclastic component Angular block fragments	Pyroclastic component Brecciated material (same composition as blocks) Angular block fragments	Brecciated material (same composition as blocks) Angular block fragments
Squeeze-Ups	Inject into brecciated material	Inject into brecciated material	Inject into brecciated material
Shear Planes	Limited (associated with squeeze-ups)	Associated with dihedral block planes	Intersect through outcrop Displace blocks
Channels	Metres wide Solid flow interior	10's metres wide Layered, thin jointed to massive coherent lava	None observed
Levees	Low angle Evident from channelized lava		Limited
% Solid	>70 %	25 – 70 %	<25 %

Table 4.1. Lava flow classification of rubbly-a'a, blocky a'a and blocky lava flows of Lyttelton Volcano.

4.5. Geochemical Trends and Relationship

4.5.1. Previous Geochemical Studies

Of note is the high phenocryst component within blocks at both Whakaraupo and Major Hornbrook sequences, when compared to typical Lyttelton lava of almost aphyric basalts within the coherent interiors of a'a flows. In light of this an overview of geochemical data from previous studies on Lyttelton Volcano was made. A common theme encountered within studies was cyclic magmatic processes (Coates, 1976; Altaye, 1989; Slaughter, 1995; Neumayr, 1998).

Coates (1976) summary and interpretation of the lava flows of north-eastern Lyttelton noted the presence of cyclic phenocryst content in the lavas. Plagioclase, augite and olivine phenocrysts were scarce for large stratigraphic intervals and then rapidly increase in abundance to a maximum before decreasing towards the succeeding less porphyritic interval. Following each porphyritic maxima a major pyroclastic horizon occurs, with Coates (1976) identifying five major pyroclastic horizons on north-eastern Lyttelton Volcano. Altaye (1989) followed with an examination of the Lyttelton lavas designating sequences of an evolving magmatic source, divided into Lyttelton main-phase, and Mt Pleasant Formation, stratigraphically above the Major Hornbrook blocky lava flow sequence. Neumayr's (1998) analysis of the Lyttelton 1 lava pile highlighted an overall maturation of the Lyttelton 1 magma system evolution with time. While within this major trend, smaller cyclic variations of increasing and decreasing porphyricity are evident for the main phenocryst phases.

All of the above studies suggest fractional crystallisation (Coates, 1976; Altaye, 1989; Slaughter, 1995; Neumayr, 1998), which have been constantly interrupted through cyclic eruptive and magmatic processes. Neumayr (1998) further hypothesised that oscillations represented repeated injections of fresh magma into the Lyttelton 1 chamber and small scale fractionation recharge sequences.

4.5.2. Analysis

In light of the characterisation of Lyttelton Volcano's distinctive a'a-blocky lava flow horizons, a review of Neumayr's (1998) geochemical data has been undertaken. Neumayr's (1998) methodology targeted the prominent spurs along the north-western crater rim being sampled and analysed, and then combined into a continuous geochemical evolution. In the stratigraphic context of Lyttelton Volcano, these spurs represent isolated sections through Lyttelton lava flow stack, which need to be put into the context of the volcanics evolution through definition of their association with a lava sequence or a'a-blocky lava flow horizon.

Sampled sections, primarily along the major inner harbour spurs, display highly variable mineral percentages throughout stratigraphic sequences (Figure 4.23). An important association between increased feldspar content and decreasing clinopyroxene and olivine contents, and blocky lava horizons is evident. With the intersection points of sample lines and mapped blocky lava flow units, coinciding with a peak in feldspar mineral volume (Figure 4.23).

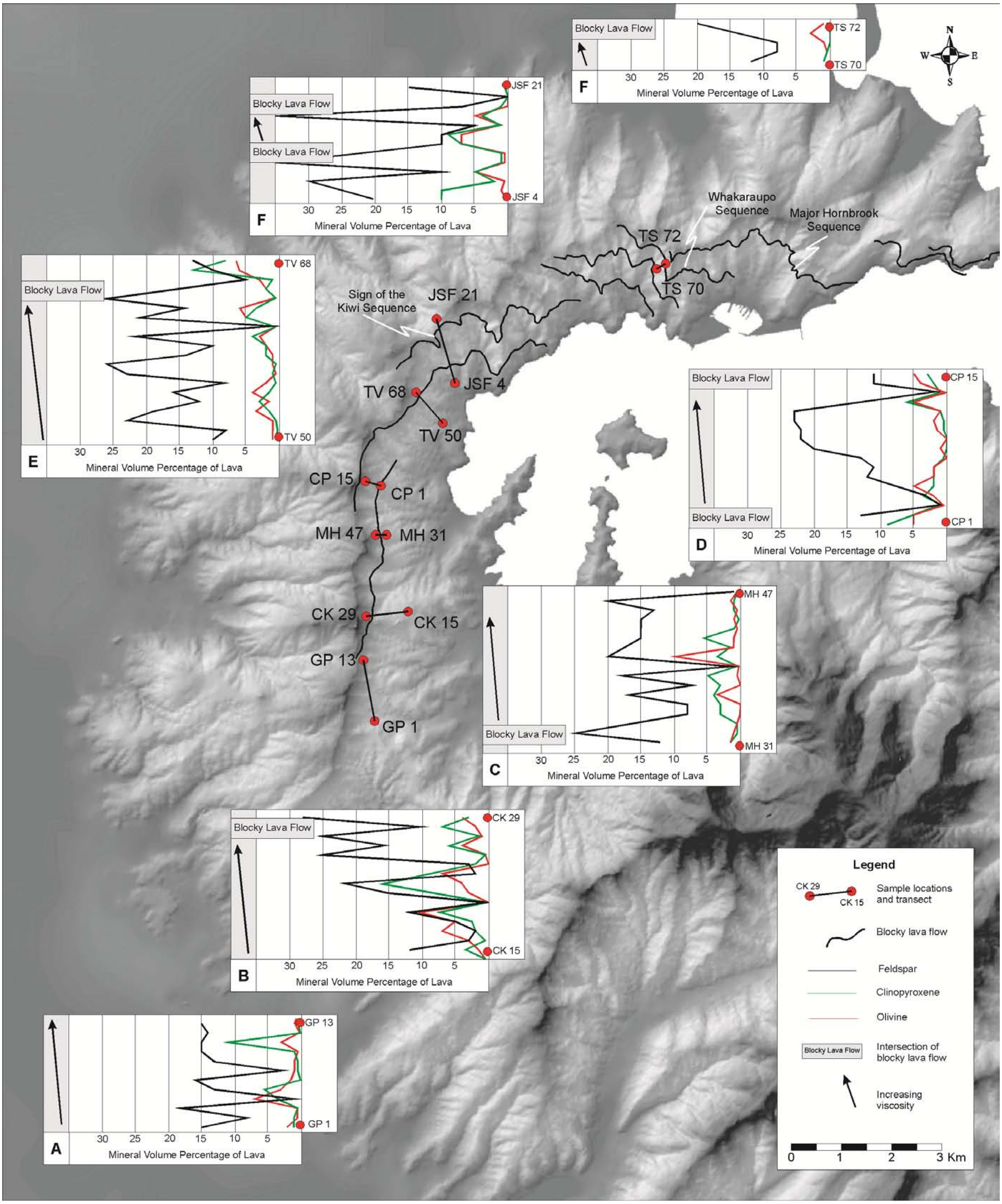

Figure 4.23. Location and trends of Neumayr (1998) geochemical analysis and relationship to blocky lava flows of Lyttelton Volcano. Where sample points and lines intersect blocky lava flow horizon, a distinct relationship between feldspar content, hence viscosity is evident, supportive of magmatic cycles.

4.5.3. Interpretation: Magma Cycles

An important observations on Lyttelton Volcano is the evolving trend of lava geochemistry from the oldest lavas exposed in Gebbies Pass (south-west) to those exposed at Sumner (north-east; Sewell et al., 1992; Neumayr, 1998). Pinel and Jaupart (2004), note that the progressive evolution of lavas over time, indicate formation of a magma reservoir in volcanic fields.

Cyclic magmatic variations are only expressed when chemical, isotopic, or mineral variations are plotted against time or stratigraphic position. The resulting plots enable identification of chemical trends within a volcano, to physical field features and relationships encountered in the field, i.e. volcanic collapse at Stromboli Volcano (Francalanci et al., 1989) and Tahiti Nui (French Polynesia; Hildenbrand et al., 2004). Chesner and Rose (1984) study on the Fuego volcanic complex (Guatemala) identified magma batches based on mineral compositions (Figure 4.24). Similar geochemical and mineralogical studies at Fuego de Colima, Mexico (Robin et al., 1991) and Basse Teree, Lesser Antilles Arc (Samper et al., 2007), have further highlighted magma cycles in volcanic complexes.

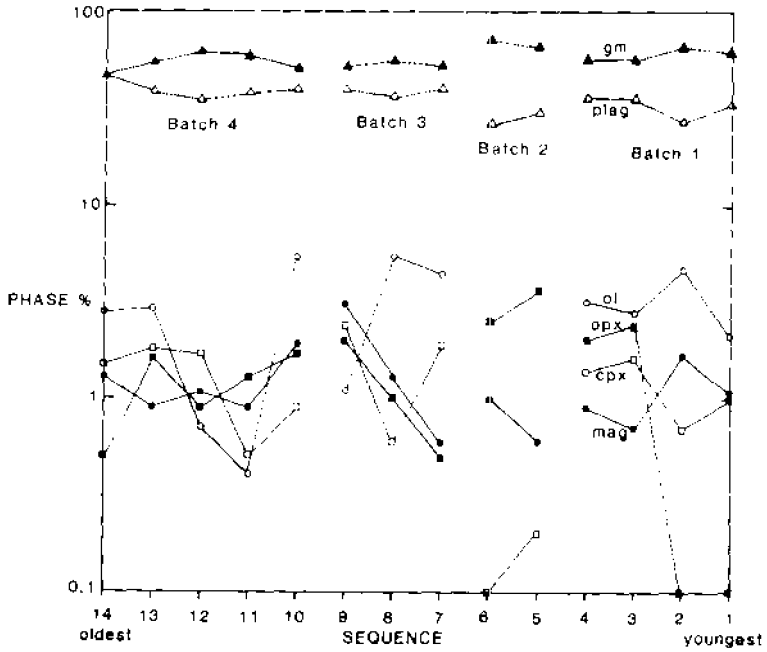

Figure 4.24. Magma batches of based on petrography from the Fuego volcanic complex, Guatemala (Chesner and Rose, 1984).

It is therefore proposed that the Lyttelton lava flow sequence represents cyclic magma batches. The relationship between magmatic phases and extrusive / eruptive styles is evident with the close association of blocky lava horizons and peaks in feldspar content (Figure 4.23). This is a similar relationship observed at Fuego de Colima (Robin et al., 1991) where magmatic cycles alternate from short mixing to long crystal fractionation, resulting in short explosive to long effusive / extrusive phases, respectively. A factor highlighted by Robin et al. (1991) is this cyclic activity conflicts with Luhr and Carmichael (1980) model of explosive phases at the end of each cycle.

The Lyttelton lava flow sequences could conform to either Robin et al. (1991) or Luhr and Carmichael (1980) cyclic models. North-eastern Lyttelton Volcano blocky lava flow horizons are infiltrated and overlain by pyroclastic and epiclastic deposits, indicating a change to explosive eruptive style, followed by degradation of and deposition onto the volcanic surface (Figure 4.15). The Whakaraupo Sequence has the best example of this with primary red ash, infiltrating the matrix poor upper horizon of the blocky flow, ultimately mantling the upper surface, prior to volcaniclastic deposition. Exposures of brecciated lavas between the Tors and the Bridle Path (Figure 2.27B) also have similar relationship, with brecciated lavas being locally covered by pyroclastic deposits and then covered by volcaniclastic sequences. This is suggestive of the effusion of blocky lava, a phase of explosive activity followed by a period of volcanic quiescence and degradation.

The brecciated lava horizons encountered throughout the Lyttelton Volcano structure represent highly viscous lavas, evident through the flow rheology and high phenocryst contents. In the transition from a'a to blocky lava flows crystallinity is a key factor, influencing crustal cooling, the ability to flow and associated strength (Kilburn, 2001). Highlighted within the geochemical trend is the increase in feldspar phenocryst content, increasing the crystallinity and therefore the observed transition from a'a to blocky lava flows.

4.6. Summary

- Distinct lava flow sequences are evident on Lyttelton Volcano, intersecting the erosional crater rim obliquely.
- No major individual unconformity is evident within the Lyttelton lava flow sequence.
- 10 brecciated lava flow horizons, representing blocky a'a to blocky lava flows, are recognised on the north-western side of Lyttelton Volcano within the typical a'a lava flow sequence.
- Key identification / classification of flow type are defined by; block morphology, matrix, squeeze-ups, shear planes, channels, and blocky to solid lava ratio.
- Geochemical trends indicate cyclic eruptive processes / magma system evolution, with increased crystal content, resulting in a change from blocky a'a to blocky lava flow horizons within the Lyttelton lava flow sequence.
- Eruptive episodes are marked by a'a lava flows, evolving up sequence, followed by an explosive phase, then quiescence indicated by overlying epiclastic deposits.

CHAPTER 5

PRIMARY VOLCANIC LANDFORMS AND ERUPTIVE CENTRE IDENTIFICATION

The following is a revision of the paper published in Geomorphology 104 (2009) 284-298. Doi: 10.1016/j.geomorph.2008.09.005.

5.1. Introduction

Primary volcanic landforms are features produced during active volcanism. Trends, orientations and structure of these features provide direct records of an associated volcanic structure, which can be used to identify eruptive centres of highly degraded volcanic structures. The use of primary volcanic features and the resulting geomorphic signatures requires an understanding of the volcanics involved and the relationship / modification of volcanic structure to post volcanism processes. Previous use of primary volcanic landforms has been limited by post volcanic movements and deposition (Szèleky and Karatson, 2004). Banks Peninsula provides a unique situation to observe well preserved volcanoes, in a un-deformed tectonic setting, where erosion has played a significant part in the current morphology, and where the underlying volcanic structure had significant control.

Banks Peninsula, on the east coast of the South Island, New Zealand, comprises three main volcanoes active between 11.0 to 5.8 Ma. Lyttelton Volcano (11.0 – 9.7 Ma) and the Akaroa Volcano (9.3 – 8 Ma) are the larger volcanic constructs of Banks Peninsula (Figure 5.1), with the contemporaneous Mt Herbert Volcanic Group (9.7 – 8 Ma), occurring in the central region of Banks Peninsula. Late stage activity occurred on the eroding flanks and within the degraded volcanoes (Diamond Harbour Volcanic Group (8.1 – 5.8 Ma)).

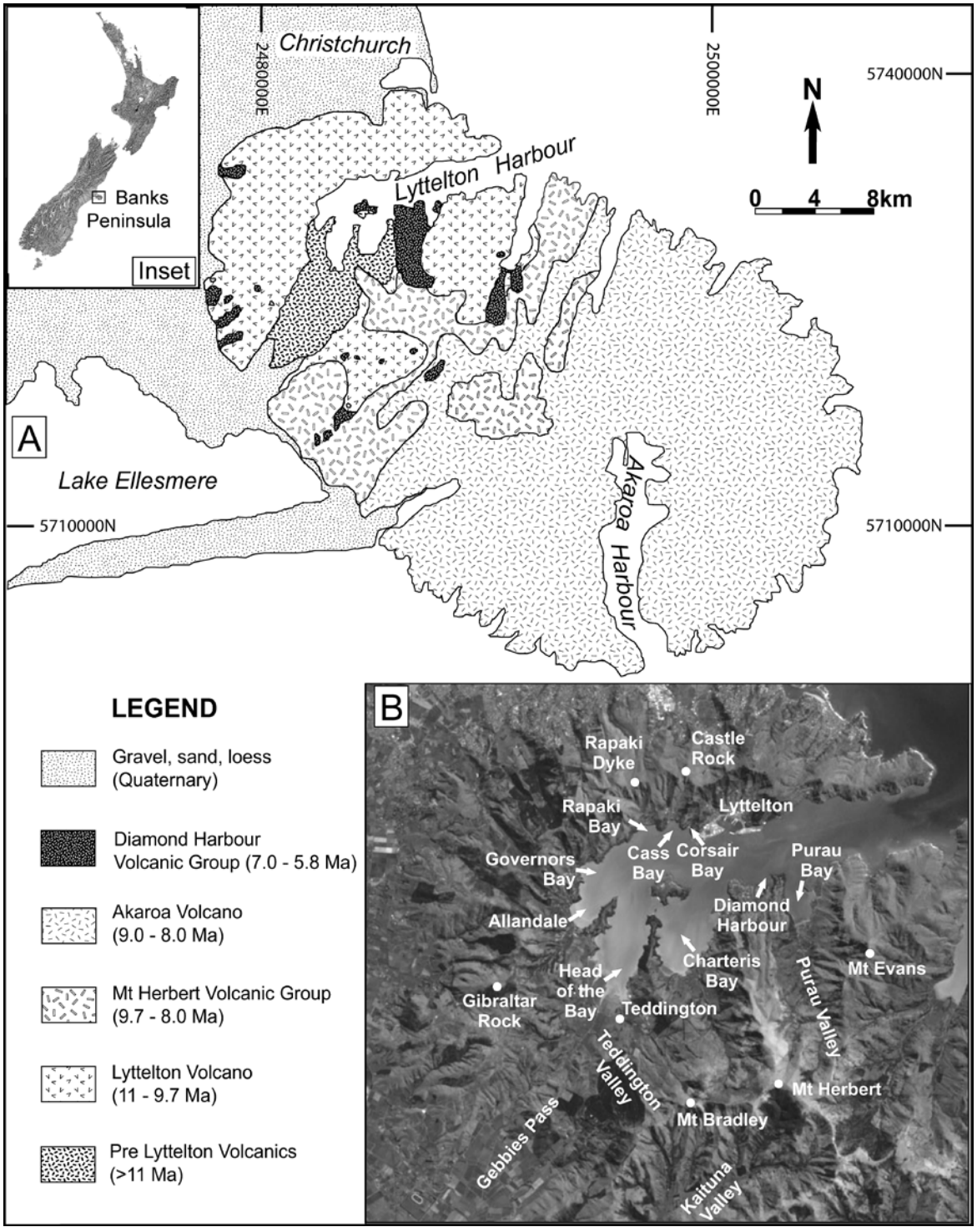

Figure 5.1. Simplified geology of Banks Peninsula.

Lyttelton Volcano (11.0 – 9.7 Ma), the oldest of this volcanic sequence has long been considered to be the result of simple large volcanic edifices, which underwent sector collapse, due to the current almost circular highly eroded caldera morphology and Lyttelton Harbour (Haast, 1879; Speight, 1916; 1938; Shelley, 1987, 1992; Sewell, 1988; Sewell et al 1992). Lyttelton Harbour has also been established as the type

section for ‘erosion calderas’ by Williams (1941). A detailed study of the geomorphology of Lyttelton Volcano using primary volcanic landforms and the projection of associated orientations is used to identify multiple eruptive centres, and reinterpret the evolution of the volcano, which is now highly modified by erosion. Individual centres are discussed, highlighting features associated with volcanic cones, such as lava flow dips and strikes, erosional crater rims, valleys, ridges, and radial dyke swarms.

5.2. Primary Volcanic Landforms: Feature Recognition

Primary volcanic landforms are those features produced by active volcanism, and the immediately following degradation, which reflect the apparent shape of a volcano just after extinction (Szèleky and Karàtson, 2004). This study classifies primary volcanic landforms into constructional, hypabyssal, and erosional volcanic features. Constructional volcanic features directly relate to the growth phases of a volcanic construct, and include lava flows, scoria cones and pyroclastic layers. Hypabyssal volcanic features are the internal features of a volcano, primarily dykes and sills. Erosional volcanic features reflect the degradation of a volcano, recorded in valley and ridge patterns and associated erosional structures, with the radial inception of features being controlled by the initial volcanic form. Lyttelton Volcano provides a unique situation where primary volcanic landform signatures are preserved in an almost pristine volcanic setting, due to the absence of post-eruptive tectonic movements (Bal, 1997), an important consideration highlighted in volcanic reconstructions by Szèleky and Karàtson (2004).

5.2.1. Constructional Volcanic Features

Lava flows are the main constructional component of a volcanic cone. These are often sourced from the main vent, although some lava flows are associated with parasitic cones. Main vent lava flows are expansive (1 to 10’s of metres thick), with flow morphology dependent on the centre of volcanism and previous topography. Lava flow orientations indicate cone-like structures with the internal stratification of lava flows interspersed with agglomerates and pyroclastic layers. Where overlapping cones

occur, earlier lavas will be centred on an earlier cone, while the higher stratigraphic lavas radiate around a younger cone.

Scoria cones and domes are the surface reflections of flank activity on volcanoes, and may also be buried by the next phase of volcanic activity. Scoria cones and domes directly reflect the internal plumbing and inherent planes of weaknesses of a volcano as they are commonly dyke-fed (Shelley, 1992). Determining the location of scoria cones and domes enables recognition of the outer flanks of a volcanic cone, allowing the identification of which eruptive centre they are associated with.

5.2.2. Hypabyssal Volcanic Features

Hypabyssal volcanic features reflect zones of weakness and stress conditions in a volcanic cone. They typically form radial dyke systems / swarms from the injection of magma (infilling fissures) through inherent weaknesses within the volcano, controlled by local gravitational forces (Shelley, 1992; Carrigan, 2000). Sills are commonly related to dykes and reflect the structural integrity of individual eruptive centres and overall volcanic structure.

5.2.3. Erosional Volcanic Features

Valley orientations record incision radial to the centre of volcanism (Karàtson et al., 1999), with initial inception during the growth and active phases of volcanism becoming the predominant erosional axis throughout landform degradation. Ridges are the inverse features left after radial incision (valley formation) of a conical volcano, representing the least eroded surface of a volcanic cone (Szèleky and Karàtson, 2004). Radial valley and ridge patterns are primary erosive features of a volcanic cone, which become accentuated / enhanced by proceeding erosion. Valley and ridge systems produce characteristic features, dependent on the amount of erosion. Initial incision produces barrancas or deeply cut ravines, radial to the cone, following the initial slopes (Cotton, 1944). Planèzes (Figure 5.2) are the sub-mature dissection of a cone, where sectors of constructional surfaces survive on the ridges between deeply eroded major consequent valleys (Cotton, 1944).

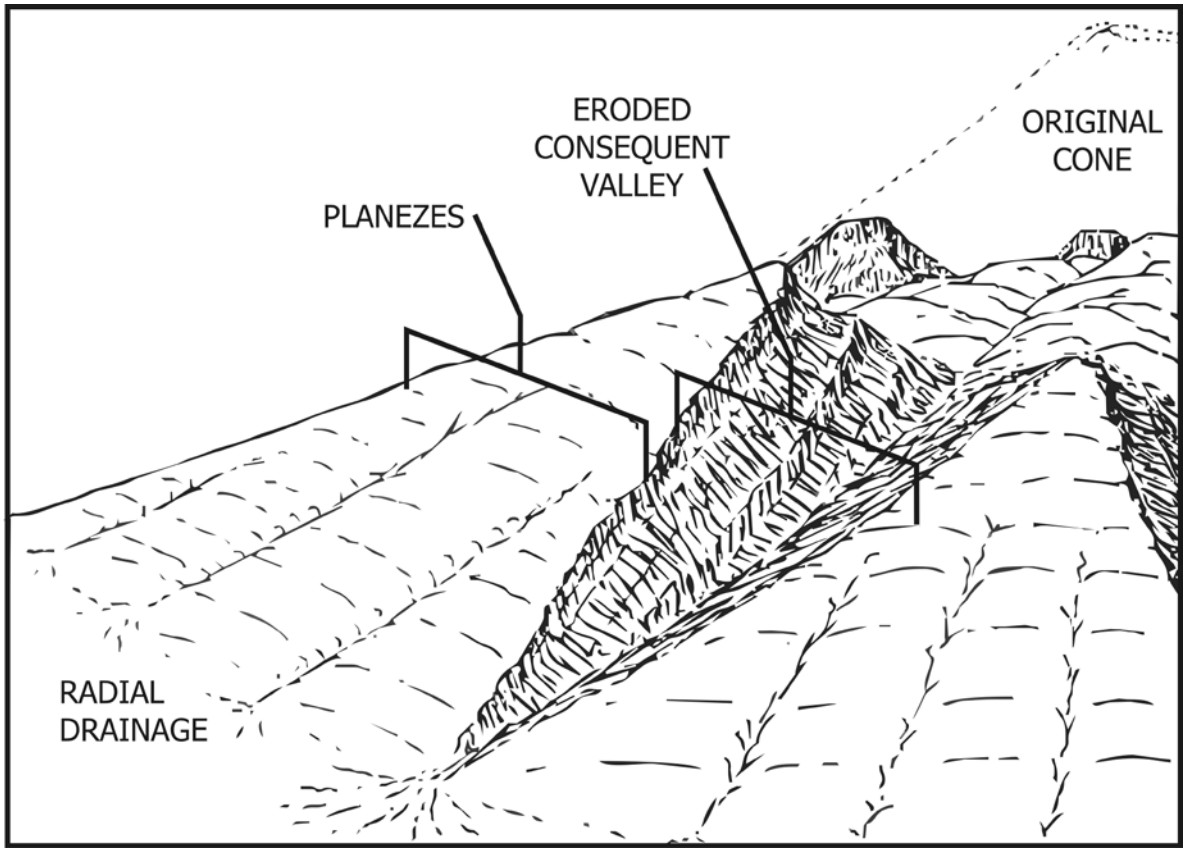

Figure 5.2. Planèze formation through inception and degradation of radial drainage (modified from Cotton, 1944). The flat profile, dip slope of the planèze is the result of being bounded on each side by escarpments that run up to a point or ridge, which orients towards the volcanic centre, or overlook an interior hollow developed by erosion of the volcanic centre (Cotton, 1944).

5.3. Methodology

Primary volcanic landforms have varying topographic signatures, each requiring a differing identification/extraction technique. This methodology follows the process used in the initial recognition of multiple volcanic centres, through the comparison of the current volcanological model to the observed deposits.

1. Aerial photograph analysis of major lava flow features, with recognition of blocky lava flows.
2. Re-plotting of dyke orientation databases, highlighting dyke assemblages.
3. Projection of valley and ridge trends, to indicate volcanic summits.
4. Recognition of further constructional and hypabyssal volcanic features intimately related to each eruptive centre.

Primary volcanic landform recognition is aided by the use of aerial photographs and digital terrain models (DTM) in ArcGIS to produce layers for the further analysis of features. Generation of layers (contour, slope aspect, hillshade, and stream features) is within ArcGIS using 3d Analyst Tools, calculated from a 10 m cell size / resolution DTM, supplied by GNS, New Zealand (projected coordinate system GD 1949 New Zealand Map Grid, on the 1949 Geographic coordinate system). Contour models presented are at 25 m contour intervals, with all figures displayed in New Zealand Grid references based on New Zealand Topographic Maps M36, M37, N36 and N37. The details of the projections and layers used in DTM analysis are expanded in each methodology sub-section.

Constructional and hypabyssal volcanic features, such as scoria cones, domes, sills and dykes, require geographic location and trends / orientation of features. This information is sourced from published geological maps (Sewell, 1988; Sewell et al., 1992), unpublished theses (Sewell, 1985; Shearer, 1986; Hibberd, 1994; McKenzie, 1995; Slaughter, 1995; Neumayr, 1998), field notes produced by Dr David Shelley over four years of field study, and field observations. Reference point data of these features is put into ArcGIS and overlaid on simplistic contour maps, providing databases for each feature.

5.3.1. Constructional Volcanic Features

Lava flow trends are identified by aerial photograph analysis, together with field observations and mapping. Ortho-corrected aerial photographs are placed in a drawing programme and observable lava flow contacts / outcrops traced. Inferred strike and dip symbols are overlain onto specifically identified areas ('v'-ing of valleys, and ridge crests contacts), and confirmed with field mapping and observations. Lava flow orientations on the outer volcanic slopes are best exposed in valley sides and ridge crests, where vegetation cover is limited. The 'v'-ing of the valleys enables perspectives of lava flow orientations to be established from lava flow relationships between valley sides (Figure 5.3). Ridge crests are identifiable features on aerial photographs, often marked by steep eroded lava faces continuous around the downhill side of a spur. This technique, rather than direct recording of strikes and dips, is used as strikes and dips

recorded at an outcrop only represent a localised lava trend that responded rapidly to underlying topography and not the overall trend of a lava flow.

Unconformable surfaces are recognisable features that represent significant time and compositional / rheological changes between eruptive products. Horizons are mapped through aerial photographs, field observations and previous mapping, and transferred into a drawing programme. These data are then exported and transferred into ArcGIS software enabling identification and the 3-D visualisation of features.

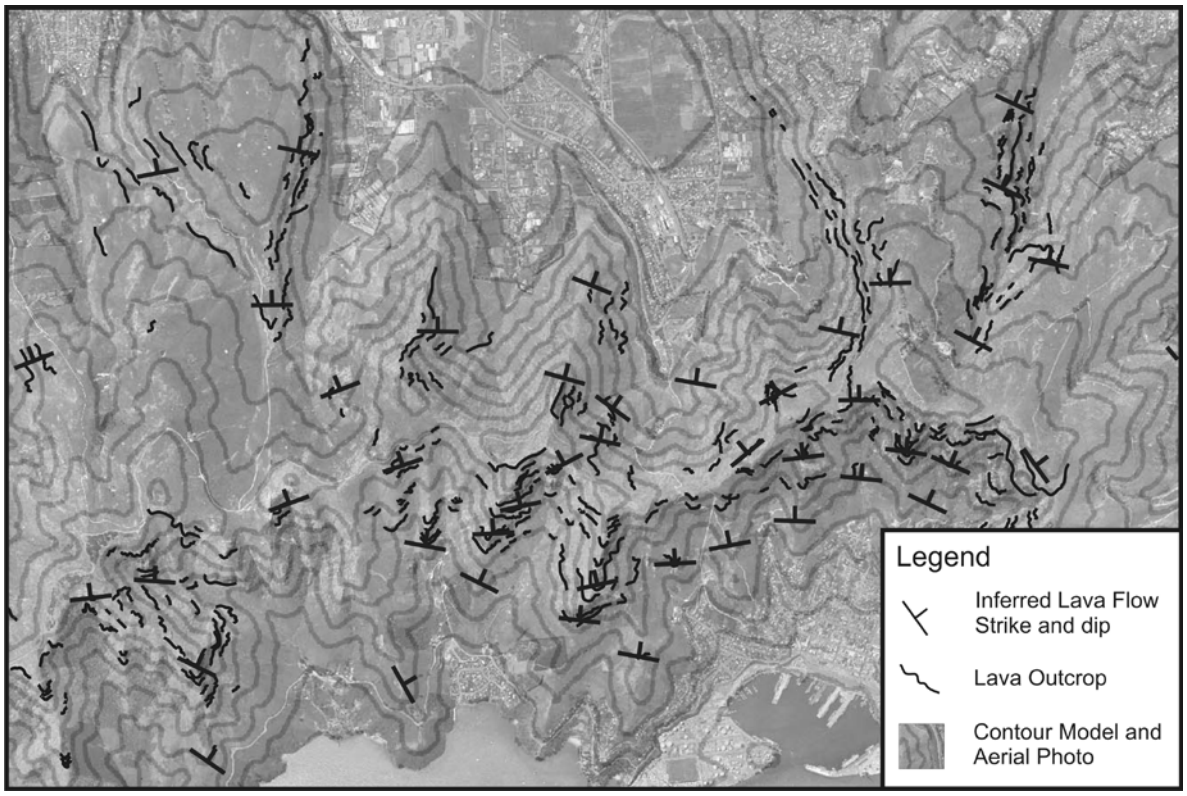

Figure 5.3. Identification and extraction of lava flow features, through the tracing of lava flow trends on aerial photographs and the projection of strikes and dips from relationship between outcrop and contour.

5.3.2. Hypabyssal Volcanic Features

Dyke orientations and projections follow the principles developed by Brandle et al. (1991) and used successfully by Ancochea et al. (1994, 1996, 1999, 2008) on the eroded volcanoes of La Palma, Tenerife, Fuerteventura, and La Gomera, where each dyke is considered to be a straight line, which converges at the hypothetical eruptive centre. This method requires each dyke recorded to be located on a base contour map

and the strike drawn, which is then digitized in a drawing programme. The next phase is the projection / lengthening of individual dyke orientations towards the central regions, using the drawing programme. Dyke orientation data is then imported into ArcGIS, and geo-rectified creating a database of dykes. Once orientations are projected, similar areas of convergence can be recognised. Where multiple dykes are recorded at one location the predominant trends are projected, reducing the doubling up of common trends. This study only uses dyke trends from near the erosional crater rim, as these dyke trends directly reflect the cone structure, due to the greater gravitational and cone stress control, which the lower (i.e. shore platform) dykes would be lacking.

5.3.3. Erosional Volcanic Features

Valleys

Valley orientations are extracted from erosional axes highlighted in ArcGIS analysis. Hillshade images are produced from a DTM (10 m resolution), overlain with stream features and a 25 m contour (calculated from the 10 m resolution DTM), highlighting the current drainage network. The longest erosional valley axes are identified in a somewhat selective process, performed by eye within the computer programme. This is to eliminate landform features modified by processes not directly related to primary volcanic landform processes (inception of a radial drainage pattern), like smaller tributaries and larger in-filled valley floors. An erosional valley axis is identified by recording the overall valley location, trend and distance, stream sinuosity, valley side steepness (relief), and fitting a best fit straight line for the longest valley segment. Valley orientations are produced by extending the identified longest valley segment into the central region / volcanic highpoint. This technique is a continuation of the techniques and hypotheses of Karàtson et al. (1999), Szèleky and Karàtson (2004), Jordan et al. (2005), and Hildenbrand et al. (2007).

Ridges

Definition and projection of ridge orientations follow similar principles to valley orientations (Figure 5.2). A hillshade image is produced from a DTM (10 m resolution),

which is overlain with a 25 m contour model and a slope aspect model. Slope aspect models are produced within ArcGIS, colour coding slope faces according to orientation, while the use of 25 m contour models with stream features overlaid, enables easy and correct placement of ridge segments. Ridge trends are drawn in ArcGIS, as straight lines on the longest uninterrupted sequence of a spur on the outer volcanic flanks. Location of a ridge's longest uninterrupted straight line segment is controlled by staying within the 'V' of the downhill contours of the ridge, and between the colour changes highlighted in the slope aspect model. This is a process performed by eye within ArcGIS. There is some bias with this process as dykes are more resistant to erosion than the surrounding rock, and may preferentially contribute to ridge formation (Shelley, 1992). Recorded ridge segments are then projected into the interior of Lyttelton Harbour using the same projection technique and hypotheses of valley segment projection.

5.4. Results

5.4.1. Constructional Volcanic Features

Lavas flows of Lyttelton Volcano are 1-10 m thick with limited pyroclastic layers and dip away from the harbour by up to 30°. Strikes identified from aerial photograph analysis are not uniform about a central point in the harbour, but appear to radiate about multiple locations within the harbour (Figure 5.4). On the Port Hills side of Lyttelton Volcano, dips radiate around the bay regions (Teddington to Lyttelton), while on the eastern side of the harbour lava flow strikes radiate over Purau and upper Teddington valleys (Figure 5.4).

Ten blocky lava flows occur as distinct horizons within the typical aa lava flows on the western inner harbour slopes (Allandale to Lyttelton) of Lyttelton Harbour. These deposits occur near the current erosional crater rim and descend to near sea level (Figure 5.4). Associated with blocky lava horizons are onlapping sequences, with shallower lava flow dips and different morphology. Typical onlapping sequences of Lyttelton Volcano are best identified when exposure is near to perpendicular to lava flow strike. Further lava flow unconformities are present to the east (Mt Evans region)

and south (south of Mt Bradley), where subsequent volcanic product cover provides preservation of remnant cone surfaces. These provide significant control on the outer surfaces of these cones, with the overall morphology of these zones indicating centres similar to strike and dip orientations.

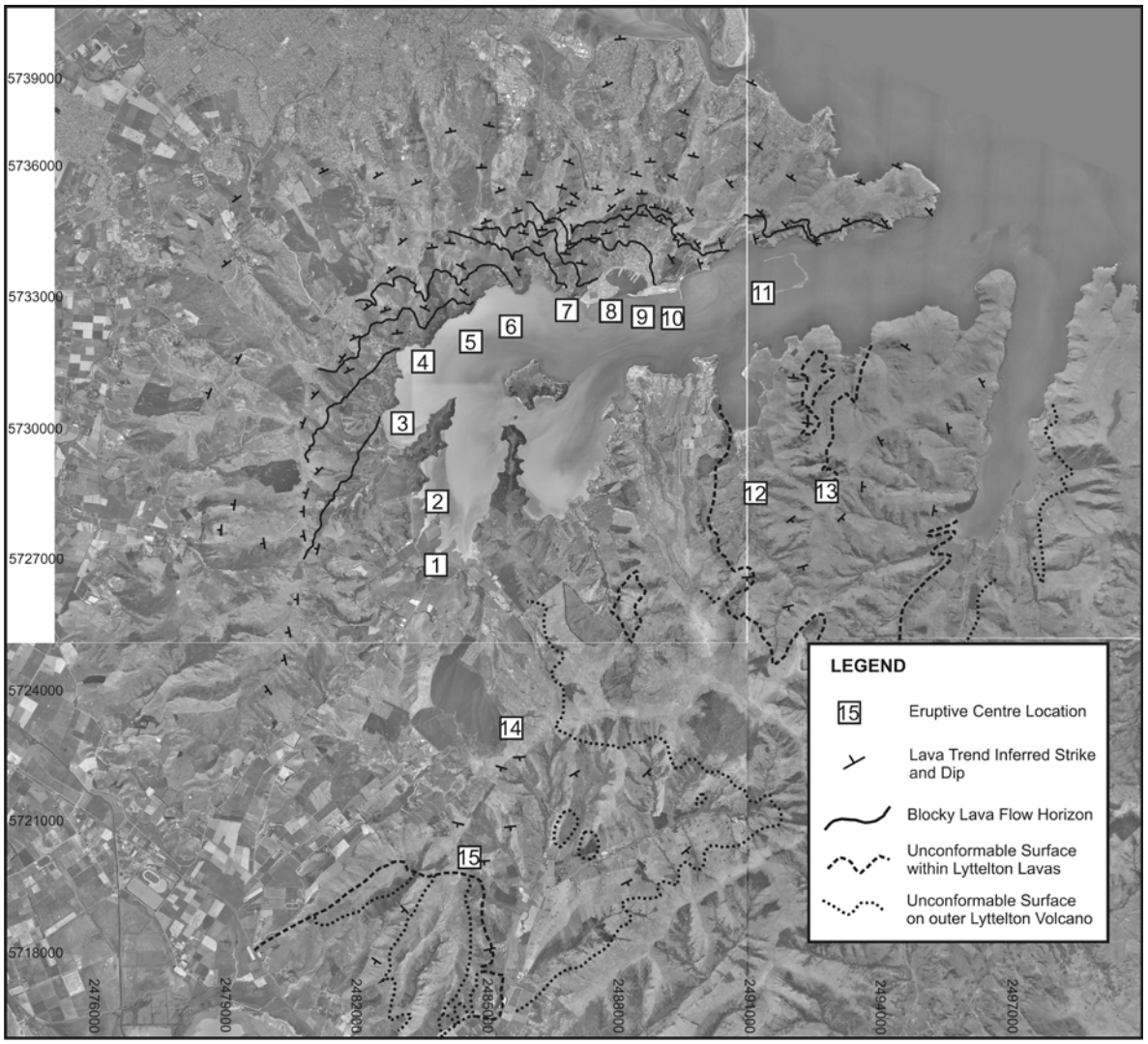

Figure 5.4. Lava flow trends (strikes and dips), blocky lava flow horizons and unconformable surfaces of Lyttelton Volcano.

Scoria cones and domes of Lyttelton Volcano occur either on the outer volcanic flanks or within lava sequences on the inner harbour slopes (Figure 5.5), with the majority being just below the erosional crater rim. Locations of scoria cones on Lyttelton Volcano are well known due to their use in building stones for Christchurch and from previous studies (Sewell, 1988; Sewell et al., 1992), and unpublished theses (Sewell, 1985; Shearer, 1986; Hibberd, 1994; McKenzie, 1995; Slaughter, 1995; Neumayr,

1998). They can be easily identified on aerial photographs because of their erosive tendencies when compared to harder lava flows. Recognised domes on Lyttelton Volcano are trachytic in composition and often have an associated dyke trending towards there longest axis, with the resulting feature forming a spur (i.e. Castle Rock and Gibraltar Rock).

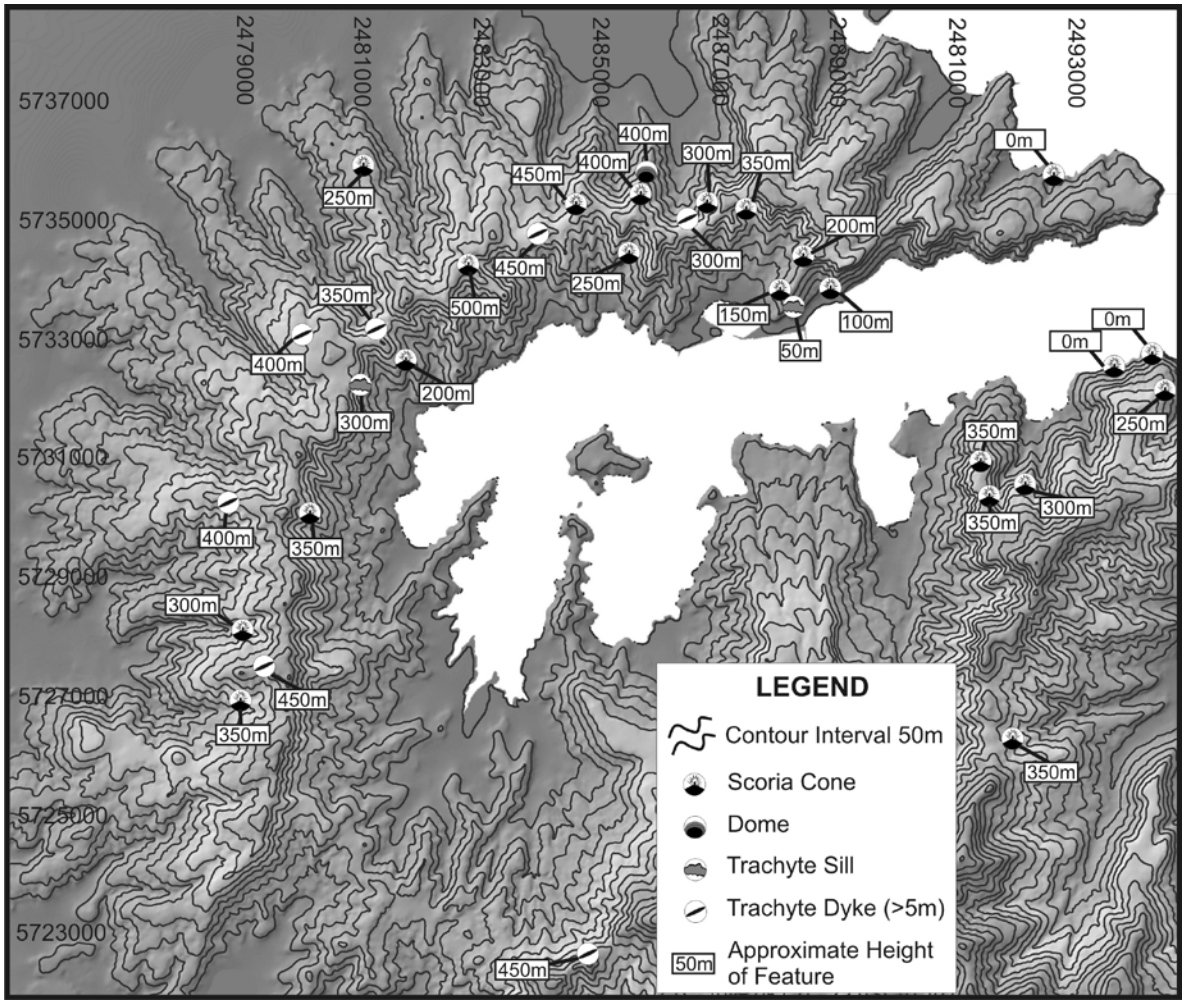

Figure 5.5. Locations of scoria cones, domes, sills and trachyte dykes (>5 m) of Lyttelton Volcano. Heights of features, in metres above sea level, are displayed in boxes.

5.4.2. Hypabyssal Volcanic Features

Dykes of Lyttelton Volcano are predominantly basaltic in composition, 1 – 2 m in width, with a blade-like form (Shelley, 1988). Large dykes (> 5 m wide) of trachytic composition are exposed along the erosional crater rim of Lyttelton Volcano and have a close affinity with blocky lava flows. These dykes are either massive (one dyking event) or are a series of dykes, often cutting through a larger dyke, producing

significant rock promontories (10's to 100's of metres) on either side of the erosional crater rim.

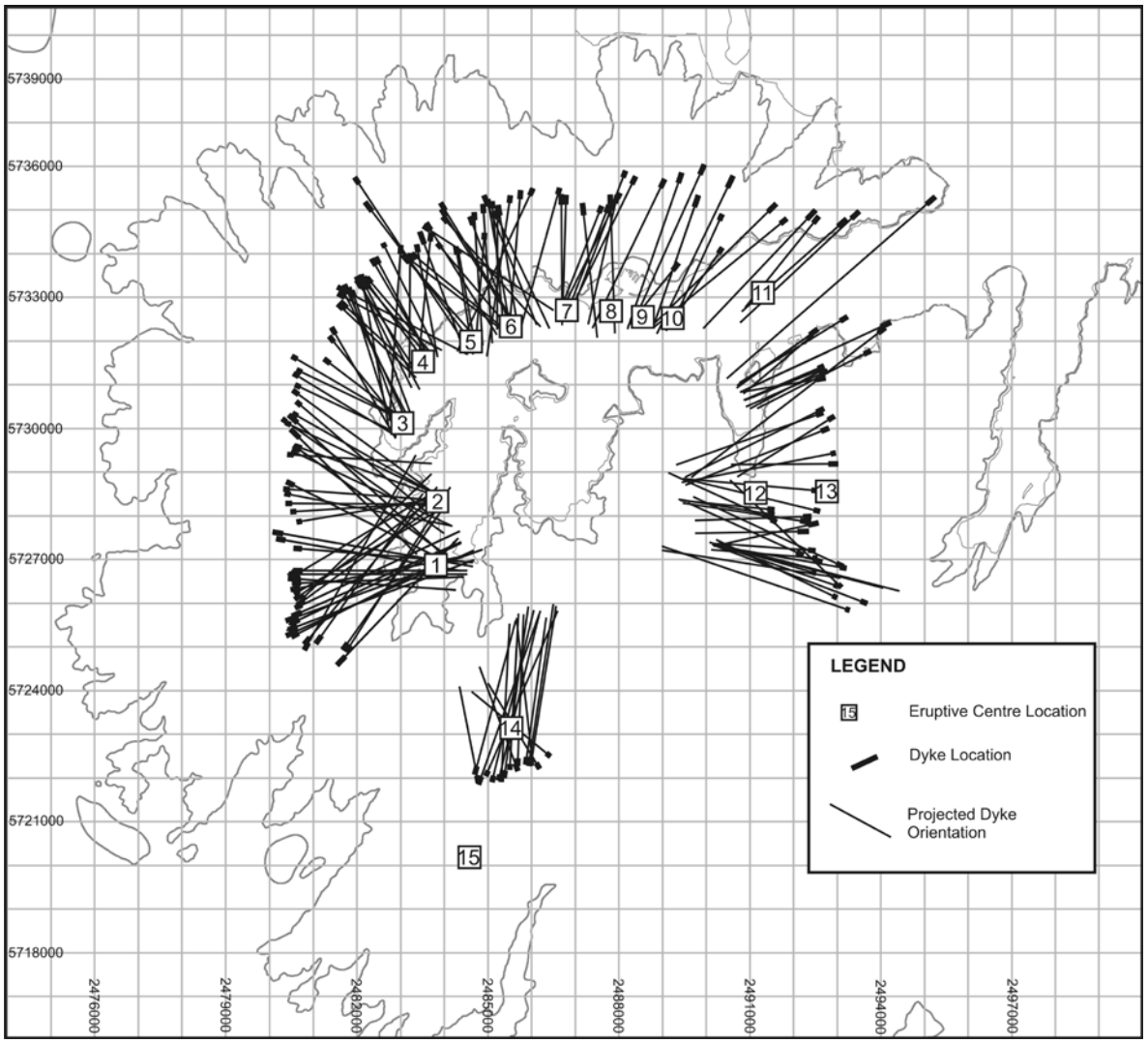

Figure 5.6. Dyke orientations and projections from the erosional crater rim into the inner Lyttelton Harbour regions. Zones of convergence are highlighted by 500 m x 500 m squares, with numbers within boxes indicating volcanic centre number. Dyke locations are highlighted by bold line segments, on the individual projected orientations.

Dyke location, orientation and projection are displayed in Figure 5.6. Large scale dykes are included in the projected dyke trends. Distinct clusters of dyke orientations converge in the harbour regions, projections beyond these convergent zones is limited due to the formation of a spaghetti effect. Two sills of Lyttelton Volcano have been recognised with locations depicted in Figure 5.5.

5.4.3. Erosional Volcanic Features

Valley orientations of the Lyttelton Volcano highlight 13 regions of convergence, radiating outwards from the harbour regions (Figure 5.7). Longest valley segments are depicted as bolder lines than the associated projected orientation. Younger valleys are observable at higher stratigraphic levels and have shorter line segment lengths when compared to the stratigraphically older and subsequently further incised valley systems. No valley orientations trend from centre 8 and centre 14. Centre 8 valleys are overprinted by following volcanism, primarily from centre 9. Centre 14's valley orientations have been overprinted by subsequent volcanism, which had the effect of covering primary erosive radial features, and initiating new erosional systems forming Kaituna Valley. Main valley orientations, longest segments are predominantly located in lower in valleys, reflecting deep incision of primary trends resulting in broader more incised valleys. Shorter valley axes are located in upper valley regions, with the lower valley axis often relating to the previous cone.

Longest ridge segments of Lyttelton Volcano have 15 zones of convergence within the harbour (Figure 5.8). Ridge segments are identified as bold segments on the end of projection lines, while ridge projections are limited to where they crosscut a ridge trend in close proximity, as these should be co-evolutionary features. Centres with limited ridge orientations are the result of later volcanism covering features, centres 7, 8, 10, 14, and 15. Longest ridge segments are located in the mid- to lower outer slopes, with upper ridge axes being shorter segments.

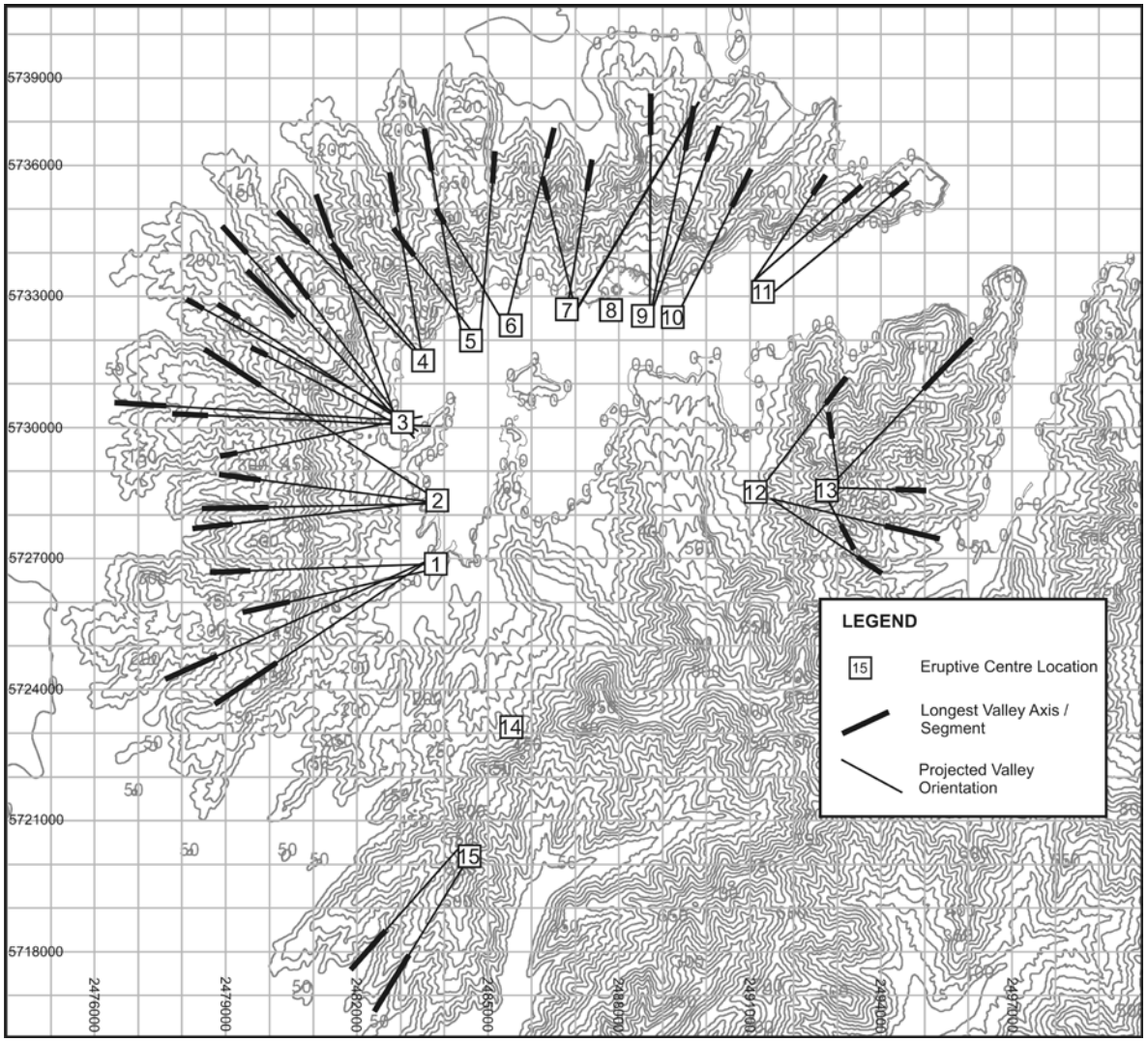

Figure 5.7. Valley orientations and projection of main valley axis into the inner Lyttelton Harbour regions. Longest valley segments are highlighted by bold sections on projections. Zones of convergence are highlighted by 500 m x 500 m squares, with numbers within boxes indicating volcanic centre number.

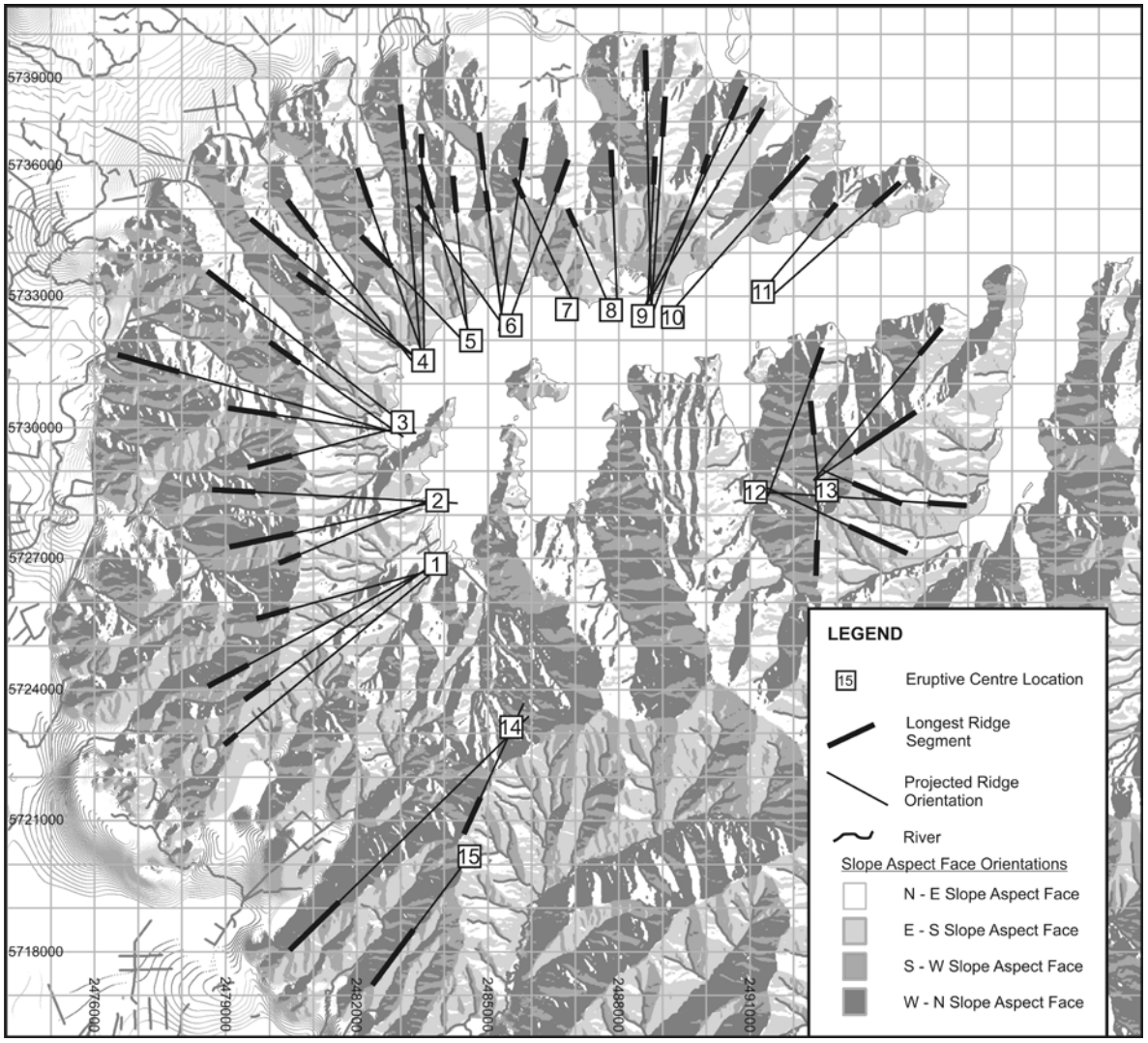

Figure 5.8. Ridge orientations and projection of longest ridge axis segments (bold lines) to inner Lyttelton Harbour regions. Zones of convergence are highlighted by 500 m x 500 m squares, with numbers within boxes indicating volcanic centre number.

5.5. Identification of Eruptive Centres

Where multiple primary volcanic landform orientations and trends (radiating lava flow strikes and dips, outer blocky lava flow horizon, marked unconformity, dyke swarms, valley or ridge orientations) converge an eruptive centre can be postulated. A zone of convergence is defined as a 500 m x 500 m grid area, a hypothetical crater rim area of a typical volcanic cone. Orientations of valleys and ridges only support the existence of a topographic highpoint, with a radiating erosive pattern. When dyke orientations and lava flow trends converging to the same zone of convergence (grid area) it is then likely these convergences represent an eruptive centre.

Lyttelton Volcanoes primary volcanic orientations and trends indicate 15 zones of convergences / eruptive centres. Each eruptive centre has a defined array of primary volcanic landform features; (Figures. 5.4, 5.6, 5.7, 5.8). Two eruptive centres (8 and 14) do not have the associated erosional primary volcanic landform features as these have been completely overprinted by subsequent volcanism. These centres are identified through the presence of a dyke swarm, blocky lava flow horizon, the orientation (trends) of associated lava flows, overlying volcanic products, and the relationship with the underlying volcanic centre. Centres 13 and 15 do not have associated dyke swarms, despite this eruptive centres can be identified with associated primary volcanic orientations and trends. Centre 13 dyke swarm could be associated with centre 12 swarm, due to the close proximity of eruptive centres. Centre 15 has a mapped vent location, and erupted directly onto the flanks of cone 14, forming mantling lava flows rather constructing a cone

5.5.1. Cone Sectors and Artefacts

Cone sectors are the preserved outer flank surfaces of individual volcanic cones / eruptive centre. Sectors are defined as regions on a volcano's outer flanks with an array of orientations from zones of convergence. Based on this relationship, cone sectors can be established for each eruptive centre. Cone sectors each have a limited overlap of features, constrained by lava flow trends, scoria cones, domes, dyke swarm, sills, and valley and ridge orientations. The upper and lower boundaries of cone sectors are recognised as a basal footprint and an erosional crater rim. A basal footprint is the sub-aerial extent of volcanic products from an eruptive centre, producing an arcuate feature at the base of the volcanic slopes. An erosional crater rim is the remnant highest feature of a volcanic cone, with the arcuate shape reflecting the curvature of the outer cone surface. These zones will also have lava flow strikes near to perpendicular to the projected eruptive centre.

Cone artefacts are remnant arcuate features of a volcanic cone, exposed due to subsequent erosion. Cone artefacts are identified through the projection of concentric ellipses around an eruptive centre, with the shape of the ellipse controlled by a basal

footprint. Cone artefacts are often identified within the internal structure of the volcano, with the relationship to individual eruptive centres defined by lava flow trends and concentric ellipses.

Fifteen cone sectors are identified on Lyttelton volcano (Figure 5.9), each with a basal footprint and erosional crater rim. Basal footprints mark the aerial limits of lava flows associated with a cone, producing Lyttelton's highly varied fan-like cone sectors. The basal footprint of centres 13 and 14 is defined by the contact with overlying volcanics, which for centre 13 is an arcuate feature on the eastern side of Port Levy. Erosional crater rims of Lyttelton Volcano are inherited features of the degrading overlapping cones inherited within subsequent morphologies. Of the 15 eruptive centres and resulting cone formations, erosional crater rims of Lyttelton Volcano produce a series of scalloped-out bites. When combining these erosional crater rims together the overall circular shape of Lyttelton Volcano's erosional crater rim, or the long-viewed caldera morphology, can be explained.

Inner harbour cone remnant features are similar arcuate features to the erosional crater rim, but are often lower flank structures with distinctive lava flow trends. Arcuate promontories are recognised on Lyttelton Volcano as inner harbour spurs between bays (Figure 5.10), which are the remnant cone surfaces that were once buried by volcanism but have since been exposed due to erosion. The best example of this feature is the spurs exposed to the south of Rapaki Bay and the spurs separating Rapaki, Cass and Corsair Bays (Figure 5.10).

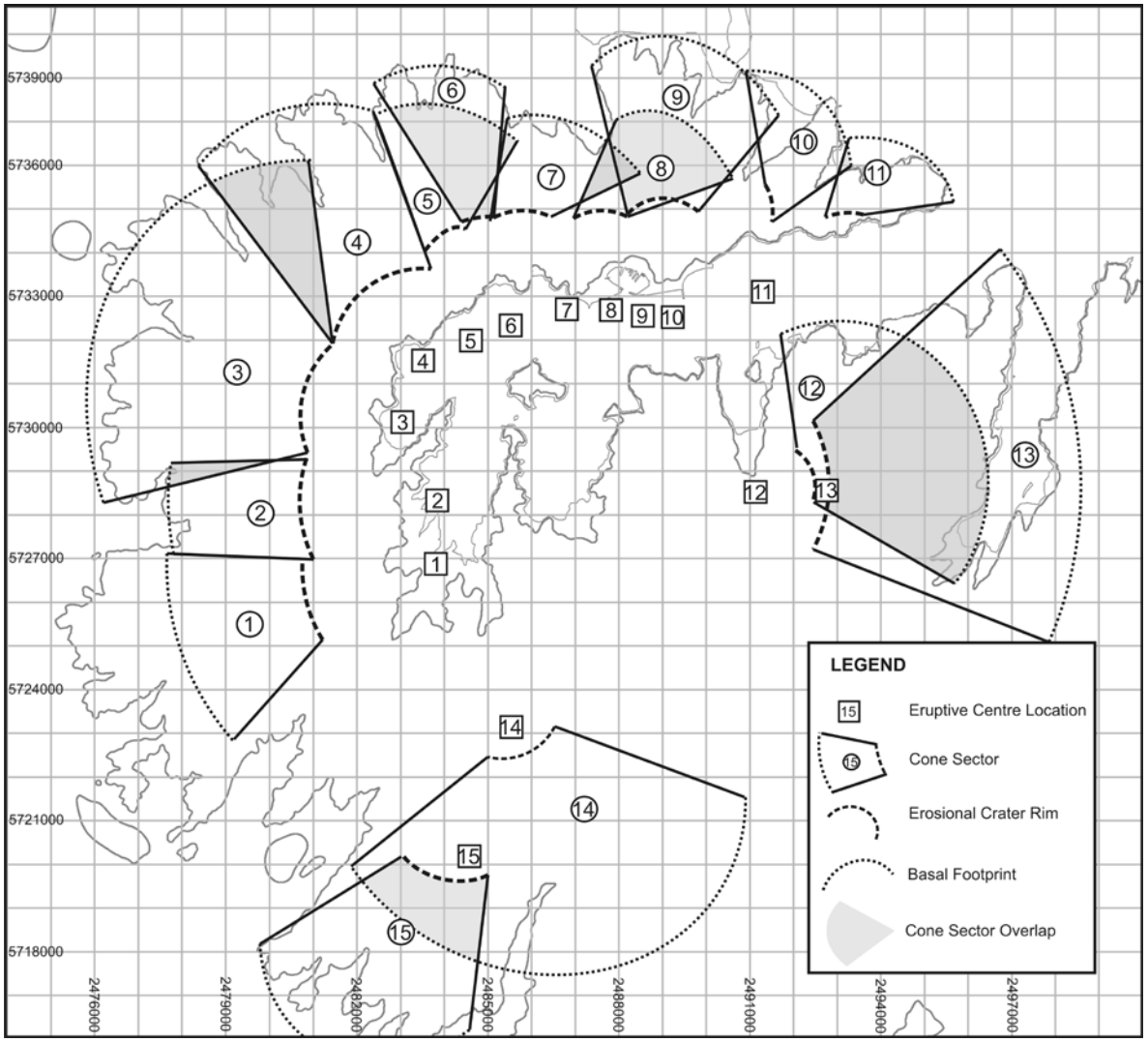

Figure 5.9. Cone sectors of Lyttelton Volcano reflect the preserved constructional components of a volcanic cone. Each cone sector has an associated erosional crater rim (dotted arcing line), basal footprint, a cone sector (area within wedges), and areas of overlap between constructional sectors (shaded regions). Relationship with eruptive centre corresponds with numbering of cone sectors.

5.6. Eruptive Centres of Lyttelton Volcano

Primary volcanic landforms indicate that Lyttelton Volcano developed from 15 eruptive centres / volcanic cones (Figure 5.11). Individual eruptive centres / cones and their interactions produced distinct lava flow morphologies, onlapping sequences, flank eruptives, intrusive events, and erosive forms.

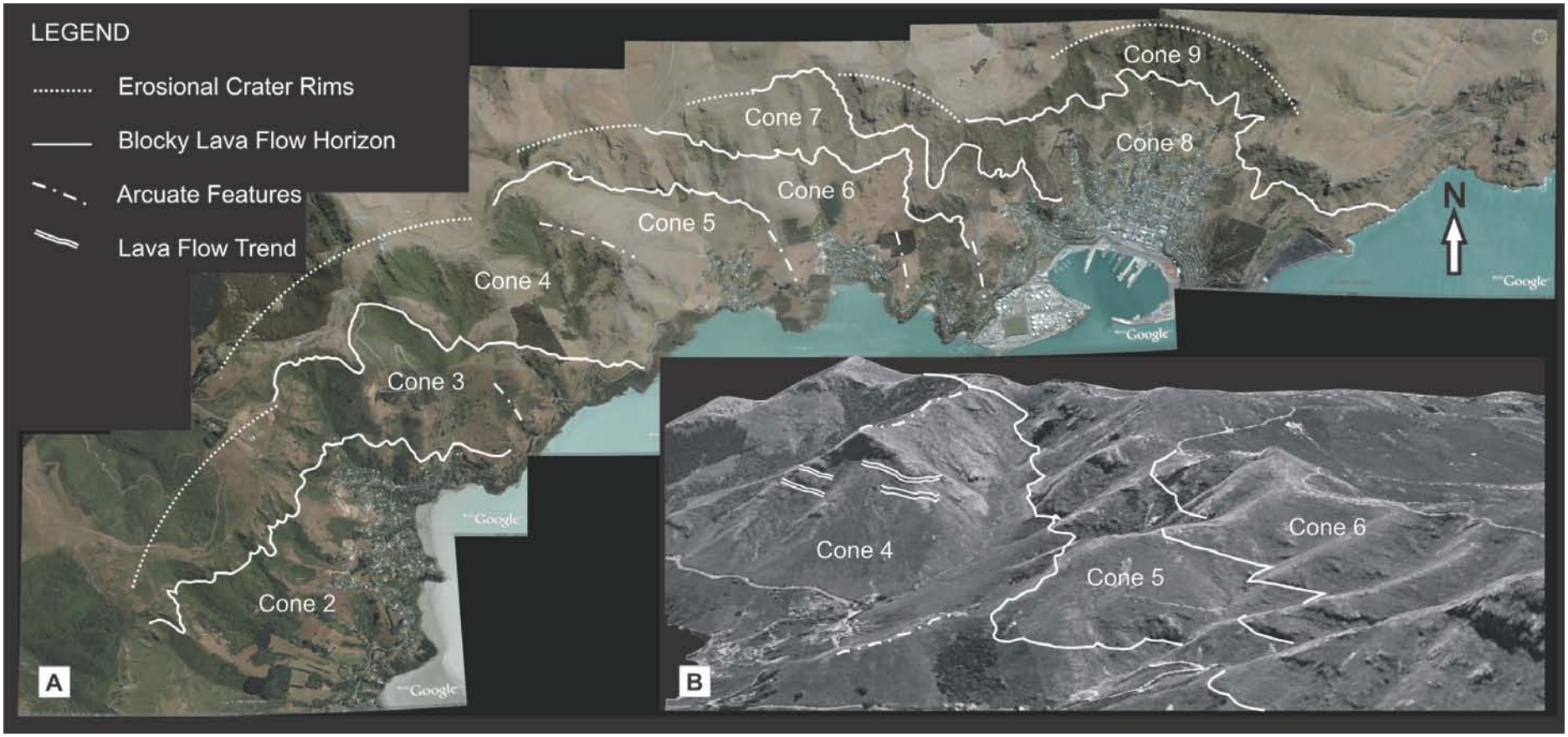

Figure 5.10. A and B Continuation of cone artefacts at the erosional crater rim, arcuate structures in the inner harbour, and cross sections of lava flows at right angles to the hypothesised centre. B) Perspective view to the southwest from near Lyttelton wharf, highlighting inner harbour arcuate features of cone 4 and overlying blocky lava horizons of cone 4 and 5.

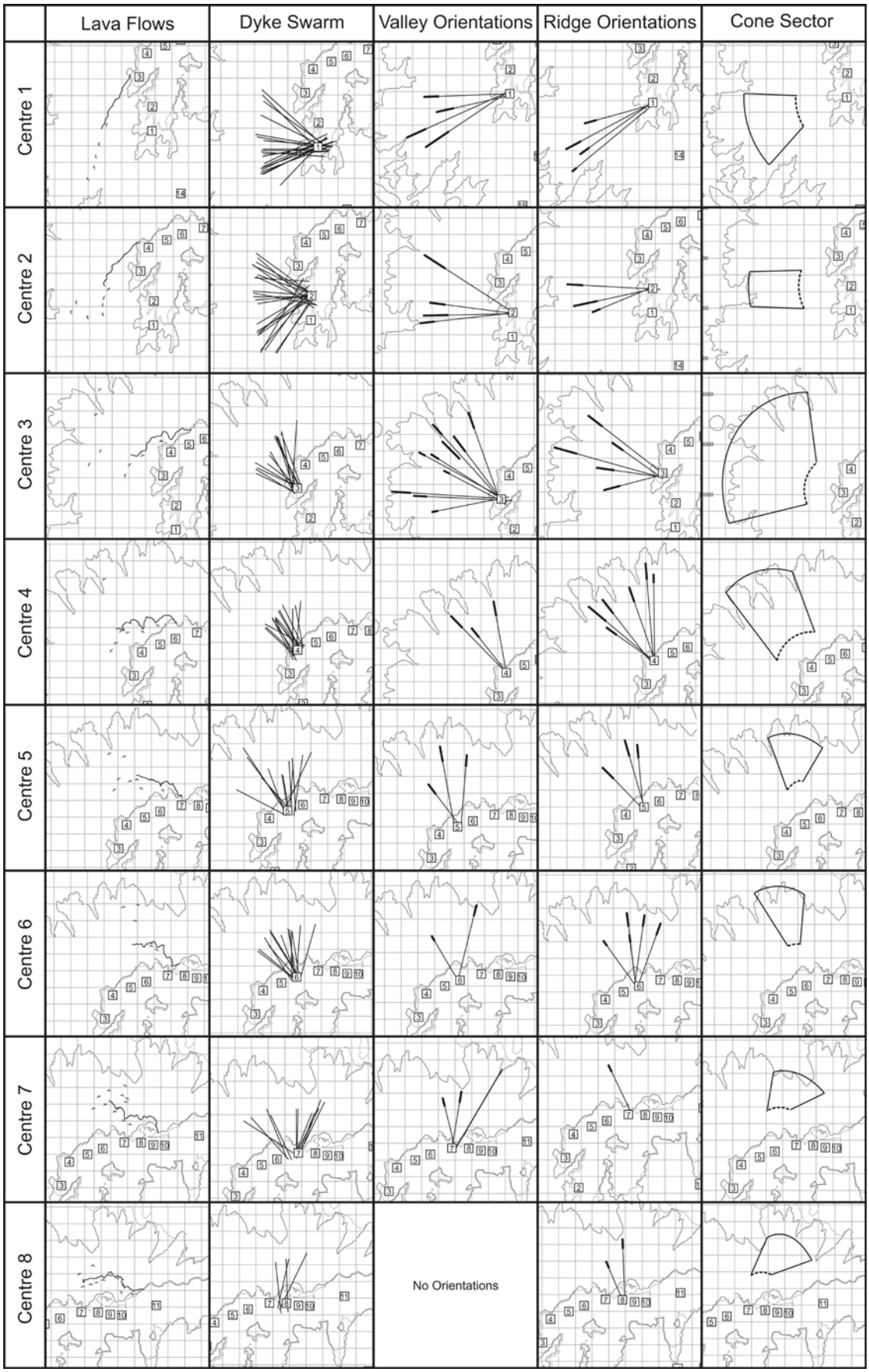
Lava Flows
Dyke Swarm
Valley Orientations
Ridge Orientations
Cone Sector
Centre 1
Centre 2
Centre 3
Centre 4
Centre 5
Centre 6
Centre 7
Centre 8
No Orientations

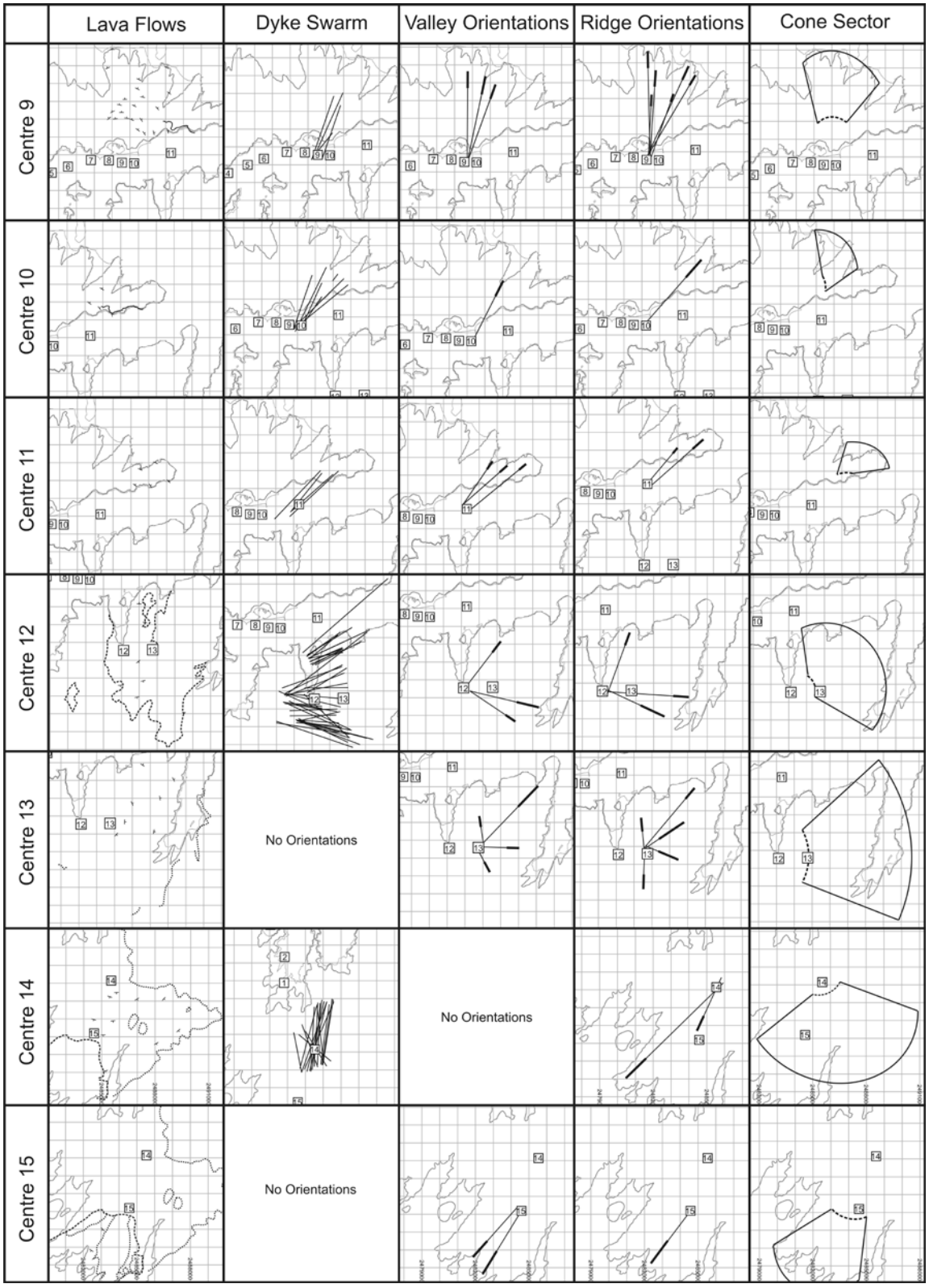

Figure 5.11. Eruptive centres / zones of convergence and cone sectors of Lyttelton Volcano, with associated lava flow trends, radial dyke swarm, valley and ridge orientations. An eruptive centre can be designated where related primary volcanic landform feature orientation arrays converge on a 500 m x 500 m zone.

5.6.1. Lava Flow Morphology

Under the previous volcano hypothesis of Lyttelton Volcano (i.e. Shelley, 1987; Sewell et al., 1992) lava flows should converge on the original summit areas, at the Head of the Bay and Charteris Bay, Lyttelton Harbour. However, lava flows around the present caldera morphology of Lyttelton Volcano are highly variable, highlighted by the lava flow strikes radiating about the fifteen eruptive centres (Figures 5.4, 5.11). Radiating lava flow strikes also reflect the sectors of erosional crater rims (Figure 5.11), as lava flow strikes parallel the arcuate structure of individual cones. Under the single cone hypothesis continuous lava sheets should dip outwards from the projected centre and those with strikes perpendicular to the caldera morphology should be correlated across the harbour. In fact there is no correlation of lava flows from one side of the harbour to the other. This is best recognised between the steeply northwest dipping lavas of Mt Evans (centres 12 and 13) and the lavas behind Lyttelton, which dip east. When projected these two sets of flows do not correlate to one another. Both sides dip into the harbour indicating they came from separate centres on either side of the harbour.

Could variable lava flow trends be the result of parasitic cones on the outer edge of a larger edifice? If this was to be assumed, beneath these parasitic cones an extensive somewhat conformable sequence of lava flows would orient towards a larger volcanic structure. There is no evidence for this larger cone structure, as all of the onlapping cone sequence on-lap onto the previous cone, with the previous cone controlling the late cone formation, evident within the perpendicular onlapping sections exposed in the inner harbour. A further aspect supporting individual cones is the defined and repetitive sequence identified within the blocky lava flow horizons, reflecting the structure of overlapping volcanic cones, with the younger cones directly overlying older ones.

An important aspect in this study is the recognition of blocky lava flow horizons, occurring at distinct horizons amongst the typical constructional aa lava flows. Blocky lava flow horizons (Figure 5.4) are interpreted as representing constructional components / periods of extensive cone growth, due to their morphology and

locations within the volcanic construct. Deposits occur near the intersection of arcuate erosional crater rim structures (zones of overlap), and represent the hypothesised flanks of a volcanic cone. Blocky lava horizons are observed to drop in height away from the hypothesised eruptive centres (erosional crater rims or at right angles from centre), reflecting the overgrowth on pre-existing volcanic cones. Scoria cones reflect the outer surface of a volcanic cone, with outer (less preserved) and inner (lava covered) scoria cones often forming on or within blocky lava horizons. Putting these data into ArcScene (ArcGIS) the distinctive dip of these units can be clearly seen (Figure 5.10), with the base of the flow mantling the outer slope / morphology of the previous volcanic structure.

5.6.2. Onlapping Sequences

Inner harbour exposures reflect a series of overlapping volcanic cones. At intersections of volcanic cones changes in lava flow orientations (observable as a change in the overall strike and dip), erosional layers (laharic material), and lava flow morphology (aa to blocky lava horizons) are observable. Where a new volcanic centre has developed on the flanks of the previous volcanic construct an onlapping lava sequence is produced. These onlapping sequences are traceable from the inner harbour up to the inner erosional crater rim, above an associated blocky lava horizon.

5.6.3. Intrusions

Associated with overlapping zones are trachytic larger dykes and sills (e.g. Castle Rock, Rapaki Dyke, and Windy Point Sill). Trachytic events are the result of intrusions being focussed in zones of weakness, at a prescribed height (steady state profile), within the distinct lithological difference produced between the aa lava sequences and blocky lava flow horizons. The trachytic composition may reflect each eruptive centre becoming more evolved over its eruptive history, with the final eruptive products being trachytic in composition and intruding into zones of weaknesses, preferentially in the newly developing zones of cone on-lap associated with a shift in eruptive centre. Few dyke orientations intrude from eruptive centres into the older underlying cone, resulting in the defined array of dyke orientations around erosional crater rims. Dykes predominantly intrude the growing cone, as intrusions penetrate weak planes in the

unbuttressed northern and eastern sides of the growing Lyttelton volcanoes rather than the underlying / earlier volcanic constructs which were structurally stronger (stabilised by the overlying growing edifice). Dyke emplacement could also reflect the volcanic structure relaxing into a steady state profile, followed by the preferential injection of material into developing structural weaknesses.

Weakness planes are also reflected in scoria cone locations on the outer surface of each cone, which directly related to the basaltic dyke swarms. Multiple dyke orientation directions are recorded near regions of onlapping lava flows (above blocky lava horizons), suggesting intrusive events from two eruptive centres. This concept of two centres being active is supported by the trends of lava flows in these regions, towards an earlier and later eruptive vent.

Shelley (1988) noted that the dykes of Lyttelton Volcano have a blade shape form; a similar form has been acknowledged by Rubin and Pollard (1987), Dieterich (1988), Ryan (1988), Parfitt (1991), and Delaney et al. (1993). Blade shape dykes are acknowledged as representing upper level (2-4 km) basaltic dykes, laterally injected as blade-like intrusions from shallow magma reservoirs beneath the summit. Dyking regimes of each volcanic centre of the Lyttelton Volcano therefore indicate shallow level magma chambers, leading to the gravitationally controlled radial dyke swarms.

5.6.4. Erosional Volcanic Features

Lyttelton Volcano's valley and ridge systems indicate a series of topographic highpoints from which radial systems propagated (Figures 5.7, 5.8). Constraining of these arrays indicates convergences within the harbour, with both valley and ridge trends showing similar trends, a feature expected from the radial incision of a volcanic cone (Figure 5.11).

Some valley and ridge systems display multiple longest segment trends, the result of two centres being recorded by lava flow overprinting and the inception of a later subsequent radial erosional system (Cotton, 1944). Initial valley and ridge systems and other topographic features of a volcanic cone can be masked completely by lava veneering / overprinting, or direct later lava flows, as at Etna, 2001 (Branca, 2003;

Behncke and Neri, 2003). Development of an overlapping volcanic cone results in the inception of a new radial drainage network in the newly erupted products. Underlying radial valley and ridge system of the previous volcanic cone are present throughout the growth of later volcanic cones, with undisturbed (by later volcanism) erosion systems (valleys) remaining active. Multiple volcanic centres result in the inception of multiple erosional volcanic feature orientations. In complex valley systems, valley axis orientations change, trending from the oldest axis at the lower sections of the valley to the younger at the top of the valley.

5.6.5. Vent Regions and Control

Assuming each volcanic centre has an erosional crater rim, and the original continuation of cone features into the interior of the harbour, Lyttelton Volcano can be described as a series of overlapping volcanic cones, younging (to the NE) down harbour. Each eruptive centre location is marked by erosion forming a distinct bay, or an associated scalloped-out region. Scalloped margins probably reflect the preferential erosion of vent regions (brecciated material), intensified through the development of Lyttelton Harbour. This geomorphic signature is lost in zones where later volcanism overprinted venting regions, predominantly in the Mt Herbert and Mt Bradley regions.

Control of the vent locations / lineament along a NE–SW orientation directly reflects underlying fault lineaments, which has up-thrusted basement lithologies in Gebbies Pass, and produced an en-echelon fault system highlighted by the Allandale Rhyolite and Governors Bay Andesite vent zones. This fault zone has acted as a conduit feeding volcanic events, with Lyttelton Volcano's eruptive centres directly reflecting these fault lineaments.

The volcanic centres in the Purau Bay region reflect a second lineament. Block-rich vent breccia is exposed along the valley floor, suggesting this was initially a fissure zone from which there were three distinct eruptive vent regions or edifices. These cones grew to a state that radial dyke inception could occur, with the central vent (centre 12) becoming the predominant cone, as reflected in the inception of the radial erosional system.

5.7. Conclusions

This chapter proposes that Lyttelton Volcano is more complex in its evolution than previously thought, with the recognition of 15 eruptive centres. Multiple eruptive centres are identified through the development of a new technique focussing on the identification, orientation, and extraction of primary volcanic landforms, constructional (lava flows, scoria cones and domes), hypabyssal (dykes and sills), and erosional (radial valley and ridge patterns) volcanic features.

Constructional features, lava flows trends are used to identify individual cones through orientations and onlapping structures, while lava flow morphology / rheology is used to highlight distinct horizons, reflecting cone growth and vent shifting. Scoria cones and domes highlight the outer flanks of a volcanic edifice often related to blocky lava horizons and dyke swarms.

Hypabyssal volcanic features include radial dyke swarms about 15 eruptive centres of Lyttelton Volcano. Late stage trachytic intrusions follow planes of weakness produced during individual cone growth, forming large dykes and domes around the erosional crater rim, and sills within blocky horizons.

Erosional volcanic features highlight radial erosion patterns, incepted during and directly after volcanism that become further accentuated by erosion with time. The orientations of primary volcanic landform valleys and ridges are the record of the original summit of a volcanic cone. Fifteen summits are identified on Lyttelton Volcano with radiating erosive patterns.

Eruptive centres are identified when clustering of primary volcanic landform trends and orientations converge on a 500 m x 500 m zone of convergence (a hypothetical crater rim). Orientations of primary volcanic landform features of Lyttelton Volcano indicate 15 eruptive centres, resulting in the formation of overlapping cones, each with a defined volcanic structure. Concentric circles are overprinted on individual eruptive centres with a related array of primary volcanic landform orientations, enabling

inception of cone sectors, reflecting the preserved sector of a volcanic cone. Constructional sector boundaries are defined by basal footprints and erosional crater rims, and used together with primary volcanic landforms (lava flows, scoria cones, and intrusions) to support the concept of multiple eruptive centres / cones.

Key to the validation of individual eruptive centres is the observation of lava flows, features directly reflecting the growth of individual cones. The orientation of lava flows reflects cone formation and the internal cone structure, best exposed in the arcuate erosional crater rim and remnant cone features of the inner harbour exposures (Figure 5.10). Lava flows near an erosional crater rim and in the corresponding cone sector conform (dip away and are near to parallel) to overlaid concentric ellipses, features observed in the field and through aerial photograph analysis. Exposures in the inner harbour provide cross-sections through the cone structure, with lava flows of cone fragments, when exposed at almost right angles to the centre, dip directly away from the associated volcanic centre. The upper ridges of these inner harbour structures also follow an arcuate structure (cone artefacts), similar to erosional crater rims. These arcuate upper ridges are remnant structures of an earlier cone structure, creating promontories between each bay, reflecting the continuation of a cone structure.

Lyttelton Volcano is a good example of a pristine volcanic setting where primary volcanic landforms can be used to identify multiple eruptive centres of conical volcanoes, even where those centres are modified by subsequent volcanism and erosion.

CHAPTER 6

RECONSTRUCTING ERODED VOLCANIC CONES:

LYTTELTON VOLCANIC COMPLEX, BANKS PENINSULA, NEW ZEALAND

6.1. Introduction

This chapter furthers the multiple eruptive centre interpretation of the highly eroded volcanic structure of Lyttelton Volcano (Hampton and Cole, 2009), through the use of primary volcanic landforms to reconstruct Lyttelton Volcano. Of significance in this study is:

1) The growth and stages of development in overlapping cones;

2) How cone development is influenced by previous topography (i.e. pre-existing cones and basement topography);

3) How a reconstructed topography can be related to the subsequent volcanism and deposition (direction / topographic control);

4) How overlapping cones have formed and then degraded to produce the current morphology;

Previous models of evolution of Lyttelton Volcano (Figure 6.1) suggested a large simple cone (Lyttelton 1) that underwent collapse, followed by the formation of a second large simple volcanic cone (Lyttelton 2) centred at Charteris Bay, slightly to the northeast of Lyttelton 1 (Shelley, 1987; Sewell and Weaver, 1992). In these models (Figure 6.1) the dominant feature is the circular crater rim, linking the high points around the eroded Lyttelton Volcano (Sewell, 1985; Shelley, 1987). Three missing segments occur in this circular crater rim; Lyttelton Harbour, Gebbies Pass and Mt Herbert, regions postulated as collapse due to the disruption of the circular crater rim.

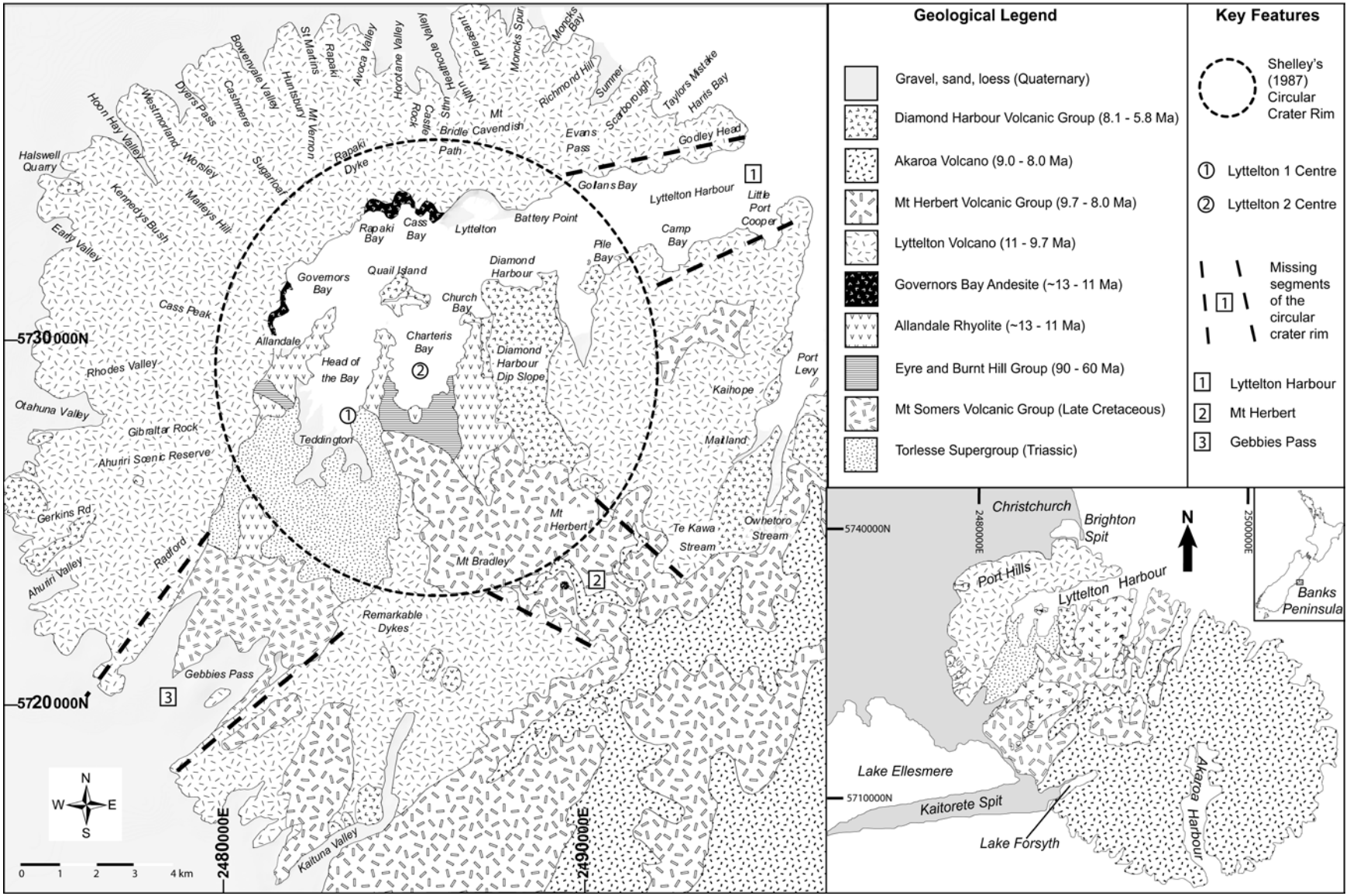

Figure 6.1. Simplified geology of Banks Peninsula and features of previous evolutionary models of Lyttelton Volcano (based on Sewell (1985) and Shelley (1987).

6.2. Data Collection and Methodology

Szèkely and Karàtson (2004) believe the upper and central parts of volcanic edifices are more prone to large scale destructive processes (i.e. sector collapse, caldera formation) during active periods, with the lower regions remaining relatively intact, and that these can be used as a reliable source in volcanic reconstructions. This is true for Lyttelton Volcano where the central, upper, and the interior sections are eroded, leaving only the lower flanks for study / reconstruction.

Volcanic reconstructions require six stages:

1. Recognition of the basement conditions / topography
2. Understanding of stratigraphy and volcanic features
3. Identification of features relating to an individual cone
4. Extraction of identified topographic information
5. Manipulation and projection of topographic data in the production of contour models
6. Triangulation of contour models producing 3D models

6.2.1. Basement

The basement or paleo-surface on which a volcano forms has a significant control on volcanic development and instability. The oldest basement lithology of Lyttelton Volcano is a fault block of Torlesse Supergroup (Figure 6.1), which is overlain by rhyolite domes and flows (Mt Somers Volcanic Group), conglomerates, and shallow marine sediments, exposed in Gebbies Pass (Sewell and Weaver, 1992). Prior to Lyttelton Volcano the Allandale Rhyolite and Governors Bay Andesites (12 – 11 Ma) erupted as a series of lava flows and domes over this basement high, with eruptive sites considered to be fault controlled (Thiele, 1983).

6.2.2. Stratigraphy and Volcanic Features

A broad morphological interpretation of Lyttelton Volcano at various stages of development and erosion can be established through examination of key stratigraphic contacts and deposits. Contacts provide critical markers for evaluating the development of the structure, while deposits provide information on the processes taking place.

Lyttelton Lava Flow Sequence

Lava flows of Lyttelton Volcano are primarily aa, 1 – 10m thick, typically with rubbly bases and tops. Interspersed within flows are pyroclastic deposits, sourced from main eruptive vents as well as from localised scoria cones on the outer flanks. Lavas young to the northeast, with the oldest lavas of Lyttelton Volcano being exposed on the western side of Gebbies Pass overlying Torlesse Supergroup and Allandale Rhyolite. Lavas in the interior of the harbour are best exposed in the cliffs near the erosional crater rim, producing distinctive spurs. Also evident within these interior harbour exposures is the onlapping sequence of lavas, younging down harbour to the northeast. These are important in the understanding of Lyttelton Volcano's evolution.

Blocky lava flows are up to 60m thick, outcropping as distinctive massive cliffs at isolated horizons within the Lyttelton lava flow sequence (Figure 6.2; Chapter 3). Deposits comprise unsorted angular blocks, intersected by distinct shear planes, lava tongues and levee structures. Blocky lava flow sequences are either overlain by epiclastic horizons, incorporating blocky rubble into the basal sections of the laharic deposits, or by near venting deposits, indicating renewed eruptive processes.

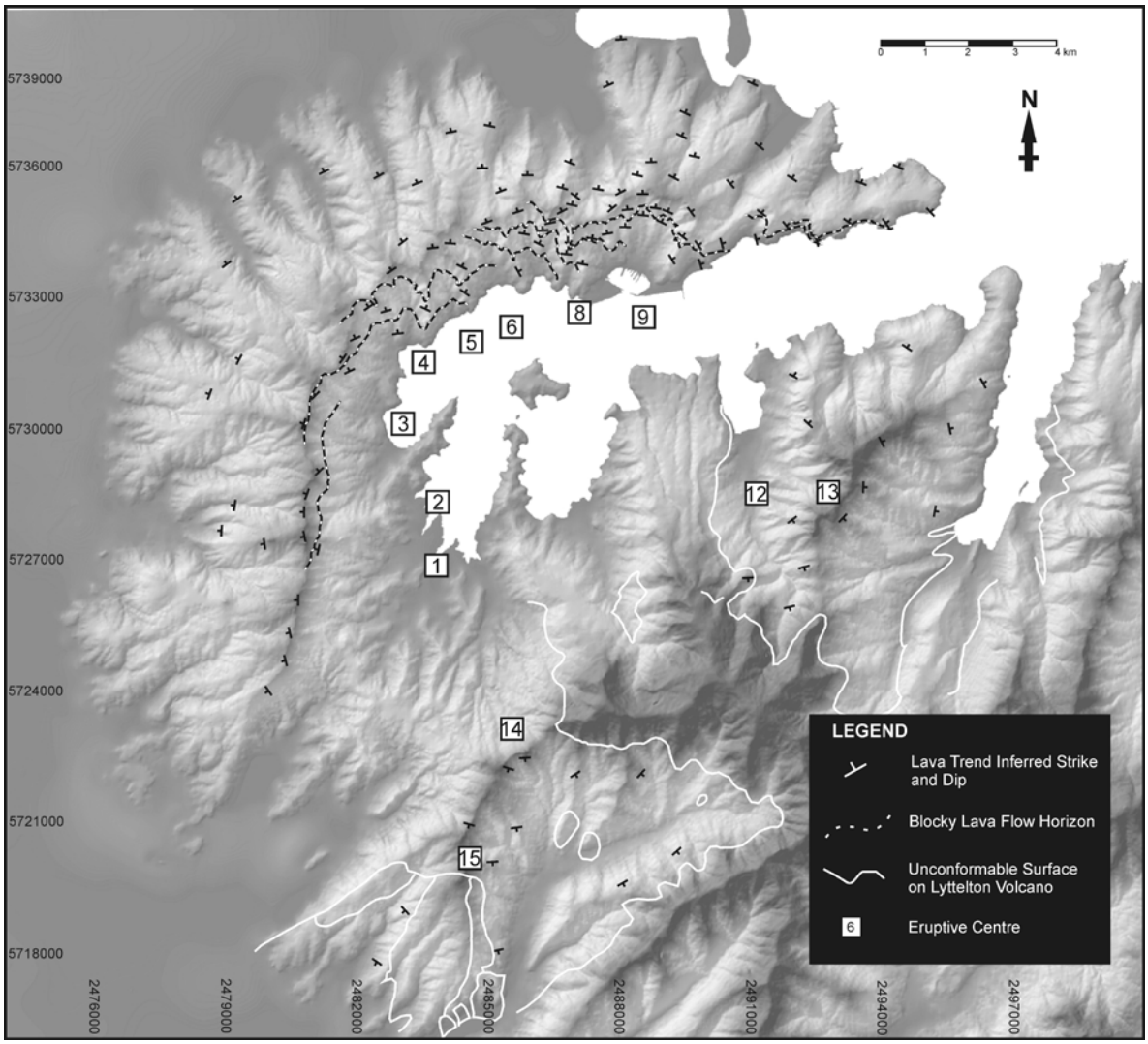

Figure 6.2. Radiating lava flow assemblages (strikes and dips) and blocky lava flow horizons. Strike and dips are inferred from aerial photograph analysis and field observations. Numbers in square boxes are locations of newly recognised eruptive centres. Tick marks indicate coordinate system GD 1949 New Zealand Map Grid).

Eruptive Packages

Many volcanoes develop through episodic behaviour, commonly exhibiting repetitive cycles (i.e. Volca de Colima, Mexico; Luhr and Carmichael, 1990), termed by Jenkins et al (2007) as episodes. The term eruptive package, defines the volcanic products erupted or emplaced over an eruptive episode (Figure 6.3). In Hampton and Cole's (2009) analysis of Lyttelton Volcano (Chapter 5), primary volcanic landforms were used to identify eruptive centres, constrained by a radiating lava flow assemblage, outer blocky lava flow surface, radial dyke swarm, radial valley and ridge pattern and an erosional crater rim. In a

continuation of this work it is proposed that the erupted material, intrusions and erosional features associated with each eruptive centre be termed an eruptive package (Figure 6.3). On Lyttelton Volcano eruptive packages are further defined using geochemical trends of lava flow stacks (Chapter Four, Neumayr (1998) geochemical analysis), where evolving a'a lava flow sequences terminate with a blocky lava flow as the magma source evolved (Figure 6.3). Blocky lava flows therefore define stratigraphic marker horizons towards the end of an eruptive package, with the outer horizon of blocky lava flows indicating a remnant volcanic surface.

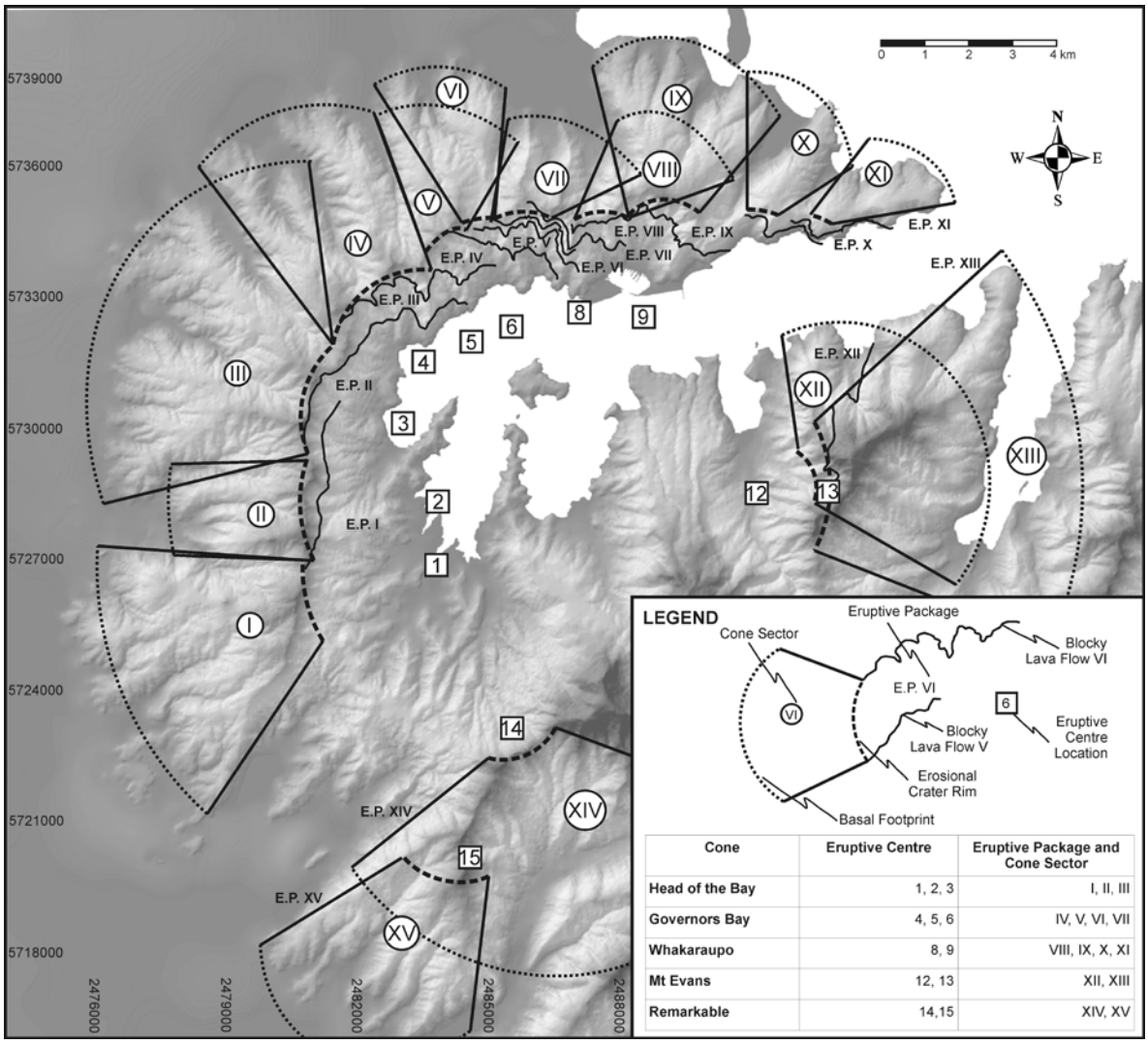

Cone	Eruptive Centre	Eruptive Package and Cone Sector
Head of the Bay	1, 2, 3	I, II, III
Governors Bay	4, 5, 6	IV, V, VI, VII
Whakaraupo	8, 9	VIII, IX, X, XI
Mt Evans	12, 13	XII, XIII
Remarkable	14,15	XIV, XV

Figure 6.3. Relationship of cones and eruptive packages on Lyttelton Volcano. Eruptive packages are defined and related to an eruptive centre, cone sector, and blocky lava flow. Note eruptive centres 10 and 11 are incorporated to be sourced from eruptive centre 9.

Overlying Lavas

Two volcanic groups directly overlie Lyttelton Volcano (Chapter 1); the Mt Herbert Volcanic Group (9.7 – 8 Ma), and the Diamond Harbour Volcanic Group (8.1 – 5.8 Ma). The Mt Herbert Volcanic Group marks a period of volcanic activity that infilled a large depression on the southeast of Lyttelton Volcano and then spread north and south. The Diamond Harbour Volcanic Group lavas are the first invasive lava flows into the interior of Lyttelton Volcano, mantling the erosive surface of Lyttelton Volcano. Diamond Harbour Volcanic Group flows which invaded the central depression (Diamond Harbour dip slope) of Lyttelton Volcano were controlled by the basement structure (Allandale Rhyolite), Mt Herbert Volcanics and Lyttelton Volcanics to the south-west and north-east sides of the flow (Figure 6.2).

Epiclastic Deposits

A series of conglomerates occur stratigraphically above the Lyttelton Volcanics, and are either covered or are interbedded with units of Lyttelton Volcano (Chapter 2), the Mt Herbert Volcanic Group, and Diamond Harbour Volcanic Group (Chapter 3). Exposures are interpreted as debris flows, occurring at variable stratigraphic levels, indicating periodic erosion of the outer slopes of the Lyttelton Volcano structure.

6.2.3. Classification of a Volcanic Cone: Intrusive and Morphological Features

A volcanic cone is the ultimate product of a series of eruptions over a period of time, and will have at least one eruptive centre, with each eruptive phase termed an eruptive package. Multiple eruptive packages relate to in an individual volcanic cone when eruptive centres are in close proximity (~1km) to each other.

Recognition of an eroded volcanic cone and its eruptive packages requires analysis of various morphological and intrusive features, in particular:

1. Radiating sequence of lava flows
2. Defined dyke swarm or regime
3. Erosional crater rim and basal footprint
4. Preserved sector on the volcano's flanks

Radiating sequence of lava flows

During the growth of a volcanic cone the eruptive centre acts as a point source, resulting in a radiating array of lava flows, providing a simplistic basis to begin identification of source regions. Lava flow paths can be predicted by a simple straight line projection (in plan view) of each related radiating lava flow assemblage up individual dip directions, with projections clustering on the eruptive source / centre. In Lyttelton Volcano's lava flow sequence (Hampton and Cole, 2009) distinct point sources / eruptive centre can be identified (Figure 6.2).

Defined dyke swarm or regime

In the development of a volcanic cone, radial dykes typically form during the late stages of eruption (Shelley, 1992; Carrigan, 2000), due to a combination of gravitational forcing and volcanic relaxation producing a radial fracture system, through which magma injects. Therefore by projecting the orientation of a dyke towards the magma propagation direction an eruptive centre can be designated (Ancochea et al., 1994; 1996; 1999; 2008). Following this principle, Hampton and Cole (2009) designated 15 eruptive centres / packages to Lyttelton Volcano (Chapter 5).

Erosional crater rim and basal footprint

Important parts of a cone are the erosional crater rim and basal footprint (Figure 6.3). An erosional crater rim directly reflects the pre-existing arcuate volcanic structure. A basal footprint is the current surface extent of a volcanic cone, or the areal extent that lava flows from a volcano were able to flow. Both of these features are arcuate, reflecting the inherent shape of the eruptive package / cone.

Cone sectors and outer cone horizons

Cone sectors represent the relatively unmodified outer flanks of a cone (Figure 6.3 and Figure 6.4; Stage 1), whereas outer cone horizons are distinct horizons within a volcanic structure, later dissected, that reflect the buried outer flank of a volcanic cone. An important aspect in the identification of cone sectors and outer cone horizons is to establish the relationships between features, defining the morphology of the volcanic structure.

Cone sectors are initially recognised from strikes and dips of lava flows, dyke swarm, valley and ridge orientations, and associated arcuate features (erosional crater rim, basal footprint, and remnant cone curvatures). The upper extent of a cone sector is defined by the erosional crater rim, with the lower limit controlled by the basal footprint. Outer cone horizons used in this study are distinctive blocky lava flow horizons and contacts with later volcanic products. Outer cone horizons are identified through field work and aerial photograph mapping, and overlaid onto contour models. Cone sectors are identified as areas of similar topographic trends representing a preserved cone remnant, whereas outer cone horizons are directly mappable.

The distribution of Lyttelton Volcano's cones and numbers of eruptive centres and packages is given in the table in Figure 6.3.

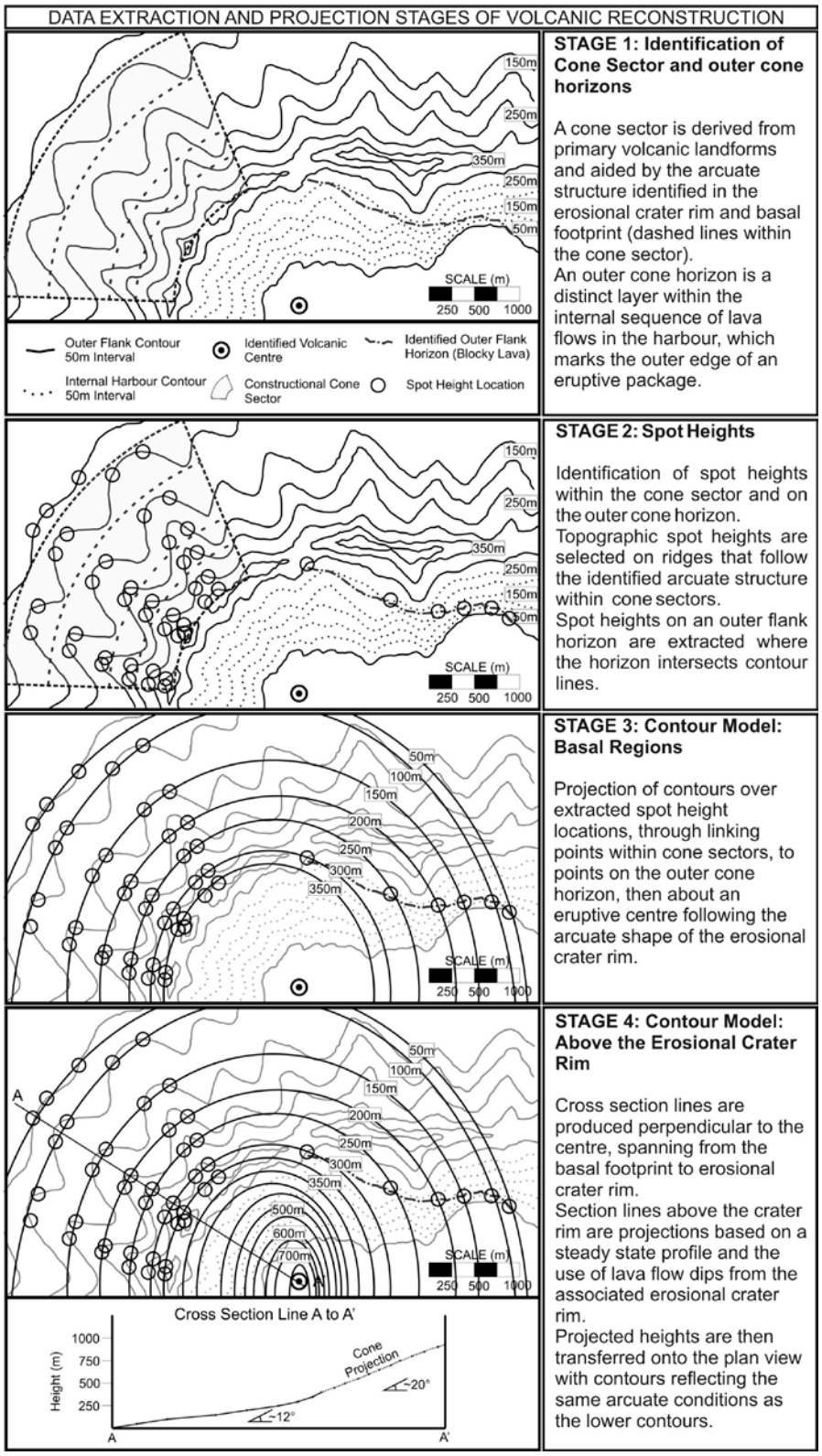

Figure 6.4. Reconstruction process. Stage 1: Cone sector and outer horizon recognition. Stage 2: Spot height identification and extraction. Stage 3: Projection of contours below the erosional crater rim. Stage 4: Projection of contours above the erosional crater rim.

6.3. Construction and Analysis

6.3.1. Spot Heights

Spot heights provide an overview of the topographic and morphological trends of the remnants of a cone (Figure 6.4: Stage 2). Identification of spot heights within a cone sector allows recognition of arcuate topographic signatures reflecting the shape of the erosional crater rim and basal footprints. Spots heights are marked at defined (50m) contour intervals on ridges (Figure 6.4; Stage 2), defining a theoretical cone surface, not the actual cone surface due to erosion (Szèkely and Karàtson, 2004). Spot heights of outer cone horizons follow a similar yet simpler process, with spot heights being extracted at the intersection of a mapped outer cone horizon and a contour (Figure 6.4; Stage 2). Spot height databases are compiled for each cone sector and related outer cone horizon for use in the next phase of contour model construction.

6.3.2. Contour Models

Contour models are constructed sequentially (oldest to youngest), with younger cone reconstructions taking into account the previous reconstructed topography. Contour models are initially constructed for the basal regions (up to the erosional crater rim), followed by the projection of the cone towards the summit,

Basement reconstruction is based on mapping of Thiele (1983) and Sewell (1985). Current topographic information is used to establish a minimal base height of the topography, while the projection of basement lithologies beneath later lava flows are purely conjectural, based on the recorded strikes and dips and the relationship to overlying lava flows. This topographic information is then combined to produce a contour model.

Basal Regions

Contour models are constructed by linking spot heights within a database (Figure 6.4; Stage 3). Spot heights are used as guide points for contour projections, with each new

contour intersecting a related spot height. Initial links are within the cone sector, followed by extrapolation towards the spot heights of the outer cone horizon. In the absence of spot heights (i.e. when the cone has been eroded), projections assume a simplistic cone model, however the recognition of overlapping cones and packages required careful analysis to conform to the physical structure of the recorded deposits. Resulting in the hypothesis of a 'talus apron' cone-building regime, where the cone structure is defined by the curvature of the erosional crater rim, basal footprint and the newly projected contours of the cone sector and between cone sector and outer cone horizon. This cone growth pattern is important as it suggests less material was erupted than required in previous models.

Above the Crater Rim

The contour model above the erosional crater rim is established by constructing a cross section of the basal contour models (Figure 6.4; Stage 4) through the cone sector, perpendicular to the identified centre. This cross section line is projected towards the hypothetical eruptive centre, at a dip recorded / inferred (of a related lava flow) from the erosional crater rim. Cross sections are drawn using Davidson and De Silva's (2000) steady state volcanic profile, in which the lower slopes of a volcanic cone have lower dips than those in the upper regions. Once a cross section has been produced above the erosional crater rim, a new set of spot heights are inputted as topographic spot heights into the plan view model, with contours radiating around the eruptive centre at similar curvatures to the basal region.

6.3.3. 3D Cone Modelling

Modelling the volcanic structure in Vulcan 7.5 enables a 3D reconstruction of each growth phase of a volcano. Direct comparisons can then be made to field observations, aerial photographs and the digital elevation model (DEM). Perspective views can also be produced to observe and compare reconstructions to the present topography.

3D models are produce from individual contour models of the previous stages of reconstruction, by a series of phases:

1) Digitise contour models in a drawing programme (i.e. CorelDraw), and export as dxf files;

2) Import dxf files into Vulcan, and verify scale and geographic projection;

3) Tidy contours, removing splines and correcting irregularities inherited during the exporting and importing process;

4) Attribute heights for each contour, establishing a 3D wireframe contour model;

5) triangulate surfaces of contour models to produce 3D renditions of the volcanic structure.

Contour models are presented as a series of diagrams (Figures 6.5 to 6.15), with overlays of associated (recorded) primary volcanic landforms (scoria cones, dyke swarm, valleys and ridges). The resulting reconstructions provide the sequence of volcanic development for Lyttelton Volcano (Figures 6.5 to 6.15), and represent the volcanic growth / evolution.

6.4. Detailed Volcanological Evolution

The following section discusses the formation of each volcanic cone in the sequence of vent progression as identified from stratigraphic relationships.

6.4.1. Basement Reconstruction (Figure 6.5)

Of significance in the development of Lyttelton Volcano is the presence of basement 'highs' at Gebbies Pass and the rhyolite 'highs', now exposed at southern end of Lyttelton Harbour. Although highly eroded these areas would have been up to 350m a.s.l., when Lyttelton Volcano began erupting, producing considerable constraining effects on cone growth. The eastern side of Charteris Bay is the one region of the basement high that was not extensively covered by Lyttelton Volcanic Group lavas, suggesting continuous exposure, a factor incorporated within the models.

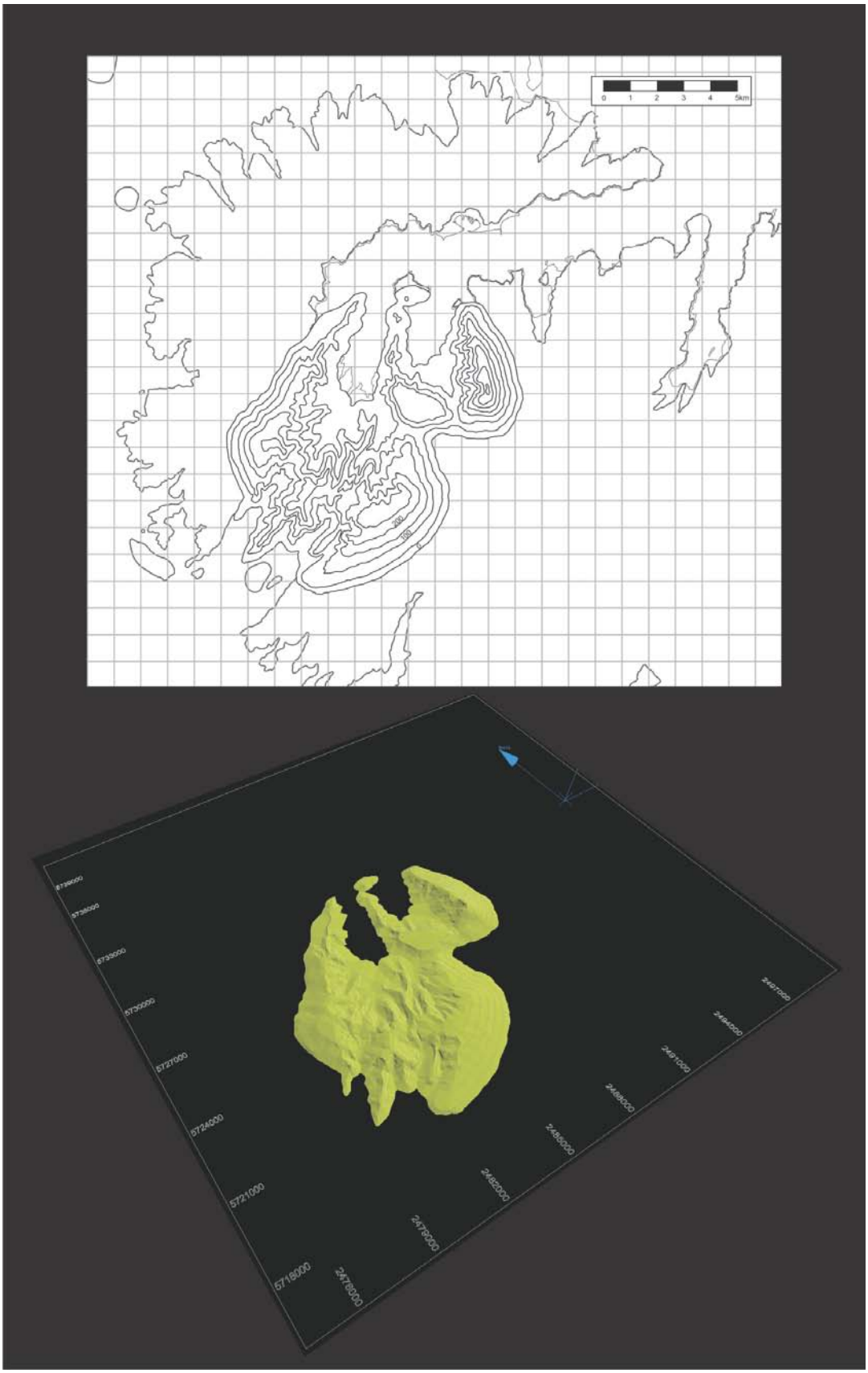

Figure 6.5. Basement contour model and reconstruction.

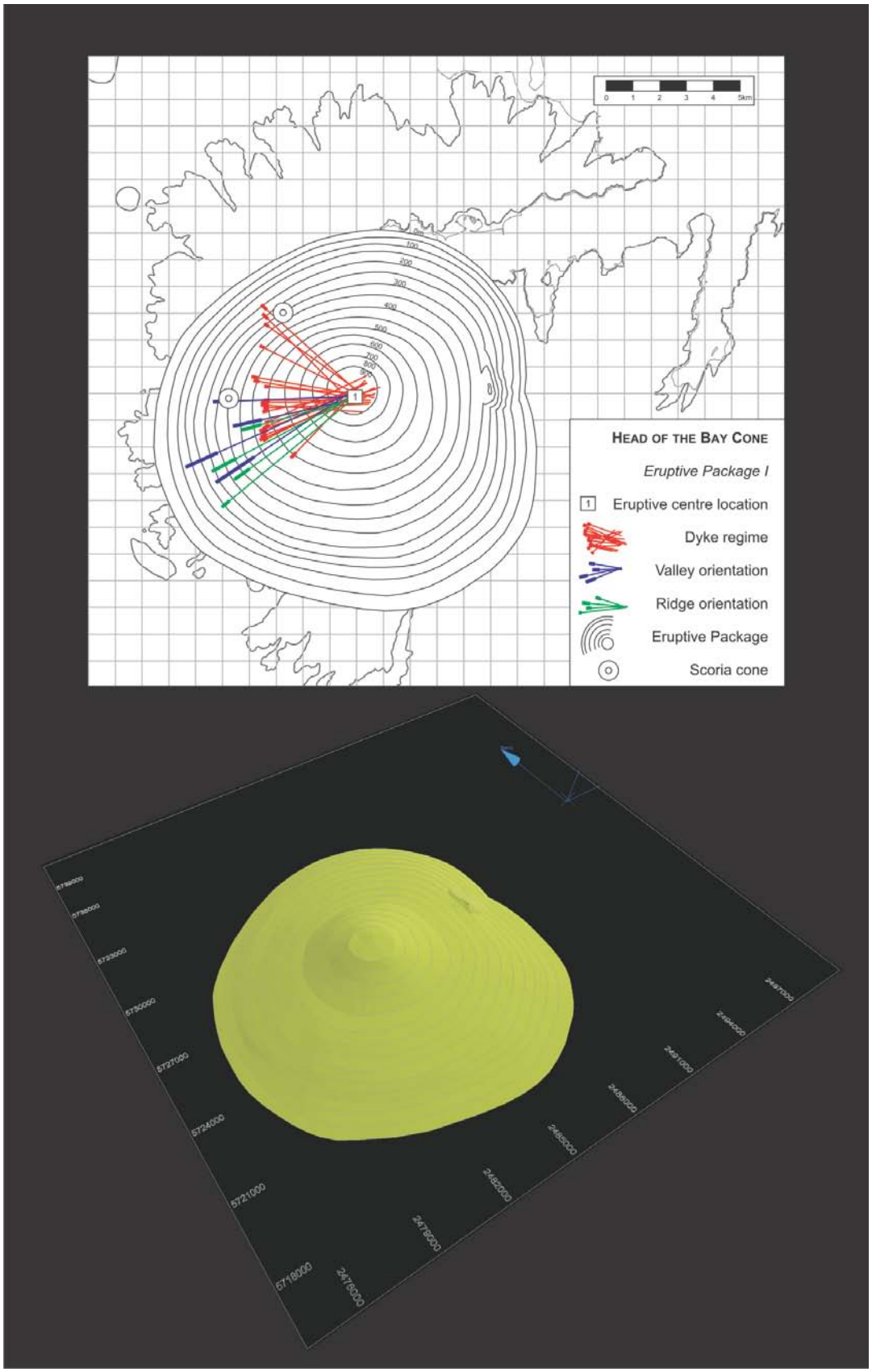

Figure 6.6. Head of the Bay Cone, eruptive package I.

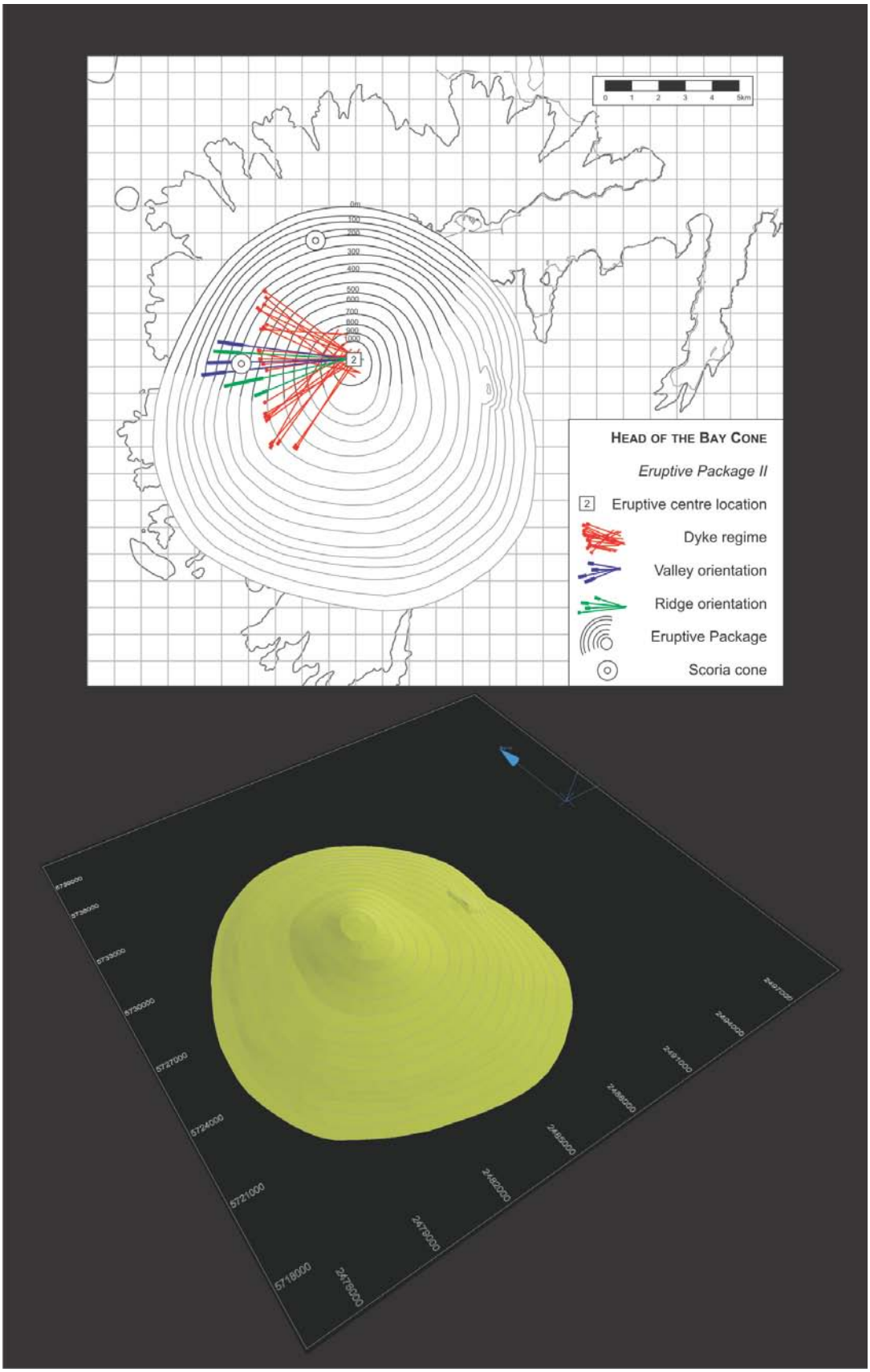

Figure 6.7. Head of the Bay Cone, eruptive package II.

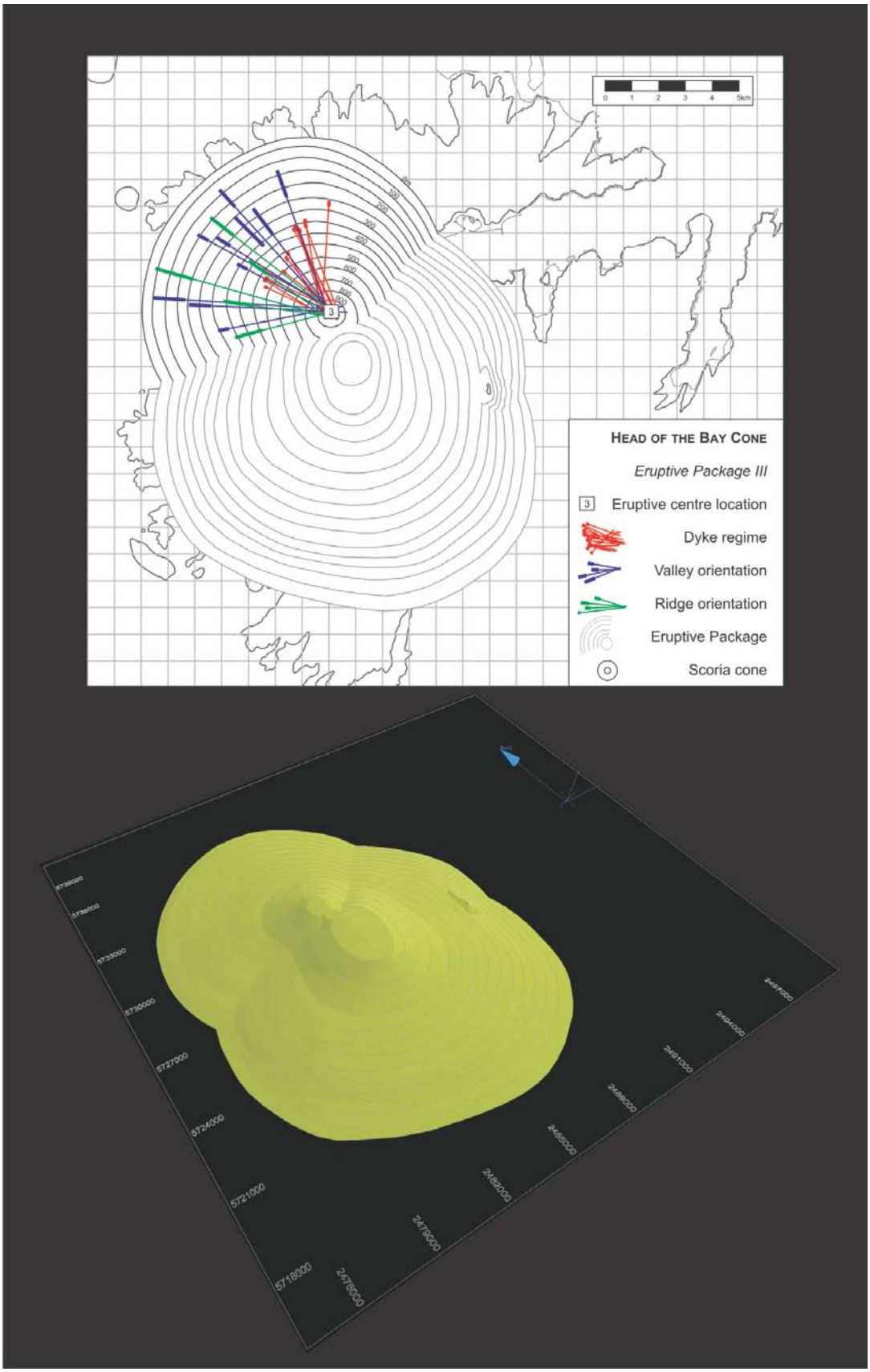

Figure 6.8. Head of the Bay Cone, eruptive package III.

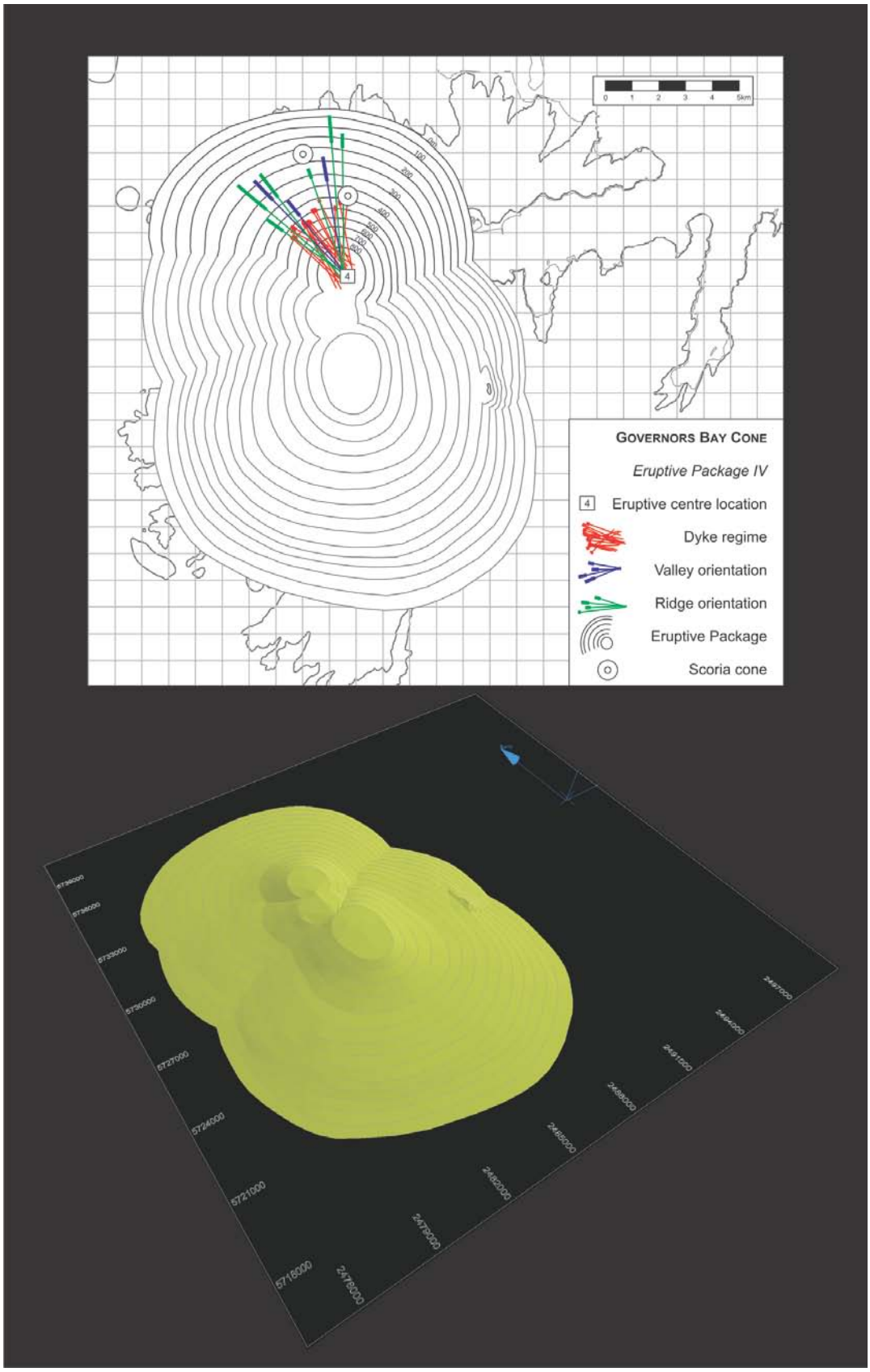

Figure 6.9. Governors Bay Cone, eruptive package IV.

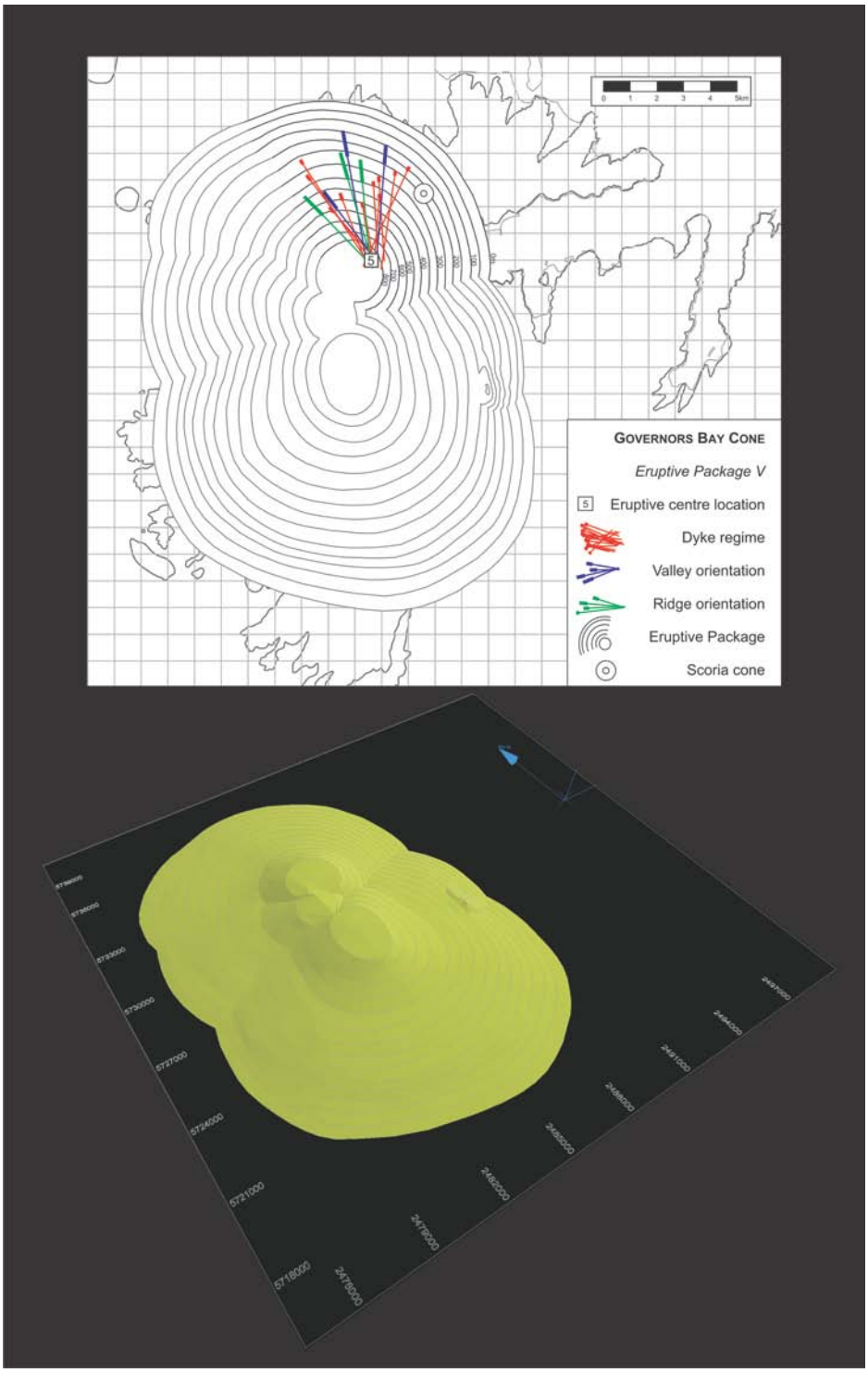

Figure 6.10. Governors Bay Cone, eruptive package V.

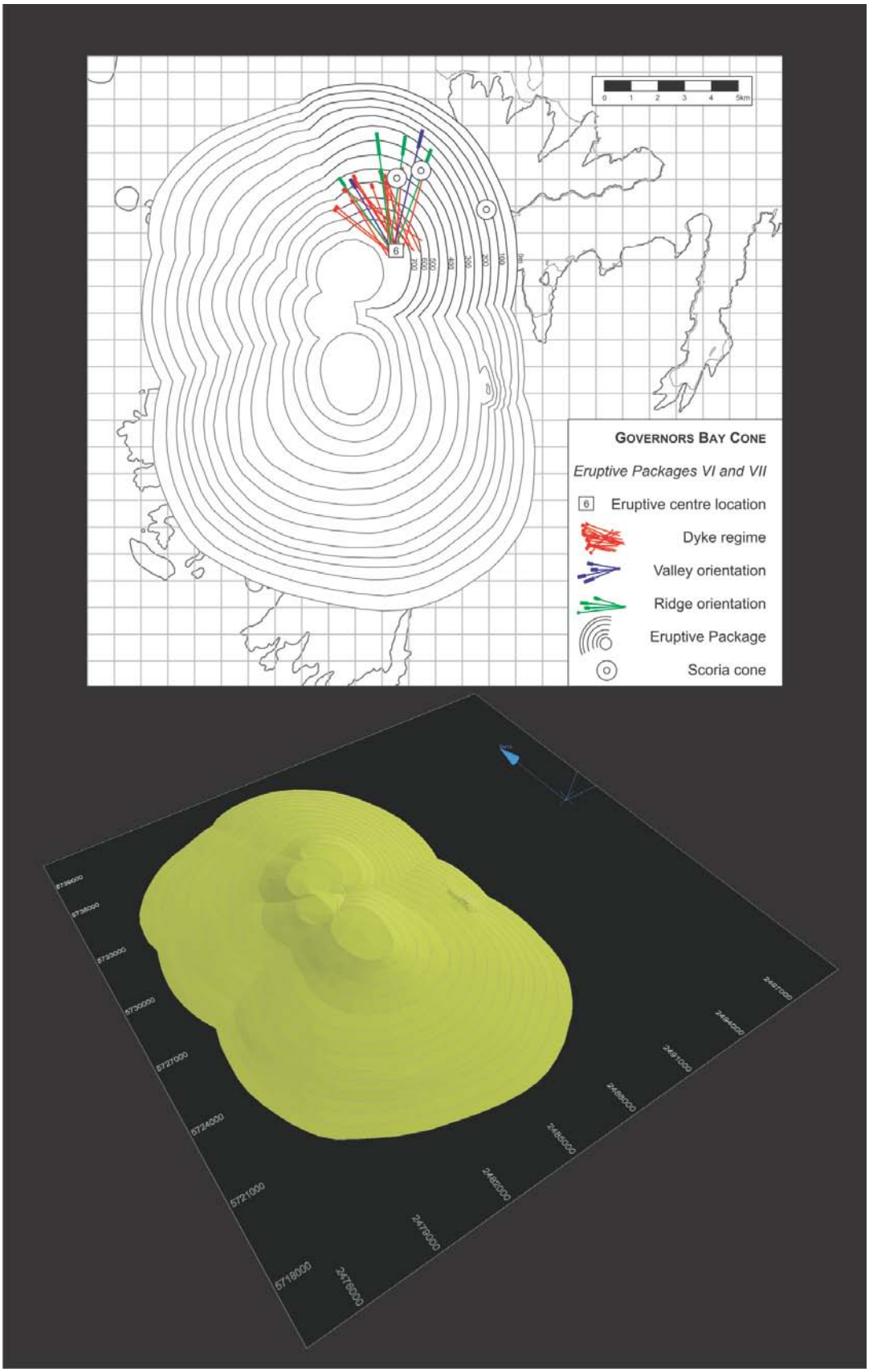

Figure 6.11. Governors Bay Cone, eruptive packages VI and VII.

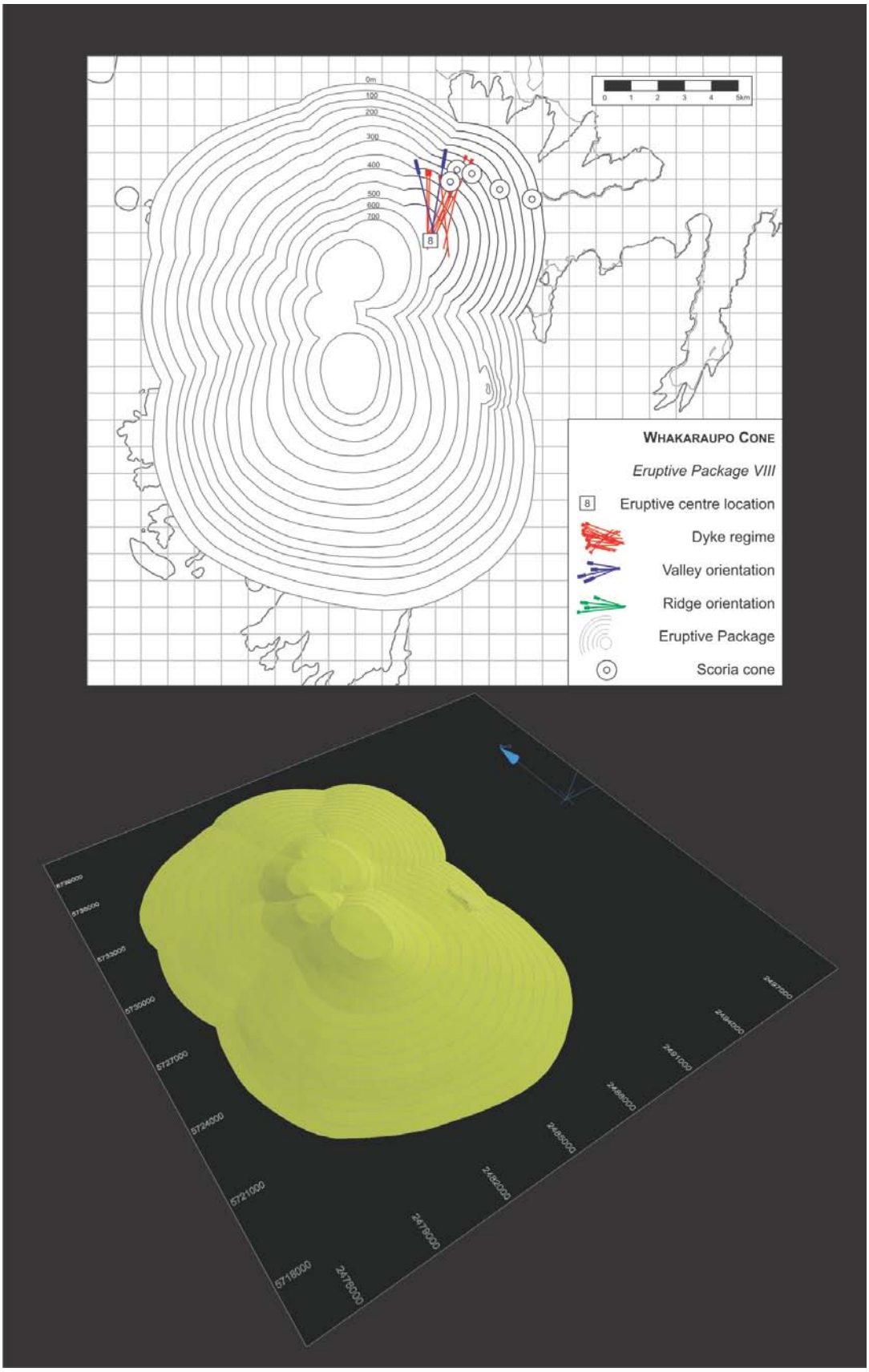

Figure 6.12. Whakaraupo Cone, eruptive package VIII.

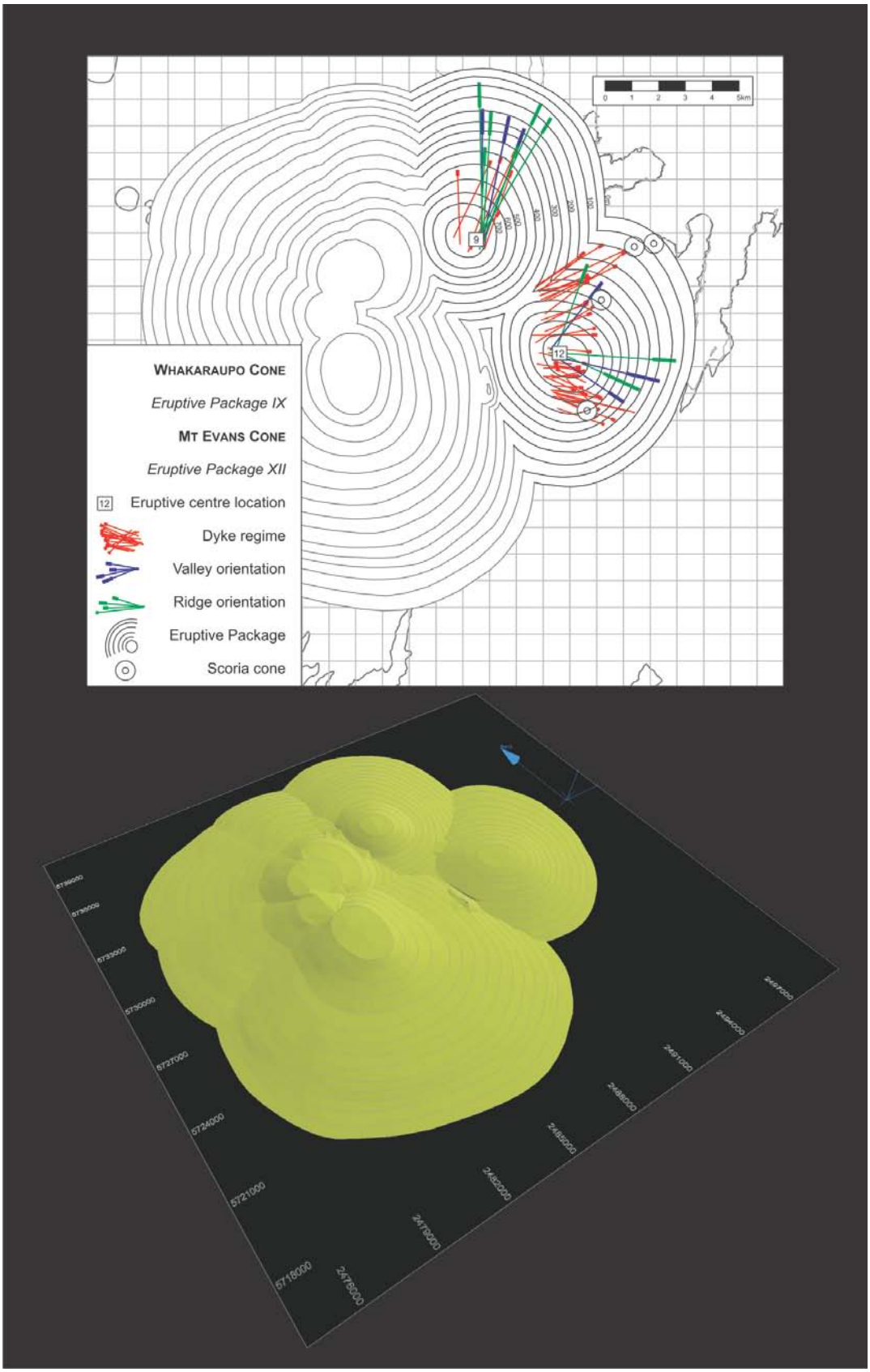

Figure 6.13. Whakaraupo and Mt Evans Cones, eruptive packages IX and XII respectively.

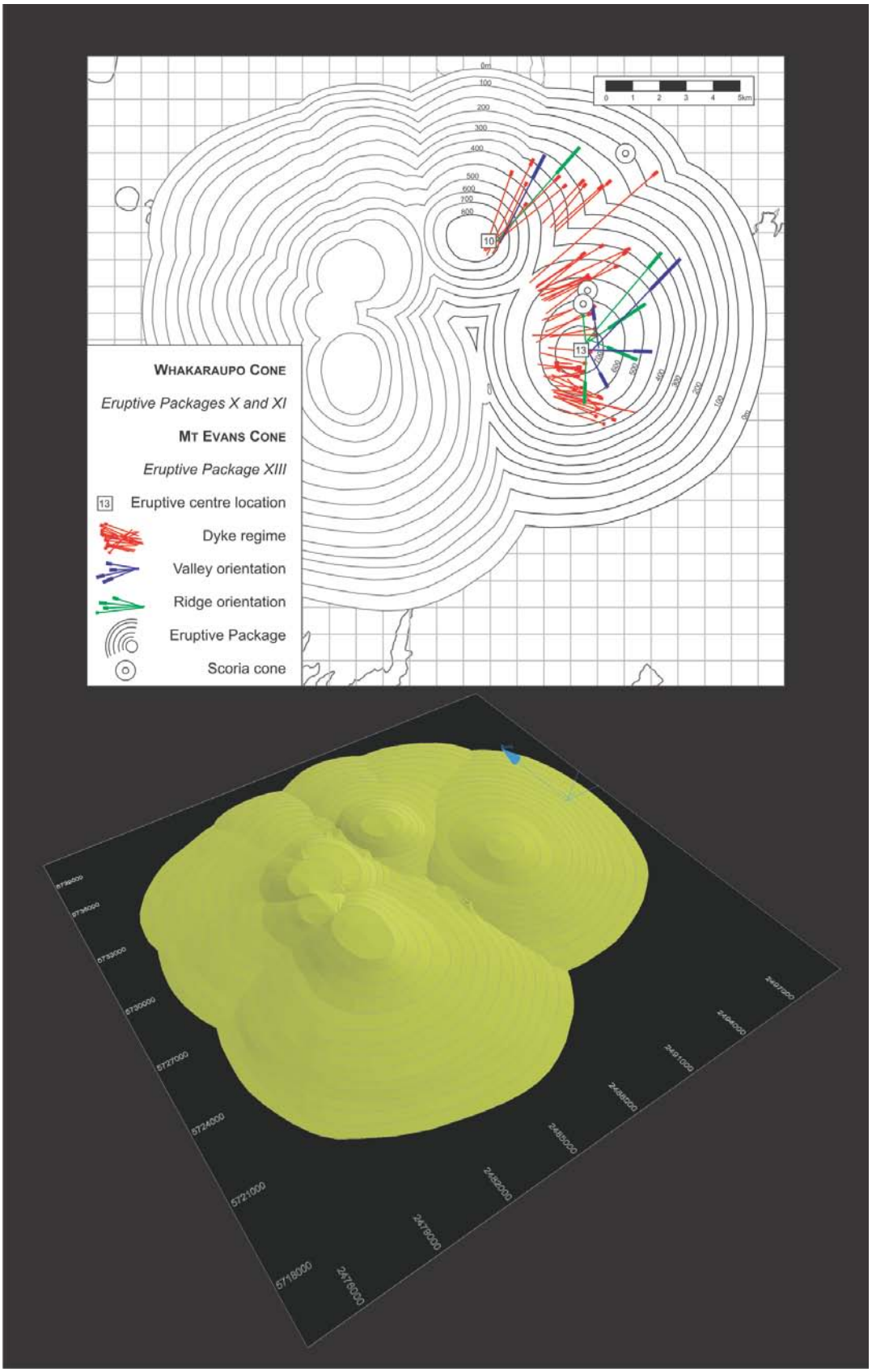

Figure 6.14. Whakaraupo and Mt Evans Cones, eruptive packages X, XI and XIII respectively.

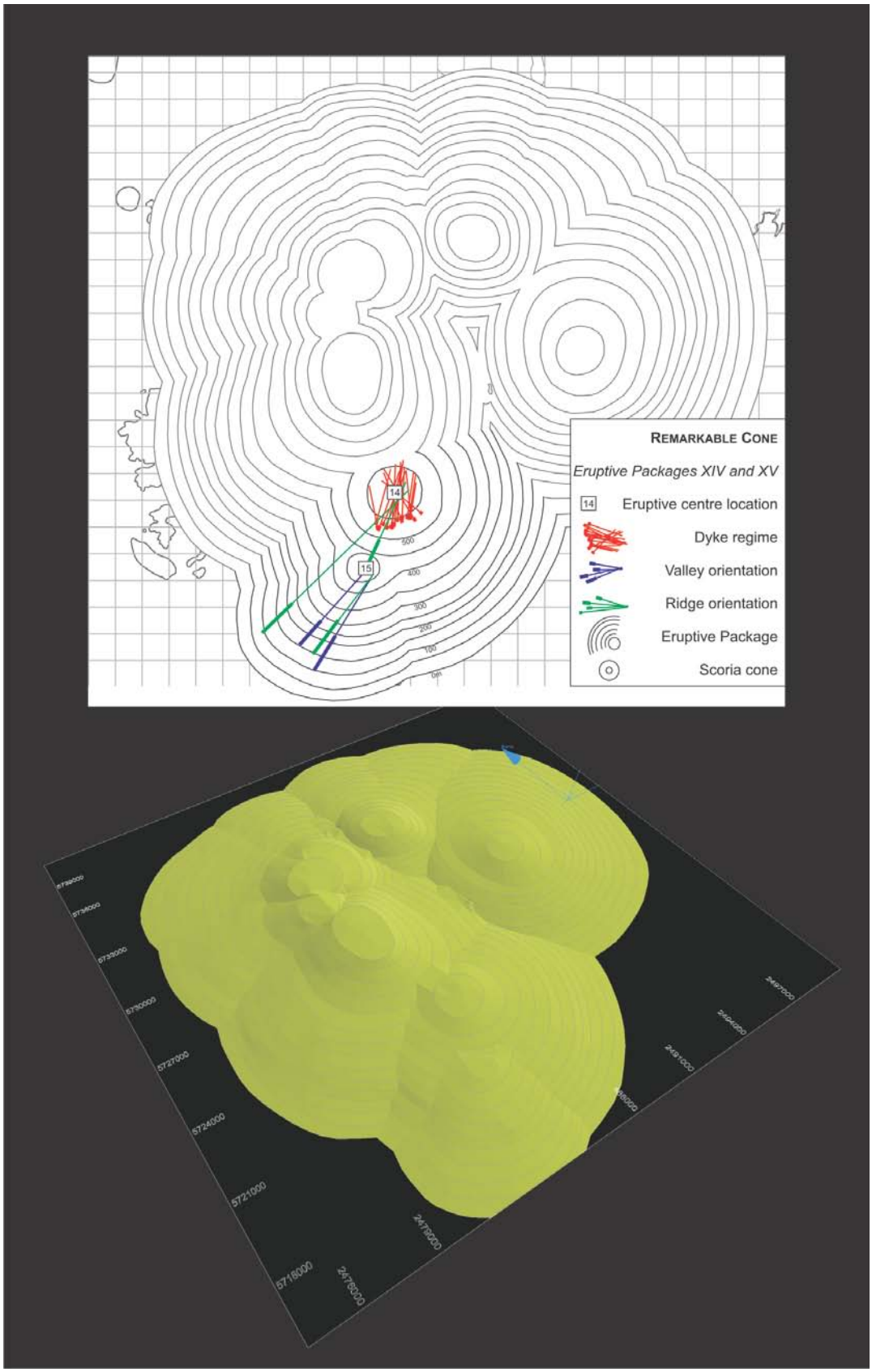

Figure 6.15. Remarkable Cone, eruptive packages XIV and XV.

6.4.2. Head of the Bay Cone: Eruptive Packages I, II, and III

Eruptive Package I (Figure 6.6)

The Head of the Bay Cone developed on the northern side of the Gebbies Pass basement high. Initial lava flows flowed to the north and then west. The growing cone was built up primarily of aa lava flows, reaching a summit of 1000m, and was asymmetric due to the underlying basement high. Dykes associated with this cone are within basement lithologies and the newly developed cone. At sea level the basal footprint reached Allandale in Lyttelton Harbour, and Ahuriri valley (for locations see Figure 6.2). A large valley developed in the northwest region of Gebbies Pass, where the basal footprint onlapped basement, while smaller radial valleys developed on the outer slopes, with the remnants observable in the Ahuriri Valley region. The basal footprint to the west may have once been more expansive, but later volcanism has modified the slope and basal footprint. Two scoria cones erupted on the flanks of this cone. The first is located in the upper reaches of Ahuriri valley, while the second is now exposed in the southern cliffs above Allandale and is overlain by lavas of eruptive package II.

Eruptive Package II (Figure 6.7)

Eruptive package II developed on the north-western flanks of the Head of the Bay Cone, resulting in limited flows to the southeast, with lavas directed to the northwest to west. The basal footprint of this cone terminated at sea level at Governors Bay, and the top of the package defined by the blocky horizon exposed in the valley. Limited radial valley development is preserved in the cone sector of this cone (three valleys north of Otahuna Valley), while Otahuna Valley is cone-controlled. Dykes of this centre are limited with the radial dyke swarm at crater rim height from Gebbies Pass to north of Cass Peak.

Two scoria cones are associated with this cone. The first is exposed in the cliff faces on the inner harbour side of Governors Bay, and is overlain by the next eruptive package. The second is exposed at a valley north of Gibraltar Rock. A further feature associated with this cone is the Gibraltar Rock trachyte dome, which overlies a blocky horizon. This dome

is fed by a large dyke, orientated to eruptive centre 2, signifying that this dyking and doming event is an intrusive product of eruptive package II.

Eruptive Package III (Figure 6.8)

Eruptive package III erupted on the eastern side of the Head of the Bay Cone, limiting flows to the south. Mantling lava flows occurred to the west and north. Steeper cone development occurred in northeast regions due to the underlying cone, initially the result of parasitic cone development. Lavas reached Quail Island where flows lapped onto basement rhyolite. A cross section of this cone is exposed in the cliffs behind Governors Bay (Figure 6.16), where the erosional crater rim and stratified lavas dipping away from Allandale can be clearly seen, with the outer cone marked by a blocky lava flow. Radial valley development is evident from Cass Peak to Marleys Hill, with deep incision in Early Valley, whereas one-controlled valley formation formed Rhodes Valley. No scoria cones are exposed on the outer flanks of this eruptive package. A large dyke also forms a prominent ridge to the west of Cass Peak.

6.4.3. Governors Bay Cone: Eruptive Package IV, V, VI, and VII

Eruptive Package IV (Figure 6.9)

The Governors Bay Cone is a slightly asymmetric cone which reached heights of 800m. Cone growth was limited to the west, south and southeast, resulting in asymmetry and the development of the slightly steeper north-eastern flank. Key features of this cone are exposed in the spur on the southern side of Rapaki Bay (Figure 6.17). The end of this spur exposes flows at right angles to flow direction, indicating an eruptive source in the region of Governors Bay. The upper trend of this spur, extending into the harbour, is a continuation of the erosional crater rim and flanks of eruptive package IV, with the lower slopes / spur between Rapaki and Cass Bay following a similar arcuate pattern.

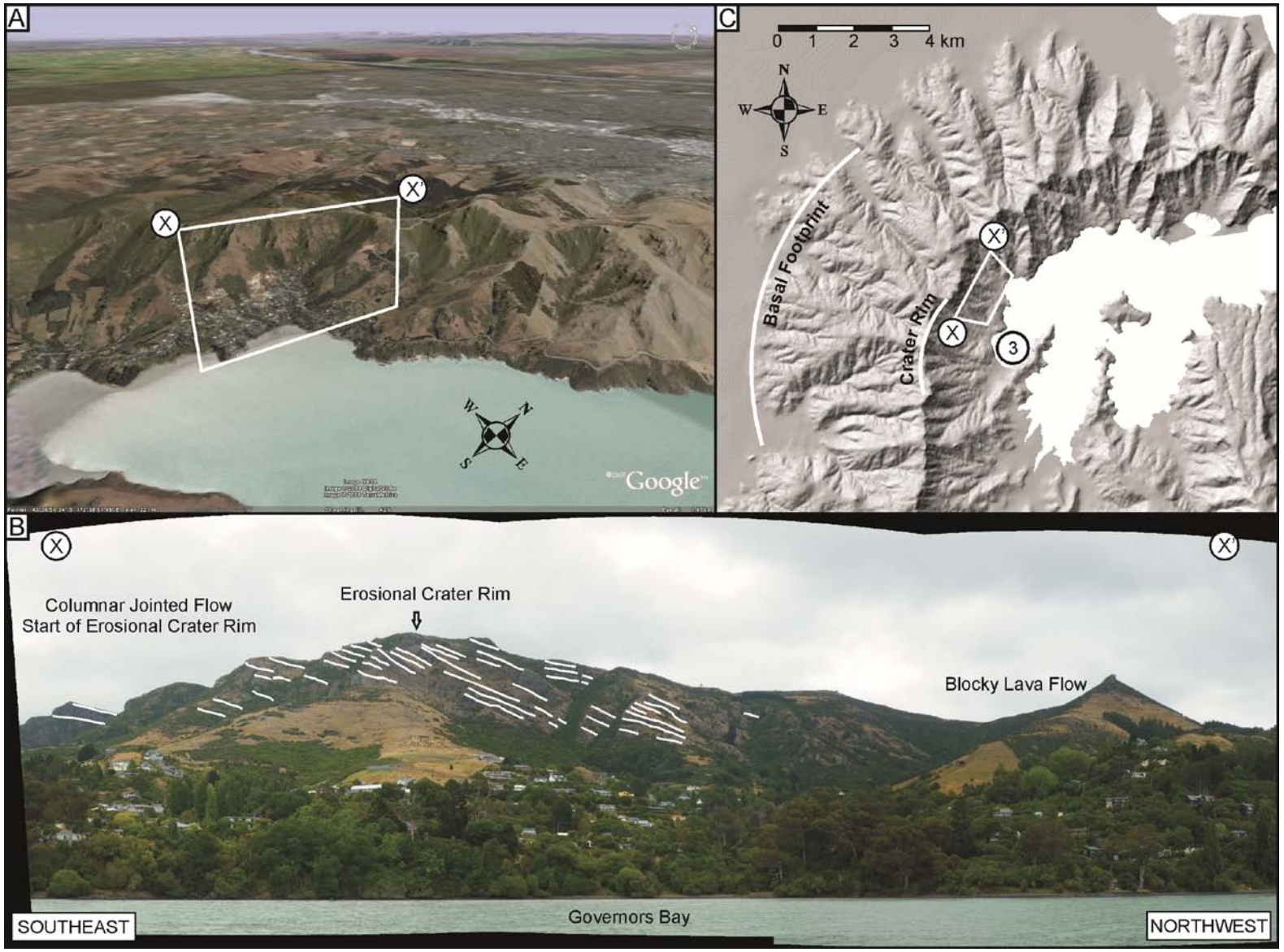

Figure 6.16. Preserved fragments of eruptive package III of the Head of the Bay Cone. A) Oblique view, Google Earth of Governors Bay. B) Photo at right angles to flow direction, indicating erosional crater rim and outer edge of cone marked by blocky lava flow. C) DEM expressing erosional crater rim and basal footprint associated with eruptive package III.

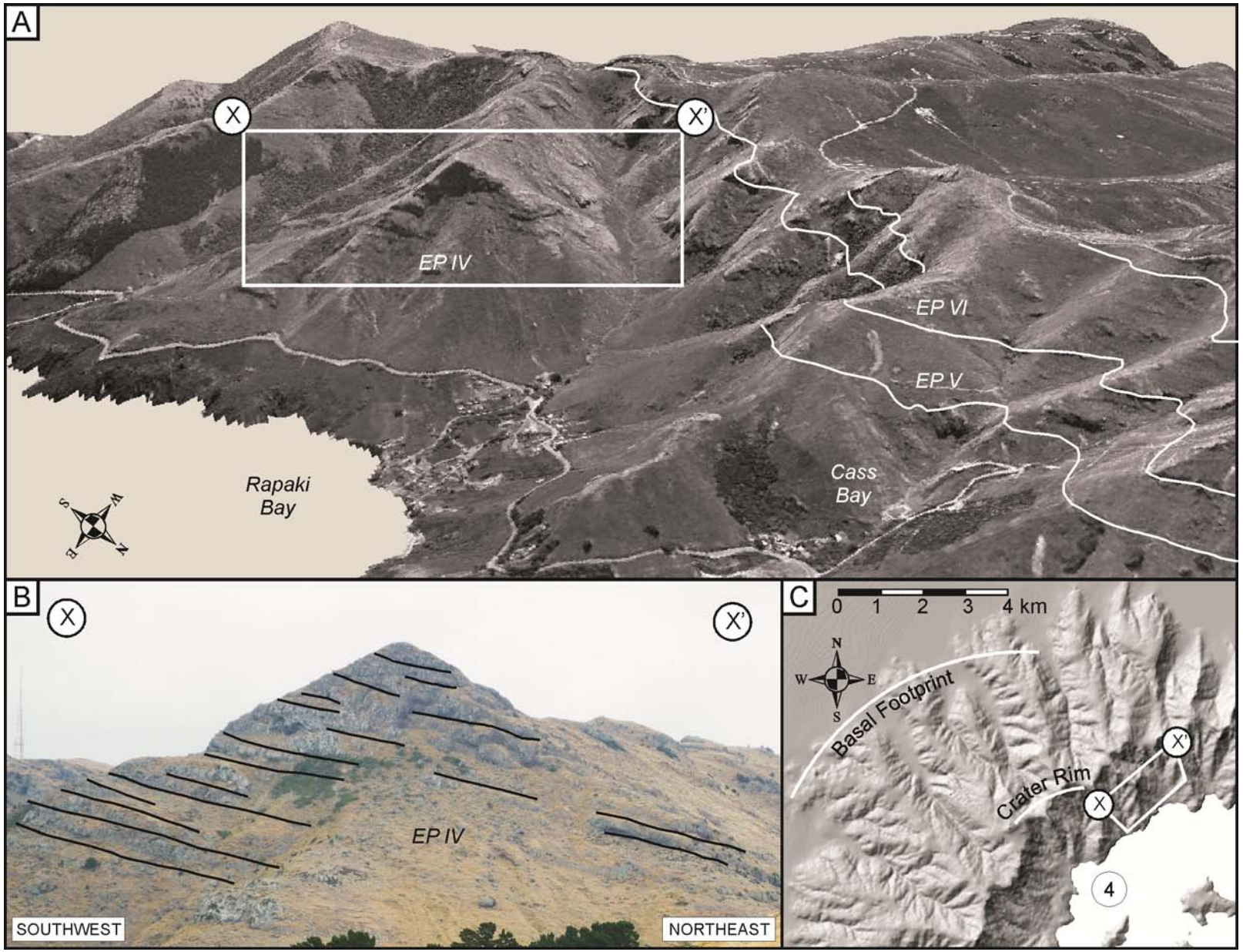

Figure 6.17. Preserved cone fragment exposure of eruptive package IV, Governors Bay Cone, on the western side of Rapaki Bay.

The basal footprint of this cone reached the headland between Cass and Rapaki Bays, and terminated at the outer spur at Hoon Hay. Radial valley formation has limited exposure due to the mantling of later lavas. A major cone-controlled valley formed at the intersection of the eruptive package III, forming the long, deeply incised Hoon Hay Valley.

Two scoria cones are related to this cone, one on the Rapaki spur near the intersection of the overlying cone, and the other at low levels on the Cashmere Spur, in Victoria Park. The latter is a dyke-fed feature, identifiable by a prominent ridge trending towards the scoria cone. A large dyke outcrops on the western side of Marleys Hill, trending towards the eruptive centre, intruding flows on the western flanks. The Multiple Dykes, a complex intersection of five intrusions exposed along the Summit Road, also relates to this cone, cutting through a blocky lava horizon at the erosional crater rim.

This cone marks a significant shift in the eruptive centre lineament, possibly due to magma migration along a fault system. This vent lineament shift is accompanied by the change from gently dipping bays in the volcanic centre region (inner harbour), to steeply dipping, cliff slopes, suggesting that the previous underlying volcanics introduced a structural control, now expressed in the eroded remnants.

Eruptive Package V (Figure 6.10)

The Governors Bay Cone then erupted lavas to the north-east, with flows mantling the northern and eastern slopes of eruptive package IV (Figure 6.17), and producing a more symmetrical shape to the growing Governors Bay Cone. Radial valley formation is preserved to the northeast of Sugarloaf, where radial valley and ridge features are semi-preserved between Huntsbury and Mt Vernon spurs, converging on the projected cone summit. Cone-controlled valley formation developed the long, incised Dyers Pass Valley.

Figure 6.18. View from Rapaki Spur to the north-eastern side of Heathcote Valley. Key features indicated are: eruptive packages (*EP#*) and scoria cone deposits (*SCD).*

One scoria cone is exposed on the flanks of this eruptive package, on the northeast tributary of Cass Valley. Remnant features of this cone are expressed as the erosional crater rim and continuation of arcuate features, producing the significant spur on the south side of Rapaki Bay. The basal footprint of this cone reached what is now Corsair Bay in the harbour, lower Cashmere and lower Rapaki Spurs on the outer flanks.

Eruptive Packages VI (Figure 6.11)

Eruptive packages VI is relatively thin, with remnant surfaces observable in Avoca Valley (Figure 6.18), to the east of Rapaki Spur. Radial valley formation is confined to the south of Rapaki Spur to Avoca Valley. Cone-controlled valley formed in the region of Bowenvale, now a long, broad incised valley. Associated with this package is the Rapaki Dyke, a large late stage trachytic intrusion through the erosional crater rim. One scoria cone is exposed in the north-eastern valley branch of Cass Bay, which has been subsequently covered by eruptive package VII.

Eruptive Packages VII (Figure 6.12)

Eruptive package VII erupted flows to the east and north, extending a basal footprint to Heathcote Valley (Figure 6.18), where the blocky lava horizon intersects the lower section of the spur. Radial valley development of this cone is primarily represented by Horotane Valley, with the two ridges either side paralleling this trend. Three scoria cones are associated with this package, Witch Hill Scenic Reserve at the erosional crater rim, Lyttelton Spur (east of township), and at Castle Rock where a scoria cone is overlain by laharic material (Figure 6.18). Associated with this eruptive package is the Rapaki Spur, now an isolated planèze, cut off from the related volcanic flanks by subsequent erosion. Cone-controlled valley formation developed in the Avoca Valley, becoming a predominant region for erosion, aiding in the development and isolation of the Rapaki Spur planèze.

6.4.4. Whakaraupo Cone: Eruptive Packages VIII, IX, X, and XI

Eruptive Package VIII (Figure 6.12)

The eruptive package VIII developed on the eastern side of the Governors Bay Cone. Lavas mantled previous flows to the northeast, whose basal footprint terminated near middle Heathcote Valley (Figure 6.18), Gollans Bay and Diamond Harbour. Five scoria cones are associated with this eruptive package, at Bridal Path, Mt Cavendish, Major Hornbrook Track, Upper Lyttelton valley, and Battery Point. The Mt Cavendish region had a series of scoria cones, now highly eroded due to limited cover of later volcanics. Erosion of the Bridal Path scoria cones formed the prominent saddle, at the summit of the track. Deposits of this cone suggest a small crater lake existed within the scoria cone, with later erosion and deposition directing lahars through these scoriaceous deposits. The Major Hornbrook Track scoria cone was covered by later lava flows, and exposed by later erosion. Upper Lyttelton Valley and Battery Point scoria cones are also highly eroded, although being overlain by a blocky lava flow, indicating a cessation of localised eruptions prior to emplacement.

There is limited evidence for radial drainage inception at this cone as these are covered by the next eruptive phases (IX, X and XI). The cone-controlled valley at the intersection of eruptive package VIII and VII formed the western incision of Heathcote Valley, a later pathway for debris flows (volcaniclastic / laharic deposits). Interspersed within this eruptive package are laharic deposits. Volcaniclastic horizons to the west of Bridal Path have channels and flow paths, aligning towards the Governors Bay Cone, indicating a major depositional paleo-valley system. Castle Rock, a shallow trachytic dome, associated with this eruptive package (Figure 6.18), which overlies lavas and laharic material representing a late stage intrusion.

Eruptive Package IX (Figure 6.13)

Eruptive package IX lavas is now well exposed in the sea cliffs and rock promontories of Sumner and Redcliffs regions. Lavas of this package were previously called the Mt Pleasant

Formation (Sewell et al., 1992). This cone reached heights of 800m, with lava flows reaching the eastern side of the present day harbour. Radial valleys developed in the Redcliffs and Sumner regions, and may have followed paths previously incised by the underlying eruptive package VIII. A cone-controlled valley developed on the western side of Heathcote Valley, intensifying erosion in the valley between the Whakaraupo Cone and the Governors Bay Cone. Significant features of this cone are the extensive laharic deposits on the outer flanks, primarily exposed in Sumner valley. These are scoria-rich, matrix-supported lahars, with fine ash beds between laharic horizons, indicating near to source pyroclastic reworking, with finer ash beds indicating ongoing eruptions during deposition.

Eruptive Packages X and XI (Figure 14)

Eruptive packages X and XI developed on the eastern side of the growing Whakaraupo Cone. Flows mantle the laharic deposits overlying eruptive package IX, and produced Godley Head and the spur between Sumner and Taylors Mistake. Lava flows were limited to the northwest, due to the topographic control from the interaction between the Whakaraupo Cone and Mt Evans Cone. Limited valley and ridge incision relates to this cone, forming Taylors Mistake valley and the saddle above Livingstone Bay. The overlapping zone of these cones, within the Evans Pass region, promoted further erosion of Sumner valley, a previous valley system. One scoria cone is identified on these eruptive packages, now exposed at sea level in Harris Bay.

6.4.5. Mt Evans Cone: Eruptive Packages XII and XIII

Eruptive Package XII (Figure 6.13)

The Mt Evans Cone was erupted in the eastern part of Lyttelton Volcano, in what is now Purau Valley. Three eruptive packages are identified within this sequence with the older package being poorly exposed on the lower eastern slopes of Purau valley. The middle package (XII) is the predominant feature in the lower Purau valley, distinguished from those on the opposite side (north-western) of the harbour cone sequence (Whakaraupo

Cone) because flows dip into the harbour (Figure 6.2). In reconstructions the early eruptive package is combined with eruptive package XII.

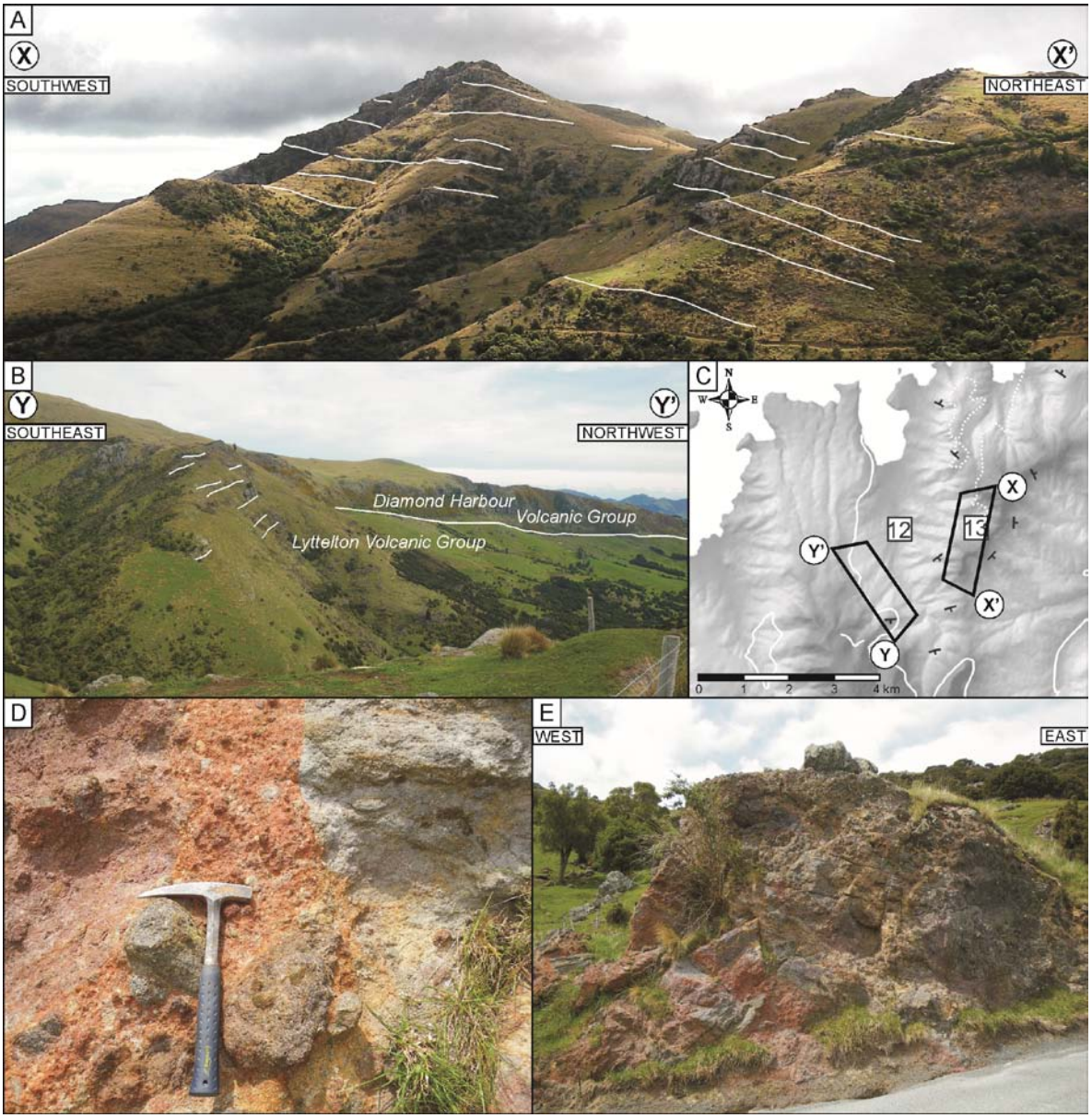

Figure 6.19. Cone structure of the Mt Evans Cone (A, B, and C) and (D and E) related near vent and hydrothermally altered deposits.

Remnant arcuate cone features are associated with this eruptive centre, most significantly the spur half way up Purau valley (Figure 6.19), while on the upper slopes of Mt Evans the descending lava flows can be easily recognised. Most of the radial valley formation of this

initial cones eruptive package is mantled by eruptive package XIII lava flows. This is best exposed on the southern side of Lyttelton Harbour, between Camp Bay and Little Port Cooper, where a significant thickness of pyroclastic deposits mantle a highly irregular, almost hummocky terrain (Figure 6.20). This hummocky terrain limited the overlying lava flows, suggesting these were small valleys incised into the eruptive package XII, which the harbour now cuts at right angles. Two scoria cones are exposed along this contact, with the pyroclastic layer covering the hummocky terrain possibly being linked to the pyroclastics emitted from these scoria cones.

Eruptive Package XIII (Figure 6.14)

Flows of the Mt Evans Cone mantle the underlying structure exposed in Purau valley. Due to the pre-existing extent of the underlying cone, flows were limited to the west and southeast. Lavas predominantly flowed east, reaching the eastern side of Port Levy, over which the Kaituna Valley Hawaiites flowed. The latter are used in this study as a distinct marker horizon, reflecting the arcuate structure of the Mt Evans Cone.

The radial drainage pattern of the Mt Evans Cone is preserved in the upper slopes, as the lower slopes, between the western and eastern sides of Port Levy, have been entirely eroded. Valley incision developed between the Mt Evans Cone and the underlying eruptive packages at overlapping contacts, promoting the inception of Camp Bay, Little Port Cooper, and the Purau – Port Levy Saddle.

The Mt Evans cone developed to the east of the predominant rhyolite high of Charteris Bay. This area of basement, up to 350m high, limited flows from the Purau Cone to the west, initiating the formation of a large valley system between the rhyolite high and the newly developed cone, which later directed flows of the Diamond Harbour Volcanic Group, to form the Diamond Harbour dip slope (Figure 6.1). A large scale cone-controlled valley system developed a proto-Lyttelton Harbour, with this valley system being at a similar orientation to the present day harbour.

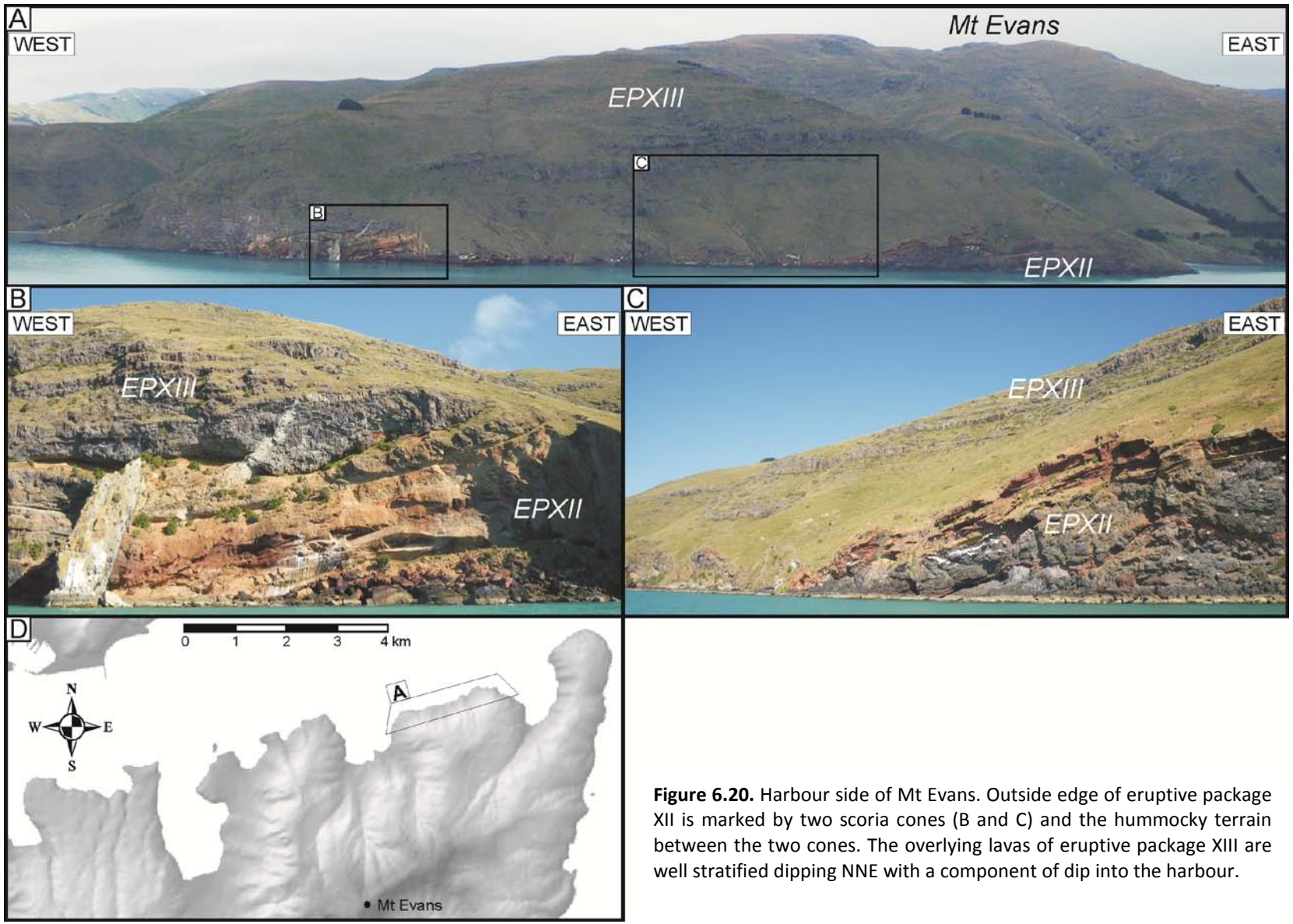

Figure 6.20. Harbour side of Mt Evans. Outside edge of eruptive package XII is marked by two scoria cones (B and C) and the hummocky terrain between the two cones. The overlying lavas of eruptive package XIII are well stratified dipping NNE with a component of dip into the harbour.

6.4.6. Remarkable Cone: Eruptive Packages XIV and XV

Eruptive Package XIV (Figure 6.15)

Eruptive package XIV was an isolated feature of Lyttelton Volcano. It is however of topographic importance in accounting for the distribution of the next phase of volcanic activity; Mt Herbert Volcanic Group. This cone developed on the south-eastern flank of the Head of the Bay Cone, limiting lavas to the southwest, with the lower flanks being covered by Mt Herbert Volcanic Group and later removed by erosion (Gebbies Pass and Kaituna Valley). Because of this the radial drainage pattern has almost entirely been lost, with only minimal ridge orientations trending towards the summit.

A distinct cone structure is evident in the Remarkable Cone structure (Figure 6.21) through observations of primary volcanic features (Figure 6.15) and distinct near vent deposits (Figure 6.21). The erosional crater rim in this region has its own arcuate trend, lava flow assemblage and distinctive near vent deposits (Figure 6.21), indicative of an isolated eruptive centre. A notable feature of the Remarkable Cone is the Remarkable Dyke (Figure 6.21), a large-scale intrusion that propagated from the eruptive centre, and intersects the erosional crater rim. This cone controlled subsequent volcanism and erosion, developing two large cone-controlled valley systems. One is in the orientation of what is now Gebbies Pass, at the intersection of the Head of the Bay Cone and the Remarkable Cone, and the second to the east at the intersection with the Purau Cone (Figure 6.15; eruptive packages XII and XIII) and older rhyolite units in Charteris Bay.

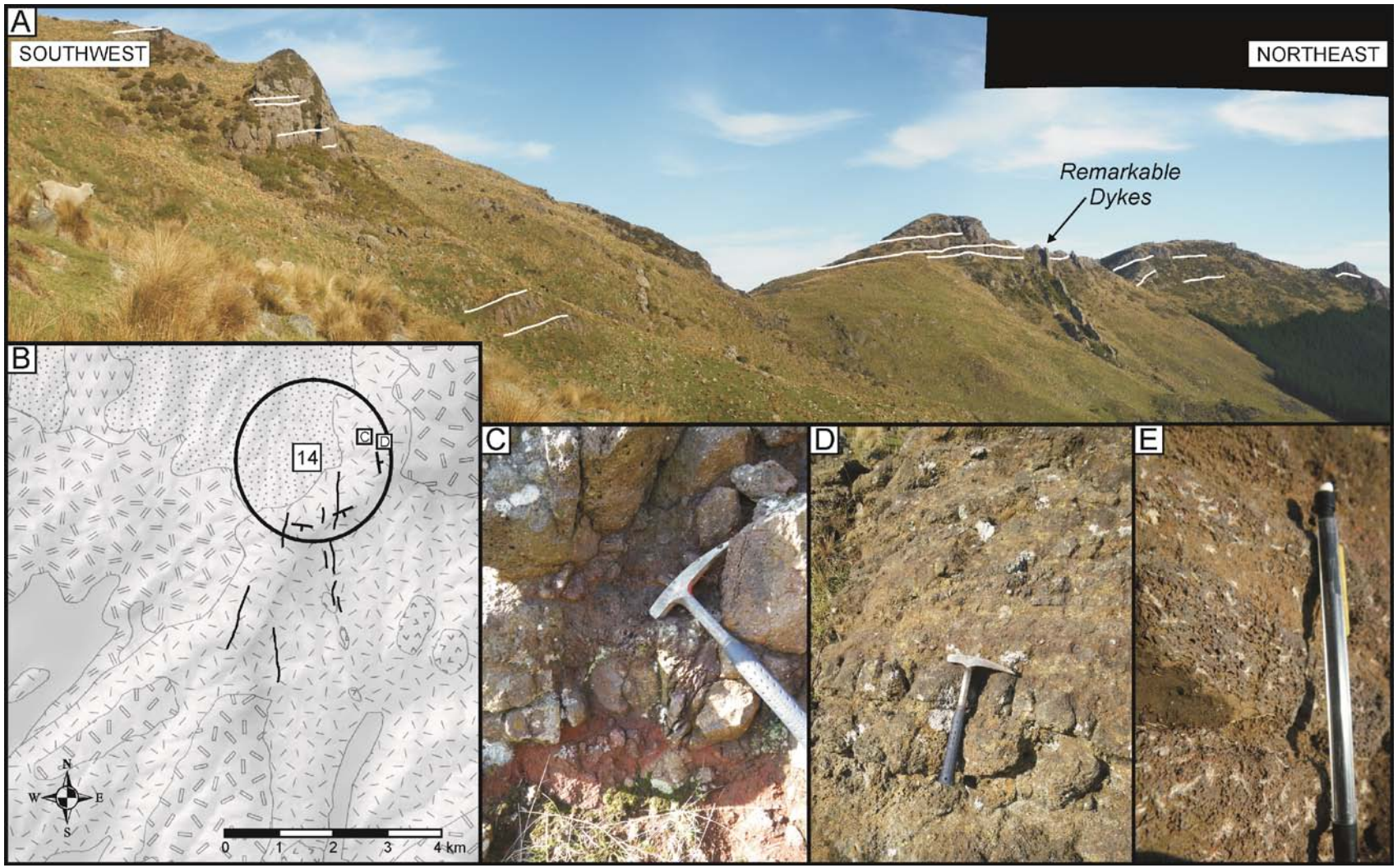

Figure 6.21. Remarkable Cone, attitude of lavas about the crater rim and associated near vent deposits. A) Oblique view of the erosional crater rim and major lava flow trends. B) Location of the erosional crater rim, inferred strikes and dips, and locations of outcrops displayed in C and D. C) Rubbly pyroclastic rich base of a thin lava flow, overlying a red pyroclastic deposit. D and E) Stratified wedded agglutinate separated by thin ash rich layers. E provides a close up of the crystal rich thin layers of welded spatter.

Eruptive Package XV (Figure 6.15)

Lavas of eruptive package XV have previously been mapped as the flows of the Mt Pleasant Formation (Sewell et al., 1992), as they are petrologically related to the lavas of eruptive packages IX to XIII, late phase eruptives of Lyttelton Volcano. This package is interpreted as a flank eruptive on the outer flanks of the Remarkable Cone, extending the basal footprint of Lyttelton's volcanics to what is now Lake Ellesmere and overprinting the incised radial pattern of eruptive package XIV. No radial dyking is associated with this package as it has a mapped vent (Sewell et al., 1992).

6.5. Discussion

In this study Lyttelton Volcano is viewed as a volcanic complex, to be termed the Lyttelton Volcanic Complex, comprised of five overlapping volcanic cones. The volcanic complex developed over a period from 11 – 9.7 Ma, with activity initiating in the south (Head of the Bay) and progressing northwards. Cone structures, zones of overlap, and degradational stages have all contributed to the formation of valleys and erosional crater rims, dictating the current form of Lyttelton Volcano. The following section discusses the features produced in the reconstruction models and compares them to present day topography and the stratigraphic relationships.

6.5.1. Features of the Reconstructed Models

In reconstructions of the Lyttelton Volcanic Complex two major erosional systems are classified; radial valleys and cone-controlled valleys (Figure 6.22 and 6.23).

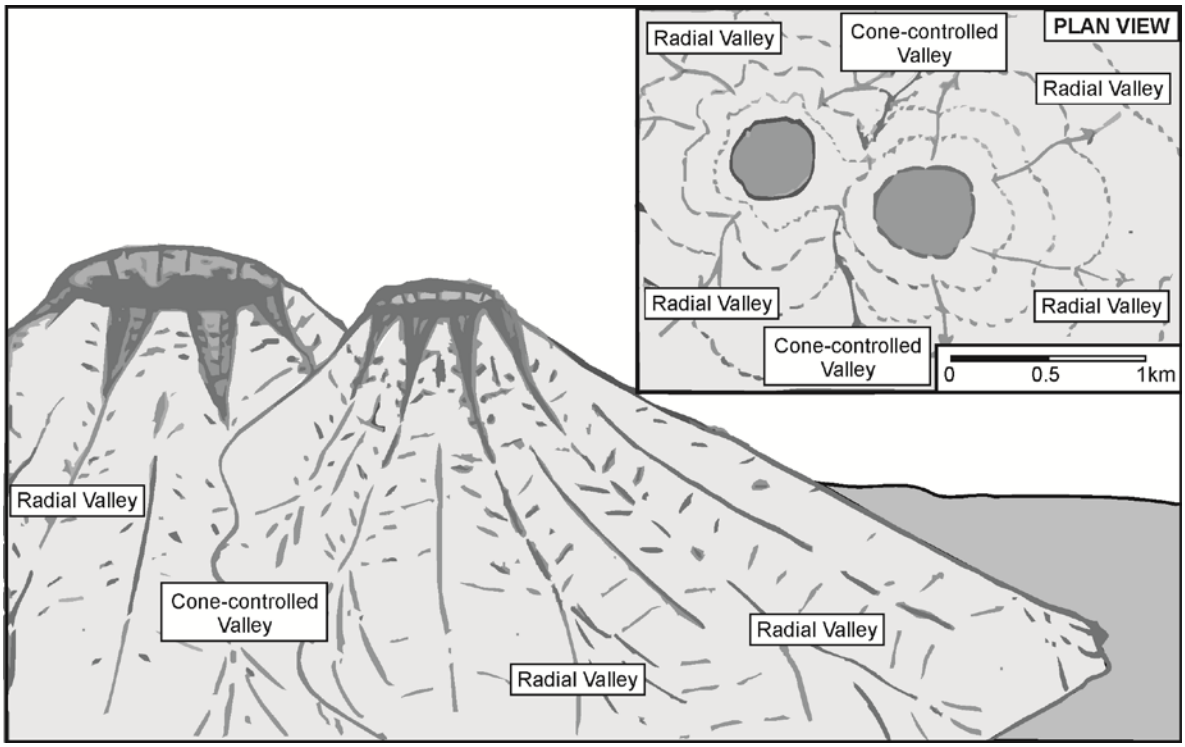

Figure 6.22. Conceptual model of radial and cone-controlled valleys. Radial valleys incise about the summit region, with cone-controlled valleys initiating between volcanic cones, based on Arenal and Chato Volcanoes (Linneman and Borgia, 1993).

Radial Valleys

Radial valleys form as stream erosion incises radially about an eruptive centre (Figure 6.22). On Lyttelton Volcano multiple radial valley systems have been recognised, each incised into an eruptive package. These valley patterns follow a similar sequence to that observed in the stratigraphy, with radiating valley systems associated with each cone, younging to the northeast. Multiple axes within a valley may result from the underlying older valleys being infilled by younger volcanics, then incised radially to the younger eruptive centre. This occurs primarily near to the erosional crater rim at the intersection of eruptive packages with older drainage systems, leaving the older system preserved on the lower volcanic slopes. Preservation of radial drainage features was promoted due to the migration of eruptive centre location, limiting lava flows and overprinting previous radial systems.

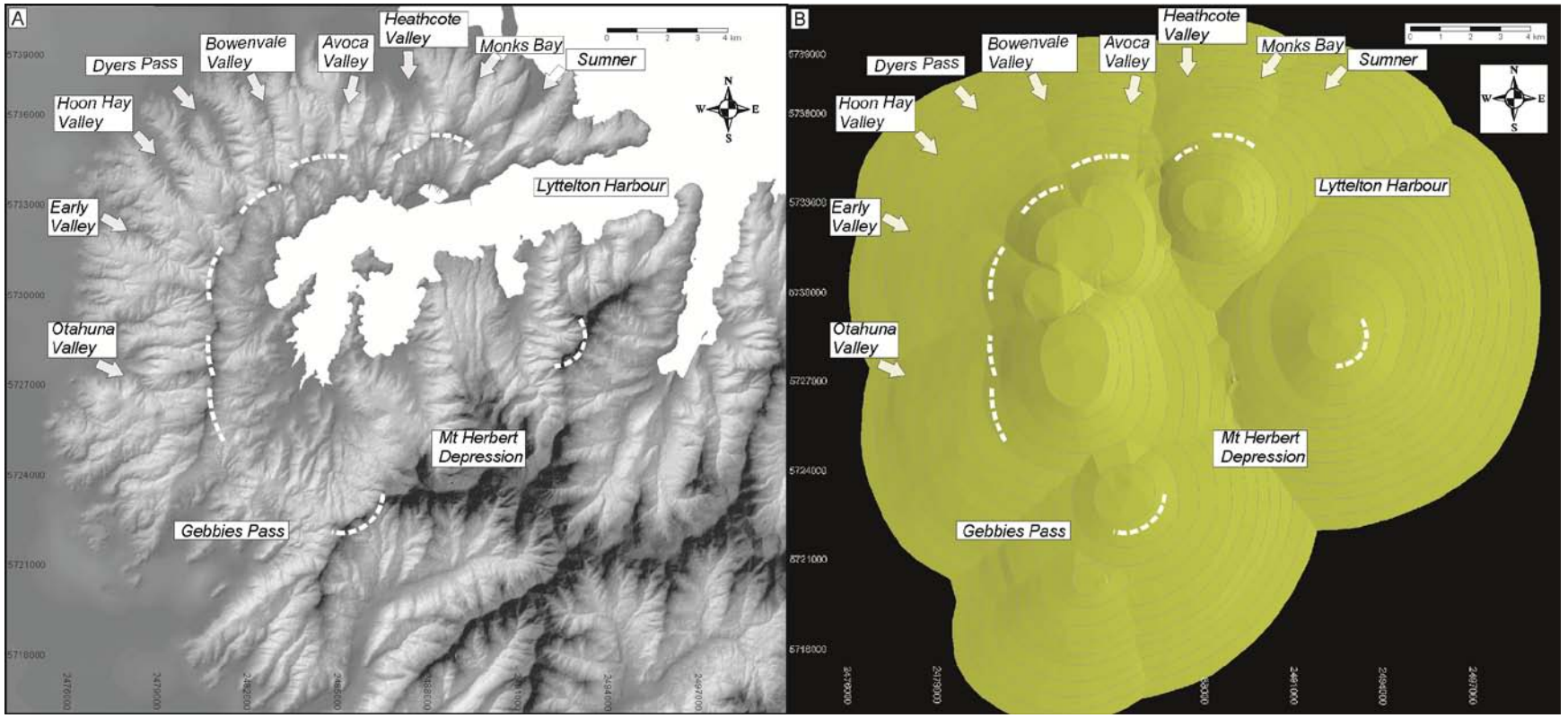

Figure 6.23. Comparison between DEM features and those produced in the reconstruction. Dashed lines indicate the present day erosional crater rim segments, while cone-controlled valleys are labelled.

Cone-controlled Valleys

Large deeply incised valleys forming between eruptive packages and cones are termed cone-controlled valleys (Figure 6.22). These cone-controlled valleys initially develop as an indent on the volcano's flank, with the orientation of the valley axis following the line of intersection between eruptive packages and cones (Figure 6.23).

These regions (Figure 6.23) become preferentially incised due to confined erosion, forming a deeply incised valley, features that will be present throughout the erosive history of the volcano. Cone-controlled valleys would have limited erosive processes in the surrounding radial valley systems, through redirection and loss of catchment area over time, because of the reduction in cone height. With time, cone-controlled valleys became the predominant features on the flanks of the volcano, incising the head-scarp of the valley towards the centre of volcanism, producing distinctive saddles at the erosional crater rim.

Linneman and Borgia (1993) have discussed the development of Arenal and Chato, Costa Rica, next to each other, and the influence of the two volcanoes on drainage patterns. They identified a zigzag pattern of the drainage, developing at the intersection between the well developed radial drainage pattern of Chato and the younger Arenal, whose flows 'flooded' the valleys of the older (Chato) cone. In comparison to the now highly eroded Lyttelton Volcanic Complex, the zigzag drainage pattern identified between Arenal and Chato would be an easily modified surface, with only the remnant of this feature remaining, as a major valley axis.

Missing Segments

Previous models of Lyttelton Volcano have been based around a circular crater rim with three distinctive missing segments discussed as sector collapse (Figure 6.1; Sewell, 1985; Shelley, 1987; Sewell et al, 1992). In the reconstructed model, missing segments (Lyttelton Harbour, Gebbies Pass, and Mt Herbert) are recognised as inter-cone valleys.

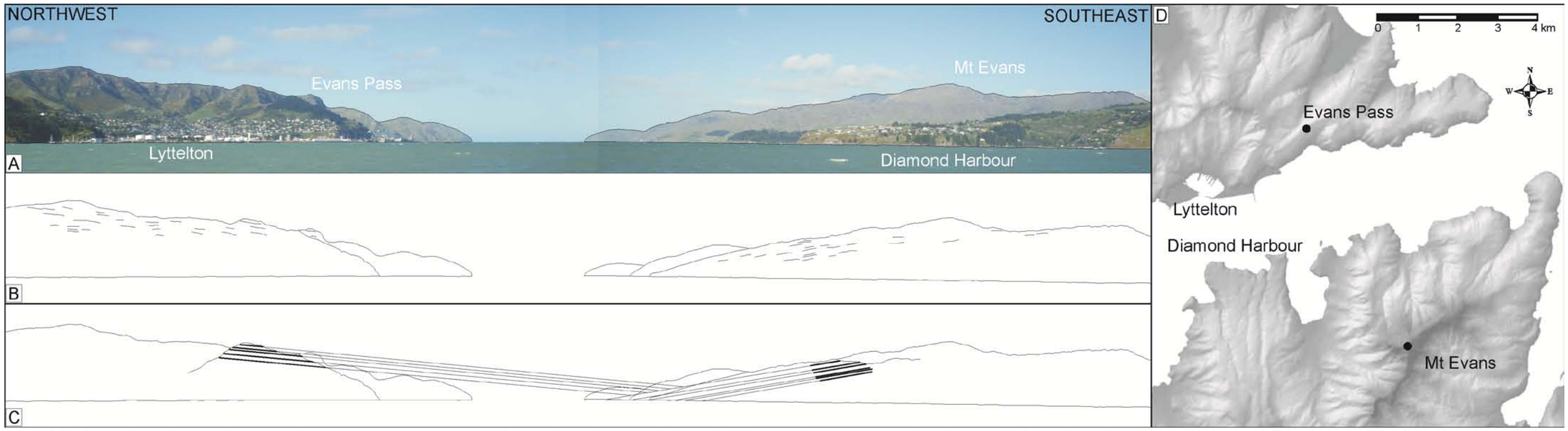

Figure 6.24. Comparison of the north-western (Lyttelton) and north-eastern (Mt Evans) sides of Lyttelton Harbour. B) Major lava flow trends of the Lyttelton and Mt Evans sides of the harbour. C) Projection of the Whakaraupo Cone (Eruptive package IX, Lyttelton side) and Mt Evans Cone lava flows (eruptive package XII), converging in the region of proto-Lyttelton Harbour.

Lyttelton Harbour: In previous models (Sewell, 1985; Shelley, 1987) the western (Lyttelton township) side of Lyttelton Volcano was linked to the eastern (Purau Valley) side (Figure 6.1). If so, correlations in height and volcanic structure should be apparent between the two sides. However field observations indicate the Lyttelton township side lavas dip (NEE) into the harbour, whereas the Purau Valley side lavas dip (NNW), towards the harbour (Figure 6.2 and 6.24). A simple projection of lava flows on a photograph looking down the harbour supports this observation (Figure 6.24), with the convergence of flows near the orientation of the present day harbour. In the new reconstructed model this region reflects an intra-conal valley (Figure 6.23), with the lavas of the Whakaraupo and Mt Evans Cones dipping into the harbour.

A distinct cone structure is apparent on the Purau Valley side (Figure 6.13, 6.14, 6.19 and 6.24). Lava flows in the lower regions of Purau Valley dip towards the harbour (NNW; Figure 6.24), while near the middle of the valley they dip towards Port Levy (NE; Figure 6.19), and begin to dip towards the east in the upper reaches. On the southern side of Purau Valley, Lyttelton Volcanic Group flows are capped by the Diamond Harbour Group. Spurs stratigraphically below this contact have distinct exposures where lavas dip towards the head of the valley (east), reflecting an arcuate cone structure that is radiating about an eruptive centre near the middle of Purau Valley (Figure 6.13, 6.14, 6.19). Near vent associated deposits are exposed on the road cuttings on the southern side of Mt Evans. These are primarily stratified ash and near vent agglutinates, and altered lava flows, indicative of a nearby eruptive source (Figure 6.19).

The Mt Herbert Region was a depression on the south-eastern side of the Lyttelton Volcanic Complex, which later infilled with eruptive products of the Mt Herbert Volcanic Group (Figure 6.1). Two distinct regions are involved in the analysis of this depression, the Purau side, exposed in Purau and the eastern side of Charteris Bay, and the south-western side exposed on the southern slopes of Mt Bradley and the north-eastern side of Gebbies Pass.

If this region represents a collapse sector then one would expect a landslide scar, and a major unconformity between pre and post-collapse deposits (Figure 6.25), like that observed at La Gomera, Canary Islands (Paris et al., 2005). As discussed in the previous section a distinct cone can be interpreted in the Purau Valley / Mt Evans region. A continuation of this cone is exposed on the eastern side of Charteris Bay (Figure 6.21), where a conformable relationship, i.e. no obvious angular unconformity (Figure 6.26), between the Lyttelton Volcanics and the overlying Mt Herbert Volcanic Group, suggesting an unmodified (when compared to a sector collapse scarp) volcanic slope.

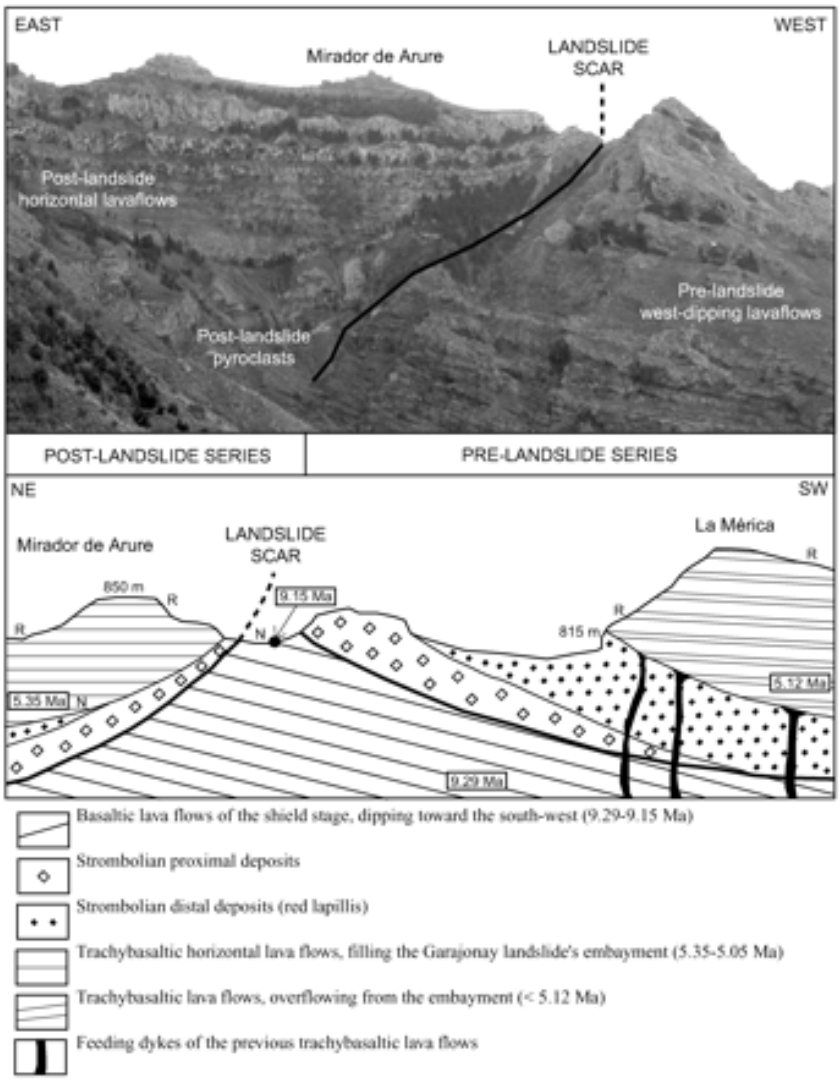

Figure 6.25. West wall of the Barranco de Valle Gran Rey, La Gomera, Canary Islands (from Paris et al., 2005). Note the post and pre landslide (collapse) series, and differing dip relationships separated by the landslide scar.

On the south-eastern side of the Mt Herbert region another distinct cone structure, the Remarkable Cone (Figure 6.22) is evident through observations of primary volcanic features (Figure 6.15) and distinct near vent deposits (Figure 6.21). The erosional crater rim in this region has its own arcuate trend, lava flow assemblage and distinctive near vent deposits (Figure 6.21), indicative of an isolated eruptive centre. To the northeast a distinct surface occurs between the onlapping Mt Herbert Volcanic Group deposits (from the northeast) and the underlying Lyttelton Volcanics. Fieldwork has established that although there is an onlapping sequence, this does not lap onto the south eastern collapse amphitheatre of Lyttelton Volcanics, but onto the eastern slope of the Remarkable Cone (Figure 6.26). The topographic effect of the Remarkable Cone is best viewed when examining the near flat, thick lava flows of Mt Bradley (Figure 6.26). These flows could not have ponded without the topographic barrier and height of the cone structure.

Gebbies Pass is a 5km wide sector 'missing' from the hypothesised circular crater rim of Lyttelton Volcano (Figure 6.1). The two sides of this sector are defined by the western erosional crater rim of Port Hills, and the eastern Remarkable Cone. On the western side there is a marked crater rim, with southerly dipping lava flows, identified and discussed earlier in this study as the remnants of eruptive package 1 of the Head of the Bay Cone, and the eastern side recognised as the Remarkable Cone, also with an isolated crater rim and cone structure. Therefore, no correlation or continuation of the previous large circular crater rim can be made.

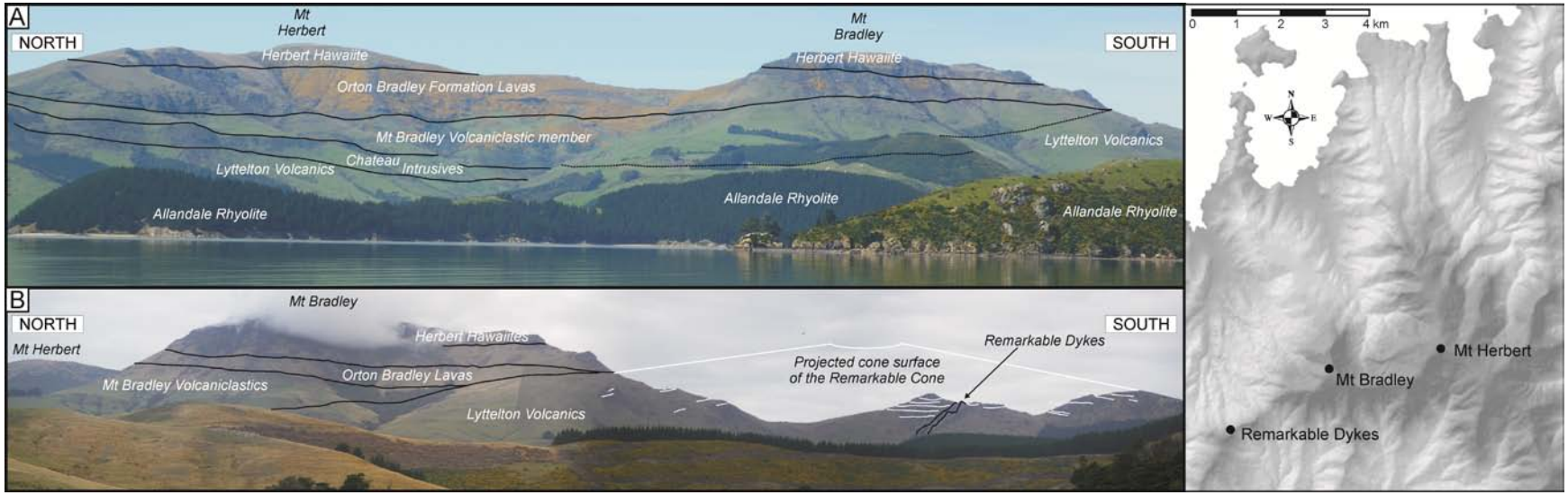

Figure 6.26. Topographic control of Lyttelton Volcanics on subsequent eruptive products of the Mt Herbert Volcanic Group.

6.5.2. Degradational Stages and Features

Under the classification review of Karàtson et al. (1999) the Lyttelton Volcanic Complex is only in the second stage of volcanic degradation, in which rapid valley incision is followed by the beheading of radial valley systems, channel capture and the formation of planèzes. Varying types and stages of erosion are evident on Lyttelton Volcano, ranging from stream flow (epiclastic deposits) to major valley and harbour formation.

Karàtson (1996) made the assumption that volcanic degradation has an initial period of intense erosion (hundreds of thousands to one million years after volcanism ceases), which then slows down to operate at a linear or quasi linear rate. Erosion on volcanic landforms increases crater and cone diameter, intracraterial valley length and valley number, and decreases cone height, average outer slope of cone, and average slope of outlet valley (Karàtson, 1996). Therefore as cones degrade the catchment area is reduced, as a result initial degradation of the volcanic structure will be intense, reducing over time, reducing catchment area due to loss of volcanic height (Karàtson et al., 1999).

The head-ward advancement of valleys has been calculated at 250 times the rate of summit lowering in the Tertiary basalts of the Shoalhaven Gorge, SE Australia (Nott et al., 1996). With the authors concluding this region will become more dissected well before the substantial decrease in height. A further control on catchment area and the erosive potential (valley incision) is base level (Karàtson, 1996; Karàtson et al., 1999), which on Banks Peninsula is controlled by relative sea level. Lowering sea-level during glacial periods would have increased the erosion potential dramatically, resulting in distinct degradational phases (intensifications) over time.

Crater Regions

Erosion in the central region of the Lyttelton Volcanic Complex has been promoted and initiated by the volcanic topography and erodability of volcanic products. Summit and crater regions of volcanoes are commonly comprised of alternating lavas and

unconsolidated pyroclastics, intersected with zones of weakness due to hydrothermal alteration (Stiltoe, 1994; Thouret, 1999; Karàtson et al., 1999). Crater regions can rapidly enlarge with erosion and through the through rapid incision of radial drainage (Karàtson, 1996), with the invasion of a drainage network into the crater (unidirectional breaching; Karàtson, et al., 1999), increasing the area of the drainage basin (Figure 6.27, erosion modified craters), further promoting erosion.

The Lyttelton Volcanic Complex is modelled to have erupted from five main eruptive centres. Each summit region would initially erode in the fore mentioned style. Yet as degradation of the volcanic complex progressed, the summit regions would become amalgamated or coalesced. Karàtson et al., (1999) classification of erosion craters / calderas identified coalesced crater clusters (Morske Oto, Mihorlat Mountains, Slovakia, and Hargita Mountains, Romania; Karàtson et al., 1992) as forming due to the highest valley breaching all of the craters or capturing all of the breached channels (Figure 6. 27).
The Valle del Bove, Mt Etna (Figure 6.28; McGuire, 1982; 1985; Chester et al., 1985; Patane et al., 2006) on Mt Etna is comprised of a succession of eruptive centres (Chester et al., 1985), with the Valle del Bove aligned along the overlapping zones of these, modified over time by periods of debris avalanches (Calvari et al., 1996; 1998), and capturing of drainage basin into a unidirectional drainage network. Crater breaching and amalgamation is the probable degradation evolution for the Lyttelton Volcanic Complex, leading to the erosion of the interior and ultimately the formation of Lyttelton Harbour, discussed next.

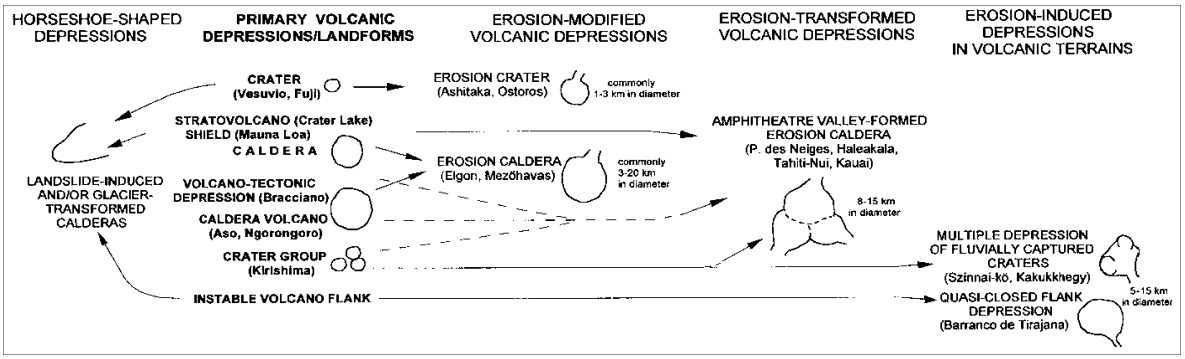

Figure 2.27. Karàtson et al,. (1999) erosional crater and caldera classification with examples. Of significance in the degradation of Lyttelton Volcano are the termed erosion transformed volcanic depression and erosion induced depressions in volcanic terrains.

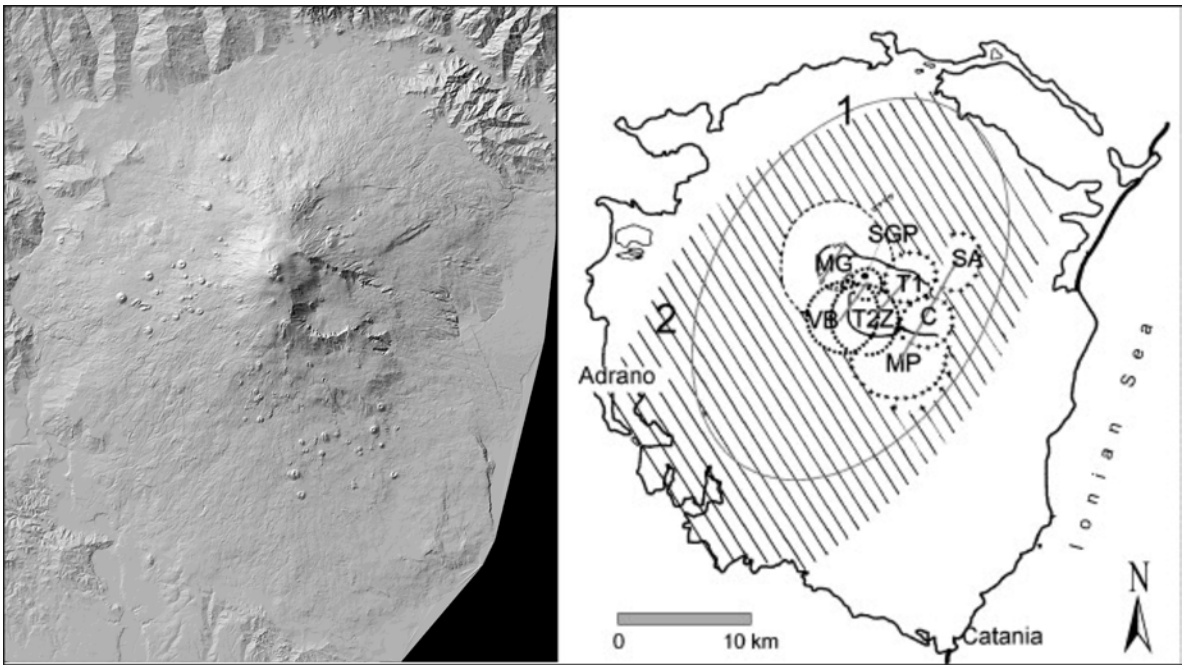

Figure 6.28. DEM of Mt Etna, Italy and the eruptive centre interpretation of Chester et al., (1985). Valle del Bove is the horseshoe shaped feature extending towards the present day summit of Mt Etna, with the orientation along the alignment of previous volcanoes. The DEM was supplied by David Karàtson, Eotvos University).

Large Inter-cone Valleys

The most significant feature of the reconstructed Lyttelton Volcanic Complex (Figure 6.23) is the large inter-cone valleys, at similar orientations to the present and recognised major erosional features; Lyttelton Harbour, Gebbies Pass, and Mt Herbert. These valleys or depressions had the largest catchment areas, which when accompanied by direct connection to the ocean had the greatest erosion levels. Ollier and Terry (1999) defined

"the valley draining the crater has a larger catchment than other radial streams and tends to erode faster than the others, enlarging the crater and modifying the centripetal drainage pattern to some extent. With time the centripetal drainage, typical of a crater, becomes more and more modified towards a dendritic pattern, typical of a normal fluvial valley."

The Mt Herbert region, oriented to the southeast was flanked on one side by the Mt Evans Cone and the other by the Head of the Bay and Remarkable Cones (Figure 6.23). It is within this valley that the next phase of volcanic activity developed, blocking off this outlet. Gebbies Pass is a large valley between the Head of the Bay and Remarkable Cones, that progressive incised, cutting down until reaching basement lithologies. Preferential erosion of this region would have been promoted by three factors: the time period between activity of the Head of the Bay Cone and the Remarkable Cone, resulting in extensive erosion; the ease of removing material directly out to sea; and the easily erodible nature of the Remarkable Cone, being near vent interbedded stratified lavas and pyroclastics (Figure 6.21).

The largest present day structure, Lyttelton Harbour (Figure 6.25), developed through the extensive erosion of the Head of the Bay, Governors and Whakaraupo Cones on the north-western side of Lyttelton Volcano, while to the northeast the Mt Evans Cone and infilled Mt Herbert region channelized these effects down a proto-Lyttelton Harbour (Figure 6.26).

Lyttelton Harbour developed due to the infilling of the Mt Herbert region, the previous outlet, promoting accumulation of water within the interior depression of the volcano. On the lower slopes head scarp incision was occurring, cutting through the lavas of the Whakaraupo and Mt Evans Cones, creating a new drainage outlet, which when linked to the sea provided a constant removal of material by longshore drift along the east coast of New Zealand. As erosion progressed up the proto-Lyttelton Harbour, preferential erosion

occurred in the central, brecciated eruptive regions, resulting in the scalloped form of bays and head scarps of the associated bay / valley system at the location of eruptive centres (i.e. Head of the Bay, Allandale, Governors Bay and Lyttelton Township).

A key feature of the reconstructed model of the Lyttelton Volcanic Complex is the development of inter-conal valleys as major erosional pathways, rather than multiple breaches incising into the interior of the volcano. Volcanic degradation on the Lyttelton Volcanic Complex can be designated through the following stages:

1. Upper regions of the volcanic structure degrade rapidly, through radial incision.
2. With loss of volcanic height through erosion, radial drainage catchments becoming reduced, limiting their erosive potential.
3. Radial valleys incise to a base level, dependent on relative sea-level and climatic conditions, reaching a steady state, aiding in the preservation of the outer volcanic structure
4. Erosion is primarily limited to inter-cone valleys, active erosional pathways with large catchment areas linked to the ocean, promoting rapid removal of material.
5. Erosion enlarged the inter-cone valleys focussing on brecciated / hydrothermally altered eruptive vent regions, producing scalloped out bays and valleys.

Erosional Crater Rim Segments

In the inception of coalescing summit craters, and the development of a single drainage pathway from this region, a segmented erosional crater rim will preferentially develop, with the volcanic height reducing in height over time. In the reconstructed model a series of scalloped erosional crater rims (Figure 6.23) have been produced, reflecting the structure of the associated volcanic cones and eruptive packages. Formation of this segmented erosional crater rim can be attributed to the erosive tendency of the volcanic structure. Lower slopes commonly record slope angles around 10° to 12°, while the upper slopes, near the crater rim have slopes≤20°, reflecting a steady state profil e (Davidson

and De Silva, 2000). A similar coalesced crater structure has been recognised in the Carpathians, Central Europe (Karàtson et al., 1999), in which the summit craters combined together when erosive forces focussed in one drainage branch, resulting in a single shared drainage basin (Figure 6.27). Control on the height of the erosional crater rim relates to the erosion of individual cones (Karàtson, 1996). The upper regions of volcanic cones were probably loose brecciated pyroclastic material, intensifying erosion on these slopes rather than the more gently dipping lower flanks.

Scoria Cones

Lavas flows and welded structures (agglutinated lavas) are less susceptible to erosion when compared to lesser or un-welded pyroclastics (Wood, 1980; Carn, 2000; Nèmeth, 2004). Erosion of scoria cones has resulted in distinctive topographic signatures, in some cases producing an erosive valley head. This greater erosive tendency has resulted in many larger valleys having an eroded scoria cone at the top of the valley, producing a scalloped out valley, and often a saddle at the top of the ridge (e.g. Bridle Path). In areas where scoria cones are away from the crater rim, smaller concaved topographic expressions are produced, either on the inner harbour region or on the outer slope, dependent of scoria cone location.

Preservation of the Volcanic Landscape

Two contrasting levels of erosion are reflected between the less eroded outer flanks and highly incised interior of the Lyttelton Volcanic Complex. As discussed earlier erosion in the interior is exacerbated by the inception of large inter-cone valleys and the coalescing of crater regions /drainage basins over time, with the outer drainage networks becoming dendritic (Ollier, 1988). Resulting in the outer flank valleys having ever reducing drainage basin areas with loss of volcanic height, reaching a steady-state (Karàtson et al., 1999). Limited erosion of the outer slope surfaces of the Lyttelton Volcano could also relate to vegetation cover, with drainage networks being reduced with vegetation cover (stabilisation), hindering fluvial erosion (Karàtson et al, 1999). It should be noted that

Banks Peninsula has only been clear-felled of trees in the last ~150 years; prior to this was heavily forested (Wilson, 1994).

6.5.3. Deposits Overlying the Reconstructed Lyttelton Volcano

Paleo-valley surfaces are identifiable through the erosive basal contacts of later sediments and volcanic deposits, providing a template of the erosional form of the volcanic complex at a given time period. This study recognises three stages of paleo-valley deposits associated with; Lyttelton epiclastic horizons, Mt Herbert Volcanic Group and the Diamond Harbour Volcanic Group.

Lyttelton Epiclastic Horizons

Epiclastic horizons are distinctive deposits preserved within the Lyttelton Volcanic Complex. They occur at distinct stratigraphic horizons within the volcanic sequence, not as one layer, that defined an unconformable surface between Lyttelton 1 and 2 as previously indicated by Shelley (1987). Distinct channels and paleo-flow directions are observable within major epiclastic horizons exposed between the Tors and the Bridle Path (Figure 2.27). These channels have flow orientations indicating a source region near Cass Bay. Overlaying this orientation onto the constructed model, a distinct relationship can be observed between paleo-flow directions and probable source regions, trending down the cone-controlled valley between eruptive packages VII and VIII. A similar aspect is observed in epiclastic deposits at Battery Point, clearly indicating a paleo valley with a similar trend to Sumner Valley.

Mt Herbert Volcanic Group (9.7 – 8 Ma)

The Mt Herbert Volcanic Group marks a period of volcanic activity that infilled and then spread east within a large depression on the southeast of Lyttelton Volcano (Figure 6.29). Of significance within the Mt Herbert Volcanic Group are the initial deposits of the Orton Bradley Formation. This sequence of lava flows, phreatomagmatic deposits, conglomerates and tuffaceous sandstones indicate a substantial body of water fuelling

phreatomagmatic phases, supporting the existence of a large depression. Further volcanic activity within this depression was controlled by the surrounding topography, restricting flows back into central Lyttelton, and to the southwest and northeast (Figure 6.29). The top flows of this group produced the flat topped, ponded lava flows, exposed on Mt Bradley. This thick lava succession stops dramatically to the southwest of Mt Bradley, limited by what was the Remarkable Cone, now heavily eroded (Figure 6.21A).

Post Lyttelton Volcanism

Volcaniclastic deposits are encountered at the present day harbour level and lower valley floors, overlying Allandale Rhyolite and Lyttelton Volcanics. Deposits are either covered by or interbedded with units of the Diamond Harbour Volcanic Group (Chapter 3). These represent debris flows and alluvial fans on the eroding flanks of Lyttelton Volcano, with those now exposed lower down within inter-cone valleys indicating long lived erosive and depositional environments (Figure 3.18).

Conglomerates in upper Kaituna Valley, upper Purau Valley and the western side of Mt Bradley are successions of well indurated, pebble to boulder, matrix to clast supported, massive conglomerate. Deposits have tuffaceous matrix due to their close association with the Mt Bradley Volcaniclastic Member of the Orton Bradley Formation, stratigraphically near the base of the Mt Herbert Volcanic Group (Hampton, 2005). Clasts are primarily Lyttelton Volcanic Group, with distinct variation in weathering profiles (extensively weathered / altered rinds, to fresh unaltered basaltic clasts).

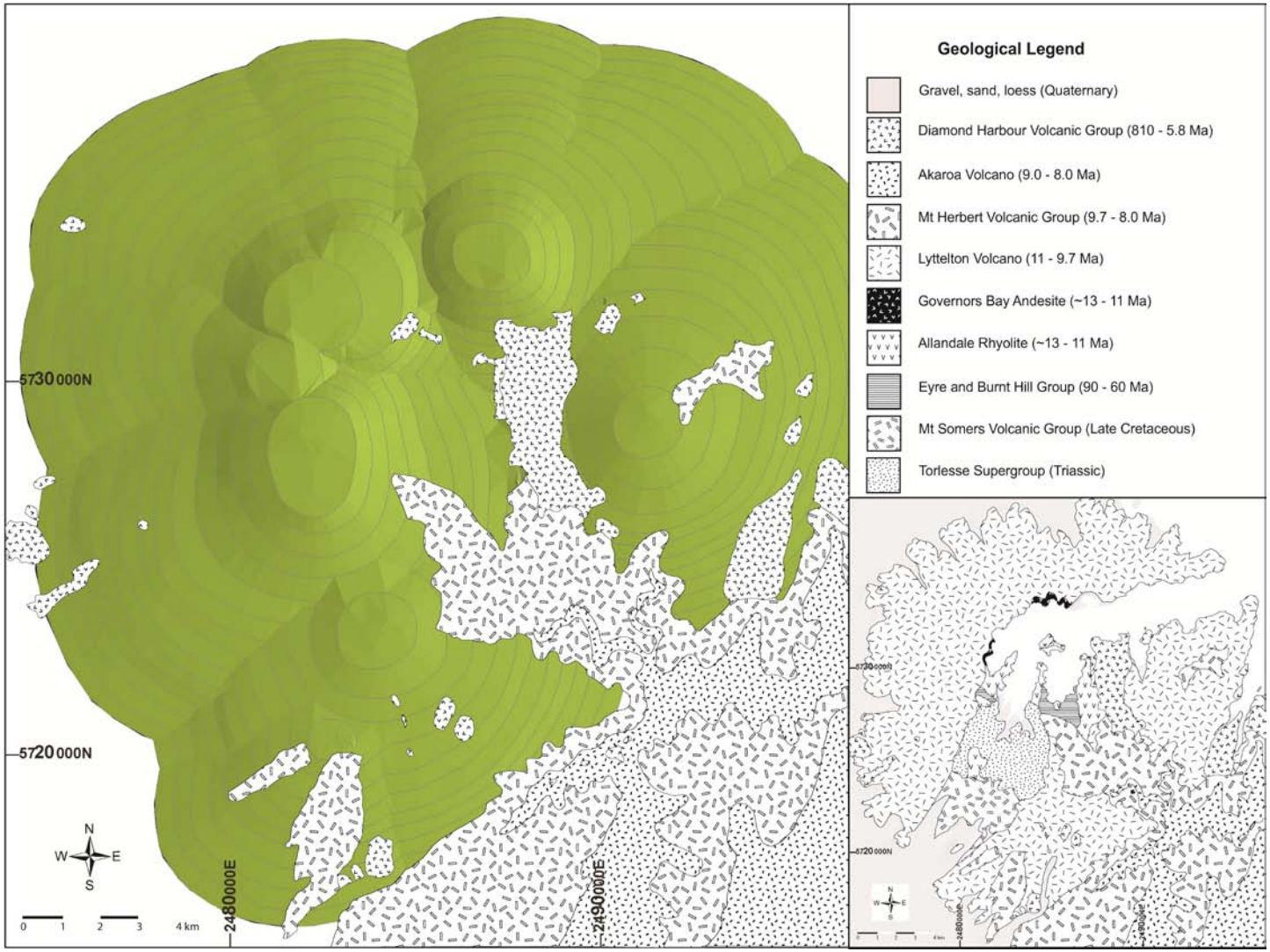

Figure 6.29. Reconstructed model of the Lyttelton Volcanic Complex and the relationship with overlying volcanic groups. Of significance is the infilling relationships of both the Mt Herbert Volcanic Group (Mt Herbert Region) and the Diamond Harbour Volcanic Group, with the latter invading a proto-Lyttelton Harbour in existence prior to 8.1 Ma.

The most significant exposures of conglomerate occur at Black Rock (between Church and Hays Bays) and the northern cliffs of Quail Island (Chapter 3). Exposures are interpreted as a succession of lake beds, fluvial channels and conglomerates with a tuffaceous matrix, indicating a surface that had limited Lyttelton Volcanic Group cover. Channels in conglomerates and lenses of interbedded tuffaceous mudstone and sandstone indicate flow conditions to the northeast, in the direction of the proto-Lyttelton Harbour. Sequences are interbedded and capped by Diamond Harbour Volcanic Group (8.1 – 5.8 Ma), supporting the hypothesis of early valley inception (Figure 6.29).

Diamond Harbour Volcanic Group

Diamond Harbour Volcanic Group lavas were the first invasive lava flows into proto-Lyttelton Harbour, mantling the erosive surface of Lyttelton Volcano (Figure 6.29). The dip slope of these flows was controlled by the basement structure (primarily rhyolite), Mt Herbert Volcanics and Lyttelton Volcanics on both the south-western (eroding Head of the Bay Cone) and north-eastern (Mt Evans Cone) sides of this flow feature (Figure 6.1 and 6.29).

In examination of the basal contacts of volcaniclastic horizons and the Diamond Harbour Volcanic Group, on Lyttelton Volcanic Group and underlying lithologies, a distinct similarity is evident between the mapped contacts and the reconstructed Lyttelton Volcanic Complex (Figure 6.29). Erosion is not taken fully into account in the reconstructions, but what becomes apparent is that this invasive series of Diamond Harbour Volcanic Group lava flows, sourced just northeast of Mt Herbert (Sewell, 1985), was channelized between the outer flanks of the Mt Evans Cone, Mt Herbert Volcanic Group and rhyolite highs on the north-eastern side of Charteris Bay valley. Lavas flowed into an established paleo-drainage network or proto-Lyttelton Harbour that was in existence by at least 8.1 Ma (earliest Diamond Harbour Volcanic Group; Figure 6.29).

6.6. Summary

- Eruptive packages are evident from cone sectors with primary volcanic landform features, distinct blocky lava flow horizons, and an intrusive regime with a radiating assemblage about an eruptive centre.
- The reconstructed model highlights a segmented erosional crater rim, resulting from the growth of overlapping eruptive packages and cones. Each cone has a distinct structure and associated deposits (cone sector), for example the Mt Evans and Remarkable Cones.
- Two erosional structures are modelled, radial valleys and cone-controlled valleys. Radial valleys reflect erosion from a cone's summit, while cone-controlled valleys are regions where eruptive packages and cones from different centres meet, allowing stream development at their intersection. With larger catchment areas, cone-controlled valleys had the potential to erode and transport extensive amounts of material away from source, ultimately forming the features of Lyttelton Harbour, Gebbies Pass, and the infilled Mt Herbert region.
- Overlying volcanic groups (Mt Herbert, and Diamond Harbour Volcanic Group) and interbedded epiclastic deposits (Chapter 3), support reconstructed surfaces. With epiclastic deposits representing deposition on the flanks and valley floors of the eroding Lyttelton Volcano. Mapped contacts mimic the underlying reconstructed surface, particularly in the Mt Herbert Volcanic Group, with the Diamond Harbour Volcanic Groups deposited on eroded surfaces, but strongly influenced by the earlier Lyttelton Volcanic structure.
- The degradation of Lyttelton Volcano can be best explained by the loss of catchment of the outer flank valleys, decreasing erosive potential. Initial erosion focussed on the volcanic highs, eroding outer radial valley systems. These catchment areas lowered over time, resulting in less erosion and greater preservation of the original volcanic structure, when compared to the increasingly eroded cone-controlled valleys.

CHAPTER 7

STRUCTURAL CONTROL AND FURTHER STUDY

7.1. Introduction

This chapter is divided into two sections. The first discusses how the tectonic setting, fault control and volcanic structure affect the location and development of eruptive centres of the Lyttelton Volcanic Complex. The second section briefly discusses wider implications to Banks Peninsula, in particular to Akaroa Volcano.

7.2. Magmatic Source and Vent Controls

Previous models (Shelley, 1987; Sewell et al., 1992) regarded Banks Peninsula as a 'wandering' hotspot, initially moving from Lyttelton 1 to Lyttelton 2, then sequentially erupting the Mt Herbert Volcanic Group, Akaroa Volcanic Group, and finally the Diamond Harbour Volcanic Group. Hoernle et al (2006) proposed decompression melting as the source of volcanism, with magma rise dependent on the amount of lithospheric removal.

Contrary to these models there is not a clear progression of volcanic activity, from Lyttelton to Akaroa Volcanoes. Volcanic activity has been focussed in three regions; the north-west, central and south-east regions of Banks Peninsula. Initial volcanism was focussed in the north-west, erupting the Allandale Rhyolite, Governors Bay Andesite, and Lyttelton Volcanics (Figure 7.1). Volcanism proceeded in the central region as the Mt Herbert Volcanic Group, followed by the Diamond Harbour Volcanic Group. Importantly Akaroa erupted simultaneously as the Mt Herbert Volcanic Group in the south-eastern region. This leads to the suggestion of at least two magma systems; one in the west, erupting the Allandale Rhyolite, Governors Bay Andesite, Lyttelton, Mt Herbert, and Diamond Harbour Volcanic Groups, and another in the east erupting the Akaroa Volcanic Group.

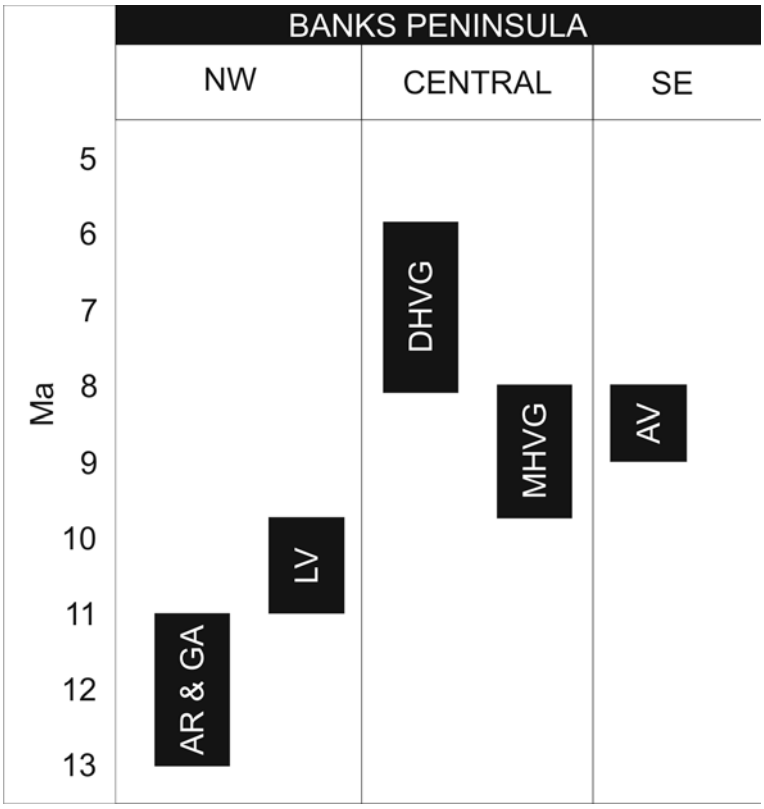

Figure 7.1. Timing and regions of volcanism on Banks Peninsula. AR, Allandale Rhyolite; GA, Governors Bay Andesite; LV, Lyttelton Volcano; MHVG, Mt Herbert Volcanic Group; AV, Akaroa Volcano; DHVG, Diamond Harbour Volcanic Group.

It is evident from stratigraphic relationships that initial Lyttelton Volcanic Group eruptions occurred to the west of Gebbies Pass (Head of the Bay), migrating down harbour (Governors Bay and Whakaraupo Cones) to Purau (Mt Evans Cone) and then back to Mt Bradley / Mt Herbert Region (Remarkables Cone and Mt Herbert Volcanic Group).

Previously two faults had been recognised on Banks Peninsula, on either side of Gebbies Pass (Figure 7.2). These have a NE – SW trend, and align with thermal springs in Purau, Heathcote Valley, Rapaki Bay, and Motukarara (Sewell et al., 1992). Little is known about the fault systems beneath the eastern Canterbury Plains, but it is here suggested that if faults were present in this region they would have a similar orientation to those identified in inland and offshore Canterbury (Figure 7.2).

An important component in the assessment of faulting regimes on Banks Peninsula is the faulted block of Torlesse exposed in Gebbies Pass. This not only has structural significance that can be extrapolated to infer deformation directions, but its relationship to subsequent

deposits provides critical information on the tilt of this block. Thiele's (1983) study suggested that the tensional stresses with the basement Torlesse Supergroup of Gebbies Pass produced faults, which acted as conduits for the Mt Somers Volcanic Group, Allandale Rhyolites and Governors Bay Andesites. A distinctive compressional tectonic regime, with NNW to SSE shortening can be approximated across the area (Associate Prof. Uwe Ring, pers comm., 2009), with deformation aligning with the Chatham Rise.

7.2.1 Fault-slip Analysis in North-Western Banks Peninsula

To constrain the tectonic boundary conditions of the Lyttelton Volcanics, fault kinematic data have been collected from two known faults in the north-western part of Banks Peninsula, from inferred fault to the south of those two faults, and from around Lyttelton Harbour (Figure 7.4).

Fault Zones

In general, the fault zones in the volcanic rocks of northern Banks Peninsula are not well exposed. They are characterized by anatomising zones of gouge, cataclasite, breccia and hematite-clay-coated fractured rock (Figure 7.4). In the centres of the fault zones grain-size reduction commonly produced gouge zone; extremely fine-grained, clayey layers of non-cohesive rock. Cataclasite is usually a cohesive fault rock in the study area. Border fault segments are zones of interlinked sets of gouge zones with minor step-over faults and small intervening blocks. Subsidiary faults are mainly made up of cataclasite, have relatively thin gouge zones (<~2 m) and hardly any intervening blocks of country rock. The subsidiary faults show a relatively simple propagation from non-fractured country rock into severely fractured cataclasite and thin gouge zones in their centres.

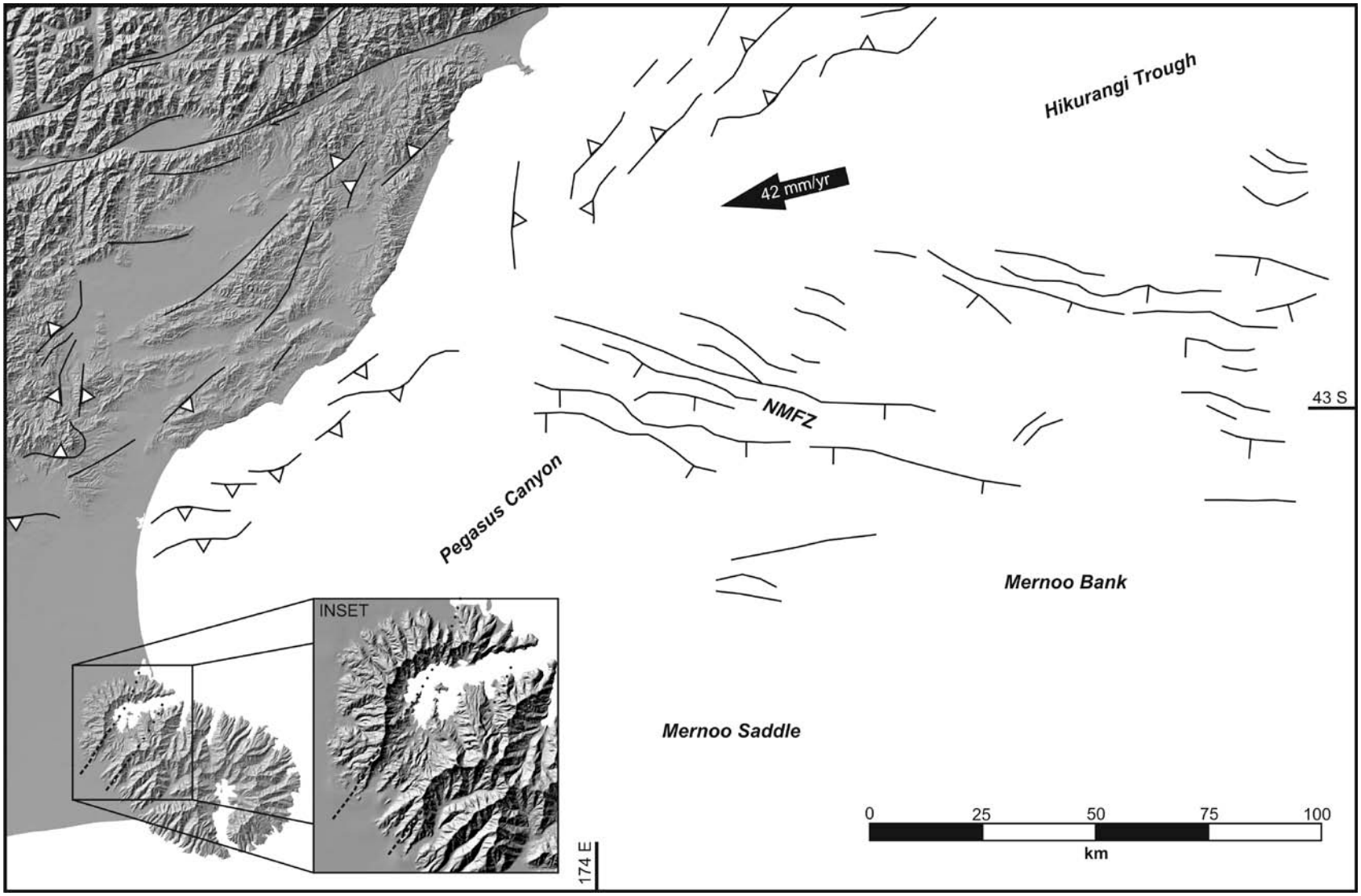

Figure 7.2. Faults systems of onshore and offshore North Canterbury (modified from Barnes, 1994). Of note is the offshore North Mernoo Fault Zone (NMFZ) at a similar trend to Banks Peninsula. Inset: hypothetical faults (dotted) on Banks Peninsula, from Sewell et al (1992). Note the parallel relationship between the bounding edges of Gebbies Pass.

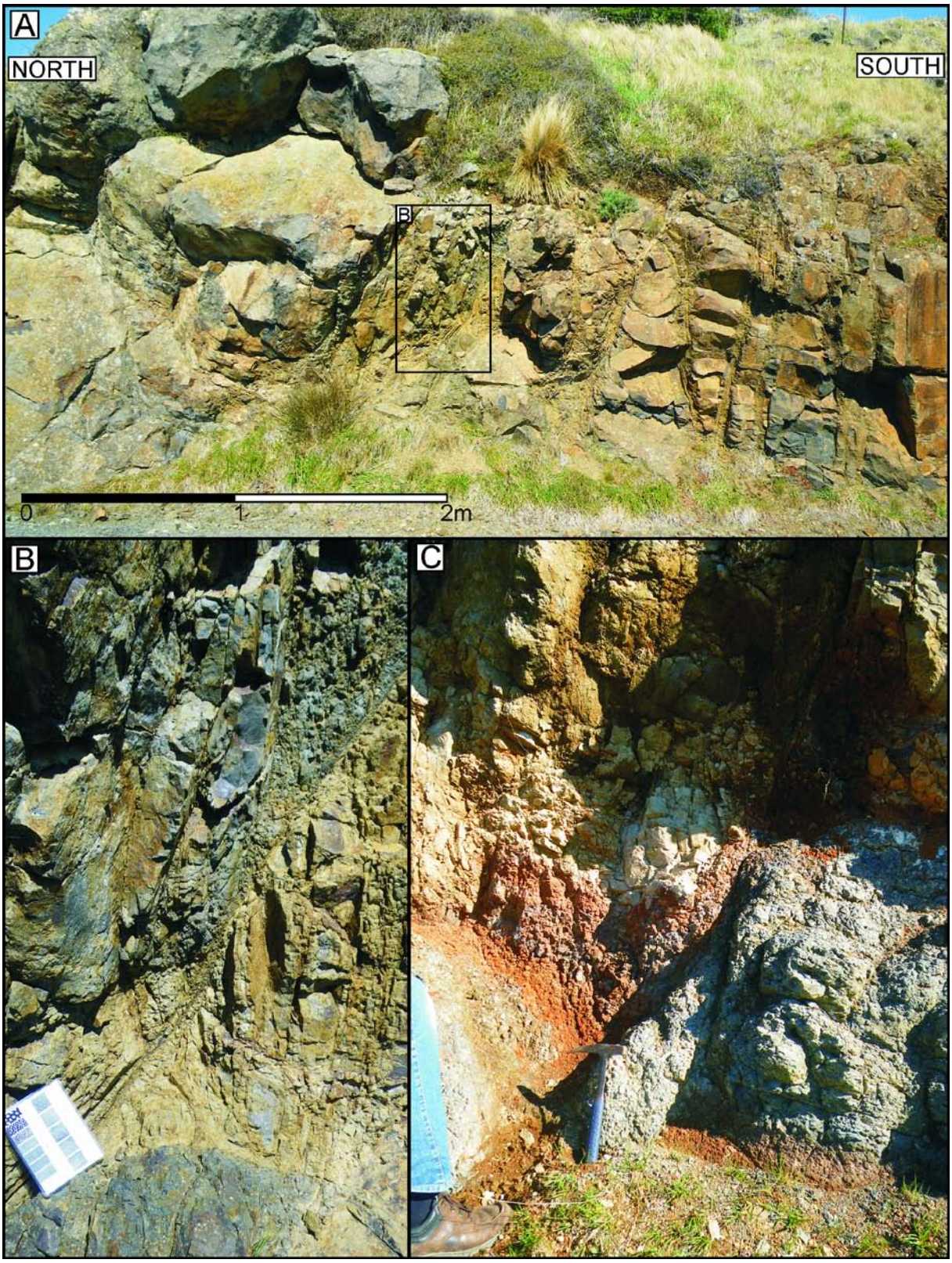

Figure 7.3. Photographs of fault zones along the Gebbies Pass Fault. (a) Several meso-scale fault zones cutting through Lyttelton volcanics near Bridle pass, Summit Road of Port Hills. Crosscutting trachyte dike at the left is hardly faulted. (b) Close-up of the fault zone shown in (a) showing pronounced cataclasis of basalt in fault zone. Note development of near-vertical secondary Riedel shears associated with normal faulting. (c) Small-scale normal faulting in basalt near Coopers Knob, Summit Road, Port Hills.

Fault-slip Analysis

To evaluate the kinematics of a fault, the orientation of primary and secondary fault planes, trend and plunge of striations and the sense of relative displacement on these planes have been mapped. A simple graphical method has been used to determine principal strain axes (program 'Fault Kinematics' written by R. Allmendinger). This method graphically constructs the principal incremental shortening and extension axes for a given population of faults. Each pair of axes lies in the movement plane of the fault (a plane perpendicular to the fault plane that contains the unit vector parallel to the direction of accumulated slip, and the normal vector to the fault plane). Furthermore, each pair of axes makes angles of 45° with each of the vectors, (Figure 7.4, inset). In order to distinguish between the shortening and extension axes it is necessary to have information on the sense of slip. Bingham distribution statistics for axial data have been used to optimize clusters of kinematic axes of a fault array (Mardia, 1972). The linked Bingham distribution is equivalent to an un-weighted moment tensor summation (a moment tensor sum in which all faults are weighted equally). With a perfect concentration of shortening and extension axes in plane strain, the positive (corresponding to extension) and negative (corresponding to shortening) eigen values will be 0.5 and -0.5 respectively with the intermediate axis of 0.

The fault zones consist of heterogeneous mesoscale zones fractured into arrays of blocks whose surfaces have a wide distribution of orientations. Individual blocks are separated by thin, slickensided surfaces with fibres and striae, which make these fault zones suitable for brittle strain analysis. The mesoscale faults occur in the vicinity of the main fault zones and increase in number towards these faults. This spatial relationship is considered to imply a genetic connection of the mesoscale faults with the mapped main fault zones. Therefore, a fault-slip analysis of the mesoscale faults allows inferring the kinematics of the main faults.

The direction and sense of shear on these surfaces have been deduced from the orientation of fibres, striae and fractures associated with the fault (Hancock, 1985). Fibre and striae orientations on slickensides from the subsidiary faults are usually simple, consistent, and are readily interpretable with the geometry of the mapped faults at a regional scale.

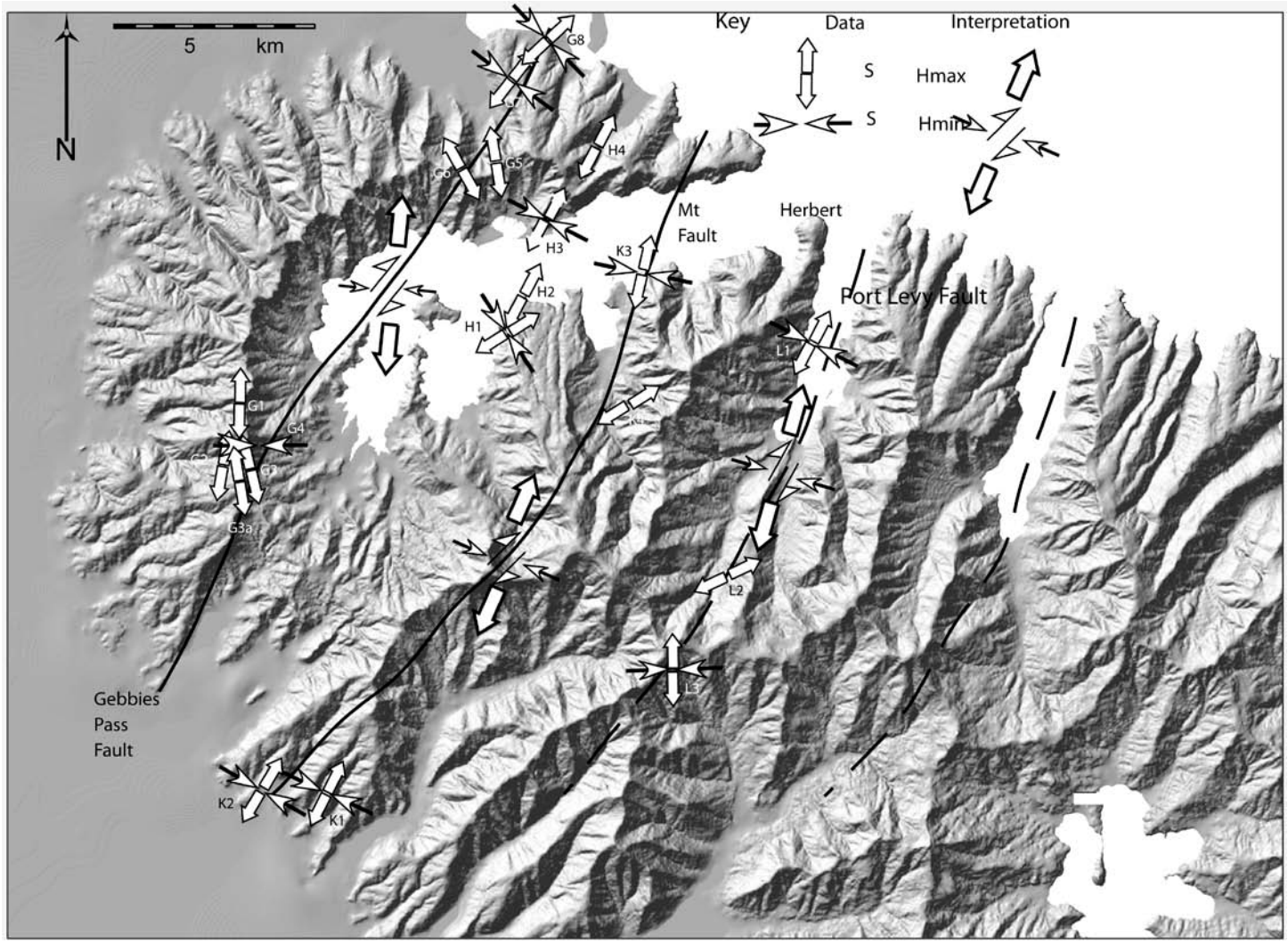

Figure 7.3. Digital elevation model of the northern part of Banks Peninsula showing the major faults and the maximum horizontal extension direction (SHmax) inferred from the fault slip data shown in Figs. c-f. In those cases where the maximum shortening direction is near the horizontal, the shortening direction has been projected into the horizontal and is also shown (SHmin). Note that both, the maximum extension and the shortening directions have been projected into the horizontal and therefore do not coincide with the strain axes shown in figures 7.4-7.7. Also shown is the interpretation of the kinematics of the major faults along which the data have been collected.

Fault-slip data

The fault-slip data from outcrops along the Gebbies Pass Fault are dominated by E-W striking normal faults (Figure 7.5) resulting from E-W extension. Some data sets from the Gebbies Pass Fault show a strong E-W shortening component (Figure 7.5e). In addition to the normal and reverse faults, N-S striking sinistral strike-slip faults occur. Overall, the fault-slip data from mesoscale faults yielded fairly consistent results, which are compatible with dextral oblique-slip normal faulting along the NE-striking Gebbies Pass Fault.

The data from the Mt Herbert Fault have a less pronounced normal faulting component than the data from the Gebbies Pass Fault (Figure 7.6). Outcrop K1 shows a dominant set of E-W striking normal faults; however, there are also two E-W striking reverse faults (Figure 7.6a). K2 shows also mixture of normal, oblique and strike-slip faulting (Figure 7.6b). The relatively large data set from outcrop K3 shows a similar mixture of faults. However, the E-W striking faults are mainly normal and oblique normal slip, whereas the N to NE striking faults are reverse slip. K4 shows a dominance of oblique normal faults but also oblique reverse faults. The extension directions of the various data set are relatively consistent and trend NE, with SE trending shortening axes. Overall, the data suggest dextral strike-slip faulting along the Mt. Herbert Fault. Compared to the Gebbies Pass Fault, the Mt Herbert Fault appears to have a less pronounced oblique normal faulting component.

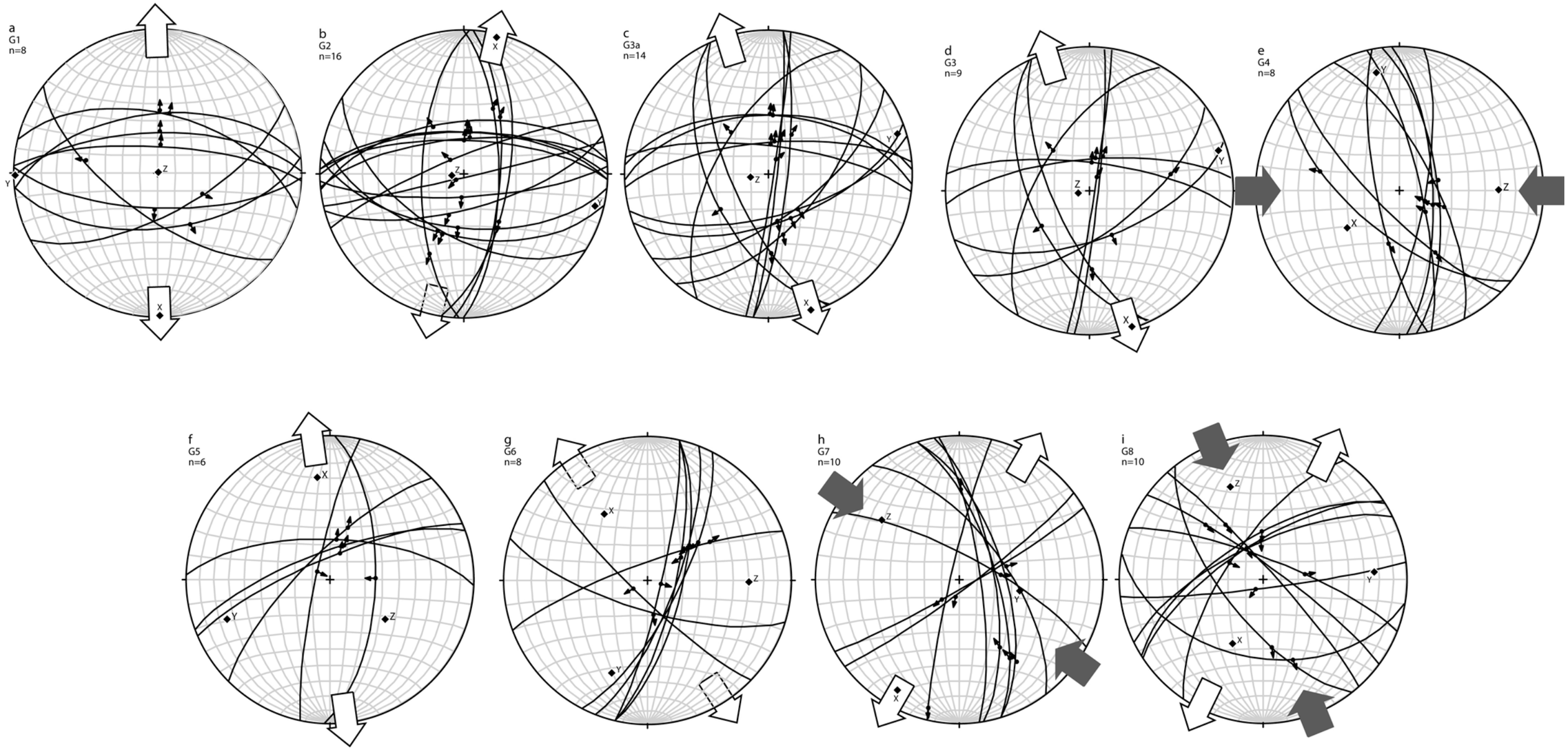

Figure 7.5. Fault-slip data from the Gebbies Pass Fault. The diagrams show great circles of fault plane and the projected trace of the associated slickenside lineation in a lower-hemisphere equal-area projection. The principal strain axes (X>Y>Z) are shown. The deduced extension directions (X) are indicated by white arrows, the shortening directions (Z) by grey arrows. The outcrop number is indicated on the upper left and can be located in Figure 7.3. The inset in the upper right shows a graphical construction of the principal incremental shortening and extension axes for a given fault; the movement plane of the fault is perpendicular to the fault plane and contains the unit vector parallel to the direction of accumulated slip and the normal vector to the fault plane; the shortening and extension axes make angles of 45° with the fault plane. Fault station G1 through G4 from outcrop ENE Gebbies Pass; outcrops G5 and G6 are from the central portion of the Gebbies Pass Fault and outcrops G7… from the northern part of the fault in the Heathcote Valley. (a) Outcrop G1 is dominated by E-W striking normal faults; consequently the calculated extension direction is N-S. (b) G2 contains more data but shows similar characteristics as G1; in addition a few N-S striking sinistral strike-slip faults occur. (c) Outcrop G3a is again similar to G2. (d) G3 has a limited data set that again shows N-S extension. (e) Outcrop 4 shows a number of N-S striking reverse faults and a few NW-striking oblique-slip normal faults. The fault pattern resulted from E-W shortening; there is minor N-S extension in the Y direction of the strain ellipsoid; the maximum extension direction X is sub-vertical. (f) Outcrop G5 shows a mixture of E-W striking normal faults and N-S striking reverse faults. (g) Outcrop G6 see also Figure 7.2 (a and b) depicts a more complicated data set with E-W striking normal and oblique-normal faults, as well as NNE striking oblique reverse faults; one NNE striking fault is a normal fault. (h) Outcrop H show a number of NNW striking faults, which either have reverse slip kinematics (NE plunging striations) or normal kinematic (ENE plunging striations). In addition strike-slip faults and a NE striking normal fault occurs. (i) G8 shows also a mix of reverse, normal and strike-slip faults that overall combine to a similar kinematic pattern of shortening and extension axes as G7.

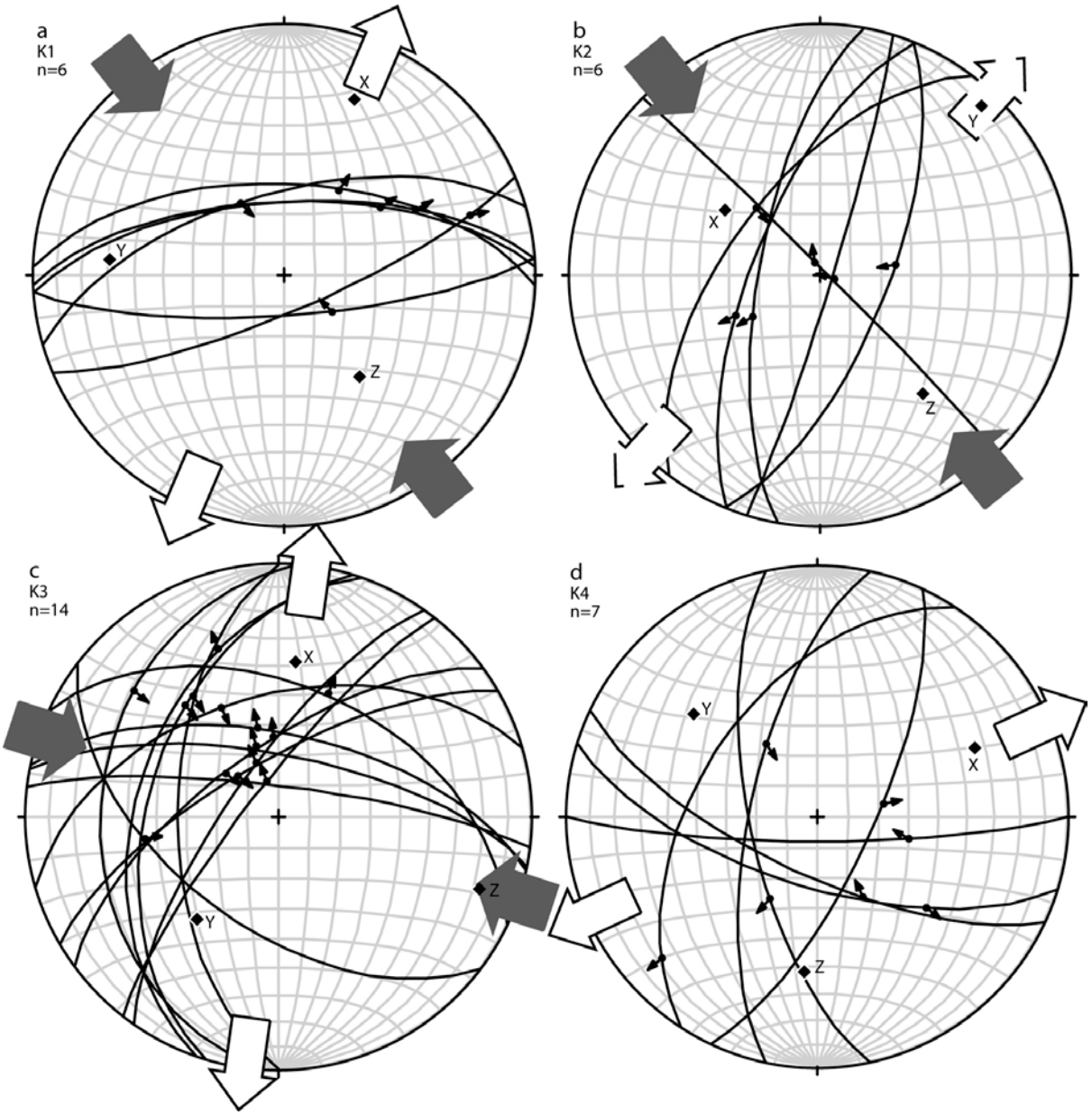

Figure 7.6. Fault-slip data from the Mt Herbert Fault. (a) Outcrop K1 is dominated by E-W striking dextral oblique-normal faults and two E-W striking dextral oblique-reverse faults. The fault pattern is compatible with dextral strike-slip faulting along the NE-striking Mt Herbert Fault (Fig. B) and a NNE trending extension and a NW- trending shortening axis. (b) K2 shows a rather messy data set with three NE-striking reverse faults and two NE-striking oblique normal faults; in addition one NW striking sinistral strike-slip fault occurs. The fault pattern resulted from NW trending shortening; the X and Y axes have very similar positive eigen values indicating a flattening strain type with two extension directions. (c) Outcrop K3 has a larger data set than K2 but the data are similar indicating WNW directed shortening and NNE extension. (d) K4 has a limited data set with oblique reverse and oblique normal faults that resulted ENE extension.

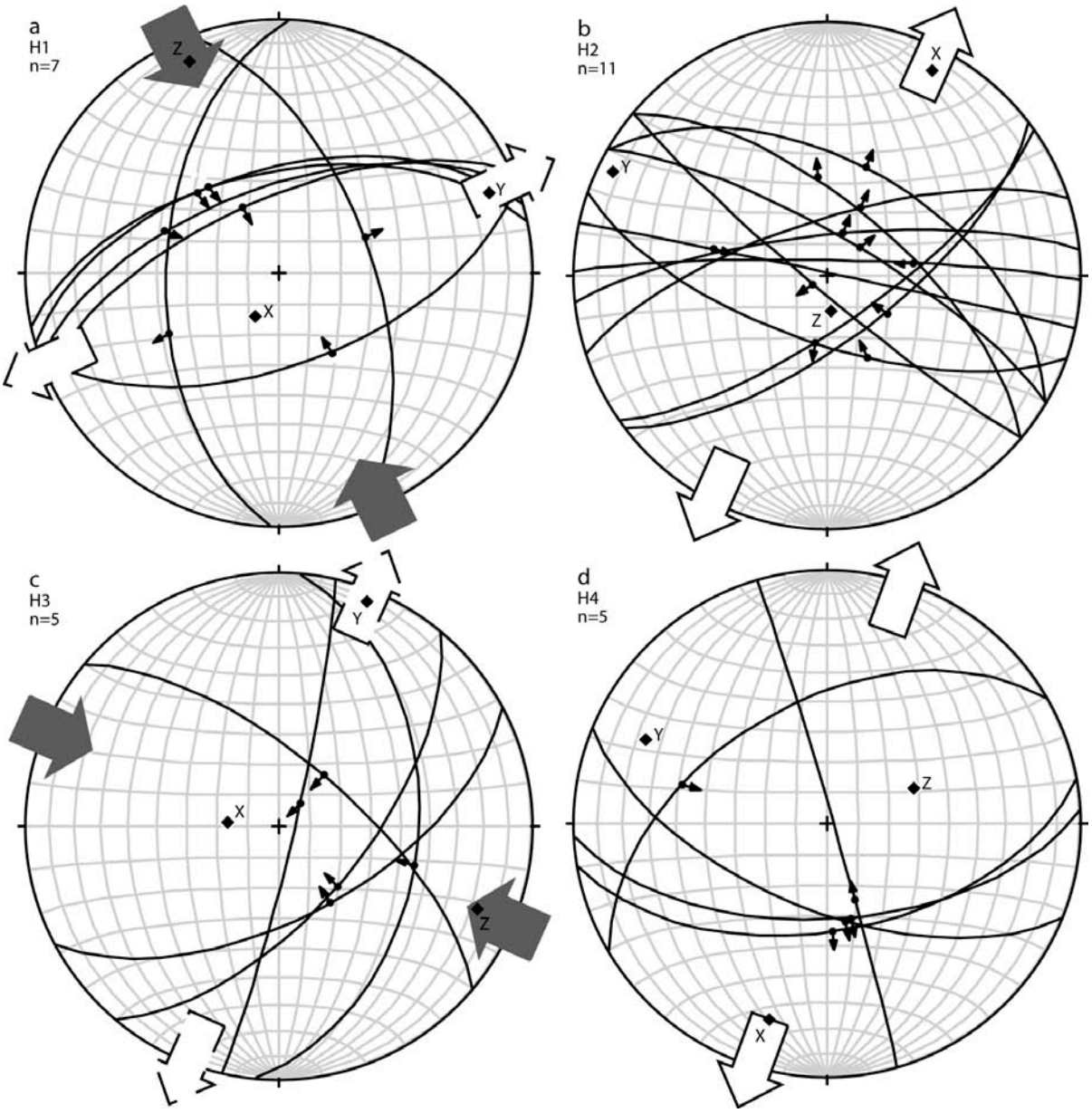

Figure 7.7. Fault-slip data from the Lyttelton Harbour region. (a) Outcrop H1 is dominated by ENE striking reverse faults; in addition two N-S striking normal faults occur. The NW trending shortening axis and the near-vertical extension axis for this fault pattern is well defined. The intermediate, Y, axis is oriented ENE. (b) H2 shows a straightforward pattern of normal and oblique normal faults that strike about E-W. Consequently the NNE trending extension direction is well constrained. (c) Outcrop H3 has three reverse faults, one normal faults and one NNE striking sinistral normal fault. The fault pattern basically resulted from WNW shortening and near vertical extension. (d) H4 has a limited data set that resembles H2 with a well-defined NNE oriented extension direction.

The fault-slip data from the Lyttelton Harbour area (Figure 7.7), between the Gebbies Pass and Mt Herbert, also show patterns that are compatible with dextral oblique slip faulting along both faults. Data sets H2 and H4 show a well-defined NNE oriented extension direction resulting from a pronounced component of normal faulting (Figure 7.7b, d). The other two data sets are more mixed and show a strong reverse faulting component resulting from NW to WNW oriented shortening. Taken together, the data suggest a mixture between strike-slip faulting and almost pure normal faulting.

Finally, some fault-slip data was collected from the Port Levy - Kaitorete Spit area (Figure 7.8), that are related to an assumed NE striking fault (Figure 7.3). The three data sets collected along the assumed fault are compatible with the data from the Gebbies Pass and Mt Herbert fault and thus would support a dextral strike-slip kinematics along the NE striking faults in northern Banks Peninsula.

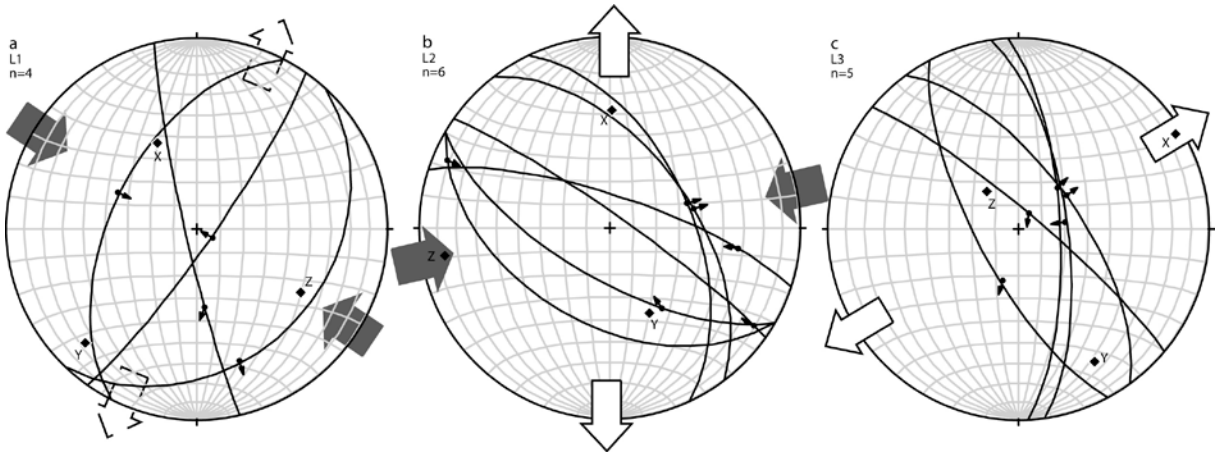

Figure 7.8. Fault-slip data from the supposed Port Levy – Kaitorete Spit Fault. (a) L1 shows two NE striking reverse faults and two oblique normal faults. The strain field is flattening with extension in X and Y; the well-defined shortening axis is NW trending. (b) K2 shows a heterogeneous data set with two NW striking dextral strike-slip faults, two NNW striking normal faults and two WNW striking oblique reverse faults. The pattern resulted from E-W shortening and N-S extension. (c) Outcrop K3 has mainly normal and oblique normal faults resulting from NE extension.

7.2.2. Dextral pull-apart model for Lyttelton Volcano

Figure 7.9 summaries the inferred tectonic model. The fault-slip data indicate a dextral strike-slip faulting along the NNE striking faults in northern Banks Peninsula. The Gebbies Pass Fault shows a relatively strong N-S extension component associated with dextral strike slip. Between the dextral Gebbies Pass and Mt Herbert faults there are segments, in

Diamond Harbour for instance, which are characterized by almost pure normal faulting due to NNE oriented extension.

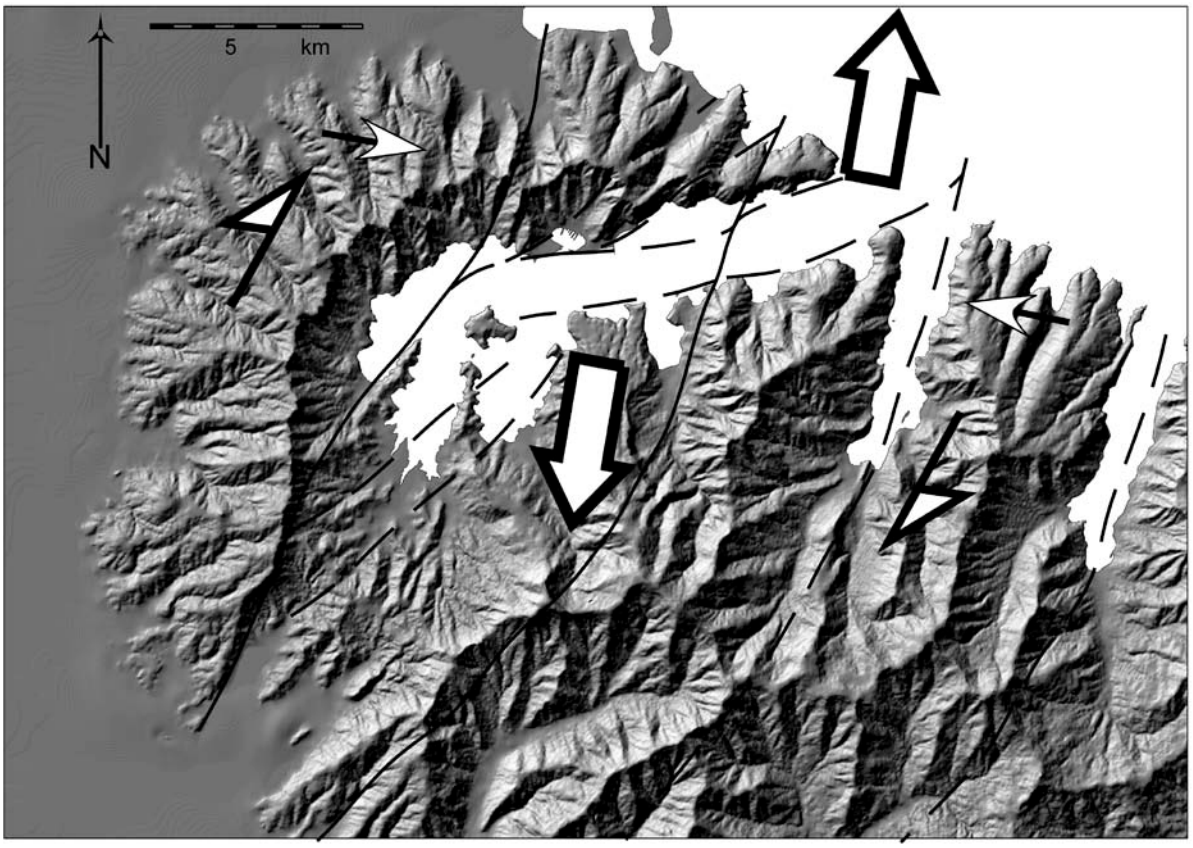

Figure 7.9. Envisaged releasing bend model for the formation of Lyttelton Harbour. The E-W oriented depocenter is interpreted as a result of a complex dextral releasing bend structure between the NNE striking dextral strike-slip to oblique slip faults.

It is proposed that, when combined the fault-slip data set suggests that Lyttelton Harbour represents a dextral pull-apart basin (Figure 7.9), with a number of releasing bend faults in the Lyttelton Harbour area, which transfer the extensional strain between the major dextral strike-slip faults.

Toprak (1998) investigated the vent distribution and its relation to regional tectonics in the Cappadocian Volcanic Province (CVP), of Turkey. Two fault systems exist in the province. One system (Miocene-Quaternary Tuz-gölü–Ecemis system) is oblique, whereas the other (late Miocene–Pliocene CVP system) is parallel to the long axis of the CVP. The polygenetic volcanoes are aligned parallel to the second system but concentrate around the major faults of the first system (Figure 7.10).

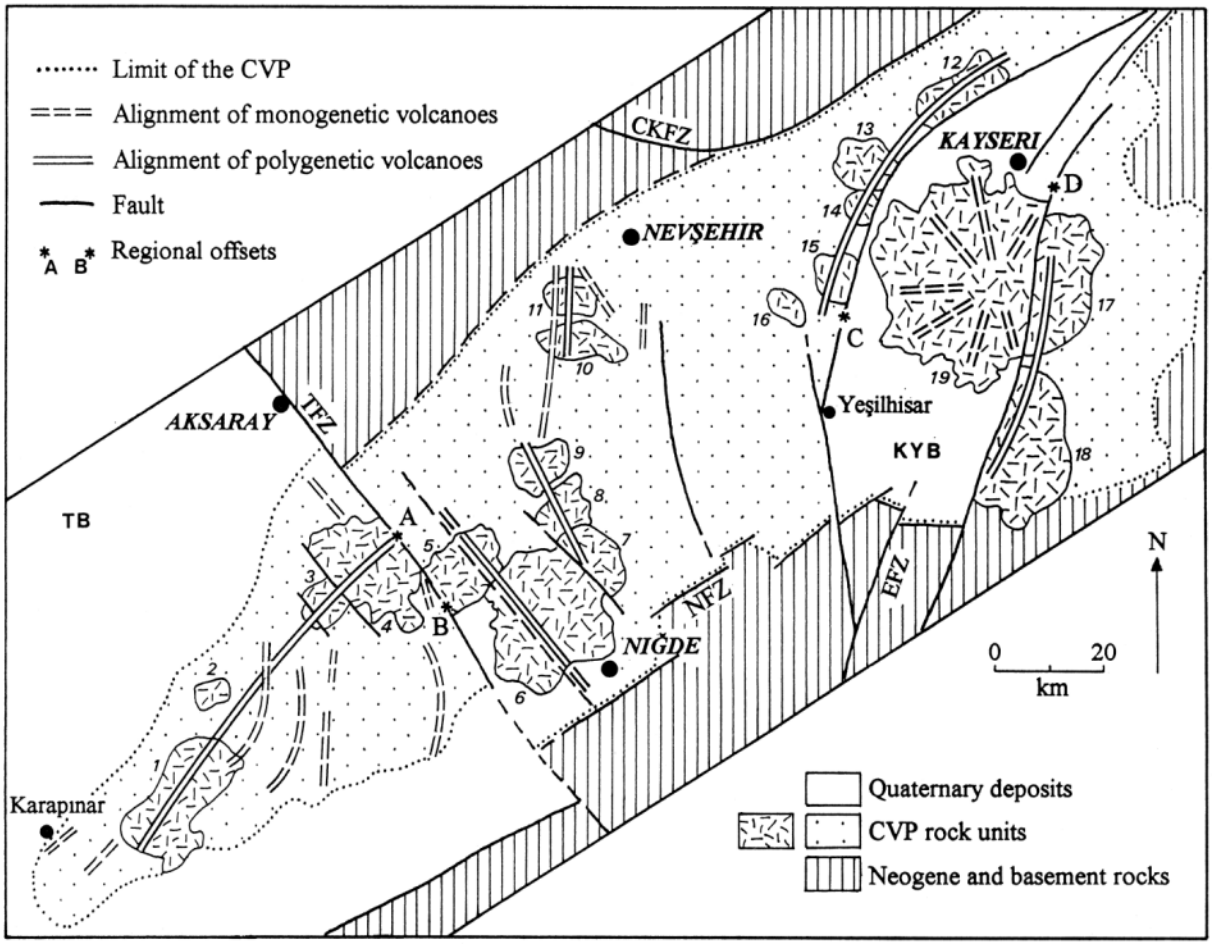

Figure 7.10. Alignment of polygenetic and monogenetic volcanoes detected within the CVP. A–B and C–D correspond to right-lateral and left-lateral offsets along the Tuzgo¨lu¨ and Ecemis faults, respectively. TB: Tuzgölü basin, KYB: Kayseri–Yesilhisar pull-apart basin.

The larger volcanic entity of Toprak (1998) study of the CVP is situated on the boundaries of the Kayseri-Yesilhisar pull-apart basin, and in some ways structurally similar to the proposed pull-apart model of Lyttelton Volcano. Lavallee et al. (2009) investigated the structural control on volcanism in southern Peru, concluding that volcanic centres lie at the intersection of active major strike-slip faults, cross cutting an older graben structure. It was also found in this study that the onset volcanism coincided with a change in tectonic regime, an aspect similar to the onset of Banks Peninsula's volcanism. Lavallee et al. (2009) further concluded that as magma ascended it deviated to local dilation zones associated with active releasing bends, an aspect intrinsically linked in the focus of vent sites at the intersection of cross cutting / releasing bend faults of Lyttelton Volcano (Figure 7.11), and also encountered in the Cofre de Perote-Pico de Orizaba volcanic chain (Conchas-Dimas et al., 2005).

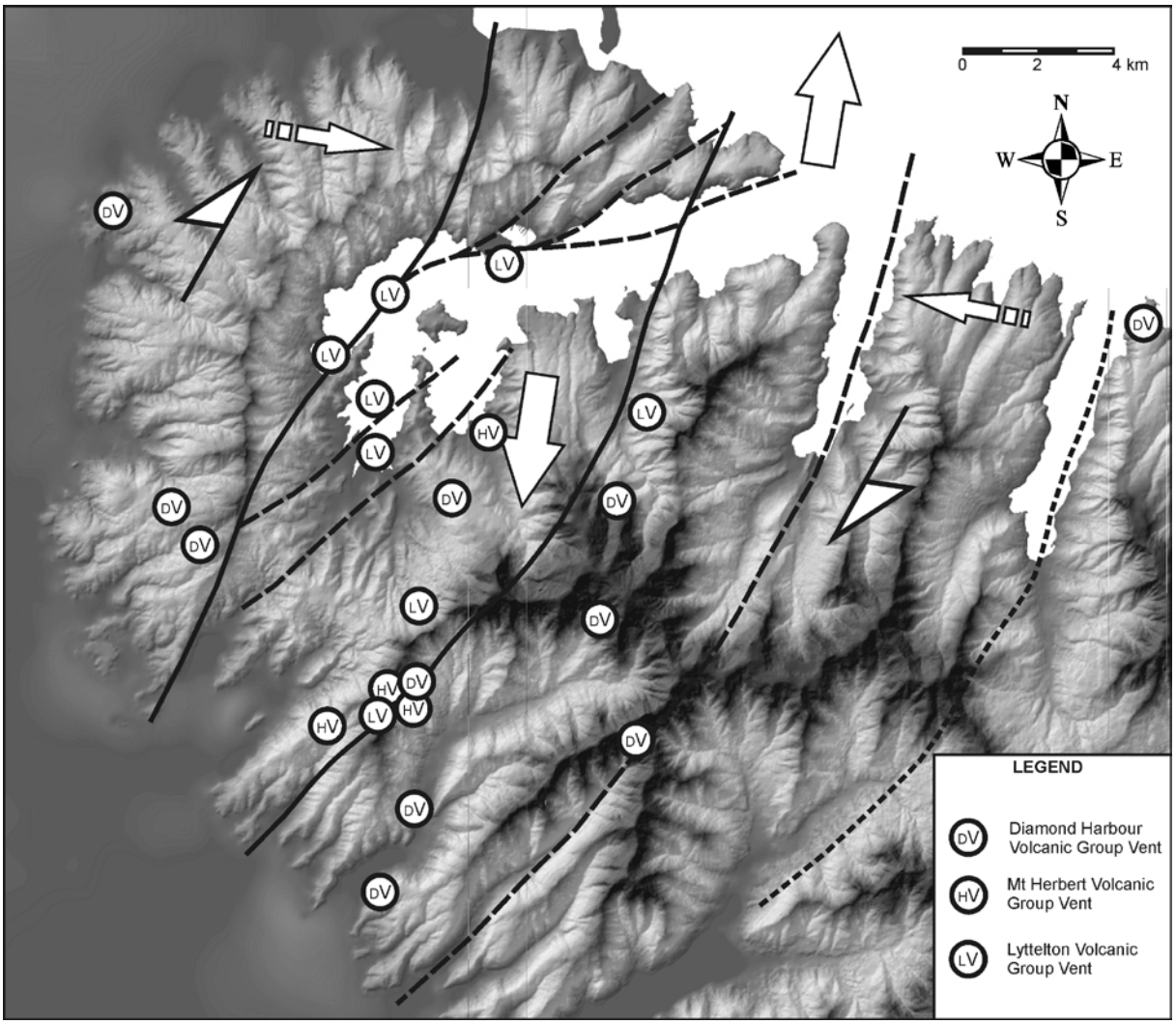

Figure 7.11. Releasing bend model of Lyttelton Volcano, oblique fault system of Banks Peninsula, and the relationship with eruptive sites of the Lyttelton, Mt Herbert and Diamond Harbour Volcanic Groups.

The Aeolian Islands are comprised of various volcanic complexes, Vulcano, Liapari and Salina (Figure 7.12). The primary faulting regime in this region is strike-slip, with movements along the fault systems in the Vulcano-Lipari-Salina region forming isolated pull-apart basins (Figure 7.12c), with the renewal of associated volcanic activity (Gioncada et al., 2003).

Links between graben and horsts and volcanism has also been detailed at the Las Sierras-Masaya volcanic complex, Nicaragua (Girard and Wyk de Vries, 2005) and Mt Etna, Italy (Patanè et al., 2006). Girard and Wyk de Vries (2005) speculated that the Managua graben and Las Sierras-Masaya volcanic complex is tectonically linked, with the graben developed in response to the regional stress field induce by the intrusive complex. This results in the formation of rhombic fault structures about the volcanic complex forming, a pull apart basin.

In the modelling of the formation of pull-apart basins (Girard and Wyk de Vries, 2005), both ductile intrusion and tectonic motion are required, highlighting the importance of tectonic regimes and faulting relationships in the development of Lyttelton Volcano.

A horst structure is hypothesised to exist and control eruptive centre sites on Mt Etna (Patanè et al., 2006). The horst aligns with the regional tectonic regime (NE) with cross cutting fractures (NE-SW and NW-SE), with the eruptive centres of Mt Etna occurring at the intersection of these. As the horst uplifted (north-eastward) volcanic activity migrated westward (Patanè et al., 2006).

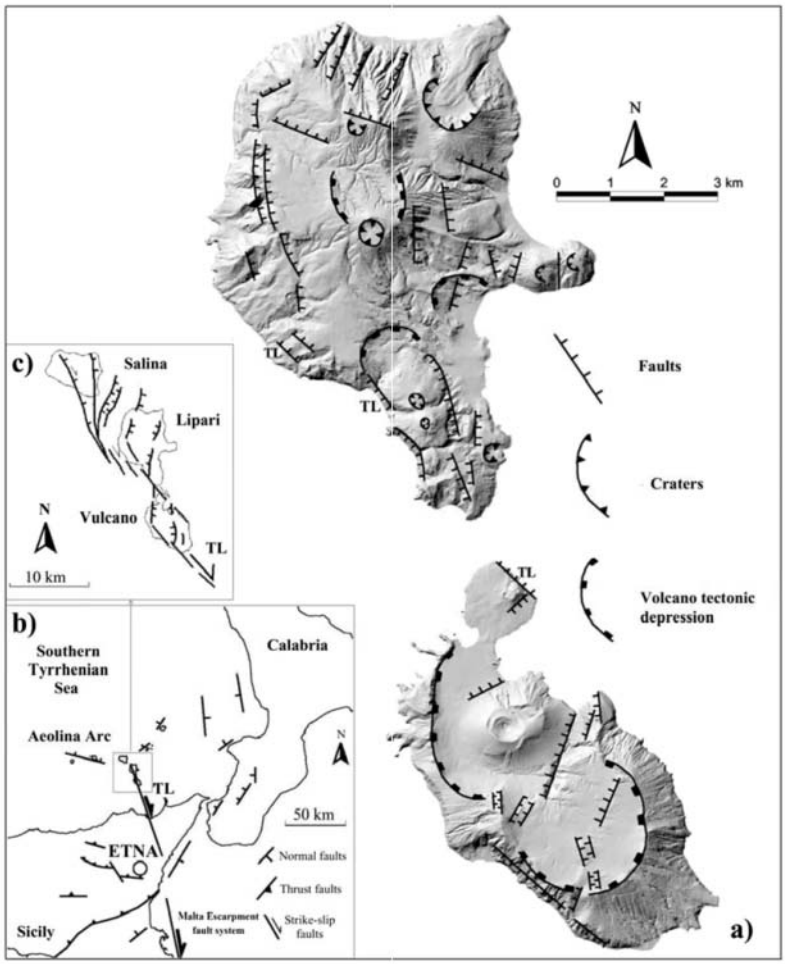

Figure 7.12. Aeolian Islands, Vulcano and Lipari, and Salina with key surface structures and interpretations (from Gioncada et al., 2003). b) Structural setting of the Aeolian arc and relationship to Mt Etna. c) Interpretation of the fault systems in the Vulcano-Liparu-Salina area. Of importance is the interpreted pull-apart basin structure (Mazzouli et al., 1995; Ventura et al., 1999).

A significant consideration in understanding the structure of the region is the elongate form of Banks Peninsula (Figure 7.2). The recognised faulting system on Banks Peninsula (Gebbies Pass) occurs along a NE – SW trend. These faults are oblique to the trend of the elongate form of Banks Peninsula, and it is here suggested that a further, possibly older, fault trend on Banks Peninsula exists along a NW –SE trend, also producing a control on eruptive centres (Figure 7.11) as observed at the CVP. This older fault system or structural control is aligned along the Chatham Rise, and at a similar trend of the extensional North Mernoo Fault Zone (NMFZ; Figure 7.2). The NMFZ developed, 8 - 6 Ma, and is related to the encroachment of the incoming Chatham Rise against the evolving, transpressive plate boundary zone. Recent studies (Sutherland et al., 2000) have proposed the Alpine Fault / transpressive plate boundary formed 25Ma, indicating structural control at this earlier age.

A broad structural control on location on eruptive sites and volcano growth is proposed by Lenat et al. (2009) study of Reunion Volcano, where two major transform faults bound the regions of the mantle plume (Figure 7.13). Here the transform faults cause decoupling deformation of the two sides, trapping the upward flow of plume material in this fault bounded zone (Sleep, 2002; Lenat et al., 2009). A similar fault / graben control directed volcanism at the Tongariro Volcanic Complex (Cassidy et al., 2009).

The age of fault activity is not directly constrained. It is recognised that fault structures affect the volcanic rocks (Figure 7.3) displacing lavas, yet the recognised faults are not prominent on aerial photographs and are, at least in part, masked by Lyttelton volcanic flows. These relationships strongly suggest that faulting was largely concurrent with the volcanic activity and has probably controlled the geometry of the volcanic vents.

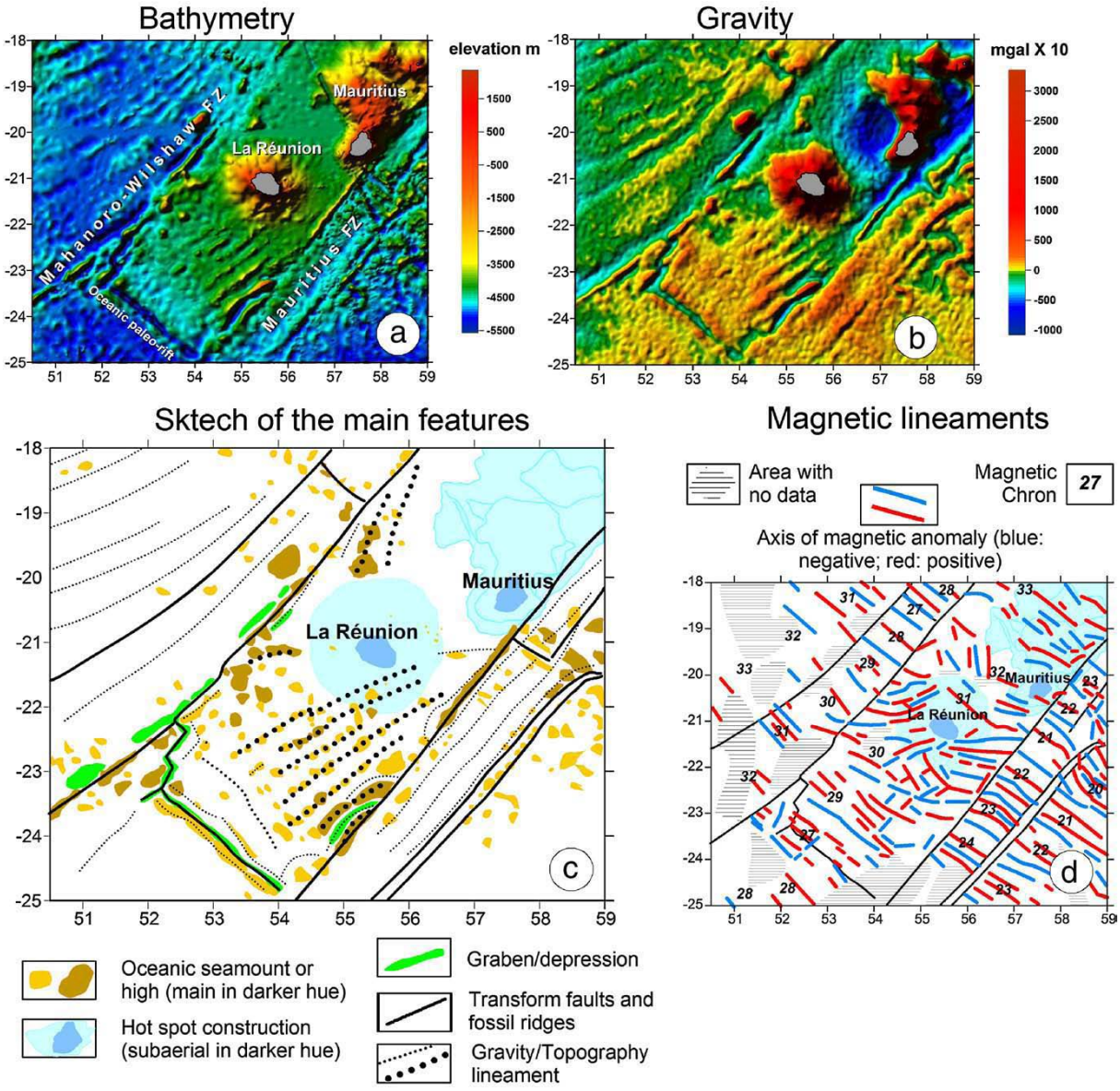

Figure 7.13. Lenat et al., (2009) transform fault boundaries of Reunion Volcano, producing an isolated block, in which mantle plume upwelling is confined to Reunion and Mauritius volcanoes are depicted in blue, while surrounding oceanic seamounts (submarine volcanoes) are in yellow and browns.

7.3.1. Topographic Influence

Topography has a distinct control on the formation of vent / centre location. Pinel and Jaupart (2004) state that the "growth of a volcanic edifice modifies the stress field at shallow depth. Magma rising vertically from a deep source region beneath the focal area may stall beneath the edifice or feed a laterally extensive dyke. Within a vertical magma column, magma overpressure reaches a maximum at some depth, which depends on buoyancy, edifice size, and density stratification.... Magma storage proceeds until differentiation leads to more evolved and buoyant magmas. Depending on the edifice size, evolved magmas may either propagate horizontally or rise vertically to feed summit eruptions." Walker (1992)

produced a schematic model (Figure 7.14) of asymmetric growth of Kilauea, Hawaii, produced through the varying position of the active rift zone (eruptive vent), with the active rift controlled by the concentration of extensional forces on the actively growing side.

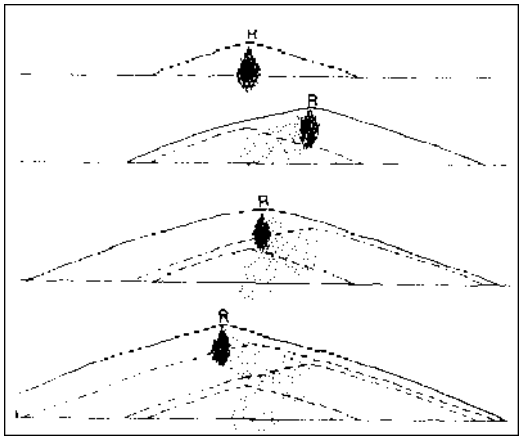

Figure 7.14. Asymmetric growth and development of a major volcano (schematically in cross section). The active rift zone (R) varies in position due to extensional stresses in the growing side (from Walker, 1992).

Marti and Geyer (2009) investigated the control of central vs. flank eruptions at Teide–Pico Viejo twin strato-volcanoes of Tenerife, Canary Islands (Figure 7.15). The morphology and size of the volcanic edifices have been changing over the last 35 ka, but has not affected the location of new eruptions (Figure 7.15). The assumed control on the pathway that magma will follow is exerted by the stress field distribution around the chamber, which is a function of the shape of the chamber. These authors have hypothesised that the location of each new eruption is preceded by the modification of the existing magma chamber (or the emplacement of a new batch of magma) that does not necessarily matches the structure of the previous one, resulting in the formation of multiple shallow reservoirs containing eruptible magma. Extensional stress fields then have a significant role in determining the position of the feeder dykes (Figure 7.15).

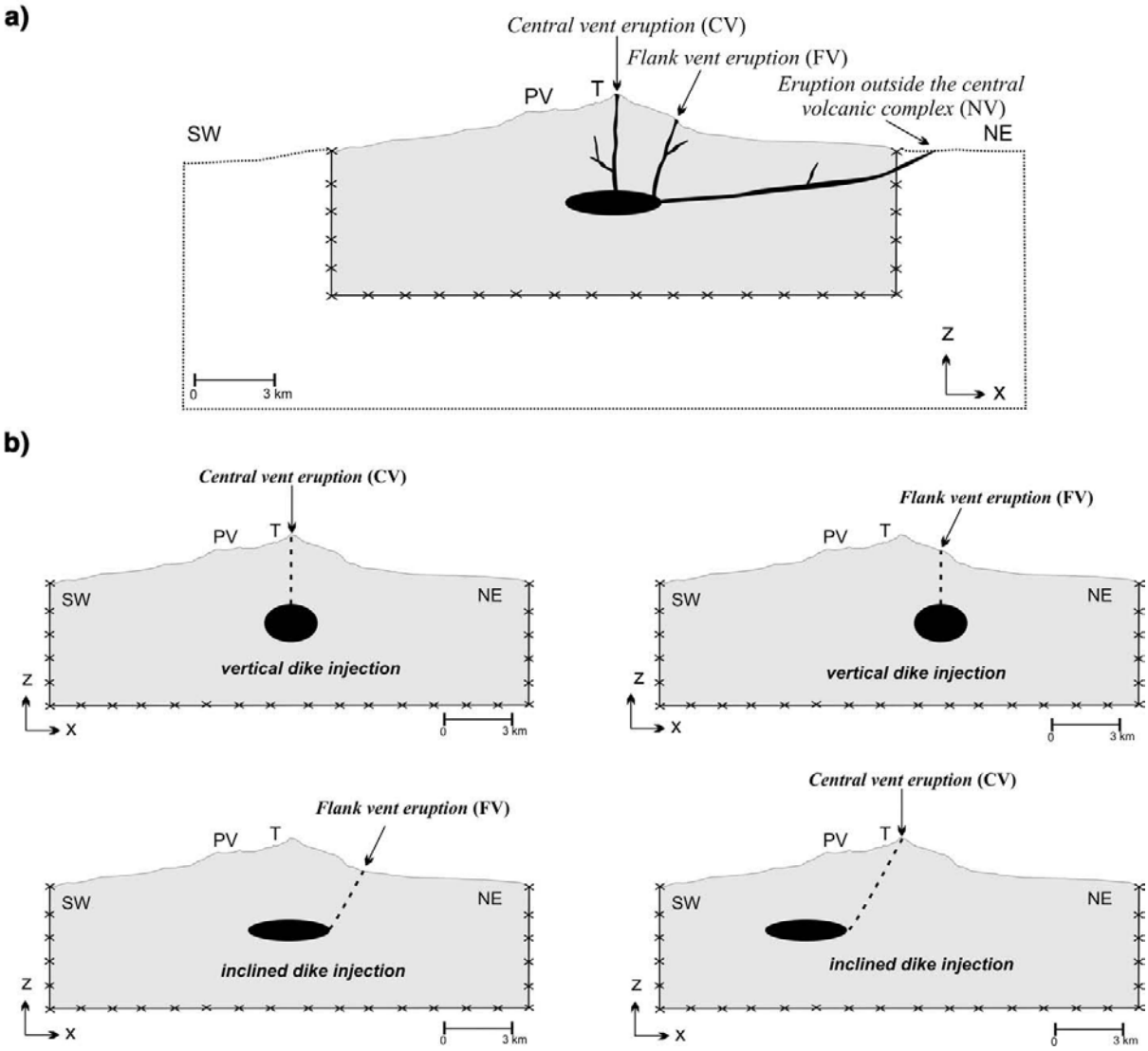

Figure 7.15. Marti and Geyer (2009) theoretical magma chamber location stress fields relative to Tiede crater, and the resulting eruptive site. a) Central vent eruption (CV), flank vent eruption (FV) and an eruption far from the central volcanic complex (NV). (b) Four different locations of the same magma chamber relative to the Teide crater, the resulting stress field configurations may lead to central vent (CV) or flank vent eruption (FV).

As a volcanic cone develops it will grow to a steady state, beyond which magma cannot propagate to the surface (Pinel and Jaupart, 2000), resulting in intrusive events (on Lyttelton Volcano observed as hawaiite and / or trachyte dykes and sills). As magma propagates into zones of inherent weakness, one may become a predominant pathway, resulting in the inception of a new eruptive centre (Marti and Geyer, 2009). This will occur in an un-buttressed section of the volcanic structure, where planes of weakness will be prevalent (Walker, 1992). The resulting eruptive centre location / migration will develop due to the volcanic structure limiting and focusing magma.

7.3.2.Dykes

In the upper levels (2-4 km) of a volcanic complex basaltic (mainly tholeiites) dykes are laterally injected as blade-like intrusions from shallow magma reservoirs beneath the summit (Rubin and Pollard, 1987; Dieterich, 1988; Ryan, 1988; Parfitt, 1991; Head and Wilson, 1992; Delaney et al., 1993). Radial dyke swarms have been described as forming due to the injection of magma through inherent weaknesses within the volcano, controlled by local gravitational forces (Shelley, 1992; Carrigan, 2000), or through the development of radial fissures perpendicular to the walls of an expanding magma chamber (Ode, 1957). In the development of an eruptive package an individual stress regime will be produced either through establishment of a shallow level magma chamber or newly developed gravitational relaxation, resulting in radial intrusion of a dyke swarm, reflected on Lyttelton Volcano through eruptive packages having a defined dyke swarm.

In the development of radial dyke swarms it is proposed that the intrusion of dykes into a volcanic cone would strengthen and buttress an edifice through infilling fractures. As discussed by Walker (1999) intrusions put a cone into tension, with only gas-rich magma batches able to propagate into the upper parts of the cone. On Lyttelton Volcano this is reflected by the distinct radial dyke swarms, with little intrusion into the pre-existing volcanic structure. It is hypothesised that this relates to the underlying structure being more stable with earlier dyking 'locking' the structure, with new fracturing occurring predominantly in under the newly developed overlying eruptive package.

A similar situation has been recognised at La Gomera (Spain), Canary Islands (Ancochea et al., 2008), where the circular shape of La Gomera is due to the progressive growth of four centres as the magmatic focus slowly migrates. It is considered the same occurred at Lyttelton Volcano, with each eruptive package erupted and then terminated with a radial dyke swarm 'locking' the structure, with the next phase of activity erupting in isolation from previous packages.

Dykes on the Mt Evans Cone have variable orientations, not all trending towards an eruptive centre. Three factors can be established to explain these:

1) All dykes that outcrop in this region have been assumed to be intrusions of Lyttelton Volcanics. This may not be the case as later dykes may relate to the Mt Herbert Volcanic Group; Hampton (2005) observed basaltic dykes intruding the Orton Bradley Formation. This later intrusive regime would have been intruded from a centre in the upper reaches of Charteris Bay.

2) The zone of dyke alignment on the northern flanks of the Mt Evans Cone could reflect the topographic influence / structural control on stress regimes on dyking. With the resulting stress conditions producing near parallel dyking, like that observed at the edges of the Valle del Bove, Mt Etna (McGuire, 1982), and Stromboli's collapsed crater region (Tibaldi, 2001).

3) This spread of dykes could reflect a rift zone, at a similar orientation to the axis of Lyttelton Harbour.

In Walter et al (2006) an investigation into gravitational spreading and rift zone formation proposed two main directions of rift development for overlapping volcanoes (Figure 7.16). These two directions are dependent on the spreading of the cones involved; if both cones are spreading (i.e. actively growing) then a rift will develop perpendicular to the boundary between cones, if only one cone is spreading then the rift zone will parallel the boundary between both volcanoes, as is the situation observed within the dykes nearer to Lyttelton Harbour.

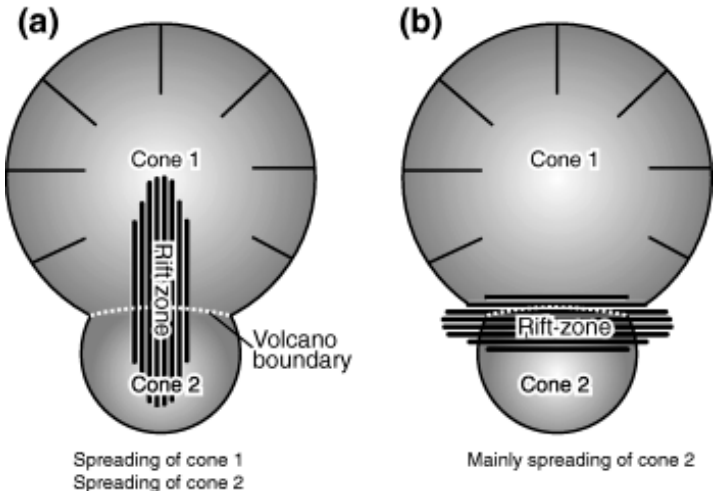

Figure 7.16. Rift zone formation on volcanic cones, controlled by rates of spreading of individual volcanic cones, from Walter et al (2006).

7.4. Comparison with Basaltic – Andesitic Volcanic Complexes

7.4.1. Volcanic Complexes

Banks Peninsula is a unique volcanic structure, both in size and shape. In this study the Lyttelton Volcano is designated as the Lyttelton Volcanic Complex comprised of five overlapping volcanic cones, each comprised of eruptive packages representing eruptive episodes or stages of volcanic construction. A volcanic complex is defined by Németh and Martin (2007) as 'a persistent volcanic vent area that has built a complex combination of volcanic landforms'.

Large volcanoes commonly form through the construction and destruction of cones (i.e. Mt Etna (Guest et al., 1985), Stromboli (Francalanci et al., 1989) Tahiti-Nui (Hildenbrand et al., 2004). Construction commonly forms volcanic cones, with their morphology dependent on tectonic setting, magma composition and eruptive style, destruction can be catastrophic, producing collapse scars and debris avalanches, features recognisable within a volcanic structure. On the Lyttelton Volcanic Complex no large scale catastrophic collapse has been identified, however epiclastic deposits indicate ongoing degradation to the complex throughout its development (Chapter 2).

Dunedin Volcanic Complex

Martin (2000) identified six stages of volcanic activity in the early history of the Dunedin Volcanic Complex, Otago Peninsula (Figure 7.17), of which four took place in subaqueous to emergent environments. Large central-vent polygenetic structures grew, with the final stage culminating in the formation of large phonolite, benmoreite, trachyandesite and mugearite domes (Martin, 2000).

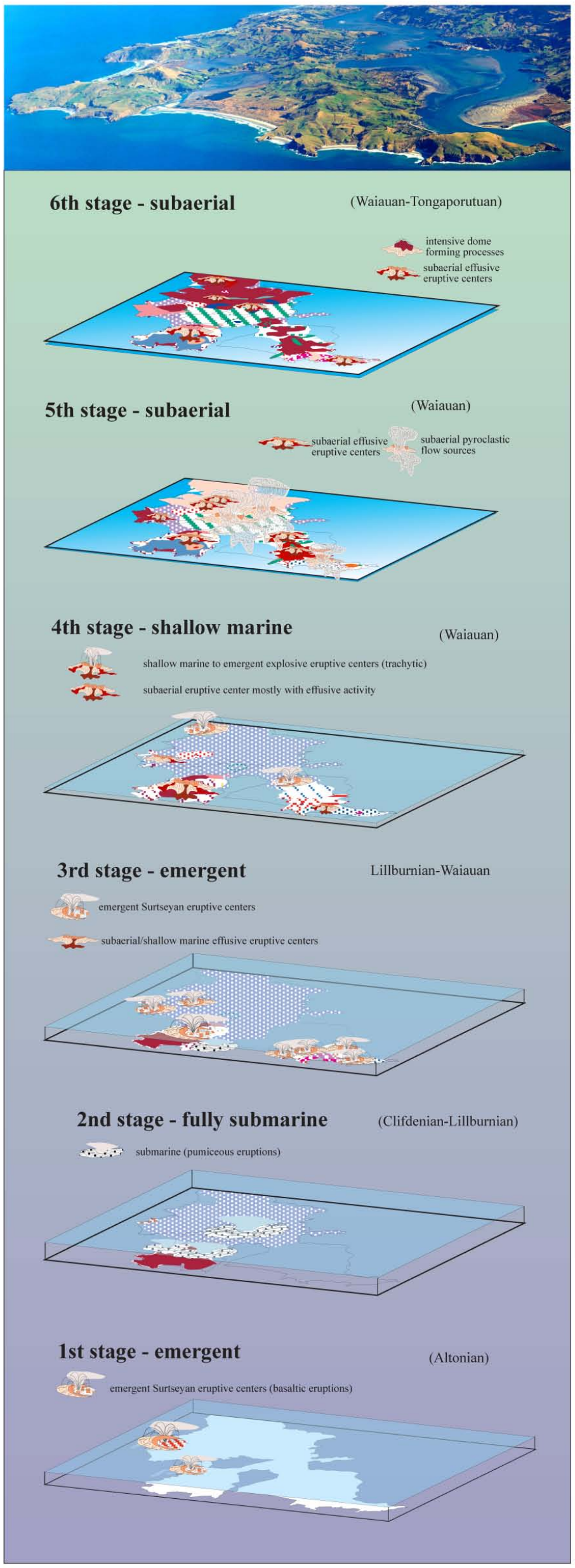

Figure 7.17. Six stage model of the early development of the Dunedin Volcanic Complex, Otago Peninsula (From Martin, 2000). Of significance is the formation of the harbour due to the paleo-valley produced from the overlapping polygenetic volcanoes.

East Australian Intra-plate Volcanism

Significant intra-plate volcanic activity has occurred in eastern Australia throughout the Cenozoic (Figure 7.18), sub-dividided by Johnson (1989) into central volcanoes, lava fields and high potassium mafic areas. Large shield volcanoes with dips 5-10°, and large basal diameters are now disected and highly eroded (i.e. Tweed, Main Range, Nandewar, Ewart et al., 1985; Johnson, 1989). Recent studies by Sutherland et al (2001; 2005) investiagted Barrington Volcano and the Belmore Volcanic Province, indicating multiple eruptive centres within these complexes (Figure 7.19).

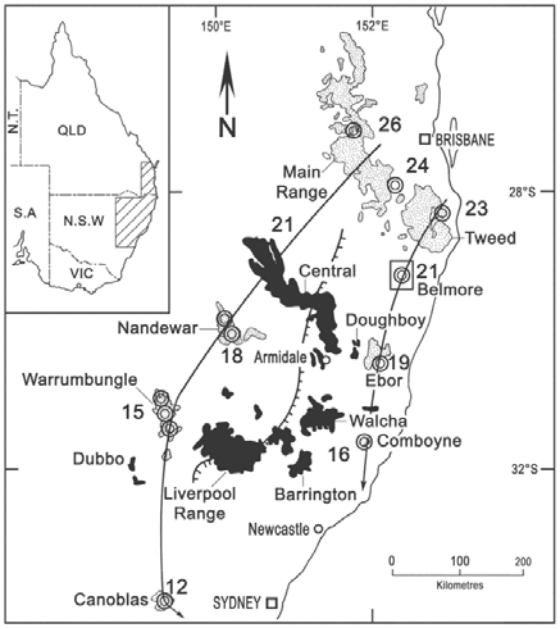

Figure 7.18. Location of intra-plate volcanism on the south-eastern coast of Australia (From Sutherland et al., 2005).

Erosion of the Barrington and Belmore Volcanic Complexes resulting in radial incision about eruptive centres (Figure 7.19; Sutherland et al., 2001; 2005). With the irregular mulitple eruptive centres of Belmore forming radial drainage on the flanks of edifices, with internal drainage (inter-cone valleys) forming between edifices and directing drainage incision (Figure 7.19 and 7.20).

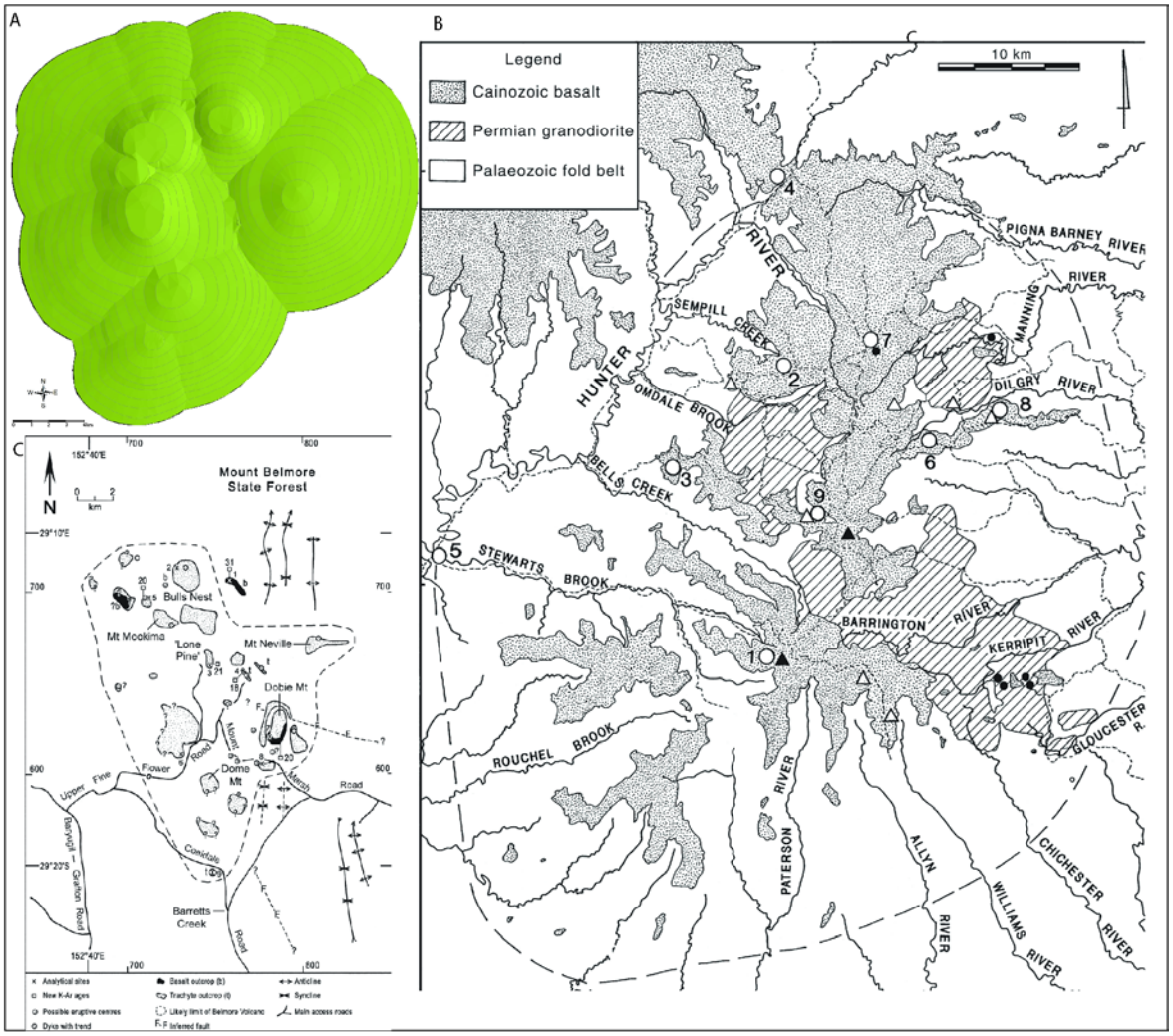

Figure 7.19. Comparative Australian intra-plate volcanoes, A) Lyttelton Volcanic Complex, B) Barrington Volcanic Complex (From Sutherland et al., 2001) and C) Belmore Volcanic Complex (From Sutherland et al., 2005).

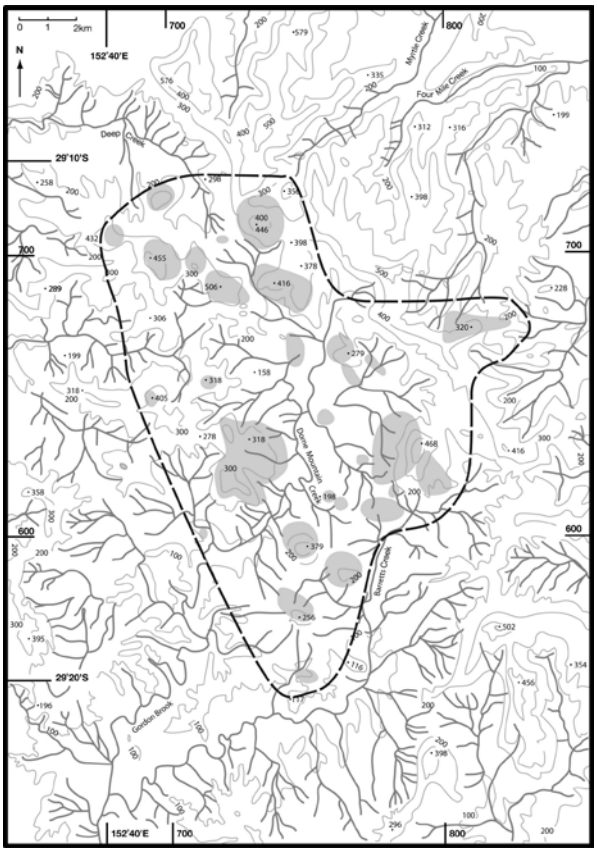

Figure 7.20. Radial valley incision and inter-cone valley drainage patterns in the highly eroded Belmore Volcanic Complex (Sutherland et al., 2005). Light grey shading depict centres of volcanism.

Colima Volcanic Complex

The Colima Volcanic Complex, Mexico, has also undergone two phases of construction, forming the overlapping volcanoes, Fuego and Nevado, both marked by horseshoe shaped avalanche calderas of explosive origin (Figure 7.21; Robin et al., 1987). Colima has steep slopes comprised of andesitic to dacitic lavas, block and ash flows, Plinian ash falls, and nuee ardentes, reaching 2500m above the surrounding ring plain (Robin et al., 1987; 1991).

San Cristobel Volcanic Complex

The San Cristobel Volcanic Complex in north-west Nicaragua is comprised of five volcanic edifices in different stages of erosion and development (Figure 7.22B; Halzett, 1986). Volcanism is tholeiitic to calc-alkaline basalts and andesites, with edifices constructed of lava flows and tephras, with few if any paroxysmal eruptions (Halzett, 1986). Of significance within the San Cristobel Volcanic Complex is the elongate form of two of the edifices (La Casita and Cerro Moyotepe; Figure 7.22B). The summit regions and form of these edifices is elongate due to the coalescing of summit craters and the shifting in the focus of activity.

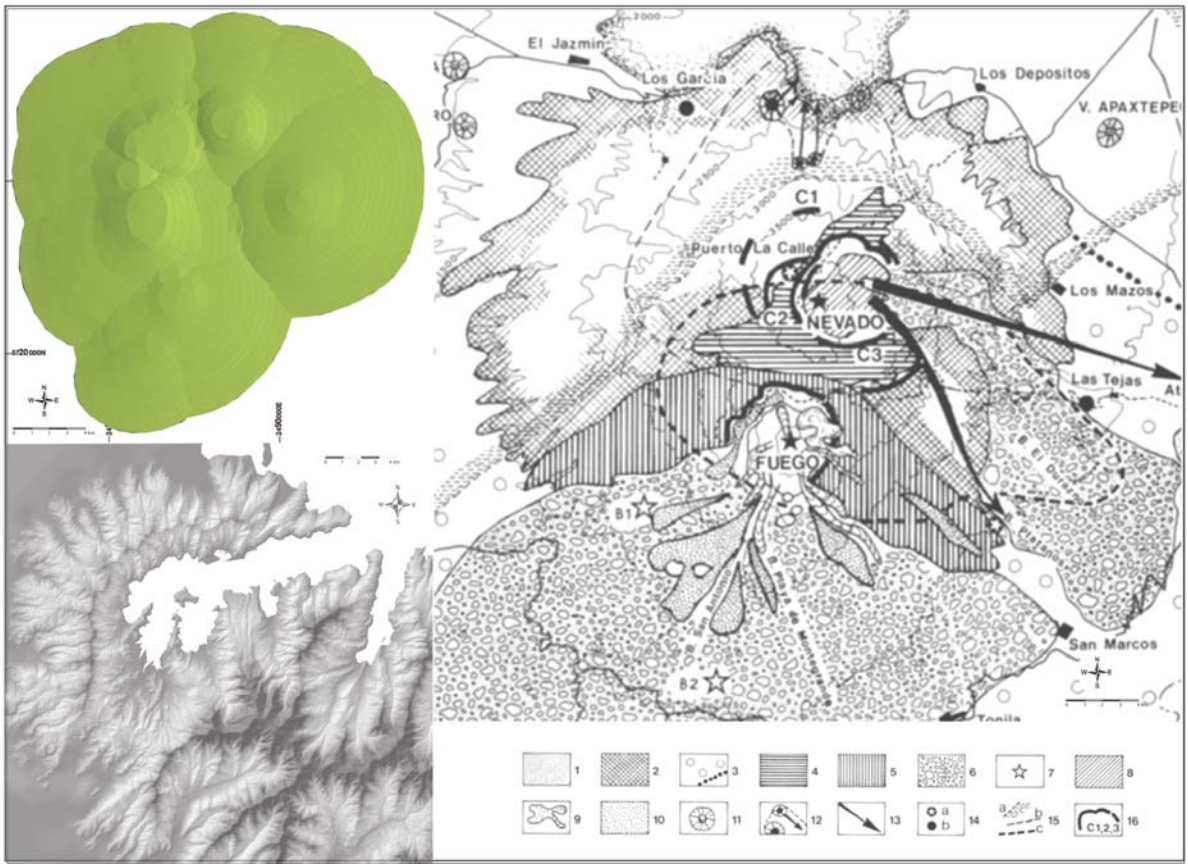

Figure 7.21. Colima Volcanic Complex and the reconstructed model of the Lyttelton Volcanic Complex (figure from Robin et al., 1987). Note the similar basal footprints between the volcanic complexes, and the pronounced horseshoe shaped amphitheatres on Fuego and Nevado Volcanoes.

Fuego Volcanic Complex

The Fuego Volcanic Complex, Guatemala (Figure 7.22F; Chesner and Rose, 1984; Chesner and Halsor, 1997) is comprised of four overlapping basaltic – andesitic centres, Fuego, Meseta, Acatenagngo, and Yepocapa, with volcanism migrating from Meseta to Fuego (younger) forming the elongate form of the volcanic complex. Of significance in this complex is the formation of two inter-cone valleys between the two somewhat separate edifices (Fuego and Meseta, to the south and Acatenagngo, and Yepocapa, to the north). There are radial valleys about each edifice, with valleys trending oblique to parallel in close proximity to the cone-controlled valleys (Figure 7.22F).

Basmus Volcano

Basmus Volcano lies on the Bismark volcanic arc of Papua New Guinea (Johnson et al., 1983). Basmus Volcano is comprised of andesitic lava flows and volcaniclastic deposits, constructed about a central vent region. The summit (2248m) is marked by two crater regions (Fig

7.22D). Basmus Volcano is beside the similar (geochemically and geomorphically) Ulawun Volcano to the northeast (Johnson et al., 1983). The flanks of the volcano steepen towards the summit (<35° dips), with a radial drainage pattern about the summit, and inter-cone valleys between the flanks of the volcano and the Nakanai Mountain ranges to the southeast (Figure 7.22D).

Tanaga Volcano

Tanaga Volcano is the central and highest (1830m) of three adjacent stratovolcanoes at the northwest end of Tanaga Island, Alaska (Figure 7.22E; Miller et al., 1998). These volcanoes are aligned, forming an elongate ridge (trending E-W), with upper slopes dipping up to 35° (Miller et al., 1998). This volcano has a similar elongate form to the San Cristobel Volcanic Complex and Fuego Volcanic Complex, due to the formation of the overlapping strato-cones. Inter-cone valleys are in the initial stages of formation, and are the main drainage networks indicated on the contour model (Figure 7.22E).

Tongariro Volcanic Complex

The Tongariro Volcanic Complex is comprised of at least nine cones built during its ~275-ka history (Figure 7.22C; Cole et al., 1986; Hobden et al.1996, 2002). Each edifice has a distinct structure, forming the summit region of the older northern end of the elongate volcanic complex (Figure 7.22C). Collapse and glaciations have modified these features but radial drainage is still visible. Ngauruhoe, the youngest cone has grown to bury the eroding older Tongariro cones (Figure 7.22C).

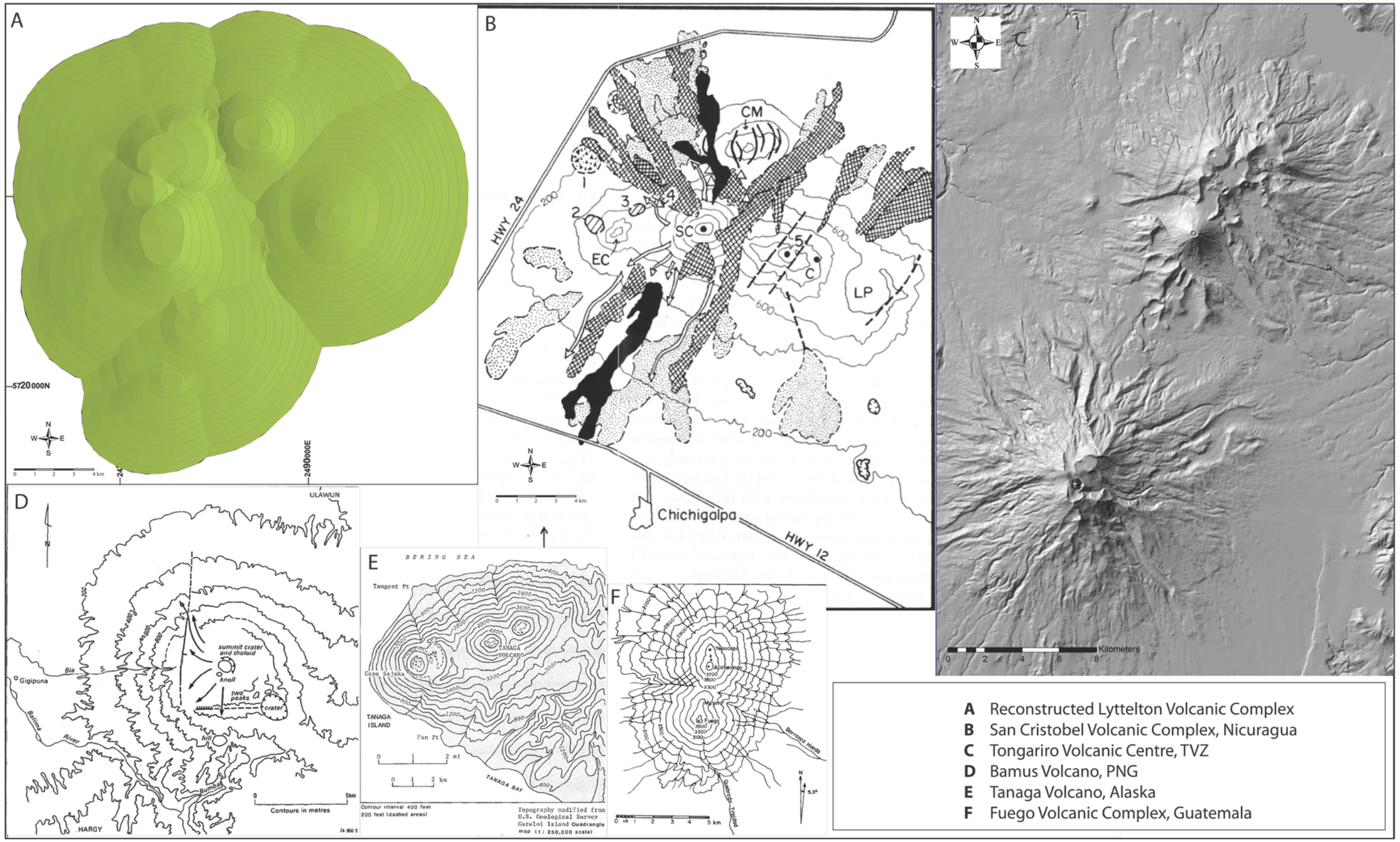

Figure 7.22. Comparative volcanic complexes. A) Reconstructed Lyttelton Volcanic Complex. B) San Cristobel Volcanic Complex: *San Cristobel SC; El Chonco EC; La Casita C; Cerro Moyotepe CM; La Pelona LP* (Halzett, 1986). C) DEM of the Tongariro Volcanic Complex, Ruapehu lies to the south. Note the overlapping eruptive centres in the northern sector of the Tongariro Volcanic Centre, and the radial erosion pattern. Ngauruhoe Volcano lies to the south of the northern sector. D) Basmus Volcano, Papua New Guinea (Johnson et al., 1983), has a similar basal footprint and radial morphology to the Governors Bay and Whakaraupo cones of the Lyttelton Volcanic Complex. E) Tanaga Volcano, Alaska (Miller et al., 1998), has an elongate ridge pattern with young radial incision. The edifice is predominantly incised by inter-cone valleys. F) Fuego Volcanic Complex, Guatemala (Chesner and Rose, 1984), elongate ridge formed through four overlapping eruptive centres. Radial drainage is incised about each edifice with pronounced inter-cone valleys occurring between edifices.

7.4.2. Comparisons

Slope Angle and Volcanic Products

The Colima Volcanic Complex (Robin et al., 1987) has a similar basal footprint to the Lyttelton Volcanic Complex (Figure 7.21), yet Colima has significantly steeper slopes and markedly different styles of eruption (block and ash flows, Plinian eruptions, nuee ardentes, effusive cone building andesitic to dacitic lavas) and history of catastrophic collapse (Robin et al., 1987; 1991). This is similar in evolution to that suggested by Shelley (1992) and Nuemayr (1998), in terms of volcanic height and structure (Lyttelton was estimated at 2500m a.s.l. (Figure 1.7), while Colima is 2500m above the surrounding ring plain), explosive catastrophic collapse, and overlapping cones. As there is no evidence of catastrophic collapse on the Lyttelton Volcanic Complex, with the preserved flanks dipping between 12 - 20°, significantly lower than that of Colima, Lyttelton has a significantly different volcanic morphology.

The San Cristobel, and Fuego Volcanic Complexes are similar in overlapping volcanic structure, lower slope angle, and chemistries like that modelled and observed for the Lyttelton Volcanic Complex. Basmus Volcano, Papua New Guinea, has a similar basal footprint size, slopes and volcanic height as the reconstructed Governors and Whakaraupo cones (Figure 7.22A and 6.3), with the crater region being marked by multiple eruptive vents (Johnson et al., 1983). The Dunedin Volcanic Complex is modelled as overlapping polygenetic volcanoes (Martin, 2000), similar to that proposed in this study for the Lyttelton Volcanic Complex.

Crater and Summit Regions

Elongate ridges and coalesced craters are modelled in the reconstructed Lyttelton Volcanic Complex (Figure 7.22A), and are proposed to have formed by the migration of volcanic focus, like that observed at San Cristobel Volcanic Complex, Fuego Volcanic Complex, Tanaga Volcano (Chesner and Rose, 1984; Halzett, 1986; Chesner and Halsor, 1997; Miller et al., 1998). Overlapping eruptive centres have been documemted at Barrington Volcano and Belmore Volcanic Province (Sutherland et al., 2001; 2005), which are similar in composition and geomorphology to the Lyttelton Volcanic Complex (Figure 7.19).

Geochemical Trends

The Lyttelton Volcanic Complex has similar geomorphology, volcanic structure, and geochemical evolutionary trends to the overlapping Fuego Volcanic Complex of Guatemala (Chapter 4: 4.5.3; Figure 7.22F; Chesner and Rose, 1984; Chesner and Halsor, 1997). Shifts in volcanic centre and eruptive products from varying centres have marked geochemical signatures, as highlighted in Chapter 4: 4.5.3. Lava flow sequences of the Lyttelton Volcanic Complex have an overall evolving geochemical signature, with smaller cyclic magma variations occurring throughout. These cyclic variations result in cyclic eruptive episodes, with a short initial explosive event is the result of a mechanical magma mixing process and the effusive phase corresponding to the longer phase of differentiation, like that observed at the Colima Volcanic Complex (Robin et al., 1987) and Fuego Volcanic Complex (Chesner and Rose, 1984; Chesner and Halsor, 1997).

Volcanic Degradation and Features

Radiating erosion patterns about individual edifices on volcanic complexes is common, with inter-cone valleys forming the intersection of cones (i.e. Fuego Volcanic Complex; Figure 7.22F and Basmus Volcano 7.22D). The radial drainage pattern at the northern end of the Tongariro Volcanic Complex (Figure 7.22C) supports the reconstructed model of Lyttelton Volcanic Complex in the formation of overlapping edifices with individual radial drainages on a multiple centred volcanic complex.

The drainage evolution of the Lyttelton Volcanic Complex (Chapter 6: 6.5.2.) is similar to that for the Belmore Volcanic Complex (Sutherland et al., 2005), with initial radial incision of edfices and the direction / control on drainage from the surrounding volcanic topography. Topographic control has resulted in the formation of large inter-cone valleys, which directed the long term degradaton processes, similar to that porposed in the formation of Lyttelton Harbour, Mt Herbert region and Gebbies Pass. the The formation of Dunedin Harbour is modelled by Martin (2000) as developing from overlapping volcanic edifices (Figure 7.17), which divided the volcanic accumulation into a western ridge and an eastern peninsula (Martin, 2000), a similar cone-controlled valley formation as proposed for Lyttelton Harbour (Figure 6.22).

7.5. Implications for Akaroa Volcano

In this analysis of Lyttelton Volcano, multiple eruptive centres with complex volcanic forms have been proposed. Akaroa Volcano is significantly larger than Lyttelton Volcano, but a similar origin is considered likely. The following section provides an initial analysis of the volcanic morphology, and an indication of what additional work needs to be done.

7.5.1. Geomorphic Analysis

Following the procedures outlined in Chapter 5 (Primary Volcanic Landforms and Eruptive Centre Identification), an initial investigation into Akaroa Volcano's geomorphology has been performed on valley and ridgeline trends.

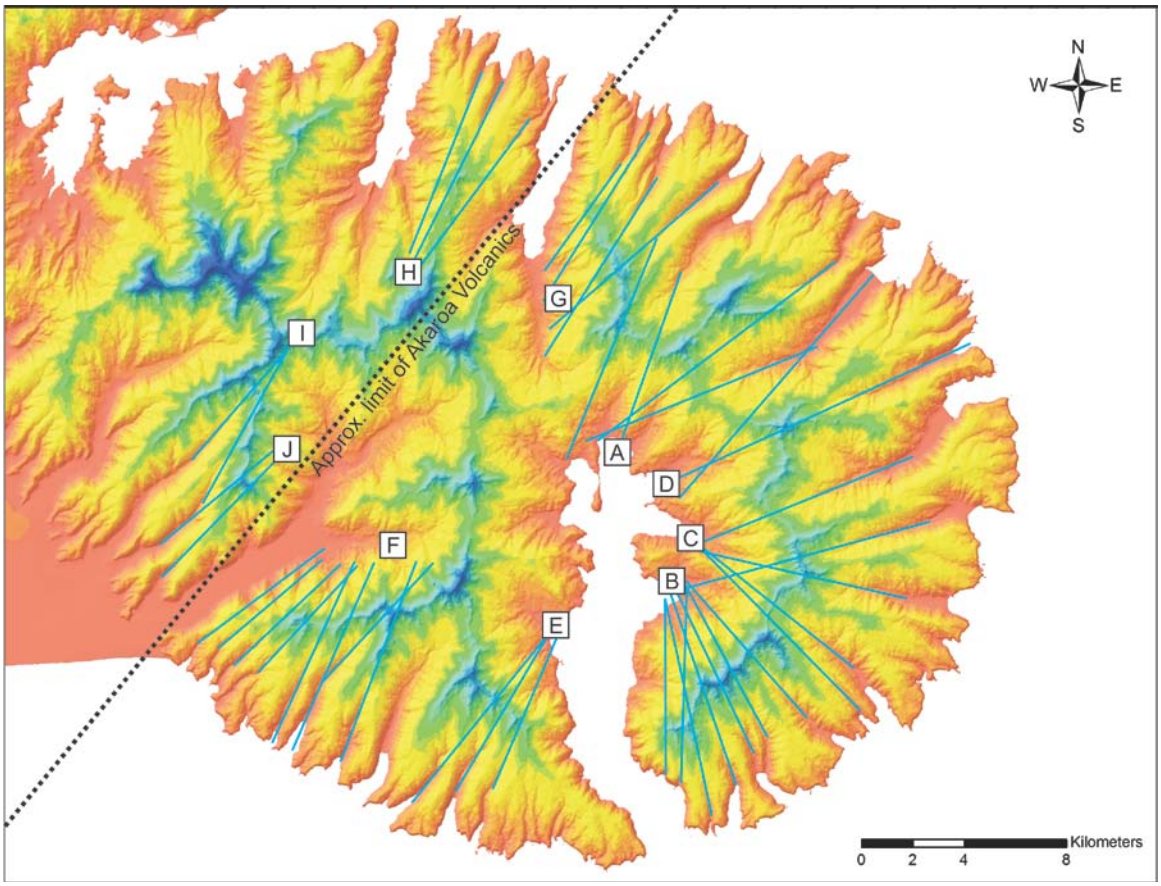

Figure 7.23. Radial valley systems and their projected trends of Akaroa Volcano and central Banks Peninsula. Letters indicate zones of convergence.

Valleys and Ridges

Due to Akaroa's larger scale, more distinct morphological features are identifiable than at Lyttelton Volcano. In valley analysis 10 zones of convergence can be identified, with ridges in

close proximity to a corresponding valley orienting to the same zone of convergence (Figure 7.23 and 7.24). In ridge and valley analysis two trends / orientations in a system is clearly recognisable, with the younger system at higher relief.

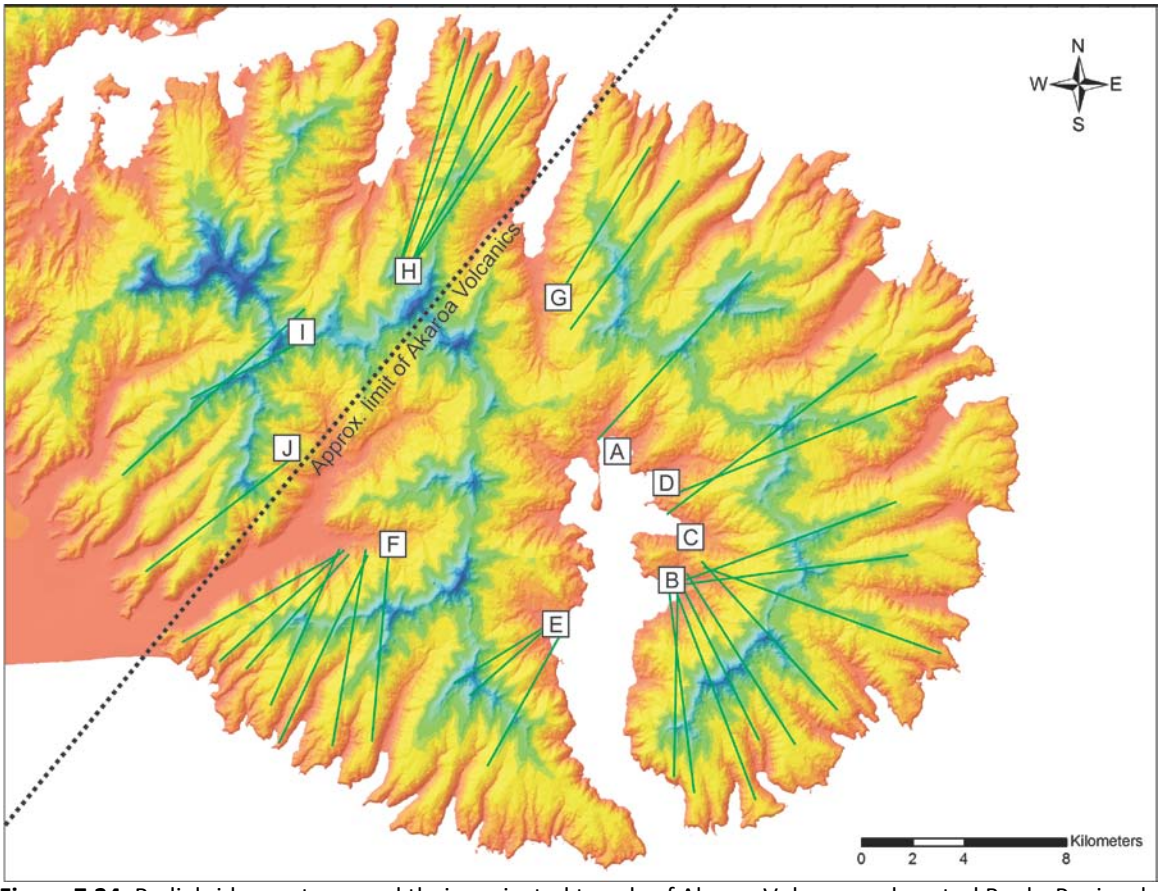

Figure 7.24. Radial ridge systems and their projected trends of Akaroa Volcano and central Banks Peninsula.

Crater Rims and Basal Footprints

Like Lyttelton Volcano the erosional crater rim of Akaroa can be subdivided into a series of crater rim sections, which are able to be correlated to zones of convergence determined from orientations of ridges and valleys. Associated with crater rims is a basal footprint, or the present aerial extent of the volcanic form. On Akaroa there is a good correlation between both crater rims and basal footprints, and the associated ridge and valley trend and zone of convergence (Figure 7.23, 7.24 and 7.25). The relationship between these features is used to define a cone sector with the upper and lower limits designated by the crater rim and basal footprint. In this instance of Akaroa Volcano, each cone sector is clearly defined by an abrupt change in basal footprint (Figure 7.25).

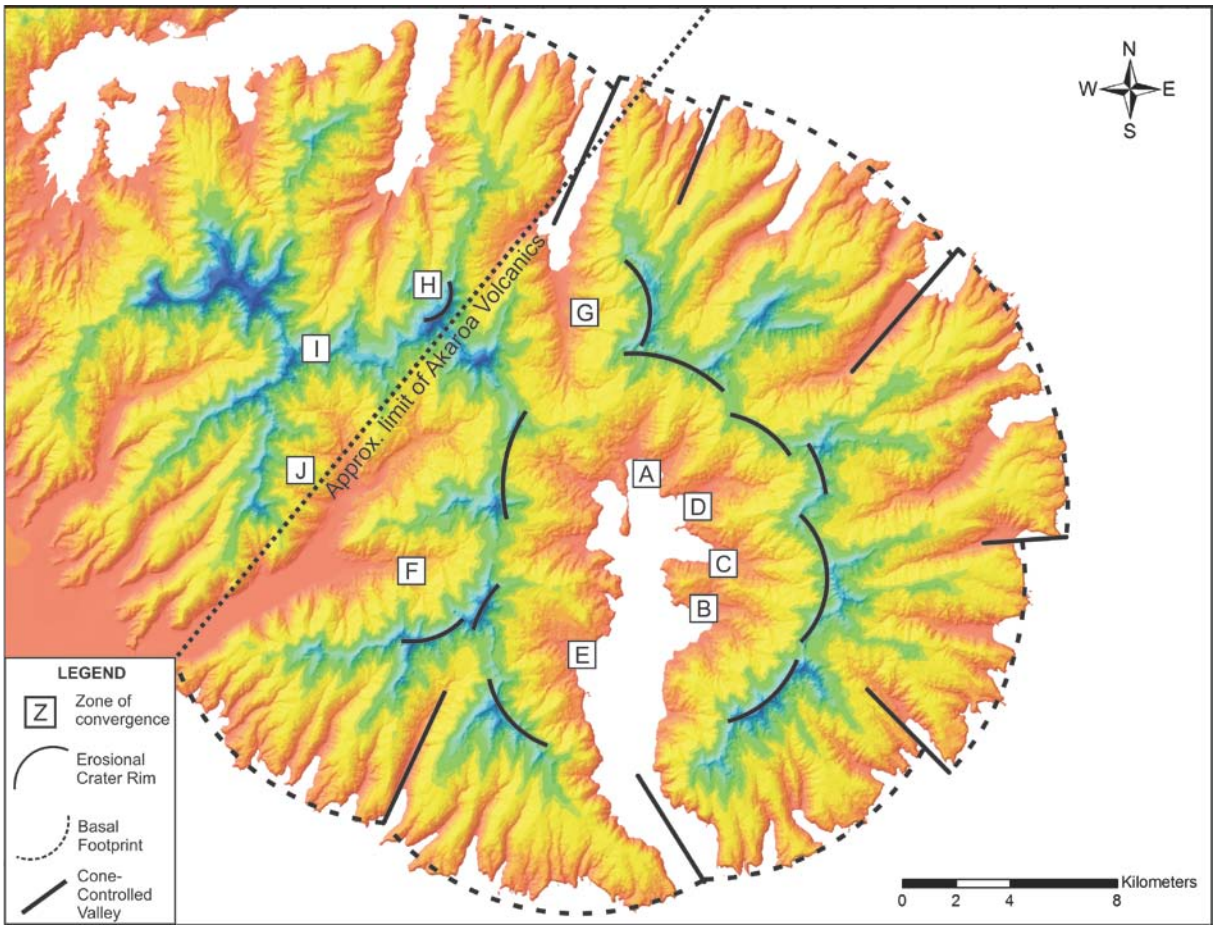

Figure 7.25. Crater rims, basal footprints and cone-controlled valleys of Akaroa Volcano and central Banks Peninsula.

Eruptive Centre Identification

Eruptive centres are identifiable through a correlation of various geomorphic trends. In this initial review ten eruptive centres are proposed, based on the identified cone sectors and primary volcanic trends of valleys and ridges. As stated earlier this is a very initial and limited analysis of Akaroa and central Banks Peninsula, requiring further investigation.

A clear relationship between cone sectors and eruptive centres on Akaroa is evident. However away from both Lyttelton and Akaroa Volcanoes, in central Banks Peninsula, trends vary away from these larger structures. The area between these two volcanoes is infilled by the eruptive products of primarily the Mt Herbert Volcanic Group, and to a lesser degree the Diamond Harbour Volcanic Group. Limited Akaroa Volcanics erupted in this central region, with Sewell et al., (1992) indicating the Mt Sinclair Formation and Te Oka Formation erupting from vents on the flanks of Akaroa Volcano in the region of central Banks Peninsula (Figure 1.6). This supports the geomorphic analysis that the eruptive centres highlighted away from

Akaroa Volcano, either relate to flank eruptives of Akaroa Volcano, or the Mt Herbert Volcanic Group. The eruptive site would have developed a topographic high, from which erosion incised, producing the distinct ridge and valley features, oblique from the main Akaroa Volcano structure.

7.5.2. Schematic Reconstruction

A complete reconstruction is beyond the scope of this thesis however a schematic model has been developed based on initial investigations (Figure 7.26).

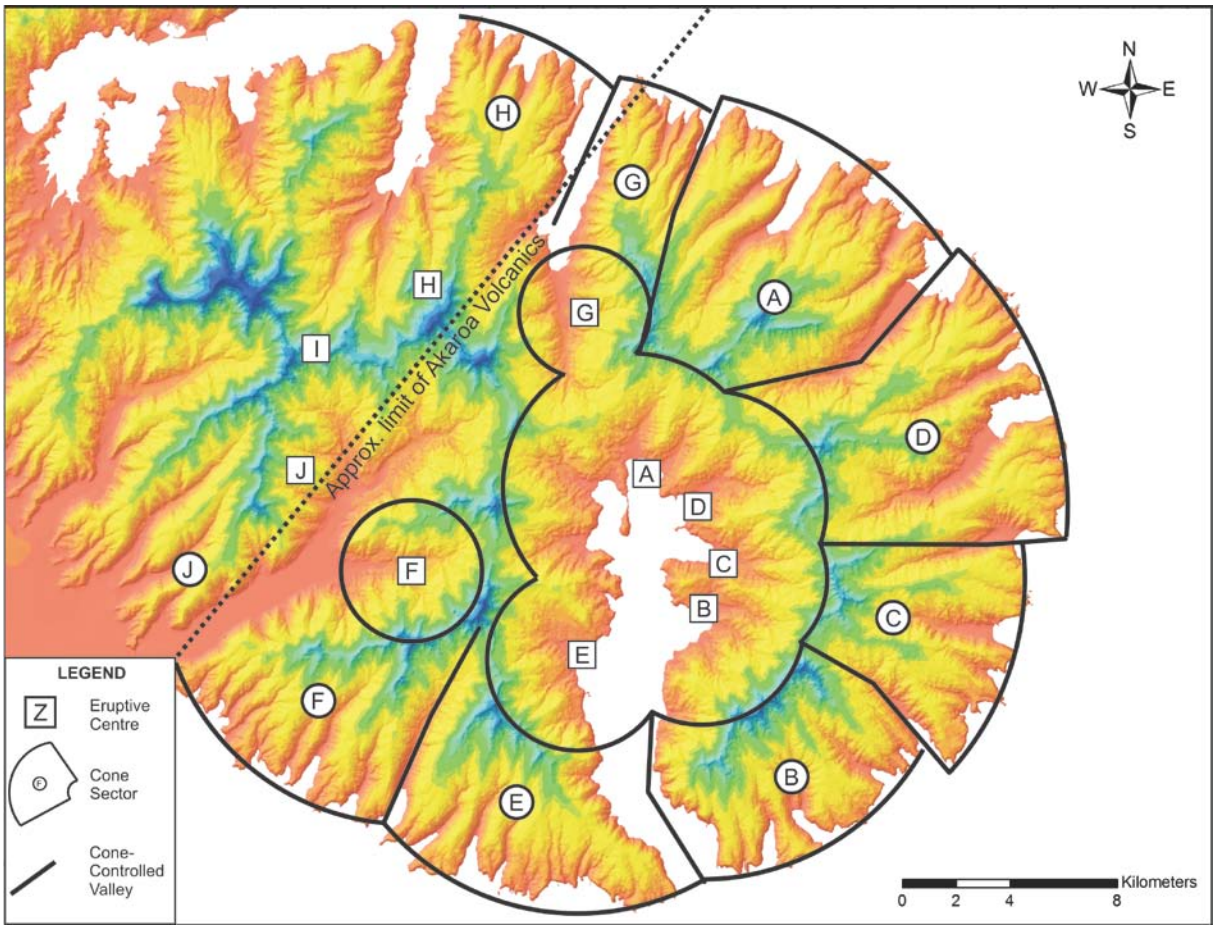

Figure 7.26. Crater rims, basal footprints and cone-controlled valleys of Akaroa Volcano and central Banks Peninsula.

Radial valleys incise about each eruptive centre, with these corresponding to the valley systems designated in the morphometric analysis. Cone-controlled valleys are clearly identifiable at the intersection of cone sectors (Figure 7.25 and 7.26). On Akaroa the major cone-controlled valley systems align with present day larger bay topographies. Some cone-

controlled valleys do not display an associated erosional form, being infilled by later volcanic activity, identifiable through the younger erosional incision.

The major bay and harbour systems associated with Akaroa Volcano and central Banks Peninsula can be viewed as erosional features with erosion focussed in these regions due to the existing volcanic structure. As at Lyttelton Volcano, inter-conal valleys are the main erosive features resulting in the formation of the deeply incised bays and valleys, with planezes preserved near the outer volcanic slopes. Akaroa Harbour initially incepted in the same manner as these inter-conal valleys, but due to the volcanic complex formed, and the cluster of vent sites about the volcanic centre erosion became intensified. This resulted in craters amalgamating into a large drainage basin, with one outlet to the south, progressively forming Akaroa Harbour. Two further valleys / bays are of significance as they incised into central Banks Peninsula. Little River Valley on the south-eastern side and Pigeon Bay to the north-east, are both valleys controlled by the contemporaneous and inter-fingering lavas of the Mt Herbert and Akaroa Volcanic Groups. With the distinct change in slope aspects, one dipping from the east to west (Akaroa) and the other from the west to east (Mt Herbert), resulting in the large paleo-valleys that over time have been progressively enlarged.

7.6. Further Investigations

7.6.1. North-western Banks Peninsula

- Age determination of the Governors Bay Andesite exposure on the Governors Bay to Corsair Bay shore platform. And further investigation into their relationship to Lyttelton Volcanics; are these near vent eruptives of the eruptive centres (identified in this study)?
- Analysis of the interaction between the Allandale Rhyolite and the Governors Bay Andesite, following the contacts highlighted by Thiele (1983).
- Investigation into the Foleys Rd quarry, Teddington. This area is mapped as Torlesse Supergroup, but on initial examinations it is comprised of highly altered intrusive volcanics.
- Further analysis of volcaniclastic deposits of Black Point, including clast composition and tuffaceous component sources.

- Systematic dating of the volcanic sequences of Banks Peninsula.

7.6.2. Akaroa and Central Banks Peninsula

- Dorsey (1988) investigated Akaroa Volcano, and produced a similar rose diagram to that for Lyttelton Volcano (Shelley, 1988). Dorsey's (1988) dyke data set is however mainly from the shore-platform, and as stated in Chapters 5 and 6, dykes at lower volcanic levels do not reflect a radiating intrusive form, as this occurs higher in the volcanic structure. Further investigation is required to locate and record dykes on and away from the inner harbour shore platform to indicate their origin.
- Lava flow analysis on Akaroa Volcano requires further study, with confirmation of inferred strikes and dips to be confirmed through field work. Identification of significant flow types, like Lyttelton Volcano's aa to blocky lava flows to aid in the identification of lava flow packages.
- Further investigations into the formation of the Little River – Okuti Valley system, the lavas on both sides of Lake Forsyth, and the sea cliffs of Kaitorete Spit.
- Identification of the source region or vent sites of the Akaroa's late stage Mt Sinclair and Te Oka Formations.
- Relationship of the domes, intrusives and parasitic vents (scoria cones) to the structure of Akaroa Volcano. An aspect currently being investigated by Master students Eva Hartung and Aleysha Trent.

7.7. Summary

- At least two magma systems are postulated to have fed Banks Peninsula Volcanism, as simultaneous volcanism occurred in both the north-western and south-eastern regions of Banks Peninsula.
- Two distinct controls can be postulated in the development of Lyttelton Volcano, with implications on Banks Peninsula volcanism. The first is from the tectonic (fault) systems of the Canterbury region, and the second due to volcanic structure, heavily influenced by the first.

- Through fault slip analysis three dextral strike-slip, NNE striking faults have been recognised in the north-western region of Banks Peninsula.
- Faulting analysis suggests Lyttelton Harbour is the result of a pull-apart basin, with a number of releasing bend faults.
- Lyttelton Volcano's pull-apart basin model is similar to that recognised in the Cappadocian Volcanic Province of Turkey, where two phases of faulting controls the location of polygenetic and monogenetic volcanoes. With an older fault system in an NW-SE trend while the younger system trends NNE, evolving as the transpressive plate boundary of New Zealand developed.
- Topographic control influenced magma migration in the volcanic structure, with volcanic cones reaching a steady state beyond which magma cannot propagate, initiating in an intrusive regime. The resulting magma pathway modifies, resulting in a new eruptive site controlled by extensional stress fields, primarily on the un-buttressed flanks of the volcanic complex.
- In an initial geomorphic analysis of Akaroa Volcano multiple eruptive centres can be identified, with cone-controlled valleys forming the now deeply incised valley systems.
- Akaroa Harbour formed due to the erosion of a large inter-conal valley, combined with the amalgamation and intensified erosion of the multiple crater regions of central Akaroa Volcano.

CHAPTER 8
CONCLUSIONS

In this study Lyttelton Volcano is viewed as a volcanic complex, comprising five overlapping volcanic cones (Figure 8.1). The Lyttelton Volcanic Complex developed between 11 – 9.7 Ma, with activity initiating in the south (Head of the Bay) and progressing northwards. The five overlapping cones are (Figure 8.1); Head of the Bay, Governors Bay, Whakaraupo, Mt Evans, and Remarkable Cones, each comprised of stratified lava flows, pyroclastic deposits, radial dyke regimes, interbedded epiclastic deposits, and outer flank scoria cones.

Each cone formed through constructional or eruptive phases (Figure 8.1). This study has isolated periods of volcanic construction, through stratigraphic relationships, lava flow trends and flow types, a related dyking regime, and radial erosional features (i.e. ridges and valleys), with each period of construction being termed an eruptive package. Lyttelton Volcanic Complex eruptive packages commonly terminate with a rubbly a'a to blocky lava flow, identifiable within the typical Lyttelton lava flow stack through characteristic blocky appearance and the tendency of these thick deposits to form cliff faces, amongst the typical a'a lava flows.

Geochemical trends within the Lyttelton Volcanic Complex indicate an evolving magma source over time. Within this evolving trend are cyclic eruptive phases trends, identified on the basis of crystal content / volumes plotted against stratigraphic location and lava flow rheology. Within each eruptive package, crystal content fluctuates, but there is a common trend of increasing feldspar content, with peak levels corresponding to a blocky lava flow horizon, indicating the role of this increased crystalinity and lava flow rheology.

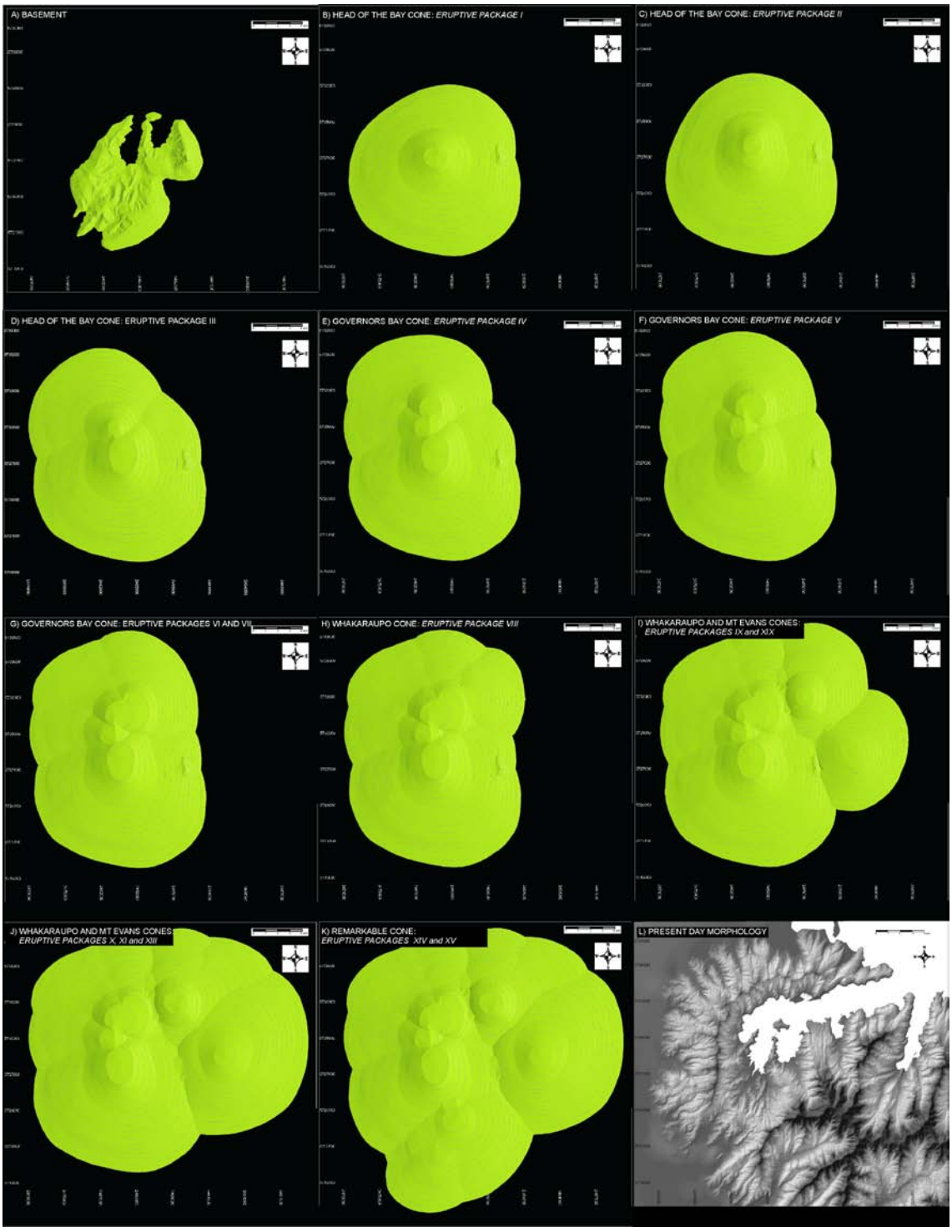

Figure 8.1. Stages of development in the reconstructed model for the Lyttelton Volcanic Complex.

Commonly directly overlying blocky lavas are pyroclastic deposits from central vent explosive eruptions. This style of cyclic magma evolution is also common at other volcanic complexes, and is related to discreet magma batches within the higher levels of the edifice. As each magma batch evolves, crystal content increases, limiting the

ability of the volcanic system, over time, to erupt. An evolving magma can result in the explosive eruptions following effusive eruptives, and / or result in the intrusion of hypabyssal features such as dykes and domes, of more evolved compositions (i.e. trachyte).

In Lyttelton Volcanic Complex the termination of an eruptive package or phase of activity is marked by a radial dyke swarm, reflecting the stress state within the edifice at the time of emplacement. These radial dyke regimes relate to the development of an eruptive package, where an individual stress regime will be produced either through establishment of a shallow level magma chamber or a newly developed stress field due to gravitational relaxation in the newly constructed edifice, resulting in radial intrusion of a dyke swarm.

At least two magma systems are postulated to have fed Banks Peninsula volcanism, with simultaneous volcanism occurring in both the north-western and south-eastern regions of Banks Peninsula. Two distinct controls, tectonic and volcanic structure, are postulated for the development of Lyttelton Volcanic Complex, with implications for Banks Peninsula volcanism.

Fault slip analysis indicates three dextral strike-slip, NNE striking faults in the north-western region of Banks Peninsula. The Lyttelton Volcanic Complex resulted from development of a pull-apart basin, with a number of releasing bend faults (intersection points of cross cutting faults), which controlled the location of eruptive sites. The elongate form of Banks Peninsula is postulated to relate to the upward constraining of magmatism in a north-west / south-east fault bounded zone.

Volcanic structure further influences the pathway magma can propagate. Once a cone reaches a steady state most magmas do not reach the surface forming a dominantly intrusive regime (an aspect recorded within lava flow geochemistry). This results in a new eruptive site primarily on the un-buttressed flanks, controlled by extensional stress fields. New eruptive sites either result in the eruption and formation of a new

cone, or as further cone growth recorded as an eruptive package. Each eruptive package records an eruptive episode related to a magma batch.

Scoria cones formed and erupted on the outer flanks of cones and eruptive packages throughout the evolution of the Lyttelton Volcanic Complex. As a result scoria cones mark the once outer horizon of an edifice, and are used as such within the reconstructions. Scoria cones in the Bridle Path – Mt Cavendish region are incised, reworked and overlain by a series of epiclastic deposits interpreted as debris flows to hyper-concentrated flows. Epiclastic deposits are sourced and interbedded with primary volcanic deposits (lava flows and pyroclastics) indicating ongoing activity during volcanic degradation. Channels within epiclastic horizons indicate drainage networks on the flanks of the Lyttelton Volcanic Complex, primarily aligned in paleo-valleys.

Two distinct erosional structures are modelled on the reconstructed Lyttelton Volcanic Complex; radial valleys and cone-controlled valleys. Radial valleys reflect radial erosion about a cone's summit, while cone-controlled valleys are regions where eruptive packages and cones from different centres meet, allowing stream development. Each edifice initially erodes in the fore mentioned style, yet as degradation of the volcanic complex progressed, the summit regions would become amalgamated or coalesced. Invasion of a drainage network into coalesced crater regions results in unidirectional breaching, increasing the area of the drainage basin and thus the potential to erode and transport extensive amounts of material away, ultimately forming Lyttelton Harbour, Gebbies Pass, and the infilled Mt Herbert region. Lyttelton Harbour is the result of intensified erosion, in a region of coalesced craters with highly altered and brecciated near vent material being eroded and transported down a unidirectional cone-controlled valley, which had a similar orientation to the present harbour.

The present day "erosional crater rim" of the Lyttelton Volcanic Complex is a series of scalloped out segments, relating to the erosion of remnant cone structures. Original crater rim morphology, although now highly enlarged, is the result of the coalescing of

craters and the inception of a unidirectional drainage system, Lyttelton Harbour. Evidence of this drainage system on the Lyttelton Volcanic Complex is preserved in inner harbour exposures. Epiclastic deposits on the south-eastern side of Lyttelton Harbour indicate a paleo-valley system (paleo-Lyttelton Harbour) predominantly dipping to the NNW to NNE since 8.1 Ma. With the mapped contacts of overlying volcanic groups mimicking an un-eroded Lyttelton Volcanic Complex surface.

South-eastern Lyttelton Harbour epiclastic deposits deposited from debris flows and transitional hyper-concentrated debris flows, with finer tuffaceous units depositing in meander bends and paleo-depressions in an alluvial fan system, over a long period (1 - 6 MY) of sedimentation / erosion. The catchment and paleo-valley of this system was topographically controlled by the pre-volcanic basement, Lyttelton Volcanics and Mt Herbert Volcanic Group. Late stage Diamond Harbour Volcanic Group lava flows (Kaioruru Hawaiite and Stoddart Basalt) infilled paleo-channels within the alluvial fan, with lava flows topographically constrained by the paleo-valley system to the south-east, and by the less eroded north-western side of proto-Lyttelton Harbour, forming the Diamond Harbour dip slope.

The morphology of the Lyttelton Volcanic Complex also directed / controlled the eruptive sites, style and resultant morphology of the Mt Herbert Volcanic Group. Of significance is the paleo-valley formed between the Mt Evans, Head of the Bay and Remarkable Cones, which progressively infilled with volcanic products, ultimately resulting in the development of the near flat lying lavas at the summits of both Mt Bradley and Mt Herbert.

Lyttelton Volcanic Complex degradation and preservation of features (planèze) can be explained through loss of catchment of the outer flank valleys, decreasing their erosive potential. Initially erosion incised volcanic highs, eroding outer radial valley systems, but as these catchment areas reduced over time, there was less erosion resulting in the greater preservation of the volcanic structure. Cone-controlled valleys, with larger catchment area, generally formed larger deeply incised valleys.

Previous interpretations of the Lyttelton Volcano hypothesised collapse to Lyttelton 1 and 2 Volcanoes. Through PCT image analysis of Lyttelton Volcano, it is apparent that no single eruptive centre or circular erosional crater rim is concentric around the originally proposed Lyttelton 1 (Head of the Bay) eruptive centre. No distinct remnant block or volcanic collapse features are evident in seismic profiles offshore, which when combined with distinct epiclastic horizons interbedded with lava flows of north-eastern Lyttelton Volcano, does not support volcanic collapse an origin of Lyttelton Harbour.

In an initial geomorphic analysis of south-eastern Banks Peninsula, 10 eruptive centres can be identified. Akaroa Volcano is considered to have formed through the development of five central and two parasitic, fault controlled eruptive vents. Central vents coalesced with time, which like Lyttelton Volcano, was deeply eroded by a cone-controlled valley at similar orientation to the present day Akaroa Harbour. Further cone-controlled valleys formed the now deeply incised valley and bay systems. However further work needs to be done to fully understand the structure of Akaroa Volcano.

REFERENCES

Acocella, V., and Neri, M., 2009. Dike propagation in volcanic edifices: Overview and possible developments: Tectonophysics. 471, 67-77.

Adams, C.J., 1981. Migration of Late Cenozoic volcanism in the South Island of New Zealand and the Campbell Plateau. Nature. 294, 153-155.

Altaye, E., 1989. The Geology and Geochemistry of the North Eastern Sector of Lyttelton Volcano, Banks Peninsula, New Zealand. Master's Thesis, University of Canterbury, Christchurch.

Ancochea, E., Hernán, F., Cendrero, A., Cantagrel, J.M., Fuster, J.M., Ibarrola, E., Coello, J., 1994. Constructive and destructive episodes in the building of a young Oceanic Island, La Palma, Canary Islands, and genesis of the Caldera de Taburiente. Journal of Volcanology and Geothermal Research. 60, 243-262.

Ancochea, E., Brändle, J.L., Cubas, C.R., Hernán, F., Huertas, M.J., 1996. Volcanic complexes in the eastern ridge of the Canary Islands: the Miocene activity of the island of Fuerteventura. Journal of Volcanology and Geothermal Research. 70, 183-204.

Ancochea, E., Huertas, M.J., Cantagrel, J.M., Coello, J., Fúster, J.M., Arnaud, N., Ibarrola, E., 1999. Evolution of the Cañadas edifice and its implications for the origin of the Cañadas Caldera (Tenerife, Canary Islands). Journal of Volcanology and Geothermal Research. 88, 177-199.

Ancochea, E., Brandle, J.L., Heurtas, M.J., Hernan, F., Herrera, R., 2008. Dike-swarms, key to reconstruction of major volcanic edifices: the basic dikes of La Gomera (Canary Islands). Journal of Volcanology and Geothermal Research. 173, 207-216.

Andrews, P.B., Field, B.D., Browne, G.H., McLennan, J.M., 1987. Lithostratigraphic nomenclature for the Upper Cretaceous and Tertiary sequence of central Canterbury, New Zealand. New Zealand Geological Survey record. 24, 40.

Avery, M., 2000. The transition of andesitic Lava from ‘a’a’ to ‘blocky’ flow, Mt Ruapehu New Zealand. Masters Thesis, University of Canterbury, Christchurch.

Aydar, E., Gourgaud, A., Ulusoy, I., Digonnet, F., Labazuy, P., Sen, E., Bayhan, H., Kurttas, T., Tolluoglu, A. U., 2003. Morphological analysis of active Mount Nemrut stratovolcano, eastern Turkey: evidences and possible impact areas of future eruption: Journal of Volcanology and Geothermal Research. 123, 301-312.

Bal, A., 1997. Sea caves, relict shore and rock platforms: evidence for the tectonic stability of Banks Peninsula, New Zealand. New Zealand Journal of Geology and Geophysics. 40, 299-305.

Ballance, P.F., 1984. Sheet flow dominated gravel fans of the non marine Middle Cenozoic Simmler Formation, Central California: Sedimentary Geology. 38, 337-359.

Barley, M.E., Weaver, S. D., De Laeter, J. R., 1988. Strontium isotope composition and geochronology of intermediate-silicic volcanics, Mt Somers and Banks Peninsula, New Zealand: New Zealand Journal of Geology and Geophysics. 31, 197-206.

Barnes, P.M., 1994. Continental extension of the Pacific Plate at the southern termination of the Hikurangi subduction zone: The North Mernoo Fault Zone, offshore New Zealand. Tectonics. 13 (4), 735-754.

Behncke, B., and Neri, M., 2003. The July - August 2001 eruption of Mt Etna (Sicily). Bulletin of Volcanology. 65, 461-476.

Belousov, A.B., 1996. Deposits of the 30 March 1956 directed blast at Bezymianny Volcano, Russia: Bulletin of Volcanology. 57, 649-662.

Belousov, A., Belousova, M., Voight, B. (1999). "Multiple edifice failures, debris avalanches and associated eruptions in the Holocene history of Shiveluch volcano, Kamchatka, Russia." Bulletin of Volcanology. 61(5), 324-342.

Best, J.L., 1992. Sedimentology and vent timing of a catastrophic volcaniclastic mass flow, Volcan Hudson, Southern Chile: Bulletin of Volcanology. 54, 299-318.

Blair, T.C., 1987. Sedimentary processes, vertical stratification sequences, and geomorphology of the Roaring River alluvial fan, Rocky Mountain National Park, Colorado: Journal of Sedimentary Petrology. 57, 1-18.

Borgia, A., Ferrari, L., Pasquare, G., 1992. Importance of gravitational spreading in the tectonic and volcanic evolution of Mount Etna: Nature. 357, 231-235.

Bradshaw, J.D., Andrews, P.B., and Adams, C.J. (Editor), 1981. Carboniferous to Cretaceous on the Pacific margin of Gondwana: The Rangitata Phase of N.Z. 5th International Gondwana Symposium, Wellington, New Zealand.

Brailsford, B., 1981. The Tattooed Land: The Southern Frontiers of the Pa Maori: Wellington, A.H. Reed.

Branca, S., 2003. Geological and geomorphological evolution of the Etna volcano NE flank and relationships between lava flow invasions and erosional processes in the Alcantara Valley (Italy). Geomorphology 53, 247-261.

Brandle, J.L., Ancochea, E., Cubas, C.R., and Hernan, F., 1991. Analisis de enjambres de diques radiales utilizando un metodo matematico. Geogaceta. 10, 97-100.

Bret, L., Fevre, Y., Join, J.-L., Robineau, B., and Bachelery, P., 2003. Deposits related to degradation processes on Piton des Neiges Volcano (Reunion Island): overview and geological hazard: Journal of Volcanology and Geothermal Research. 123, 25-41.

Browne, G.H., and Naish, T.R., 2003. Facies development and sequence architecture of a late Quaternary fluvial-marine transition, Canterbury Plains and shelf, New Zealand: implications for forced regressive deposits: Sedimentary Geology, 158, 57-86.

Brown, L.J., and Weeber, J.H., 1992. Hydrogeological implications of geology at the boundary of Banks Peninsula volcanic rock aquifers and Canterbury Plains fluvial gravel aquifers. New Zealand Journal of Geology and Geophysics. 37, 181-193.

Cacho, L.G., Diezgil, J. L., Arana, V., 1994. A large volcanic debris avalanche in the Pliocene Roque-Nublo Stratovolcano, Gran-Canaria, Canary-Islands. Journal of Volcanology and Geothermal Research. 63, 217-229.

Calvari, S., and Groppelli, G., 1996. Relevance of the Chiancone volcaniclastic deposit in the recent history of Etna Volcano (Italy). Journal of Volcanology and Geothermal Research. 72(3-4), 239-258.

Calvari, S., Tanner, L.H., and Groppelli, G., 1998. Debris-avalanche deposits of the Milo Lahar sequence and the opening of the Valle del Bove on Etna volcano (Italy): Journal of Volcanology and Geothermal Research. 87, 193-209.

Campbell, J.D., and Coombs, D.D., 1966. Murihiku Supergroup (Triassic-Jurassic) of Southland and south Otago. New Zealand Journal of Geology and Geophysics. 9, 393-398.

Carlson., J.R., Grant-Mackie, J.A., Rodgers, K.A., 1980. Stratigraphy and sedimentology of the Coalgate area, Canterbury, New Zealand. New Zealand Journal of Geology and Geophysics. 23, 179-192.

Carn, S.A., 2000. The Lamongan volcanic field, East Java, Indonesia-physical volcanology, historic activity and hazards: Journal of Volcanology and Geothermal Research. 95, 81-108.

Carracedo, J.C., 1999. Growth, structure, instability and collapse of Canarian volcanoes and comparisons with Hawaiian volcanoes: Journal of Volcanology and Geothermal Research. 94, 1-19.

Carrigan, C.R., 2000. Plumbing Systems. In: Sigurdsson, H, Houghton, B., McNutt, S.R., Rymer, H., Stix, J. (Eds.), Encyclopedia of Volcanoes. Academic Press. California. 219-235.

Cas, R.A.F., Wright, J. V., 1987. Volcanic successions, modern and ancient: a geological approach to processes, products, and successions. Allen & Unwin, London; Boston.

Cassidy, J., Ingham, M., Locke, C.A., and Bibby, H., 2009. Subsurface structure across the axis of the Tongariro Volcanic Centre, New Zealand: Journal of Volcanology and Geothermal Research. 179, 233-240.

Chesner CA, Halsor SP. 1997. Geochemical trends of sequential lava flows from Meseta volcano, Guatemala. Journal of Volcanology and Geothermal Research. 78(3-4), 221-237.

Chesner CA, Rose Jr WI. 1984. Geochemistry and evolution of the Fuego Volcanic Complex, Guatemala. Journal of Volcanology and Geothermal Research. 21(1-2), 25-44.

Chester DK, Duncan, A. M., Guest, J. E., and Kilburn, C. R. J. 1985. Mount Etna: The anatomy of a volcano. London: Chapman and Hall.

Clavero, J., Sparks, R., Huppert, H., Dade, W., 2002. Geological constraints on the emplacement mechanism of the Parinacota debris avalanche, northern Chile: Bulletin of Volcanology. 64, 40-54.

Coates, G.F., 1976. A Stratigraphic Study of the Lyttelton Volcano. B.Sc. Hons Thesis. University of Canterbury, Christchurch.

Cole, J.W., Graham, I. J., Hackett, W. R., Houghton, B. F., 1986. Volcanology and petrology of the Quaternary Composite Volcanoes of Tongariro Volcanic Centre, Taupo Volcanic Zone, in Smith, I.E.M., ed., Late Cenozoic Volcanism in New Zealand, Volume 23, Royal Society of New Zealand Bulletin. 7-20.

Concha-Dimas, A., Cerca, M., Rodriguez, S. R.,Watters, R. J., 2005. Geomorphological evidence of the influence of pre-volcanic basement structure on emplacement and deformation of volcanic edifices at the Cofre de Perote-Pico de Orizaba chain and implications for avalanche generation: Geomorphology. 72, 19-39.

Cotton C.A., 1944. Volcanoes as landscape forms. Whitcombe & Tombs limited, Christchurch, New Zealand.

Coussot, P., and Meunier, M., 1996. Recognition, classification and mechanical description of debris flows: Earth-Science Reviews. 40, 209-227.

Cronin, S.J., Neall, V. E., Palmer, A. S., 1996. Geological history of the north-eastern ring plain of Ruapehu volcano, New Zealand: Quaternary International. 34, 21-28.

Davidson, J., and DeSilva, S., 2000. Composite volcanoes. In: Sigurdsson, H, Houghton, B., McNutt, S.R., Rymer, H., Stix, J. (eds.), Encyclopedia of Volcanoes. Academic Press. California. 663-681.

Delaney, P.T., Miklius, A., Arnadottir, T., Okamura, A.T., Sako, M.K., 1993. Motion of Kilauea volcano during sustained eruption from the Puu Oo and Kupaianaha vents, 1983–1991. Journal of Geophysical Research. 98, 17801–17820.

Dieterich, J.H., 1988. Growth and persistence of Hawaiian volcanic rift zones. Journal of Geophysical Research. 93, 4258-4270.

Dorsey, C.J., 1981. The Stratigraphy, Petrography, and Geochemistry of the Diamond Harbour Group, Banks Peninsula. Honours Thesis, University of Canterbury, Christchurch.

Dorsey, C.J., 1988. The geology and geochemistry of Akaroa volcano, Banks Peninsula, New Zealand. PhD Thesis, University of Canterbury, Christchurch, New Zealand.

Druitt, T.H., 1995. Settling behaviour of concentrated dispersions and some volcanological applications: Journal of Volcanology and Geothermal Research. 65, 27-39.

Duncan, A.M., Guest, J. E., Stofan, E. R., Anderson, S. W., Pinkerton, H. and Calvari, S. , 2004. Development of tumuli in the medial portion of the 1983 as flow-field, Mount Etna, Sicily: Journal of Volcanology and Geothermal Research. 132.

Elsworth, D., Voight, B., 1996. Evaluation of volcano flank instability triggered by dyke intrusion, in McGuire, W.J., Jones, A. P., Neuberg, J., ed., Volcano instability on the Earth and other planets. 45-53.

Enos, P., 1977. Flow regimes in debris flow: Sedimentology. 24, 133-142.

Ewart, A., Chappell, B. W., LeMaitre, R. W., 1985. Aspects of the mineralogy and chemistry of the intermediate-silicic Cainozoic volcanic rocks of eastern Australia. Part 1: Introduction and geochemistry: Australian Journal of Earth Sciences. 32, 359 - 382.

Favalli, M., and Pareschi, M.T., 2004. Digital elevation model construction from structured topographic data: The DEST algorithm: Journal of Geophysical Research. 109, F04004.

Favalli, M., Karátson, D., Mazzuoli, R., Pareschi, M., and Ventura, G., 2005. Volcanic geomorphology and tectonics of the Aeolian archipelago (Southern Italy) based on integrated DEM data: Bulletin of Volcanology. 68, 157-170.

Finn, C.A., Mueller, R.D., Panter, K.S., 2005. A Cenozoic diffuse alkaline magmatic province (DAMP) in the southwest Pacific without rift or plume origin. Geochemistry, Geophysics, Geosystems. 6. Q02005

Fisher, R.V., 1983. Flow transformations in sedimentary gravity flows. Geology. 11, 273-274.

Fisher, R.V., Schmincke, H.-U., 1984. Pyroclastic Rocks: Springer, Heidelberg.

Forsyth, P.J., Barrell, D.J.A., Jongens, R., 2008. Geology of the Christchurch Area, 1:250000 geological map 16: Lower Hutt, Institute of Geological & Nuclear Sciences.

Francalanci L, Manetti P, Peccerillo A. 1989. Volcanological and magmatological evolution of Stromboli volcano (Aeolian Islands): The roles of fractional crystallization, magma mixing, crustal contamination and source heterogeneity. Bulletin of Volcanology. 51(5), 355-378.

Frost, M.J., 1965. Centre finding in systems of lines: Geological Magazine. 102, 445-450.

Gee, M.J.R., Watts, A. B., Masson, D. G., Mitchell, N. C., 2001. Landslides and the evolution of El Hierro in the Canary Islands: Marine Geology. 177, 271-293.

Gioncada, A., Mazzuoli, R., Bisson, M., and Pareschi, M.T., 2003. Petrology of volcanic products younger than 42 ka on the Lipari-Vulcano complex (Aeolian Islands, Italy): an example of volcanism controlled by tectonics: Journal of Volcanology and Geothermal Research. 122, 191-220.

Giordano, G., De Rita, D., Fabbri, M., and Rodani, S., 2002. Facies associations of rain-generated versus crater lake-withdrawal lahar deposits from Quaternary volcanoes, central Italy: Journal of Volcanology and Geothermal Research. 118, 145-159.

Girard, G., Wyk de Vries, B. van., 2005. The Managua Graben and Las Sierras-Masaya volcanic complex (Nicuragua); pull-apart localization by an intrusive complex: results from analog modelling: Journal of Volcanology and Geothermal Research. 144, 35-57.

Gloppen, T.G., Steel, R. J., 1981. The deposits, internal structure and geometry in six alluvial fan-fan delta bodies (Devonian Norway)-a study in the significance of bedding sequences in conglomerates., in Ethridge, F.G., Flores, R. M., ed., Recent and ancient nonmarine depositional environments: models for exploration, Volume 31: Tulsa, Oklahoma, Soc. Econ. Paleont. Mineral., Spec. Publ., 49-69.

Guest, J.E., Chester, D.K., Duncan, A.M., 1985. The Valle del Bove, Mount Etna: its origin and relation to the stratigraphy and structure of the volcano - reply: Journal of Volcanology and Geothermal Research. 26, 384-386.

Haast, J., 1860. Report of a geological survey of Mount Pleasant, presented to His Honour the Superintendent of Canterbury, and laid before the Provincial Council, December 20, 1860. Printed at the 'Times' Office, Lyttelton.

Haast, J., 1878. On the Geological Structure of Banks Peninsula. Transactions and proceedings of the New Zealand Institute. 11, 495.

Haast, J.V., 1879. Geology of the Provinces of Canterbury and Westland, New Zealand: a report comprising the results of official explorations. [s.n.], Christchurch.

Hackett, W.R., and Houghton, B.F., 1989. A facies model for a quaternary andesitic composite volcano: Ruapehu, New Zealand: Bulletin of Volcanology. 51, 51-68.

Hazlett, R.W., 1987. Geology of the San Cristobal volcanic complex, Nicaragua: Journal of Volcanology and Geothermal Research. 33, 223-230.

Hampton, S.J., 2005. Volcanic Geology of the Orton Bradley Formation. B.Sc. (Hons) Thesis, University of Canterbury, Christchurch.

Hampton, S.J., and Cole, J.W., 2009. Lyttelton Volcano, Banks Peninsula, New Zealand: Primary volcanic landforms and eruptive centre identification. Geomorphology. 104, 284-298.

Hancock, P.L., 1985. Brittle microtectonics; principles and practice: Journal of Structural Geology, 7, 437-457.

Harrison, S., and Fritz, W. J., 1982. Depositional features of March 1982 Mount St. Helens sediment flows Nature. 299, 720-722.

Head, J.W., Wilson, L., 1992. Magma reservoirs and neutral buoyancy zones on Venus: implications for the formation and evolution of volcanic landforms: Journal of Geophysical Research. 97, 3877-3903.

Hibberd, T.J., 1994. The Geology of the Coopers Knob Area, Lyttelton Volcano, Banks Peninsula. BSc (Hons) Thesis, University of Canterbury, Christchurch, New Zealand.

Hildenbrand A, Gillot P-Y, Le Roy I., 2004. Volcano-tectonic and geochemical evolution of an oceanic intra-plate volcano: Tahiti-Nui (French Polynesia). Earth and Planetary Science Letters. 217(3-4), 349-365.

Hildenbrand, A., Gillot, P.-Y., and Marlin, C., 2008. Geomorphological study of long-term erosion on a tropical volcanic ocean island: Tahiti-Nui (French Polynesia). Geomorphology. 93,460-481.

Hobden, B.J., Houghton, B F., Lanphere, M. A., I.A Nairn, I. A., 1996. Growth of the Tongariro volcanic complex: new evidence from K-Ar age determinations. New Zealand Journal of Geology and Geophysics. 39, 151-154.

Hobden, B., Houghton, B., and Nairn, I., 2002. Growth of a young, frequently active composite cone: Ngauruhoe volcano, New Zealand. Bulletin of Volcanology. 64, 392-409.

Hoke, L., Poreda, R., Reay, T., Weaver, S.D., 2000. The subcontinental mantle beneath southern New Zealand, characterised by helium isotopes in intraplate basalts and gas-rich springs. Geochemica et Cosmochimica Acta. 64, 1489-2507.

Hoernle, K., White, J.D.L., van den Bogaard, P., Hauff, F., Coombs, D.S., Werner, R., Timm, C., Garbe-Schönberg, D., Reay A., Cooper, A.F., 2006. Cenozoic intraplate volcanism on New Zealand: Upwelling induced by lithospheric removal. Earth and Planetary Science Letters. 248(1-2), 335-352.

Hurlimann, M., Garcia-Piera, J. O., Ledesma, A., 2000. Causes and mobility of large volcanic landslides: application to Tenerife, Canary Islands: Journal of Volcanology and Geothermal Research. 103, 121-134.

Hurlimann, M.M., J., Ledesma, A., 2004. Morphological and geological aspects related to large slope failures on oceanic islands: The huge La Orotava landslides on Tenerife, Canary Islands: Geomorphology. 62, 143-158.

Irvine, P., 2003. Lahar deposits of north-east Lyttelton 1 Volcano. BSc (Hons) Thesis, University of Canterbury, Christchurch, New Zealand.

Jaggar, T.A., 1930. Distinction between pahoehoe and a'a or block lava. The Volcano Letter. 281, 1-3.

Jenkins, S.F., Magill, C.R., McAneney, K.J., 2007. Multistage volcanic events: A statistical investigation: Journal of Volcanology and Geothermal Research. 161, 275-288.

Johnson, A.M., 1970. Physical processes in geology: San Francisco, Freeman Copper.

Johnson, R.W., Knutson, J., Taylor, S. R., 1989. Intraplate volcanism in eastern Australia and New Zealand: Sydney, Cambridge University Press.

Johnson, R.W., McNab, R. P., Arculus, R. J., Ryburn, R. J., Cooke, R. J. S., Chappell, B. W., 1983. Bamus volcano, Papua New Guinea: dormant neighbour of Ulawun, and magnesian-andesite locality: Geologische Rundschau. 72, 207-223.

Johnston, W.B., 1969. Modification of the natural environment by man, in Knox, G.A., ed., The natural history of Canterbury: Wellington, Reed.

Jordan, G., Meijninjer, B.M.L., Van Hinsbergen, D.J.J., Meulenkamp, J.E., van Dijk, P.M., 2005. Extraction of morphotectonic features from DEMs: Development and applications for study areas in Hungary and NW Greece. International Journal of Applied Earth Observation and Geoinformation. 7, 163 – 182.

Karátson, D., Thouret, J-C., Moriya, I., Lomoschitz, A., 1999. Erosion calderas: origins, processes, structural and climatic control. Bulletin of Volcanology. 61, 174 – 193.

Karátson, D., Németh, K., Székely, B., Ruszkiczay-Rüdiger, Z., and Pécskay, Z., 2006. Incision of a river curvature due to exhumed Miocene volcanic landforms: Danube Bend, Hungary: International Journal of Earth Sciences. 95, 929-944.

Kilburn CRJ. 2000. Lava flows and flow fields. In: Encyclopedia of Volcanoes, (Sigurdsson H, ed). San Diego: Academic Press, 291-306.

Kilburn, C.R.J. and Guest, J.E., 1993. Aa lavas of Mount Etna, Sicily. In: Kilburn, C.R.J., and Luongo, G., (eds.) Active Lava Flows: Monitoring and Modelling. UCL Press, London. 73-106.

Kim, S.B.C., S. K.; and Chun, S. S., 1995. Bouldery deposits in the lowermost part of the Cretaceous Kyokpori Formation, SW Korea: cohesionless debris flows and debris falls on a steep gradient delta slope: Sedimentary Geology. 98, 97-119.

Kouli, M., and St. Seymour, K., 2006. Contribution of remote sensing techniques to the identification and characterization of Miocene calderas, Lesvos Island, Aegean Sea, Hellas: Geomorphology. 77, 1-16.

Lavallée, Y., de Silva, S.L., Salas, G., and Byrnes, J.M., 2009. Structural control on volcanism at the Ubinas, Huaynaputina, and Ticsani Volcanic Group (UHTVG), southern Peru: Journal of Volcanology and Geothermal Research. 186, 253-264.

Lavigne, F., and Thouret, J.-C., 2003. Sediment transportation and deposition by rain-triggered lahars at Merapi Volcano, Central Java, Indonesia: Geomorphology. 49, 45-69.

Lecointre, J.A., Neall, V.E., Wallace, R.C., and Prebble, W.M., 2002. The 55- to 66-ka Te Whaiau Formation: a catastrophic, avalanche-induced, cohesive debris-flow deposit from Proto-Tongariro Volcano, New Zealand. Bulletin of Volcanology. 63, 509-525.

Le Friant, A., Harford, C.L., Deplus, C. Boudon, G., Sparks, R.S.J., Herd, R.A., Komorowski, J.C., 2004. Geomorphological evolution of Montserrat (West Indies): importance of flank collapse and erosional processes Journal of the Geological Society. 161, 147-160.

Lenat, J.-F., Merle, O., Lespagnol, L., 2009. La Reunion: An example of channeled hot spot plume: Journal of Volcanology and Geothermal Research. 184, 1-13.

Ligget, K.A., and Gregg, D.R., 1965. Geology of Banks Peninsula, South Island. In: B.N.a.K. Thompson, L.D. (eds.), New Zealand Volcanology, South Island. Department of Scientific and Industrial Research Information Series.

Linneman, S.R., and Borgia, A., 1993. Kinematics and dynamics of lava flows, Arenal Volcano, Costa Rica. Abstracts with Programs – Geological Society of America. 15, 6, p530.

Lirer, L., Vinci, A., Alberico, I., Gifuni, T., Bellucci, F., Petrosino, P., and Tinterri, R., 2001. Occurrence of inter-eruption debris flow and hyperconcentrated flood-flow deposits on Vesuvio volcano, Italy: Sedimentary Geology. 139, 151-167.

Lo Giudice, E., and Rasà, R., 1992. Very shallow earthquakes and brittle deformation in active volcanic areas: The Eatnean region as an example: Tectonophysics. 202, 257-268.

Lowe, D.R., 1982. Sediment gravity flows: II. Depositional models with special reference to the deposits of high-density turbidity currents: Journal of Sedimentary Petrolology. 52, 279 - 297.

Luhr JF, Carmichael, I.S.E. 1980. The Colima volcanic complex, Mexico - Post caldera andesites from Volcan Colima Contributions to Mineralogy and Petrology. 71, 343-372.

Luhr, J.F., Carmichael, I.S.E., 1990. Petrological monitoring of cyclical eruptive activity at Volcan de Colima, Mexico. : Journal of Volcanology and Geothermal Research. 42, 235-260.

McBirney, A.R., 1990. A historical note on the origin of calderas: Journal of Volcanology and Geothermal Research. 42, 303-306.

MacDonald, G.A., 1953. Pahoehoe, aa, and block lava. American Journal of Science. 251, 169-191.

McDonald, G.A., 1973. Volcanoes: New Jersey, Prentice Hall.

McGuire, W.J., 1982. Evolution of the Etna Volcano: information from the southern wall of the Valle del Bove caldera. Journal of Volcanology and Geothermal Research. 13, 241 - 271.

McGuire, W.J., 1985. The Valle del Bove, Mount Etna: its origin and relation to stratigraphy and structure of the volcano: discussion: Journal of Volcanology and Geothermal Research. 26, 377 - 386.

McGuire, W.J., 1996. Volcano instability: a review of contemporary themes. In: W.J. McGuire, Jones, A. P., Neuberg, J. (eds), Volcano Instability on the Earth and Other Planets. The Geological Society, London.

McKenzie, C.J., 1995. The volcanic geology of the Southern Mt Evans - Upper Purau Valley Area, Lyttelton Volcano, Banks Peninsula. BSc (Hons) Thesis, University of Canterbury, Christchurch, New Zealand.

McPhie, J., Doyle, M., Allen, R., 1993. Volcanic Textures. A guide to the interpretation of textures in volcanic rocks: Tasmania, Tasmanian Government Printing Office.

Mardia, K.V., 1972. Statistics of directional data: London, Academic Press.

Martí, J., and Geyer, A., 2009. Central vs flank eruptions at Teide-Pico Viejo twin stratovolcanoes (Tenerife, Canary Islands): Journal of Volcanology and Geothermal Research. 181, 47-60.

Martin, U., 2000. Eruptions and deposition of volcaniclastic rocks in the Dunedin volcanic complex, Otago Peninsula, New Zealand, PhD Thesis, University of Otago, Dunedin, New Zealand.

Martin, U and Németh, K., 2007. Blocky versus fluidal peperite textures developed in volcanic conduits, vents and crater lakes of phreatomagmatic volcanoes in Miocene/Pliocene volcanic fields of Western Hungary, Journal of Volcanology and Geothermal Research. 159, 164–178.

Masson, D.G., Watts, A.B., Gee, M.J.R., Urgeles, R., Mitchell, N.C., Le Bas, T.P., and Canals, M., 2002. Slope failures on the flanks of the western Canary Islands: Earth-Science Reviews. 57, 1-35.

Mathisen, M., McPherson, J., 1991. Volcaniclastic deposits: implications for hydrocarbon exploration. In: Fisher, R.V., and Smith, G.A., (eds.), Sedimentation in Volcanic Settings, SEPM Special Publication. 45, 27–36.

Mazzuoli, R., Tortorici, L., Ventura, G., 1995. Oblique rifting in Salina, Lipari and Vulcano islands (Aeolian islands, southern Italy): Terra Nova. 7, 444-452.

Miller, T.P., McGimsey, R.G., Richter, D.H., Riehle, J.R., Nye, C.J., Yount, M.E., Dumoulin, J.A., 1998. Catalog of the historically active volcanoes of Alaska, Open file report 98-582: Anchorage, Department of the Interior U.S. Geological Survey.

Moore, J.G., Clague, D.A., Holcomb, R.T., Lipman, P.W., Normark, W.R., and Torresan, M.E., 1989. Prodigious submarine landslides on the Hawaiian Ridge, Journal of Geophysical Research. 94, 17465–17484.

Moore, J.G., Chadwick, W.W. Jr., 1995. Offshore geology of Mauna Loa and adjacent areas, Hawaii. In Geophysical Monograph 92, Mauna Loa Revealed: structure, composition, history, and hazards, ed. by J.M. Rhodes and J.P. Lockwood, American Geophysical Union, Washington, D.C. 21-44.

Neall, V.E., 1975. Climate-controlled tephra redeposition on Pouakai ring plain, Taranaki, New Zealand: New Zealand Journal of Geology and Geophysics. 18 317–326.

Nemèth K. 2004. The morphology and origin of wide craters at Al Haruj al Abyad, Libya: maars and phreatomagmatism in a large intracontinental flood lava field? Zeitsschrift fur Geomorpholgie. 47(1), 29-49.

Nemèth, K., and Martin, U., 2007. Practical Volcanology: Lecture notes from understanding volcanic rocks from field based studies. Occasional Papers of the Geological Institute of Hungary. 207

Neumayr, R.E.E., 1998. The geology of Lyttelton 1 volcano. MSc Thesis, University of Canterbury, Christchurch, New Zealand.

Norini, G., Groppelli, G., Capra, L., and De Beni, E., 2004. Morphological analysis of Nevado de Toluca volcano (Mexico): new insights into the structure and evolution of an andesitic to dacitic stratovolcano: Geomorphology. 62, 47-61.

Nott J, Young, R., McDougall, I. 1996. Wearing down, wearing back, and gorge extension in the long-term denudation of a highland mass: quantitative evidence from the Shoalhaven catchment, Southeast catchment, Southeast Australia Journal of Geology. 104, 224-232.

Ode, H., 1957. Mechanical analysis of the dike pattern of the Spanish Peaks area, Colorado. Geological Society of American Bulletin, 68: 567 - 576.

Oehler, J.F., Lénat, J. F., Labazuy, P., 2008. Growth and collapse of the Reunion Island volcanoes: Bulletin of Volcanology. 70, 717-742.

Ollier, C.D., 1988. Volcanoes: Blackwell, Oxford.

Ollier, C.D., and Terry, J.P., 1999. Volcanic geomorphology of northern Viti Levu, Fiji: Australian Journal of Earth Sciences: An International Geoscience Journal of the Geological Society of Australia. 46, 515 - 522.

Palmer, B.A., and Neall, V.E., 1991. Constraining lithofacies architecture in ring plain deposits related to edifice construction and destruction, the Quaternary Stratford and Opunake Formations, Egmont Volcano, New Zealand. Sedimentary Geology. 74, (1-4), 71-88.

Palmer, B.A., Alloway B. V., Neall, V. E., 1991. Volcanic-debris-avalanche deposits in New Zealand - Lithofacies organization in unconfined, wet-avalanche flows, Sedimentation in Volcanic Settings, SEPM Special Publication No.45, 89-98.

Patanè G, La Delfa S, Tanguy J-C. 2006. Volcanism and mantle-crust evolution: The Etna case. Earth and Planetary Science Letters. 241(3-4), 831-843.

Parfitt, E.A., 1991. The Shape of Dikes Emplaced Laterally Within Volcanic Edifices. Abstracts of the Lunar and Planetary Science Conference. 22, 1027.

Paris, R., Guillou, H., Carracedo, J.C., Perez Torrado, F.J., 2005. Volcanic and morphological evolution of La Gomera (Canary Islands), based on new K-Ar ages and magnetic stratigraphy: implications for oceanic island evolution Journal of the Geological Society. 162, 501-512.

Perez-Torrado, F.J., Paris, RCabrera, M.C., Schneider, J-L., Wassmer, P., Carracedo, J-C., Rodriguez-Santana, A., Santana, F., 2006. Tsunami deposits related to flank collapse in oceanic volcanoes: The Agaete Valley evidence, Gran Canaria, Canary Islands: Marine Geology. 227, 135-149.

Pierson, T.C., and Scott, K. M., 1985. Downstream dilution of a lahar: transition from debris flow to hyperconcentrated streamflow Water Resources Research. 21, 1511-1524.

Pinel V, and Jaupart, C. 2000. The Effect of Edifice Load on Magma Ascent Beneath a Volcano. Philosophical Transaction of the Royal Society of London. 358, 1515-1532.

Pinel, V., Jaupart, C., 2004. Magma storage and horizontal dyke injection beneath a volcanic edifice: Earth and Planetary Science Letters. 221, 245-262.

Ponomareva, V.V., Pevzner, M. M., Melekestsev, I. V., 1998. Large debris avalanches and associated eruptions in the Holocene eruptive history of Shiveluch Volcano, Kamchatka, Russia: Bulletin of Volcanology. 59, 490-505.

Reubi, O., and Hernandez, J., 2000. Volcanic debris avalanche deposits of the upper Maronne valley (Cantal Volcano, France): evidence for contrasted formation and transport mechanisms: Journal of Volcanology and Geothermal Research. 102, 271-286.

Riggs, N.R., Busby-Spera, C. J., 1990. Evolution of a multi-vent volcanic complex within a subsiding arc graben depression: Mount Wrightson Formation, Arizona: Geological Society of America Bulletin. 102, 1114-1135

Roa, K., 2003. Nature and origin of toreva remnants and volcaniclastics from La Palma, Canary Islands. Journal of Volcanology and Geothermal Research. 125(3-4), 191-214.

Robin, C., Mossand, P., Camus, G., Cantagrel, J.-M., Gourgaud, A., and Vincent, P.M., 1987. Eruptive history of the Colima volcanic complex (Mexico): Journal of Volcanology and Geothermal Research. 31, 99-113.

Robin, C., Camus, G., Gourgaud, A. 1991. Eruptive and magmatic cycles at Fuego de Colima volcano (Mexico). Journal of Volcanology and Geothermal Research. 45(3-4), 209-225.

Rubin, A.M., Pollard, D.D., 1987. Origins of blade-like dikes in volcanic rift zones. U.S. Geolological Survey Professional Paper Volume. 1350, 1449 – 1470.

Ryan, M.P., 1988. The mechanics and three-dimensional internal structure of active magmatic systems - Kilauea Volcano, Hawaii. Journal of Geophysical Research. 93, 4213-4248.

Samper A, Quidelleur X, Lahitte P, Mollex D. 2007. Timing of effusive volcanism and collapse events within an oceanic arc island: Basse-Terre, Guadeloupe archipelago (Lesser Antilles Arc). Earth and Planetary Science Letters. 258(1-2), 175-191.

Schmincke, H.-U., 2004. Volcanism Berlin, Springer-Verlag.

Sewell, R.J., 1985. The volcanic geology and geochemistry of central Banks Peninsula and relationships to Lyttelton and Akaroa volcanoes. PhD Thesis, University of Canterbury, Christchurch, New Zealand.

Sewell, R.J., 1988. Late Miocene Volcanic Stratigraphy of Central Banks Peninsula, Canterbury, New Zealand. New Zealand Journal of Geology and Geophysics. 31, 41-64.

Sewell, R. J., and Gibson, I.J., 1988. "Petrology and geochemistry of Teirtary rocks from inland Central and South Canterbury." New Zealand Journal of Geology and Geophysics. 31, 41 - 64.

Sewell, R.J., Weaver, S. D., and Thiele, B. W., 1989. Lyttelton sheet M36 BD. New Zealand Geological Survey DSIR, Wellington, New Zealand.

Sewell, R.J., Weaver, S. D., and Reay, M. B., 1992. Geology of Banks Peninsula. Scale 1:100,000. Institute of Geological and Nuclear Sciences Map 3. Institute of Geological and Nuclear Sciences Ltd, Lower Hutt.

Shearer, J.C., 1986. The Geology of Governors Bay Road - Dyers Pass Area. BSc (Hons) Thesis, University of Canterbury, Christchurch, New Zealand.

Shelley, D., 1987. Lyttelton-1 and Lyttelton-2, the 2 Centers of Lyttelton-Volcano. New Zealand Journal of Geology and Geophysics. 30, 159-168.

Shelley, D., 1988. Radial Dikes of Lyttelton Volcano - Their Structure, Form, and Petrography. New Zealand Journal of Geology and Geophysics. 31, 65-75.

Shelley, D., 1992. Port Hills; radial dikes, spatter cones and shapes of the two Lyttelton Volcanoes. In: Campbell J.K., (ed.) Geological Society of New Zealand Field Trip Guides, Christchurch Conference. 95 – 102.

Slaughter, G.N., 1995. The Geology of the Mt Evans Area: Implications for the Stratigraphy of Lyttelton Volcano. BSc (Hons) Thesis, University of Canterbury, Christchurch, New Zealand.

Sleep, N.H., 2002. Local lithospheric relief associated with fracture zones and ponded plume material: Geochem. Geophys. Geosyst. 3 (12), 8506.

Smith, G.A., 1986. Coarse grained nonmarine volcaniclastic sediment: terminology and depositional process: Geological Society of America Bulletin. 97, 1-10.

Smith, G.A., 1987. The influence of explosive volcanism on fluvial sedimentation: the Deschutes Formation (Neogene) in central Oregon: Journal of Sedimentary Petrology. 57, 613-629.

Smith, G.A., Lowe, D.R., 1991. Lahars: volcano-hydrologic events and deposition in the debris-flow–hyperconcentrated-flow continuum. In: Fisher, R.V., Smith, G.A. (eds.), Sedimentation in Volcanic Settings. Soc. Econ. Paleontol. Mineral. Spec. Publ. 45, 59–70.

Sohn, Y.K., Kim, S. B., Hwang, I. G., Bahk, J. J., Choe, M. Y., Chough, S. K. , 1997. Characteristics and depositional processes of large scale gravely gilbert type forests in the Miocence Doumsan fan delta, Pohang Basin, SE Korea: Journal of Sedimentary Research. 67, 130-141.

Sohn, Y.K., Rhee, C. W., Kim, B. C., 1999. Debris flow and hyperconcentrated flood-flow deposits in an alluvial fan, Northwestern part of the Cretaceous Yongdong Basin, Central Korea: The Journal of Geology. 107, 111-132.

Sohn, Y.K., 2000. Coarse-grained debris-flow deposits in the Miocene fan deltas, SE Korea: a scaling analysis: Sedimentary Geology. 130, 45-64.

Speight, R., 1917. Geology of Banks Peninsula. Transaction of the New Zealand Institute. 49, 365-392.

Speight, R., 1938. The dykes of the Summit Road, Lyttelton. Transaction of the Royal Society of New Zealand. 68, 82-99.

Speight, R., 1943. Geology of Banks Peninsula – a revision. Transaction of the Royal Society of New Zealand. 73, 13-26

Sillitoe, R.H., 1994. Erosion and collapse of volcanoes: Causes of telescoping in intrusion-centered ore deposits: Geology. 22, 945-948.

Stipp, J.J., and McDougall, I., 1968. Geochronology of the Banks Peninsula Volcanoes, New Zealand. New Zealand Journal of Geology and Geophysics. 11, 1239-1260.

Sutherland, R., Davey, F., and Beavan J., 2000. Plate boundary deformation in South Island, New Zealand, is related to inherited lithospheric structure. Earth and Planetary Science Letters. 177, 141-151.

Sutherland, F.L., and Fanning, C.M., 2001. Gem-bearing basaltic volcanism, Barrington, New South Wales: Cenozoic evolution, based on basalt K–Ar ages and zircon fission track and U–Pb isotope dating: Australian Journal of Earth Sciences: An International Geoscience Journal of the Geological Society of Australia. 48, 221 - 237.

Sutherland, F.L., Graham, I.T., Zwingmann, H., Pogson, R.E., and Barron, B.J., 2005. Belmore Volcanic Province, northeastern New South Wales, and some implications for plume variations along Cenozoic migratory trails: Australian Journal of Earth Sciences: An International Geoscience Journal of the Geological Society of Australia. 52, 897 - 919.

Sutton, R., 1993. Volcaniclastic rocks of the Orton-Bradley Formation, Banks Peninsula. Masters Thesis, University of Canterbury, Christchurch.

Szekely, B., Karàtson, D., 2004. DEM-based morphometry as a tool for reconstructing primary volcanic landforms: examples from the Borzsony Mountains, Hungary. Geomorphology. 63, 25-37.

Taylor, S.R., McLennan, S.M., and McCulloch, M.T., 1983. Geochemistry of loess, continental crustal composition and crustal model ages: Geochimica et Cosmochimica Acta. 47, 1897-1905.

Thiele, B., 1983. Basement geology of the Lyttelton Volcano, Banks Peninsula. Masters Thesis, University of Canterbury, Christchurch.

Thouret, J.-C., 1999. Volcanic geomorphology--an overview: Earth-Science Reviews. 47, 95-131.

Tibaldi, A., 1996. Mutual influence of dyking and collapses at Stromboli Volcano, Italy. In: B. McGuire, Jones, A. P., Neuberg, J. (Editor), Volcano instability on the earth and other planets. The Geological Society, London.

Tibaldi, A., 2001. Multiple sector collapses at Stromboli volcano, Italy: how they work: Bulletin of Volcanology. 63, 112-125.

Timm, C., Hoernle, K., Van Den Bogaard, P., Bindeman, I., and Weaver, S., 2009. Geochemical evolution of intraplate volcanism at Banks Peninsula, New Zealand: Interaction between asthenospheric and lithospheric melts. Journal of Petrology. 50 (6), 989-1023.

Todd, S.P., 1989. Stream driven, high density gravelly traction carpets: possible deposits in the Trabeg Conglomerate Formations, SW Ireland and theoretical considerations of their origin: Sedimentology. 36, 513-530.

Toprak, V., 1998. Vent distribution and its relation to regional tectonics, Cappadocian Volcanics, Turkey. Journal of Volcanology and Geothermal Research. 85, 55-67.

Ui, T., Takarada, S., and Yoshimoto, M., 2000. Debris avalanches. In: Sigurdsson, H, Houghton, B., McNutt, S.R., Rymer, H., Stix, J. (Eds.), Encyclopedia of Volcanoes. Academic Press. California. 617-626.

Vallance, J.W., 2000. Lahars. In: Sigurdsson, H, Houghton, B., McNutt, S.R., Rymer, H., Stix, J. (Eds.), Encyclopedia of Volcanoes. Academic Press. California. 601-616.

Van Wyk de Vries, B., and Francis, P., 1997. Catastrophic collapse at stratovolcanoes induced by gradual volcanic spreading: Nature. 387, 387-390.

Ventura, G., Vilardo, G., Milano, G., and Pino, N.A., 1999. Relationships among crustal structure, volcanism and strike-slip tectonics in the Lipari-Vulcano Volcanic Complex (Aeolian Islands, Southern Tyrrhenian Sea, Italy): Physics of The Earth and Planetary Interiors. 116, 31-52.

Vespermann, D., Schmincke, H. U. , 2000. Scoria cones and tuff rings, in Sigurdsson, H., Houghton, B. F., McNutt, S. R., Rymer, H., Stix, J, ed., Encyclopedia of Volcanoes: San Diego, Academic Press. 683-694.

Vessel, R.K., Davies, D. K., 1981. Non marine sedimentation in an active fore arc basin, in Ethridge, F.G., Flores, R. M., ed., Recent and Ancient Nonmarine Depositional Environments Models for Exploration, Volume 31, Society of Economic Paleontologists and Mineralogist Special Publication. 31-45.

Voight, B., and Ellsworth, D., 1997. Failure of volcanic slopes: Geotechnique. 47, 1-31.

Wadge, G., Francis, P. W., Ramirez, C. F., 1995. The Socompa collapse and avalanche event: Journal of Volcanology and Geothermal Research. 66, 309-336.

Walker GPL. 1992. "Coherent intrusion complexes" in large basaltic volcanoes a new structural model. Journal of Volcanology and Geothermal Research 50, 41-54.

Walker, G.P.L., 2000. Volcanic rift zones and their intrusion swarms. Journal of Volcanology and Geothermal Research. 21–34.

Walter, T.R., Klugel, A., and Munn, S., 2006. Gravitational spreading and formation of new rift zones on overlapping volcanoes, Terra Nova 18, 26–33.

Weaver, S.D., 1980. An introduction to the geology of the Lyttelton Volcano. In: Weaver, S.D., and Lewis, D.W., (eds.), Geological Society of New Zealand, Christchurch Conference Field Trip Guides. H2-H9.

Weaver, S.D. and Sewell, R.J., 1986. Cenozoic volcanic geology of Banks Peninsula. New Zealand Geological Survey Record. 13, 39-63.

Weaver, S.D., and Smith, I.E.M. (eds.), 1989. New Zealand Intraplate Volcanism. Intraplate Volcanism in Eastern Australia and New Zealand. 157-188.

Wells, S.G., and Harvey, A. M., 1987. Sedimentologic and geomorphic variations in storm generated alluvial fans, Howgill Fells, northwest England: Geological Society of America Bulletin. 98, 182-198.

White, J.D.L., Houghton, B.F., 2006. Primary volcaniclastic rocks: Geology. 34, 677-680.

Williams, H., and McBirney, A.R., 1979. Volcanology. Freeman, Cooper and Company. San Francisco, California, USA.

Williams, H., 1941. Calderas and their origin. Bulletin of the Department of Geological Sciences, University of California. 25, 239-346.

Wilson, H.D., 1994. Regeneration of native forest on Hinewai Reserve, Banks Peninsula: New Zealand Journal of Botany. 32, 373-383.

Wood, C.A., 1980. Morphometric analysis of cinder cone degradation Journal of Volcanology and Geothermal Research. 8, 137-160.

Wright, J.V., Self, S., Fisher, R. V., 1981. Towards a facies model for ignimbrite-forming eruptions, in Self, S.S., R. S. J., ed., Tephra studies: Dordrecht, Holland, D. Reidel. 433-439.

Yamamoto, T., Nakamura, Y., Glicken, H., 1999. Pyroclastic density current from the 1888 phreatic eruption of Bandai volcano, NE Japan. Journal of Volcanology and Geothermal Research. 90, 191-207.